

**Development of a Downscaling Scheme for a Coarse
Scale Soil Water Estimation Method**

Case Study -- Great Letaba River in South Africa

Dissertation

zur Erlangung des akademischen Grades doctor rerum naturalium

(Dr. rer.nat.)

vorgelegt dem Rat der Chemisch-Geowissenschaftlichen Fakultät der
Friedrich-Schiller-Universität Jena

von Diplom-Geographin Cornelia Scheffler
geboren am 20. August 1978 in Karl-Marx-Stadt (jetzt Chemnitz)

-
1. Gutachter: Prof. Dr. rer. nat. Wolfgang-Albert Flügel, Jena
 2. Gutachter: Univ. Prof. Dr. techn. Wolfgang Wagner, Wien
- Tag der öffentlichen Verteidigung: 02.07.2008
-

ACKNOWLEDGMENT

Working on this dissertation these last few years has been a challenge, combining achievements and setbacks with joy and sometimes with tears. Without the support, guidance and patience of the following people this work would not have been possible.

Special thanks go to Prof. Dr. Wolfgang-Albert Flügel who gave me the opportunity to write this dissertation in Jena and for his guidance, support and advice over the last years. I am also grateful to Prof. Dr. Wolfgang Wagner who supported this work. The discussions with him lead to the ideas that are presented in this work.

The discussions with Dr. Peter Krause helped me to work through the technical as well as some challenging argumentative problems with my study. His constructive criticism helped me to focus my ideas and to describe them more clearly. I am also thankful to him for reading the dissertation draft within a short time period.

I am very grateful to all my colleagues of the Department for Geoinformatics, Hydrology and Modelling, in particular, Dr. Jörg Helmschrot, Dr. Sven Kralisch, Dr. Manfred Fink, Björn Pfennig, and Daniel Varga who have given their time to discuss pieces of my work with me and who have also offered valuable advice. Special thanks also go to Rainer Hoffmann, the system administrator, who helped with any occurring technical problem.

I am grateful indebted to my friend and colleague Antje Vogel for proofreading and her constructive comments to improve this dissertation. Thanks to Markus Reinhold, Evelin Matejka, Cornelia Barth and Timothy Steele for proof-reading this dissertation.

Thanks to all agencies and institutes providing data for this study: to the Institute for Photogrammetry and Remote Sensing (IPF) at the Technical University of Vienna, to the South Africa Weather Service, in particular to Tracey Gill, to the Council for Scientific and Industrial Research (CSIR) and the Agricultural Research Council (ARC) for providing the land-cover data, to the

ACKNOWLEDGEMENT

School of Bioresources Engineering and Environmental Hydrology in Pietermaritzburg, to the Department of Water Affairs and Forestry for providing the data on geology. Special thanks go to the people with whom I had such a great time during the field trip in South Africa: Ralda de Wet, Danie Viljoen, the Family Lorentz and Susann Carter.

Many thanks for financial support from the Marianne und Dr. Fritz Walter Fischer-Stiftung, whose support made this research possible.

For their continuous and encouraging support, I want to thank all my friends -- in particular, Lydia Franke, Kathleen Neumann, Daniela Knorr, Katrin Geiseler and Cornelia Koch.

Special thanks go to my parents and to my brother for their endless support and the trust in me.

I am especially indebted to my partner Hisham Zerriffi who believed in me and who encouraged me to persist whenever I lost my faith in finishing this work. It is to him that I dedicate this work.

CONTENT

<u>LISTS OF FIGURES</u>	<u>V</u>
<u>LIST OF TABLES</u>	<u>VII</u>
<u>ABBREVIATIONS</u>	<u>IX</u>
<u>LIST OF PARAMETERS</u>	<u>XIII</u>
<u>ABSTRACT.....</u>	<u>XV</u>
<u>KURZFASSUNG.....</u>	<u>XVII</u>
<u>CHAPTER 1 INTRODUCTION</u>	<u>1</u>
<u>CHAPTER 2 RESEARCH REVIEW</u>	<u>5</u>
2.1 SOIL MOISTURE IN THE HYDROLOGICAL CYCLE	6
2.1.1 DEFINITION OF SOIL MOISTURE.....	7
2.1.2 CALCULATION OF SOIL MOISTURE	9
2.2 ESTIMATION OF THE SOIL WATER CONTENT AND ITS MONITORING	10
2.2.1 ESTIMATION OF THE SOIL WATER CONTENT USING REMOTE SENSING TECHNIQUES....	10
2.2.1.1 Microwave Techniques for Soil Water Retrieval	11
2.2.1.2 Fundamentals of Active Microwave Remote Sensing	13
2.2.1.3 The ERS Macro-Scale Soil Water Estimates	16
2.2.2 SOIL MOISTURE GENERATION IN LAND SURFACE MODELING.....	21
2.2.2.1 Classification of Models	21
2.2.2.2 Determination of Soil Moisture Using Land Surface Modeling.....	23
2.3 ON TEMPORAL AND SPATIAL SCALING OF SOIL MOISTURE.....	25

2.3.1 SCALE DEPENDENT SPATIAL AND TEMPORAL DISTRIBUTION OF SOIL MOISTURE VARIABILITY 27

2.3.2 THE UP- AND DOWNSCALING PROCESS..... 29

2.3.2.1 Upscaling methods..... 30

2.3.2.2 Downscaling Methods 32

2.4 RESEARCH NEEDS 33

CHAPTER 3 SCIENTIFIC OBJECTIVES AND METHODOLOGICAL APPROACH 35

3.1 STEP I: HYDROLOGICAL SYSTEM ANALYSIS AND DELINEATION OF HYDROLOGICAL RESPONSE UNITS..... 37

3.1.1 HYDROLOGICAL SYSTEM ANALYSIS 37

3.1.1.1 Data Analysis of Hydro-Meteorological Time Series..... 38

3.1.1.2 Spatial Data Modeling 39

3.1.2 DELINEATION OF HYDROLOGICAL RESPONSE UNITS 40

3.2 STEP II: RAINFALL-RUNOFF MODELING WITH J2000..... 42

3.2.1 MODULAR DESIGN OF J2000..... 43

3.2.2 INPUT DATA PREPARATION 46

3.2.3 MODEL PARAMETERIZATION AND CALIBRATION..... 47

3.2.3.1 Automatic Parameter Estimation using Sensitivity Analysis..... 48

3.2.3.2 Prediction of Model Uncertainty 50

3.3 STEP III: ANALYSIS OF THE MACRO-SCALE SOIL WATER ESTIMATES WITH THE SIMULATED SOIL WATER TIME SERIES..... 51

3.3.1 RETRIEVING THE CATCHMENT AREA COVERED BY ONE ERS-SCATTEROMETER FOOTPRINT 51

3.3.2 DELINEATION OF THE HRU-SOIL WATER INDEX (SWI_{HRU}) 51

3.3.3 PROCEDURES FOR EVALUATION OF THE TIME SERIES AT FOOTPRINT SCALE..... 53

3.3.3.1 Decomposition of Time Series..... 53

3.3.3.2 Agreement Criteria..... 54

3.3.3.3 Procedures for Evaluation of the Time Series at HRU Scale..... 55

CHAPTER 4 STUDY AREA AND DATA BASE 57

4.1 STUDY AREA 58

4.1.1 CLIMATE 58

4.1.2	RUNOFF AND WATER BALANCE.....	61
4.1.3	GEOLOGY	63
4.1.4	SOIL.....	64
4.1.5	LAND COVER AND LAND USE.....	65
4.2	DATA BASE.....	67
4.2.1	HYDRO-METEOROLOGICAL TIME SERIES	67
4.2.1.1	Rainfall Data	67
4.2.1.2	Temperature Data.....	68
4.2.1.3	Additional Climatological Parameters	69
4.2.1.4	Runoff Data.....	69
4.2.2	SPATIAL DATASETS (GIS-DATASETS)	70
4.2.3	THE REMOTELY SENSED SOIL WATER DATASET	71
 <u>CHAPTER 5 RESULTS AND DISCUSSION.....</u>		73
5.1	SYSTEM ANALYSIS AND DELINEATION OF HYDROLOGICAL RESPONSE UNITS	74
5.1.1	DATA ANALYSIS AND SYSTEM ANALYSIS.....	74
5.1.1.1	Rainfall Data Analysis	74
5.1.1.2	Runoff Data Analysis.....	74
5.1.1.3	Temporal Relationship between Rainfall and Runoff in the Great Letaba River	77
5.1.1.4	Analysis of the Additional Datasets.....	80
5.1.1.5	Summary of the Data Analysis	81
5.1.2	SPATIAL DATASETS.....	82
5.1.3	DELINEATION OF HYDROLOGICAL RESPONSE UNITS	83
5.2	RAINFALL–RUNOFF MODELING USING J2000.....	89
5.2.1	MODEL PARAMETERIZATION	89
5.2.1.1	Land Cover Information	89
5.2.1.2	Information on Soil Data	90
5.2.1.3	Information on Geology Data	91
5.2.2	MODELING RESULTS	92
5.2.3	SENSITIVITY ANALYSIS.....	96
5.3	ASSESSMENT AND EVALUATION OF THE MACRO-SCALE SOIL WATER ESTIMATES .	100
5.3.1	DELINEATION AND CHARACTERIZATION OF THE ERS-SCATTEROMETER FOOTPRINTS IN THE CATCHMENT.....	101

CONTENT

5.3.2 COMPARISON OF REMOTELY SENSED SOIL WATER AND MODELED SOIL WATER TIME SERIES AT FOOTPRINT SCALE..... 103

5.3.3 DEVELOPMENT OF THE DOWNSCALING SCHEME..... 111

5.3.4 IMPACT OF MODEL CALIBRATION PARAMETER ON THE DOWNSCALING PARAMETERS
..... 131

CHAPTER 6 SUMMARY, CONCLUSIONS AND FUTURE RESEARCH..... 133

6.1 SUMMARY AND CONCLUSIONS 133

6.2 FUTURE RESEARCH 138

REFERENCES..... 141

APPENDIX..... 161

LISTS OF FIGURES

FIGURE 2-1: THE GLOBAL WATER CYCLE (SOURCE: ENTIN, HOUSER ET AL.(2007:P.9)).....	6
FIGURE 2-2: SOIL WATER AND ITS COMPONENTS (MODIFIED AFTER DONAHUE, MILLER ET AL (1983:P.171)).....	8
FIGURE 3-1: FLOWCHART OF THE METHODOLOGICAL APPROACH	37
FIGURE 3-2: FLOWCHART METHODOLOGICAL STEPS IN THE RAINFALL-RUNOFF MODELING	42
FIGURE 3-3: THE MODELING SYSTEM J2000 (MODIFIED FROM KRAUSE (2001:P.74 AND P.89) AND BÄSE (2005:P.25))	43
FIGURE 4-1: GEOGRAPHIC LOCATION OF THE STUDY AREA	58
FIGURE 4-2: SPATIAL DISTRIBUTION OF THE YEARLY RAINFALL AMOUNT IN THE CATCHMENT OF THE GREAT LETABA DERIVED FROM INVERSE DISTANCE WEIGHTING INTERPOLATION	59
FIGURE 4-3: MONTHLY MEAN PRECIPITATION AND EVAPORATION IN THE NORTHERN PROVINCE (DATA SOURCE: SCHULZE, MAHARAJ ET AL. 1997).....	60
FIGURE 4-4: LOCATION OF THE QUATERNARY CATCHMENTS AND RUNOFF-RAINFALL COEFFICIENTS FOR THE QUATERNARY CATCHMENTS (DATA SOURCE: MIDGELEY, PITMAN ET AL.(1994A: APPENDIX 8.6); MIDGELEY, PITMAN ET AL. (1994B), PITMAN AND MIDDLETON (1994)	62
FIGURE 4-5: THE WRB- SOIL TYPES IN THE CATCHMENT OF THE GREAT LETABA RIVER .	64
FIGURE 4-6 : RECLASSIFIED LAND COVER OF THE GREAT LETABA CATCHMENT	66
FIGURE 4-7: THE GAUGING STATION LETABA RANCH (PHOTO: SCHEFFLER, MARCH 2006)	70
FIGURE 5-1: DOUBLE MASS CURVE ANALYSIS IN THE GREAT LETABA CATCHMENT	75
FIGURE 5-2: LONG TERM (20 YEARS) EVALUATION OF PRECIPITATION AND RUNOFF	77
FIGURE 5-3: THE 20 YEARS MONTHLY AVERAGE OF PRECIPITATION AND RUNOFF.....	78
FIGURE 5-4: COMPARISON OF THE DAILY FLOW AT THE GREAT LETABA RANCH BETWEEN TWO TIME PERIODS 1993/94 AND 1998/99	79

LIST OF FIGURES

FIGURE 5-5: FLOW-CHART OF THE DELINEATION OF HRUS (MODIFIED AFTER BÄSE, HELMSCHROT ET AL. (2006)) 83

FIGURE 5-6: EXAMPLE OF A SMALLHOLDING AREA IN SOUTH AFRICA (PHOTO: SCHEFFLER, 2006)..... 86

FIGURE 5-7: SIMULATED HYDROLOGICAL DYNAMICS WITH THE DISTRIBUTED MODEL J2000, GREAT LETABA RIVER CATCHMENT (WITHOUT CATCHMENT OF THE TZANEEN DAM) 93

FIGURE 5-8: SENSITIVITY INDEX FOR THE PARAMETER OF THE SOIL WATER MODULE IN REGARD TO SIMULATED RUNOFF AND SIMULATED SOIL WATER VOLUME..... 98

FIGURE 5-9: SENSITIVITY INDEX FOR THE PARAMETER OF THE GROUND WATER MODULE IN REGARD TO SIMULATED RUNOFF AND SIMULATED SOIL WATER VOLUME 99

FIGURE 5-10: EFFECTS OF CHANGES IN FCADAPATION PARAMETER TO THE MPS-SATURATION OUTPUT, TIME PERIOD 1995/96 100

FIGURE 5-11: ERS-SCATTEROMETER FOOTPRINTS IN THE GREAT LETABA CATCHMENT 101

FIGURE 5-12: TIME SERIES WITH TREND COMPONENTS OF THE \overline{SWI}_{HRU} AND THE SWI_{ERS} FOR EACH FOOTPRINT FOR THE TIME FRAME 1993 TO 1997 104

FIGURE 5-13: X-Y-PLOTS \overline{SWI}_{HRU} AND SWI_{ERS} FOR EACH FOOTPRINT 105

FIGURE 5-14: SEASONAL ANALYSIS BETWEEN 1993 AND 1997 FOR EACH FOOTPRINT 109

FIGURE 5-15: MULTIPLE LINEAR REGRESSION: SPATIAL VARIABILITY OF THE COEFFICIENT OF DETERMINATION, FOOTPRINT ID376..... 115

FIGURE 5-16: MULTIPLE LINEAR REGRESSION: SPATIAL VARIABILITY OF THE REGRESSION COEFFICIENT M_1 , FOOTPRINT ID376..... 116

FIGURE 5-17: MULTIPLE LINEAR REGRESSION: SPATIAL VARIABILITY OF THE REGRESSION COEFFICIENT M_2 , FOOTPRINT ID376..... 117

FIGURE 5-18: MULTIPLE LINEAR REGRESSION: SPATIAL VARIABILITY OF THE INTERCEPT, FOOTPRINT ID376 118

FIGURE 5-19: RELATIVE FREQUENCY OF THE R^2 -VALUES FOR EACH FOOTPRINT ACHIEVED WITH THE LCS-SCALING PARAMETERS 122

FIGURE 5-20: R^2 -SPATIAL DISTRIBUTION FOR THE DOWNSCALING, (TIMEFRAME 1997 TO 1999), FOOTPRINT ID376 126

FIGURE 5-21: R^2 -SPATIAL DISTRIBUTION FOR THE DOWNSCALING (TIMEFRAME 1997 TO 1999), FOOTPRINT ID393 127

FIGURE 5-22: R^2 -SPATIAL DISTRIBUTION FOR THE DOWNSCALING, (TIMEFRAME 1997 TO 1999), FOOTPRINT ID394 128

LIST OF TABLES

TABLE 2-1: SCALE RANGES IN HYDROLOGY (MODIFIED AFTER BECKER (1992:P. 19) AND BLÖSCHL (1996))	26
TABLE 3-1: DATA INPUT FILES IN J2000.....	46
TABLE 4-1: AVAILABLE STATIONS WITH TEMPERATURE MEASUREMENTS	68
TABLE 4-2: PERCENTAGE OF FILLED MINIMUM AND MAXIMUM DATA FROM LYNCH (2004).....	68
TABLE 4-3: ADDITIONAL CLIMATOLOGICAL PARAMETERS	69
TABLE 4-4: GIS-DATASETS FOR THE HRU-DELINEATION.....	71
TABLE 5-1: CLASSIFICATION OF ASPECT.....	84
TABLE 5-2: CLASSIFICATION OF THE SOIL TYPES.....	85
TABLE 5-4: 1. STEP OF THE GEOLOGY CLASSIFICATION	87
TABLE 5-5: 2. STEP OF THE GEOLOGY CLASSIFICATION	87
TABLE 5-6: PARAMETERS OF THE LAND COVER CLASSES FOR THE SOIL WATER AND EVAPOTRANSPIRATION MODULE.....	90
TABLE 5-7: PARAMETERS OF THE SOIL CLASSES FOR THE SOIL WATER MODULE.....	91
TABLE 5-8: PARAMETERS OF THE GEOLOGY CLASSES FOR THE GROUNDWATER MODULE	92
TABLE 5-9: EFFICIENCY CRITERIA FOR THE SIMULATION	94
TABLE 5-10: WATER BUDGET COMPONENTS FOR THE ENTIRE MODELED PERIOD (1993 TO 1999).....	96
TABLE 5-11: PARAMETER VALUES FOR SENSITIVITY ANALYSIS	97
FIGURE 5-9: SENSITIVITY INDEX FOR THE PARAMETER OF THE GROUND WATER MODULE IN REGARD TO SIMULATED RUNOFF AND SIMULATED SOIL WATER VOLUME	99
FIGURE 5-10: EFFECTS OF CHANGES IN FCADAPATION PARAMETER TO THE MPS- SATURATION OUTPUT, TIME PERIOD 1995/96	100
TABLE 5-12: DESCRIPTION OF THE LANDSCAPE CHARACTERISTICS OF EACH FOOTPRINT	102
TABLE 5-13: SUMMARY OF COEFFICIENTS OF COMPARISON	104

LIST OF TABLES

TABLE 5-14: SUMMARY OF THE COMPARISON BETWEEN THE \overline{SWI}_{HRU} AND SWI_{ERS}
TREND COMPONENTS 108

TABLE 5-15: SUMMARY OF THE COMPARISON BETWEEN THE SEASONAL COMPONENTS
 SWI_{HRU} AND SWI_{ERS} 110

TABLE 5-16 (CONTINUED): SCALING PARAMETERS FOR THE LAND COVER AND SOIL
GROUPS..... 121

TABLE 5-17: SCALING PARAMETERS FOR AGRICULTURAL LAND UNDER CONSIDERATION
OF THE SPECIFIC SOIL, SLOPE AND ASPECT GROUP..... 125

TABLE 5-18:HRU-AMOUNT AND ITS RESPECTIVE FOOTPRINT AREA OF HRUS ACHIEVING
 R^2 OVER 0.5..... 129

TABLE 5-19: STATISTICAL SUMMARY OF THE R^2 -VALUES FOR THE LAND COVER CLASSES
..... 129

ABBREVIATIONS

ABBREVIATION	DESCRIPTION
AC	Air Capacity
AET	Actual Evapotranspiration
Alb	Albedo
ARC	Agricultural Research Council
ARMA	Auto Regressive-Moving Average
ASA	Aggregated Simulation Area
ASAR	Advanced Synthetic Aperture Radar
ASCAT	Advanced Scatterometer
Asl.	Above Sea Level
AVE	Absolute Volume Error
AVHRR	Advanced Very High Resolution Radiometer
BEEH	School of Bioresources Engineering and Environmental Hydrology
Cdf	Cumulative Distribution Function
CSIR	Council for Scientific and Industrial Research
d	Depth
dB	Decibel
DWAF	Department for Water Affairs and Forestry
E	East
ENVISAT	Environmental Satellite
ERS	European Remote Sensing Satellite
ESTAR	Electronically Scanned Thinned Array Radiometer
FAO	Food and Agriculture Organization of the United Nations
FPS	Fine Pore Storage
GCM	General Circulation Models
GHz	Giga Hertz
GIS	Geographic Information System
HH	Horizontal-Horizontal
HRU	Hydrological Response Unit
HV	Horizontal-Vertical
IDW	Inverse Distance Weighting
IPCC	Intergovernmental Panel on Climate Change
IPF	Institute for Photogrammetry and Remote Sensing
ISRIC	International Soil Reference and Information Centre
LAI	Leaf Area Index
LAT	Latitude

ABBREVIATIONS

LCS	Land Cover and Soil Group
LCSS	Land Cover, Soil Group and Slope
LCSSA	Land Cover, Soil Group, Slope, Aspect
LCSSAG	Land Cover, Soil Group, Slope, Aspect and Geology
LMS	Landscape Management Analyst
Log. NaS	Logarithmic Nash-Sutcliffe Efficiency
LON	Longitude
LPS	Large Pore Storage
LQ	Lower Quintile
MAP	Mean Annual Precipitation
Md	Median
MetOp	Meteorological Operational satellite
MPS	Medium Pore Storage
N	North
NaS	Nash-Sutcliffe Efficiency
NDVI	Normalized Difference Vegetation Index
NLC	National Land Cover
P	Precipitation
PET	Potential Evapotranspiration
PRMS	Precipitation-Runoff Modeling System
Rd	Rooting Depth
REA	Representative Elementary Area
Res	Resolution
Rhum	Relative humidity
RMSE	Root Mean Square Error
RRC	Runoff-Rainfall Coefficient
RU	Response Unit
S	South
SAR	Synthetic Aperture Radar
SAWS	South African Weather Service
SG	Soil Group
SGP97	Southern Great Plain Experiment 1997
SI	Sensitivity Index
SLURP	Semi distributed Land Use-Based Runoff Processes
SOTER	Soil and Terrain database
SOTERSAF	Soil and Terrain database for Southern Africa
SRTM	Shuttle Radar Topography Mission
sun	Sunshine Duration
SVAT	Soil-Vegetation-Atmosphere-Transfer
SWI	Soil Water Index
TM	Thematic Mapper
UL	Upper Quintile
USGS	US Geological Survey
UTM	Universal Transverse Mercator
VSC	Vegetation-Soil-Complexes

ABBREVIATIONS

VV	Vertical-Vertical
W	West
WBM	Water Balance Model
WISE	World Inventory of Soil Emission Potentials
WRB	World Reference Base for Soil Resources

LIST OF PARAMETERS

SUBSCRIPT	DESCRIPTION	UNIT []
\bar{Q}_{obs}	Mean observed runoff	[m ³ /s]
d	Intercept	[-]
e _s	Saturation vapor pressure	[hPa]
Inf	Actual infiltration rate	[mm]
Inf _{max}	Maximum infiltration rate	[mm]
inter	Lateral flow	[mm]
LPS2MPS	Calibration parameter	[-]
LPS _{act}	Actual amount stored in large pore storage	[mm]
LPS _{inflow}	Inflow rate in the large pore Storage	[mm]
LPS _{max}	Maximum large pore storage	[mm]
LPS _{outflow}	Outflow rate of the large pore storage	[mm]
m ₁	Regression coefficient for SWI _{ERS} variable of a specific HRU	[-]
m ₂	Regression coefficient for SWI _{HRU} variable of a specific HRU	[-]
MPS _{act}	Actual amount stored in medium pore storage	[mm]
MPS _{inflow}	Inflow rate in medium pore storage	[mm]
MPS _{max}	Maximum medium pore storage	[mm]
M _s	Dry soil mass	[g/cm ³]
m _s	Saturation of the surface layer	[%]
M _w	Wet soil mass	[g/cm ³]
n	Number of days	[-]
P	Precipitation	[mm]
P _{d(HRU)}	Daily Precipitation of the specific HRU	[mm]
perc	Percolation rate	[mm]
P _{sum (HRU)}	Sum precipitation between two ERS-Observations	[mm]
Q _{obs}	Observed runoff	[m ³ /s]
Q _{sim}	Predicted runoff	[m ³ /s]
R	Correlation coefficient	[-]
R ²	Coefficient of determination	[-]
R _a	Absolute humidity	[g/cm ³]
R _m	Maximum humidity	[g/cm ³]
R _u	Relative humidity	[%]
runoff _{direct}	Direct runoff	[mm]
Runoff _{subsurface}	Subsurface runoff	[mm]

LIST OF PARAMETERS

soilDiffMPSLPS	Calibration parameter	[-]
soilDistMPSLPS	Calibration parameter	[-]
soilLatVerDist	Calibration parameter	[-]
soiloutLPS	Calibration parameter	[mm]
soil _{sat}	Actual soil saturation	[%]
sw	Actual soil water content, entire soil column	[mm]
SWI _{ERS}	ERS-Soil Water Index	[%]
SWI _{HRU}	Modeled Soil Water Index for every HRU	[%]
sw _{max}	Maximum value of the actual soil water content	[mm]
sw _{min}	Minimum value of the actual soil water content	[mm]
t	Time	[d]
T	Air temperature	[°C]
T _L	Characteristic time length	[d]
T _{max}	Maximum temperature	[°C]
T _{min}	Minimum temperature	[°C]
V _t	Total soil volume	[Vol%]
V _w	Water volume	[Vol%]
w	Gravimetric water content	[%]
X	Model output	[-]
Y	Parameter change	[-]
θ	Volumetric water content	[Vol%]
ρ _{soil}	Density of soil	[-]
ρ _{water}	Density of water	[-]
σ ⁰	Backscatter coefficient	[dB]
σ ⁰ (40)	Backscatter coefficient at an incidence angle of 40°	[dB]
σ ⁰ _{dry}	Backscattering coefficient of a dry soil surface	[dB]
σ ⁰ _{wet}	Backscattering coefficient of a wet soil surface	[dB]

ABSTRACT

Many river basins worldwide are adversely impacted by poor hydrological infrastructure or are poorly characterized due to limited or no hydrologic data. This condition challenges water-management authorities. Especially in semi-arid regions because of their specific natural climatic conditions, resultant water-stressed areas and local water management authorities can benefit in balancing regional disparities between areas with water surplus and those with water shortage.

Water management can benefit from reliable prediction of the hydrological dynamics that can be made by means of distributed, physical-based (process) models. Because of the lack of sufficient or reliable data, often such models are difficult to calibrate and to validate.

This study addresses this data limitation by formulating and testing an independent validation tool for hydrological models that can be applied to downscale macro-scale soil moisture data derived from a remotely sensed scatterometer dataset. This proposed method uses the concept of hydrological response units (HRU) to analyze the spatial variability within one scatterometer footprint. The HRUs are treated as model entities in the process oriented hydrological model J2000 that was applied to the Great Letaba River catchment (ca. 4.700 km²) in South Africa. The soil water time series results were then compared to the remotely sensed dataset and the downscaling scheme derived.

First, the analysis conducted on footprint scale highlights the similarities in predicting the soil water generation over the long term and in seasonal terms. It also exhibits that the absolute values of both time series can not be used for further investigation, due to differences in the observed soil water volume.

Second, the resulted simulated soil water time series were used to establish the downscaling method. Here, the study provides promising results that allow the downscaling of the macro-scale soil water calculated dataset, based upon the landscape related parameters of land cover, soil properties and precipitation. It will also highlight the dependence of the formulated downscaling method on the model calibration application. The study findings indicate that, by linking the two concepts, hydrological modeling and remote sensing, water management authorities should be able to reduce certain prediction uncertainties of the applied models.

KURZFASSUNG

A. Einleitung und Motivation

Die Mehrheit der weltweiten Einzugsgebiete besitzt keine oder nur eine unzureichende hydrometrische Infrastruktur (SIVAPALAN, TAKEUCHI ET AL., 2003), die lokale Wasserbehörden vor besondere Herausforderungen stellt. Dies betrifft im Besonderen, die durch natürlichen Wasserstress charakterisierten semiariden Gebiete. Diese Gebiete zeichnen sich durch geringe mittlere Jahresniederschläge aus, wobei diese darüber hinaus räumlich und zeitlich sehr heterogen verteilt sind. Die regionalen Wasserbehörden werden vor die Aufgabe gestellt, die räumlichen Disparitäten von Gebieten mit Wasserüberschuss und Gebieten mit Wasserknappheit auszugleichen und die Wasserversorgung für die niederschlagsarmen Perioden sicher zu stellen.

Da hydrologische Modelle in der Lage sind komplexe Zusammenhänge darzustellen und Landschaftsveränderungen hinsichtlich ihres Einflusses auf das Ökosystem zu bewerten (SINGH, 1995), können diese als bedeutende Entscheidungshilfe im Wassermanagement eingesetzt werden. Voraussetzung für die hydrologische Modellierung ist jedoch eine ausreichende Datenlage (SINGH, 1995; BEVEN, 2001A). Die Modellierung ist daher in Gebieten mit einer limitierten Datenlage nur begrenzt einsetzbar.

Ein wichtiger Parameter in der hydrologischen Modellierung ist die Bodenfeuchte, die als Steuerungsfaktor zwischen Hydrosphäre, Biosphäre,

Atmosphäre und Pedosphäre (YU, CARLSON ET AL., 2001) fungiert. Hier, könnte die Fernerkundung, die in der Lage ist, Bodenfeuchte in hoher zeitlicher Auflösung abzubilden, als ein wichtiges Instrument zur Validierung und Kalibrierung von hydrologischen Modellen eingesetzt werden.

In den Studien von WAGNER, LEMOINE ET AL. (1999A; 1999B) und WAGNER, NOLL ET AL. (1999) wurde ein Algorithmus entwickelt, auf dessen Basis ein globaler Datensatz des Bodenwassergehaltes aus den Messungen des C-Band Scatterometers an Bord der *European Remote Sensing* (ERS)-Satelliten 1 und 2 erstellt wurde. Die Daten beinhalten den aus den Messungen der oberen Bodenschicht abgeleiteten Indexes für den Bodenwassergehalt (*Soil Water Index* = SWI_{ERS}) mit einer räumlichen Auflösung von 50 km. Allerdings wird die Einsatzfähigkeit dieses Datensatzes in der hydrologischen Modellierung aufgrund der groben räumlichen Auflösung von Hydrologen angezweifelt.

Daraus ableitend, ist das übergeordnete Ziel der vorliegenden Arbeit die Evaluierung des makroskaligen Indexes des Bodenwassergehaltes für eine Verwendbarkeit in der mesoskaligen hydrologischen Modellierung. Hierfür müssen die Daten des makroskaligen Indexes auf mesoskalige Ebenen verlagert werden. Für einen solchen Skalentransfer ist der Einsatz einer geeigneten Disaggregierungsmethode notwendig. Im Mittelpunkt der Arbeit steht daher die **Entwicklung eines Disaggregierungskonzeptes zur skalenübergreifenden Verwendbarkeit des makroskaligen Indexes des Bodenwassergehaltes für die mesoskalige hydrologische Modellierung.**

Für die Entwicklung dieses Verfahrens werden Referenzdaten benötigt. Da die Erfassung der Bodenfeuchte mit punktuellen Feldmessungen auf der räumlichen Ebene der Fernerkundungsdaten (50 km) nicht möglich ist, müssen andere Informationsquellen genutzt werden. Hierfür bietet sich die Modellierung der Niederschlags-Abflussbeziehung, mit einer hohen räumlichen und zeitlichen Auflösung, an. Die Bodenfeuchte wird als Teilergebnis dieser Beziehung gewonnen, und mit den makroskaligen Daten des Bodenwasserindex verglichen, um in der späteren Folge die Methode zur Disaggregation abzuleiten. Die vorliegende Arbeit liefert dabei in den folgenden Punkten einen wichtigen Beitrag in der Forschungslandschaft, um den Einsatz von Fernerkundungsprodukten in der Hydrologie zu erweitern:

- Die Entwicklung einer Disaggregierungsmethode, die es erlaubt makroskalige Informationen des Bodenwassergehaltes in eine kleinere räumliche Ebene zu transferieren,
- Die Bestimmung von Schlüsselparametern, die die Bodenfeuchteverteilung in der jeweiligen Skalenebene (makroskalig = 50 km, mesoskalig = \varnothing 0,7 km²) beeinflussen sowie deren Einbeziehung in die Disaggregierungsmethode,
- Die Anwendung und Überprüfung der entwickelten Disaggregierungsmethode von Modellabhängigkeiten sowie
- Die Beurteilung der Anwendbarkeit des makroskaligen Bodenwasserindex in der mesoskaligen hydrologischen Modellierung.

B. Stand der Forschung

Obwohl nur etwa 0.001 % der weltweiten Wasserreserven im Bodenkompartment als Bodenfeuchte gespeichert werden, stellt die Bodenfeuchte eine wichtige Größe im hydrologischen Kreislauf dar (DINGMAN, 2002:P.55). Zur Abschätzung der Bodenfeuchte können die drei Methoden angewendet werden: 1) punktuelle Feldmessungen 2) Erfassung der Bodenfeuchte mittels der Mikrowellenfernerkundung und 3) Landschaftsmodellierung. Dabei sind nur die letzten zwei für eine flächige Abschätzung der Bodenfeuchte einsetzbar.

Fernerkundungsmethoden, insbesondere die Instrumente der Mikrowellenfernerkundung, beinhalten ein großes Potenzial zur Erfassung des Bodenwassergehaltes. Hierfür können zwei Systeme eingesetzt werden. Zum einen die passiven Instrumente (Radiometer), welche die „Eigenstrahlung der Erde“ messen (HENDERSON AND LEWIS, 1998). Die sogenannte Helligkeitstemperatur steht in einer inversen Beziehung zum Feuchtigkeitsgehalt der obersten Bodenzentimeter. Zum anderen werden aktive Instrumente, das *Radio Detection and Ranging* (Radar) eingesetzt, die ihrerseits elektromagnetische Strahlung erzeugen und den zurück gestreuten Anteil dieser Strahlung messen. Beispiele für aktive Systeme sind *Synthetic Aperture Radar* (SAR), Altimeter und das Scatterometer.

Der *Einsatz von Mikrowellen zur Abschätzung des Bodenwassergehaltes* ist aufgrund der elektromagnetischen Eigenschaften von Mikrowellen möglich (ULABY, DUBOIS ET AL., 1996). Das Rückstreuungssignal wird von den folgenden Faktoren beeinflusst: 1) die Frequenz des gemessenen Mikrowellensignals bestimmt das Eindring- und Durchdringungsvermögen. Mikrowellen mit längerer Wellenlänge, zum Beispiel L- und C-Band, und somit geringerer Frequenz können tiefer in die Bodensäule eindringen. 2) Die jeweilige Eindringtiefe hängt des Weiteren auch von der aktuellen Bodensättigung ab. Je trockener der Boden desto tiefer können Mikrowellen in den Boden eindringen. 3) Der Rückstreuungskoeffizient wird des Weiterem vom Einfallswinkel beeinflusst. Der Anteil des reflektierten Signals steigt, je stärker die beobachtete Fläche in Richtung Antenne geneigt ist. 4) Die Oberflächenrauigkeit der untersuchten Fläche bestimmt die Stärke der Rückstreuung. Je rauer eine Fläche ist desto diffuser ist die Reflexion und desto höher der Anteil der rückgestreuten Strahlung. 5) Die Dielektrizitätskonstante beschreibt die Permittivität (dieelektrische Leitfähigkeit) von Materialien und ist ein Maß für die Ausbreitungsgeschwindigkeit des ausgesendeten Signals. Ein steigender Feuchtigkeitsgehalt im Boden wird durch einen Anstieg in der Dielektrizitätskonstante beschrieben und in dessen Folge durch Zunahme des rückgestreuten Signals.

Verschiedene Studien wie beispielsweise NJOKU AND ENTEKHABI (1996), MORAN, MCELROY ET AL. (2006), KERR (2007), beschäftigten sich mit der **Extraktion der Bodenfeuchte aus Fernerkundungsdaten**. Der erste globale fernerkundlich erfasste Bodenwasser- Datensatz (SCIPAL, WAGNER ET AL., 2002) wurde aus den Scatterometer- Daten an Bord der *European Remote Sensing* Satelliten (ERS) 1 und 2 extrahiert (WAGNER, LEMOINE ET AL., 1999A; WAGNER, LEMOINE ET AL., 1999B; WAGNER, NOLL ET AL., 1999). Die Aufnahmefrequenz beträgt 5,3 GHz (C-Band) und der Satellit kann bis zu 5 cm (WAGNER, SCIPAL ET AL., 2003) in den Boden eindringen. Die daraus abgeleitete Zeitreihe repräsentiert den oberflächennahen Wassergehalt, der „vom Sensor abgetasteten“ Bodenschicht. Der aktuelle Messwert wird in Beziehung zum höchsten und niedrigsten Wassergehalt im Betrachtungszeitraum gesetzt. Die daraus resultierende Bodensättigung (m_s) repräsentiert einen Durchschnittswert über einer vegetationslosen Oberfläche und / oder einer nur spärlich bedeckten Landoberfläche, wie beispielsweise Grasland oder agrarische Nutzflächen.

Dieser Wert wird anschließend zur Ableitung des Trendindikators, dem *Soil Water Index* (SWI_{ERS}) verwendet (WAGNER, LEMOINE ET AL., 1999A; WAGNER, LEMOINE ET AL., 1999B; WAGNER, NOLL ET AL., 1999). Dieser wird mittels eines einfachen Infiltrationsmodells ermittelt. Das Infiltrationsmodell besteht aus zwei Schichten: die obere stellt die vom Sensor erfasste Bodenschicht dar. Darunter befindet sich der Bodenwasserspeicher, welcher nur von der aufliegenden Schicht beeinflusst wird. Prozesse mit benachbarten Flächen wie zum Beispiel laterale Zu- und Abflüsse, Transpiration, Grundwasserzufluss, sowie aufwärtsgerichtete Prozesse werden hierbei vernachlässigt (WAGNER, 1998). Im Ergebnis ergibt sich eine SWI_{ERS}- Zeitreihe mit einem Wertebereich zwischen 0 und 100 % für eine Fläche von 50 km (ERS-Footprint) (WAGNER, LEMOINE ET AL., 1999B; WAGNER, NOLL ET AL., 1999).

Die zweite Möglichkeit der flächigen Abschätzung der Bodenfeuchte umfasst den *Einsatz der Landschaftsmodellierung*, in welcher die aktuelle Bodenfeuchte als Nebenprodukt der Niederschlags-Abfluss Modellierung berechnet wird. Der Nachteil dieser Methode ist, dass die Genauigkeit der berechneten Bodenfeuchte stark von den Eingangsdaten sowie von der Modellstruktur beeinflusst wird (SINGH, 1995). Der Vergleich der existierenden hydrologischen Modelle zeigte wesentliche Unterschiede in der zugrunde liegenden Modellkonzeption. Ein wichtiges Unterscheidungsmerkmal stellt die Repräsentation der landschaftlichen Heterogenität (Landbedeckung, Boden, Topographie und Geologie) dar. Hier können zwei wesentliche Modelltypen unterschieden werden (SINGH, 1995): 1) Blockmodell („lumped“) und 2) räumlich gegliederte („distributive“) Modelle. In den Blockmodellen erfolgt keine Unterscheidung der räumlichen Variabilität, während räumlich verteilte Modelle die Variabilität mittels räumlich verteilter homogener Modelleinheiten wiedergeben.

Für die Entwicklung einer Disaggregierungsmethode ist die Berücksichtigung der räumlichen und zeitlichen Bodenfeuchtegeneration von entscheidendem Interesse. Dieser Forderung wird durch die Ableitung von distributiven prozessorientierten Modelleinheiten nachgekommen werden. Diese Einheiten werden anschließend in einem distributiven hydrologischen Modell als Modellentitäten verwendet.

Die Untersuchung der verschiedenen distributiven Modelltypen offenbarte Unterschiede in der Konzeption des Bodenkompartimentes. In der

Niederschlags-Abfluss Modellierung werden die folgenden Konzepte zur Generation der Bodenfeuchte angewendet. 1) Betrachtung des Bodenkompartmentes als einen Einzelspeicher (MANABE, 1969; IRANNEJAD AND SHAO, 2002) 2) Erweiterung des Einzelspeicher- Konzeptes durch die Implementierung einer oberflächennahen Bodenschicht, die durch die grenzschichtnahen Prozesse gesteuert wird (IRANNEJAD AND SHAO, 2002) 3) vertikale Unterteilung der Bodensäule in zwei oder mehrere nacheinander folgende Bodenschichten (LEAVESLEY, LICHTY ET AL., 1983; IRANNEJAD AND SHAO, 2002) und 4) Unterteilung in mehrere parallele Bodenkompimente, die ihrerseits einzelne Speicher darstellen (SCHULLA AND JASPER, 1998; KRAUSE, 2001).

Der Vergleich der einzelnen Konzepte zeigte, dass das vierte Konzept, aufgrund der stärkeren Berücksichtigung bodenphysikalischer Parameter, der Realität am nächsten kommt. Aus diesem Grund wurde sich bei der Niederschlags-Abfluss Modellierung für das distributive, prozessorientierte Modellsystem J2000 entschieden. Dieses Modell bestimmt den Bodenwasserhaushalt basierend auf parallel geschalteten Bodenspeichern.

Einen weiteren Schwerpunkt bildete die Herausarbeitung von *Einflussfaktoren*, welche die *räumliche und zeitliche Variabilität der Bodenfeuchte* beeinflussen. In Abhängigkeit der Skala lassen sich verschiedene Parameter bestimmen. Auf Mikroebene (<0,1 km²) wird die Verteilung der Bodenfeuchte vor allem durch Topographie, Vegetation und Bodeneigenschaften bestimmt (BEVEN AND KIRKBY, 1979; MOHANTY, SKAGGS ET AL., 2000; JACOBS, MOHANTY ET AL., 2004). Einige Studien geben Hinweise darauf, dass die Art der Bodenbearbeitung sowie die Vorfeuchte ebenfalls eine entscheidende Rolle spielen (FAMIGLIETTI, DEVEREAUX ET AL., 1999; WESTERN, GRAYSON ET AL., 1999). Auf der Mesoskala (<1000 km²) stellen Topographie (Exposition und Hangneigung), Vegetation und Bodeneigenschaften nach wie vor die bestimmenden Parameter dar (BEVEN AND KIRKBY, 1979; BARDOSSY AND LEHMANN, 1998; MARTINEZ, HANCOCK ET AL., 2007). In einigen Studien, wie beispielsweise in GRAYSON, WESTERN ET AL. (1997); WESTERN, GRAYSON ET AL. (1999) und WILSON, WESTERN ET AL. (2005) wurden jedoch Indikatoren gefunden, dass die Variabilität auf dieser Ebene bereits vom Klima beeinflusst wird. Auf der Makroskala (>1000 km²) ändern sich die Einflussfaktoren. In dieser räumlichen Ebene wird die Verteilung in erster Linie durch klimatische

Faktoren, vor allem durch Niederschlag und Evapotranspiration beeinflusst (BLÖSCHL, 1996; VINNIKOV, ROBOCK ET AL., 1996; GÓMEZ-PLAZA, ALVAREZ-ROGEL ET AL., 2000).

Um Informationen von einer Skalenebene in eine höhere bzw. niedrigere Skalenebene zu transferieren, erfolgt die Anwendung von *Aggregierungs- und Disaggregierungsmethoden*. Die Aggregation umfasst, den Informationstransfer von einer kleineren Skalenebene in eine höhere, während Disaggregation den umgekehrten Prozess, die Informationsübertragung von der höheren Ebene in eine niedrigere Skalenebene, beschreibt (BECKER, 1992).

In der Literatur werden **Disaggregierungsansätze** von grob aufgelöster Bodenfeuchte Datensätzen beschrieben. Zum Beispiel wurden makroskalige Bilder zum Bodenwassergehalt mittels Bodentextur und Vegetationswassergehalt von 10 km auf 1 km disaggregiert (KIM AND BARROS, 2002A). Allerdings, zeigte diese Methode eine starke Abhängigkeit von lokalen Bedingungen, denn die Topographie wurde aufgrund der Einzugsgebietscharakteristik nicht berücksichtigt. Allerdings wird die Topographie als ein treibender Faktor für die Variabilität der oberflächennahen Bodenfeuchte beschrieben. Eine andere Methode verwendeten WAGNER, PATHE ET AL. (SUBMITTED) zur Disaggregation des rückgestreuten Mikrowellensignals des *Advanced Synthetic Aperture Radar (ASAR)*. Die Autoren beschrieben den Zusammenhang zwischen der regionalen und lokalen Ebene basierend auf einer linearen Beziehung.

Aus den oben genannten Ausführungen lässt sich der **Forschungsbedarf** auf dem die vorliegende Arbeit aufbaut, ableiten. Im Mittelpunkt steht die Entwicklung eines dynamischen, nicht an lokale Bedingungen geknüpften Disaggregierungskonzeptes, in dem alle beeinflussenden Faktoren der räumlichen und zeitlichen Bodenfeuchteverteilung auf ihren Einfluss zur Beschreibung der Verteilung auf mesoskaliger Ebene bewertet werden und gegebenenfalls im Konzept berücksichtigt werden können.

C. Methodische Vorgehensweise

Zur Entwicklung des Disaggregierungskonzeptes wurden die folgenden methodischen Schritte durchgeführt: Erstens, die Abschätzung der mesoskaligen Bodenfeuchteverteilung als Referenzdatensatz der

Disaggregation erfolgte mittels des Einsatzes eines distributiven Modellsystems, welches auf dem Konzept der homogenen Modellierungseinheiten beruht (*Hydrological Response Unit* = HRUs) (FLÜGEL, 1995; FLÜGEL, 1996). Voraussetzung für die Ableitung der HRUs ist die **integrierte hydrologische Systemanalyse**, die auf der Aufnahme und Bewertung hydrologisch relevanter Systemkomponenten wie Topographie, Boden, Geologie und Vegetation sowie der Analyse der hydro-meteorologischen Zeitreihen basiert (FLÜGEL, 2000).

Die abgeleiteten HRUs dienen als Modellentitäten im **Modellsystem J2000** (KRAUSE, 2001). Das Modell J2000 ist ein distributives, prozessorientiertes Modell, das sich in einzelne Systemmodule (Interzeptionsmodul, Schneemodul, Bodenmodul, Grundwassermodul und das Reach-Routing Modul) untergliedert. Für jede Modelleinheit (HRU) werden die Abflusskomponenten im Bodenmodul (Oberflächenabfluss, Zwischenabfluss) und Grundwassermodul (Basisabfluss, unterteilt in schnellen und langsamen) ermittelt. Diese berechneten Werte der Abflusskomponenten werden anschließend in die nächste HRU weitergegeben und den dort ermittelten Abflussmengen der jeweiligen Komponenten zugeführt. Dies wiederholt sich bis ein Vorflutersegment erreicht wird. Innerhalb der Vorflutersegmente wird das Wasser dann zum Gebietsauslass geführt. Die Bodenfeuchte wird hierbei als Teilkomponente der Wasserbilanz berechnet, in dem der Niederschlag einer Modellfläche prozessorientiert auf die Prozesse der Evapotranspiration, der Bodenspeicherung und des Abflusses aufgeteilt wird.

Das Modellsystem J2000 besitzt 30 direkte Modellparameter, deren **Kalibrierung** in zwei Schritten erfolgte. In einem ersten Schritt wurde der dem Einzugsgebiet entsprechende Parameterbereich mit den Effizienzmaßen Nash-Sutcliffe Effizienz (NASH AND SUTCLIFFE, 1970) (NaS), logarithmischer Nash-Sutcliffe Effizienz (log. NaS), Bestimmtheitsmaß (R^2) sowie dem absoluten Volumenfehler (AVE) bestimmt. In einem zweiten Schritt wurde die Auswirkungen eventueller Parameter auf den Abfluss und den aktuellen Bodenwassergehalt mit Hilfe der **Sensitivitätsanalyse** untersucht. Des Weiteren wurde die erhaltene Simulation der Niederschlags-Abfluss-Beziehung im Great Letaba auf ihre Plausibilität hin geprüft. Dies erfolgte mittels Überprüfung der Wasserbilanz sowie durch Vergleich der berechneten Evapotranspiration mit Literaturdaten.

Im Anschluss an die Modellierung erfolgte die Evaluierung der beiden Datensätze. Um die modellierten Zeitreihen der Bodenfeuchte mit den fernerkundlich erfassten Werten des Bodenwassergehaltes (SWI_{ERS}) vergleichen zu können, erfolgte die **Berechnung des simulierten Bodenwasserindex** (SWI_{HRU}) (SCHEFFLER, KRAUSE ET AL., 2007). Hierfür wurde der aktuelle Bodenwassergehalt berechnet, der sich aus der Aufsummierung aller drei Bodenspeicher, Mittelporen-, Grobporen- und des Feinporenspeichers, ergibt. Im anschließenden Schritt wird dieser berechnete aktuelle Bodenwassergehalt zum höchsten und niedrigsten gemessenen Wert im jeweiligen Betrachtungszeitraum in Beziehung gesetzt. Der so erhaltende Index (SWI_{HRU}) bildet die Grundlage für die weitere Analyse. Zudem wird das Testgebiet von mehreren ERS-Footprints abgedeckt. Daher müssen die im jeweiligen ERS-Footprint liegenden HRUs bestimmt werden.

Um einen Vergleich der Zeitreihen auf der räumlichen Ebene der fernerkundlichen Daten ermöglichen zu können, ist die Berechnung eines flächengewichteten Mittelwertes des simulierten Bodenwassergehaltes über alle im Gebiet des jeweiligen Footprints liegenden HRUs notwendig. Diese sich daraus ergebende Zeitreihe ($\overline{SWI_{HRU}}$) wurde dem SWI_{ERS} gegenübergestellt. Mittels eines Dekompositionsverfahrens (CLEVELAND, 1979; CLEVELAND, CLEVELAND ET AL., 1990) erfolgte die Unterteilung der Zeitreihen, $\overline{SWI_{HRU}}$ und SWI_{ERS} , in Trend- und saisonale Komponente. In dieser Analyse werden Übereinstimmungen sowie Abweichungen in den Tendenzen der jeweiligen Komponenten bestimmt.

Aufbauend auf den Ergebnissen dieser Analyse erfolgte die Entwicklung der Disaggregierungsmethode. Das in WAGNER, PATHE ET. AL (SUBMITTED) vorgestellte Konzept beschreibt die Verteilung des „mesoskaligen“ Rückstreuungssignals als lineare Funktion des „makroskaligen“ Rückstreuungssignals. Es zeigte sich jedoch, dass der Niederschlag eine wichtige Größe darstellt und demzufolge im Model berücksichtigt werden muss. Hieraus ableitend kam ein **multiple lineares Regressionsmodell** mit dem SWI_{HRU} der jeweiligen Modelleinheit als abhängige Variable und den SWI_{ERS} und Niederschlag als unabhängige Variablen zur Anwendung.

Es wird davon ausgegangen, dass die naturräumlichen Eigenschaften der Modelleinheiten (HRUs) sich in einer landschaftscharakteristischen Kombination (Landbedeckung, Boden, Topographie und Geologie) der

Regressionskoeffizienten widerspiegeln. Zur Bestimmung dieser Charakteristika wurden die HRUs hinsichtlich ihrer Landschaftseigenschaften **gruppiert**. Die Verteilung der Regressionsparameter innerhalb der Gruppen wurde mit Hilfe von **deskriptiven Statistikmerkmalen** beschrieben. Zur Überprüfung der Disaggregierungsmethode wurden die gefundenen Skalierungsparameter in der Disaggregierung eines weiteren Zeitraumes eingesetzt und bewertet.

D. Untersuchungsgebiet und Datenlage

Das Untersuchungsgebiet des Great Letaba befindet sich im Nordosten Südafrikas und umfasst eine Fläche von ca. 4700 km². Es erstreckt sich von 330 m Höhe über NN im Nordosten bis auf 2121 m NN in den Ausläufern der Drakensberge im Westen.

Geologisch gesehen, gehört das Gebiet des Great Letaba zu sehr alten Formationen. Mit Ausnahme der Gebirgsregion im Westen des Einzugsgebietes, wurde das Gebiet in der präkambrischen Periode geologisch geformt (DU TOIT AND HAUGHTON, 1954; VEGTER, 1995). Die Ausläufer der Drakensberge sind geologisch jünger und wurden während der Hebung der Drakensberge im Proterozoikum gebildet (DU TOIT AND HAUGHTON, 1954; VEGTER, 1995). Diese Differenzierung ist auch im anstehenden Gestein sichtbar. Während die Ausläufer der Drakensberge durch Granit und Diorite gekennzeichnet sind, wird der Osten durch Gneis und Granitoid geprägt. Diese Zweiteilung spiegelt sich ebenfalls in den anstehenden **Böden** wieder. In den Hochlagen des Einzugsgebietes finden sich tiefgründig entwickelte Böden wie Acrisols, Nitisols und Lixisols, die in Gebieten mit großer Hangneigung von Leptosolen abgelöst werden (FAO, 2003). Der zentrale Teil sowie der Osten des Gebietes sind durch den Regosol beschrieben (FAO, 2003). Die **Vegetation** des Einzugsgebietes wird durch eine Savannenlandschaft charakterisiert, die im Oberlauf des Great Letaba von Wäldern abgelöst wird. Des Weiteren werden 26 % der Fläche des Great Letaba Einzugsgebietes intensiv agrarisch genutzt, wobei auf 9 % dieser Fläche Bewässerungsfeldwirtschaft durchgeführt wird (CSIR AND ARC, 2005).

Die Zweiteilung des Gebietes findet sich auch in der hohen räumlichen und zeitlichen Variabilität des **Niederschlags** wieder, welche zu einem

natürlichem Wasserstress führt. Die durchschnittliche jährliche Niederschlagssumme beträgt 760 mm (LYNCH, 2004), wobei in den Gebirgslagen bis zu 1751 mm und in den Tieflagen nur 419 mm (LYNCH, 2004) gemessen werden. Zur räumlichen Disparität, kommt eine hohe zeitliche Variabilität. Etwa 85 % des jährlichen Niederschlags fallen im Zeitraum von Oktober bis März. Aufgrund dieser hohen zeitlichen Variabilität des Niederschlags kann während der niederschlagsarmen Jahreszeit ein periodisches Trockenfallen der Flüsse beobachtet werden. Zum Ausgleich dieser jahreszeitlichen Schwankung befinden sich im Flusslauf große Stauanlagen und zahlreiche kleinere Speicherbecken, die zur Wassersicherung der Bedarfsgruppen (z.B. Landwirtschaft und Bevölkerung) dienen.

Für die Niederschlags-Abfluss Modellierung des Einzugsgebietes des Great Letaba wurden die **hydro-meteorologische Zeitreihen** (Niederschlag, Temperatur, relative Feuchte, Sonnenscheindauer, Windgeschwindigkeit sowie Abflussdaten) als Eingangsdatensätze verwendet. Des Weiteren standen für die Ableitung der Modellentitäten, die folgenden **GIS-Datensätze** zur Verfügung. Zur Bestimmung der topographischen Information, wie Höhenlage, Exposition und Hangneigung wurden die *Shuttle Radar Topography Mission (SRTM)*-Daten (U.S. GEOLOGICAL SURVEY EROS DATA CENTER AND NASA, 2007) verwendet. Digitale hydrogeologische Karten dienten der Ableitung des geologischen Untergrunds im Untersuchungsgebiet. Die Bodeninformationen wurden aus den *Soil and Terrain Database for Southern Africa (SOTERSAF)* (FAO, 2003) entnommen. Die *National Land Cover (NLC) South Africa 2000* (CSIR AND ARC, 2005) diente als Datengrundlage zur Gewinnung der Landbedeckungsinformationen.

E. Ergebnisse und Diskussion

1) Hydrologische Systemanalyse und Ableitung von hydrologisch ähnlich reagierenden Flächen

Um eine gute und realitätsnahe Niederschlags-Abfluss Modellierung durchführen zu können, müssen die Modelleingangsdaten, hydrometeorologische Zeitreihen sowie die GIS-Datensätze zur Ableitung der Modelleinheiten, auf Homogenität und Konsistenz (BEVEN, 2001B) untersucht werden. Die Auswertung der hydrometrischen Zeitreihen (Abfluss,

Niederschlag und Temperatur) sowie die einhergehende Systemanalyse im Untersuchungsgebiet des Great Letaba ergab, dass die Bewässerungsfeldwirtschaft und die in diesem Zusammenhang entstanden Stauanlagen einen entscheidenden Einfluss auf die Abflussdynamik im Einzugsgebiet haben. Dies musste bei der Niederschlag-Abfluss Modellierung berücksichtigt werden. So wurde in die Modellkalibrierung das Einzugsgebiet der großen Stauanlagen im Oberlauf des Great Letaba nicht miteinbezogen.

Bei der Überprüfung der GIS-Daten zeigte sich, dass die Rohdaten des digitalen Geländemodells, die SRTM-Daten, Lücken aufwiesen, welche gefüllt wurden. Aus den korrigierten SRTM-Daten wurden die Topographieparameter Exposition und Hangneigung sowie das Gewässernetz abgeleitet, die in der weiteren Folge zur Ableitung der Modelleinheiten (HRU) verwendet wurden. Die Modelleinheiten wurden durch Reklassifizierung, Überlagerung und Verschneidung der GIS-Datensätze Landbedeckung, Boden, Hangneigung, Exposition und Geologie abgeleitet (FLÜGEL, 1995; FLÜGEL, 1996). Abschließend erfolgte die Eliminierung der Splitterpolygone. Die so erzeugten HRUs stellen verteilte, hinsichtlich ihres hydrologischen Prozessgefüges homogene Einheiten dar. Im Ergebnis wurden 8051 HRUs als Modellentitäten für das hydrologische Modellsystem J2000 abgeleitet.

2) Niederschlags-Abfluss Modellierung im Einzugsgebiet des Great Letaba

Die Modellierung der **Niederschlags-Abfluss-Beziehung** erfolgte für den Zeitraum 1993 bis 1999, wobei der Zeitraum von Februar 1993 bis September 1997 zur Kalibrierung und der Zeitraum von Oktober 1997 bis Dezember 1999 zur Validierung herangezogen wurde.

Der visuelle Vergleich der simulierten Abflusskurve mit den beobachteten Abflusswerten zeigte, dass das Modellsystem in der Lage ist, die Abflussdynamik im Gebiet des Great Letaba abzubilden. Auch die Gütekriterien weisen (Kalibrierungszeitraum: NaS = 0,80; Validierungszeitraum NaS = 0,77), auf eine gute Modellsimulation hin.

Allerdings wurden auch Defizite in der Modellierung deutlich. Infolge der starken landwirtschaftlichen Nutzung im Untersuchungsgebiet und der damit einhergehenden Bewässerungswirtschaft wurde die Abflussmenge entlang des Flussverlaufes reduziert. Mit der aktuellen Version des Modells

J2000 konnten Bewässerungs- und Stauanlagen sowie deren Management nicht in der Modellierung berücksichtigt werden und demzufolge kam zur Überschätzung einiger Abflussereignisse von seitens des Modells (SCHEFFLER, BÄSE ET AL., 2007).

Darüber hinaus zeigte es sich, dass Abweichungen zwischen simuliertem und beobachtetem Abfluss unter anderem auf Ungenauigkeiten in den Eingangsdatensätzen zurückzuführen sind. So wies die Auswertung der Niederschlags- und Abflussdaten von Einzelereignissen darauf hin, dass die Dichte der vorhandenen Niederschlagsstationen nicht ausreicht, um die räumliche Niederschlagsverteilung detailliert wieder zu geben. Das führte dazu, dass lokale Einzelereignisse vom Modell nicht erfasst und somit unterschätzt wurden (SCHEFFLER, BÄSE ET AL., 2007).

Um die Kalibrierungsparameter des Modellsystems zu bestimmen, welche das Modellierungsergebnis beeinflussen, erfolgte die Durchführung einer **Sensitivitätsanalyse**. Hierfür wurden alle Kalibrierungsparameter des Modells um jeweils 10 % ihres ursprünglichen Wertes erhöht und reduziert. Die Parameteränderungen wurden an den Volumenänderungen der Abflussmenge bzw. des Bodenwassergehaltes am Gebietsauslass bestimmt. Die größten Volumensänderungen in Bezug auf die simulierte Abfluss- und Bodenwassermenge ergaben sich bei einer Modifikation des Kalibrierungsparameters *FC_{adaptation}*. Dieser Parameter steuert das Volumen des im Boden gespeicherten Wassers. Die durch die Modifikation dieses Parameters entstandene Variation des Bodenwassergehaltes muss bei der Entwicklung des Disaggregierungskonzeptes berücksichtigt werden, um die Abhängigkeit der entwickelten Methode von den voreingestellten Modellparameter zu bestimmen und bewerten zu können.

3) Evaluierung des makroskaligen Indexes des Bodenwassergehaltes und die Entwicklung des Disaggregierungskonzeptes

Um die Evaluierung des makroskaligen Index des Bodenwassergehaltes (SWI_{ERS}) durchführen zu können, wurde zunächst der **simulierte Index des Bodenwassergehaltes** (SWI_{HRU}) berechnet. Anschließend erfolgte die Anpassung der zeitlichen Auflösung, in dem der jeweils korrespondierte Tag zum SWI_{ERS} aus der SWI_{HRU} - Zeitreihe extrahiert wurde. Des Weiteren wurden, die in den drei Footprints liegenden HRUs (1733 HRUs (ID394) bis 3711 HRUs

(ID376)) extrahiert, wobei Wasserflächen in der weiteren Analyse nicht berücksichtigt wurden.

Im ersten Schritt der Evaluierung erfolgte die **Analyse und Bewertung der simulierten und fernerkundlichen Zeitreihen des Bodenwassergehaltes auf Ebene der Footprints** (50 km). Hierfür wurde der flächengewichteten Mittelwert der simulierten Bodenfeuchte (\overline{SWI}_{HRU}) für den jeweiligen Footprint berechnet und dem SWI_{ERS} gegenübergestellt. Des Weiteren erfolgte die Trennung der Zeitreihen \overline{SWI}_{HRU} und SWI_{ERS} in ihre Zeitreihenkomponenten. Diese Trennung wurde mit dem Zweck durchgeführt, einen Vergleich über die bisherige Entwicklung vorzunehmen und daraus Informationen über die zukünftige Entwicklung ableiten zu können (STATISTISCHES BUNDESAMT DEUTSCHLAND, 2007). Hierfür werden die Zeitreihen in die saisonale oder wiederkehrende Komponente und in die bereinigte, die Trendkomponente, welche die längerfristige Entwicklung der Zeitreihen aufzeigt, getrennt (ASSENMACHER, 1998).

Der visuelle Vergleich zeigte, dass beide Methoden, die hydrologische Modellierung sowie die Fernerkundung, sehr ähnliche Dynamiken in der Entwicklung der Bodenfeuchte aufzeigen. Dies konnte auch in der durchgeführten Regressionsanalyse zwischen den Zeitreihen der jeweiligen Komponente bestätigt werden. Für die Trendkomponente lagen die erreichten Bestimmtheitsmaße zwischen $R^2 = 0,79$ (ID376) bis $R^2 = 0,94$ (ID394). Die Saisonkomponente zeigte etwas geringere Werte mit Bestimmtheitsmaßen zwischen $R^2 = 0,74$ (ID376) und $R^2 = 0,85$ (ID393). Diese sehr große Gleichartigkeit der Zeitreihen \overline{SWI}_{HRU} und SWI_{ERS} , die auf so unterschiedlichen Konzepten aufbauen, wurde als sehr vielversprechend für die Entwicklung des Disaggregierungskonzeptes bewertet.

Des Weiteren wurde in der Analyse der Trennung der Zeitreihenkomponenten deutlich, dass starke Abweichungen in den absoluten Werten vorlagen, so dass auf weitergehende Vergleiche dieser verzichtet wurde. Diese Abweichungen sind auf Unterschiede in den beobachteten Volumina der Bodensäule der beiden Datensätze zurückzuführen. Die Grundlage für den SWI_{ERS} bilden die Messungen des Bodenwassergehaltes in der oberen Bodenschicht (<5 cm) (WAGNER, SCIPAL ET AL., 2003). Die Berechnung des sich daraus ergebenden Bodenwassergehaltes der Bodensäule erfolgt mittels eines Infiltrationsmodell, in dem angenommen wird, dass die im Oberboden

gemessene Feuchte über einen, für die jeweilige Landschaft, charakteristischen Zeitraum in den Boden infiltriert. Interaktionen mit umgebenden Bodenschichten, sowie lateraler Zu- und Abfluss und kapillarer Aufstieg werden hierbei vernachlässigt. Die simulierten Zeitreihen des Bodenwassergehaltes (SWI_{HRU}) werden allerdings unter Berücksichtigung dieser Prozesse modelliert.

Basierend auf den Ergebnissen der zuvor durchgeführten Untersuchung, erfolgte im zweiten Schritt die Beschreibung der Beziehung zwischen dem makroskaligen Fernerkundungsprodukt und den mesoskaligen simulierten Bodenwasserzeitreihen und damit einhergehend die **Entwicklung des Disaggregierungskonzeptes**. Hierfür wurde ein multiples Regressionsmodell angewendet, in dem der Bodenwasserindex der einzelnen HRUs (SWI_{HRU}) als Funktion von Niederschlag und des makroskaligen Bodenwasserindex (SWI_{ERS}) beschrieben wird.

Die im Disaggregierungsmodell integrierten Regressionskoeffizienten (Skalierungsparameter) lassen sich Funktion der Landschaftsparameter (Landbedeckung, Bodengruppe, Hangneigungs- und Expositions- sowie Geologiegruppe) darstellen, wobei deren Erklärungspotential für die entwickelte Disaggregierungsmethode untersucht wurde. Dies wurde unter Anwendung einer schrittweisen Verfahrensweise durchgeführt. Die Regressionsparameter wurden zunächst in Hinblick auf Landbedeckungs- und Bodenkombinationen gruppiert und anschließend die Disaggregierung unter Verwendung dieser Parameter durchgeführt. Das so erhaltene Ergebnis wurde mittels des Bestimmtheitsmaßes bewertet. Anschließend wurde jeweils ein weiterer Landschaftsparameter in der folgenden Reihenfolge zur Gruppierung der Regressionsparameter hinzugenommen: Hangneigung, Exposition und Geologie.

Im Ergebnis dieser Untersuchung zeigte sich, dass für nahezu alle möglichen Kombinationen von Landschaftsparametern (Landbedeckung, Bodengruppe, Hangneigungs- und Expositions- sowie Geologiegruppe) im Untersuchungsgebiet, eine Kombination von Landbedeckungs- und Bodengruppe ausreicht, die Skalierungsparameter so zu trennen, dass diese eine Disaggregierung der makroskaligen Bodenwasserindexes möglich machen. Die Ausnahme bilden landwirtschaftlich genutzte Flächen. Hier führt die

Hinzunahme von den topographischen Parametern Hangneigung und Exposition zu einer Verbesserung der Disaggregation.

Die daraus resultierenden Skalierungsparameter wurden auf den Modellierungszeitraum von Oktober 1997 bis September 1999 angewendet. Die disaggregierten Zeitreihen des Bodenwassergehaltes wurden mit den simulierten Zeitreihen verglichen. Das Ergebnis zeigt gute bis sehr gute Übereinstimmungen zwischen diesen Zeitreihen für die Landbedeckungsklassen Baumsavanne oder offenes Waldland (woodland), Buschsavanne (bushland), Grasland sowie für vegetationslose und spärlich bewachsene Flächen. Dies wird vor allem in den ermittelten Bestimmtheitsmaßen von $R^2 = 0,57$ bis $R^2 = 0,65$ (Mittelwert der Klassen) deutlich. Für städtische Flächen, Wälder sowie in Feuchtgebiete zeigten die disaggregierten Zeitreihen nur geringe Übereinstimmungen mit den simulierten Bodenwasserzeitreihen. Dies spiegelt sich in den geringen Bestimmtheitsmaßen von $R^2 = 0,27$ bis $R^2 = 0,5$ (Mittelwert der Klassen) wider. Diese Differenzen sind durch Einschränkungen der Mikrowellenfernerkundung erklärbar. Dicht bewachsene Vegetationsflächen, wie beispielsweise Wälder, können die vom Satelliten ausgesendete Strahlung nicht durchdringen. Dies bedeutet, dass der integrale Messwert des rückgestreuten Signals zu diesen Flächen keine Information über den Bodenwassergehalt liefert. Ähnliches gilt auch für Feuchtgebiete sowie städtische Flächen. Pflanzengesellschaften mit Bestandslücken, wie beispielsweise Baumsavanne, Buschsavanne, Grasland sowie vegetationslose und spärliche bewachsene Flächen erlauben hingegen, dass die von Satelliten ausgesandte Strahlung in den Boden eindringen kann. Das reflektierte Signal enthält somit Informationen zum Bodenwassergehalt unter diesen Vegetationstypen, was sich auch in den guten bis sehr guten Bestimmtheitsmaßen widerspiegelt.

Ein Grund für die eher befriedigenden Ergebnisse der angewandeten Methode im Fall der landwirtschaftlichen Flächen ist teilweise auf Defizite in der Modellstruktur des verwendeten hydrologischen Modells rückführbar. Es wird davon ausgegangen, dass infolge der Nichtberücksichtigung von stattfindenden Bewässerungsprozessen, der Bodenwassergehalt dieser Flächen von Modell unterschätzt wird. Hier zeigt es sich, dass der makroskalige Bodenwasserindex einen Zugewinn an Informationen liefert, denn Flächen unter Bewässerung werden im rückgestreuten Satellitensignal berücksichtigt.

Im Anschluss an diese Untersuchung musste die Frage geklärt werden, inwieweit die Skalierungsparameter von den Kalibrierungsparametern des Modells beeinflusst werden. Um hierüber Aussagen treffen zu können, wurden die erhalten simulierten Zeitreihen bei einer +/- 10-prozentigen Änderung des Kalibrierungsparameters *FCAdaptation* analysiert. Dieser wurde in der Sensitivitätsanalyse als sensitivster Parameter in Bezug auf das modellierte Bodenfeuchte- und Abflussvolumen bestimmt. Es zeigte sich, dass die Skalierungsparameter eine Abhängigkeit zu diesem Kalibrierungsparameter zeigen. Eine Erhöhung bzw. Reduzierung dieses Parameters führte zu einer maximalen Änderung der Skalierungsparameter von bis zu +/- 8.6 %. Ausnahmen bilden hierbei die landwirtschaftlichen Flächen bei denen Änderungen der Skalierungsparametern von fast +/- 50 % beobachtet wurden, sowie Kombinationen von Landschaftsparametern die eine Klassenstärke von unter 50 HRUs aufwiesen. Hier wird davon ausgegangen, dass aufgrund der geringen Klassendichte keine stabilen statistischen Verteilungen berechnet werden konnten.

Dieses Ergebnis ist unter Berücksichtigung der vorgenommen Annahmen sehr vielversprechend und es wird davon ausgegangen, dass die entwickelte Disaggregierungsmethode eine Anwendung des makroskaligen Bodenfeuchteproduktes auf einer kleineren räumlichen Ebene ermöglicht.

F. Schlussfolgerung und Ausblick

Das Ziel der vorliegenden Arbeit war die Entwicklung eines Disaggregierungskonzeptes zur skalenübergreifenden Verwendbarkeit des makroskaligen Indexes des Bodenwassergehaltes (SWI_{ERS}) für die mesoskalige hydrologische Modellierung. Für die Entwicklung dieser Methode wurden mittels hydrologischer Modellierung gewonnene Bodenfeuchtedaten eingesetzt. Hierfür kam das distributive, prozessorientierte Modellsystem J2000 zur Anwendung, welches als Teilergebnis der Niederschlags-Abfluss Modellierung die Bodenfeuchte liefert. Es zeigte sich, dass das Modellsystem in der Lage war, die hydrologischen Prozesse im Einzugsgebiet des Great Letaba wiederzugeben. Aufgetretene Unsicherheiten sind zum einen auf die räumlich lückenhaften Niederschlagsdaten und zum anderen auf die nicht quantifizierbare Wasserentnahme entlang des Flusslaufes zurückzuführen. Eine

Gegenüberstellung der simulierten und beobachteten Abflussdaten sowie der Vergleich der simulierten Evapotranspirationswerte mit Literaturwerten zeigte, dass die hydrologische Dynamik im Gebiet gut wiedergegeben wurde.

Die so erhaltenen mesoskaligen Zeitreihen des Bodenwassergehaltes wurden dem makroskaligen Bodenwasserindex gegenübergestellt und darauf aufbauend die Disaggregierungsmethode entwickelt. Die Ergebnisse der Anwendung der Disaggregierungsmethode zeigte für Gebiete der Baumsavanne, Buschsavanne, Grasland sowie für spärlich bewachsene und vegetationslose Flächen gute bis sehr gute Übereinstimmungen. Für Feuchtgebiete, städtische Regionen und Waldgebiete lieferte die Disaggregierungsmethode jedoch keine guten Ergebnisse. Dies ist vor allem auf Einschränkungen der Mikrowellenfernkundung in dicht bewachsenen Gebieten sowie auf versiegelten und Wasserflächen zurückzuführen. Unsicherheiten sind zudem auf die Definition des makroskaligen Bodenwasserindex zurückführbar. Der Bodenwasserindex wird als Trendindikator der Bodenfeuchte zwischen dem höchsten je gemessenen (Feldkapazität) und dem geringsten je gemessenen (Welkepunkt) Wert definiert (WAGNER, SCIPAL ET AL., 2003). Studien zeigen jedoch, dass es vor allem in semiariden Gebieten zu einer Überschreitung der Feldkapazität (KAMARA AND HAQUE, 1987; GABRIELLE AND BORIES, 1999) sowie eine Unterschreitung des Welkepunkts (KINCAID, GARDNER ET AL., 1964; ARCHER, HESS ET AL., 2002) kommen kann.

Zusammenfassend liefert die Studie trotz der obengenannten Probleme und Unsicherheiten wichtige Erkenntnisse für die Methodik von Disaggregationsverfahren und kann in dessen Folge zu einem verbesserten Verständnis der hydrologischen Prozesse und dessen Kontrollfaktoren führen. Die Arbeit liefert in den folgenden Punkten wichtige Beiträge zur Disaggregierung von makroskaligen Bodenfeuchteprodukten:

Welche Güte besitzt der makroskalige Index des Bodenwassergehaltes in Bezug auf die Verwendung in der mesoskaligen hydrologischen Modellierung?

Die Ergebnisse der vorliegenden Arbeit zeigen, dass beide Konzepte, die Abschätzung des Bodenwassergehaltes aus der hydrologischen Modellierung sowie die fernerkundlichen Daten, eine sehr große Übereinstimmung aufweisen. Aufgetretene Abweichungen in den absoluten Werten sind teilweise durch Differenzen in den beobachteten Bodenvolumina erklärbar, da der

makroskalige Bodenwasserindex auf den Messungen der oberen Bodenschicht basiert. Daher lässt sich schlussfolgern, dass der makroskalige Bodenwasserindex vor allem in Bezug auf die Dynamik des Bodenwasserhaushaltes eine potentielle Informationsquelle für die hydrologische Modellierung darstellt.

Welche Disaggregierungsmethode kann zur Beschreibung der Beziehung zwischen der makroskaligen und der mesoskaligen Verteilung des Bodenwassergehaltes angewandt werden?

Die vorliegende Arbeit bestätigt die Ergebnisse von WAGNER, PATHE ET AL. (SUBMITTED), in der der Zusammenhang der Bodenfeuchte zwischen zwei Skalenebenen über eine lineare Beziehung beschrieben wird. Allerdings muss der Niederschlag als treibende Größe der räumlichen Bodenfeuchteverteilung in das Disaggregierungsmodell integriert werden. Unter Anwendung eines multiplen linearen Regressionsmodells ist es möglich die Verteilung des Bodenwasserindex auf mesoskaliger Ebene als Funktion von Niederschlag und makroskaligen Bodenwasserindex zu beschreiben.

Welche Landschaftsparameter stellen die Kontrollfaktoren des makroskaligen Index des Bodenwassergehaltes dar und wie können diese zur Beschreibung der mesoskaligen Bodenwasserverteilung eingesetzt werden?

Die Ergebnisse dieser Studie zeigen, dass eine Gruppierung der Skalierungsparameter nach der vorherrschenden Landbedeckung- und Bodengruppe ausreicht, um Parameter zu finden, die in weiten Teilen eine sehr gute Disaggregierung ermöglichen. Eine Hinzunahme der Topographieparameter Exposition und Hangneigung zeigte nur für die landwirtschaftlichen Nutzflächen deutliche Verbesserungen.

Welcher Erfolg kann mit der entwickelten Disaggregierungsmethode erzielt werden?

Die entwickelte Disaggregierungsmethode wurde auf den Modellierungszeitraum 1997 bis 1999 am Beispiel des Einzugsgebietes des Great Letaba getestet. Die Ergebnisse zeigen, dass die Methode in der Lage ist, für bestimmte Landbedeckungsklassen gute bis sehr gute Disaggregierungsergebnisse zu erzielen. Zu diesen Landbedeckungsklassen

zählen Baumsavanne, Buschsavanne, Grasland und spärliche bzw. vegetationslose Flächen. Unbefriedigende Ergebnisse wurden für die Landbedeckungsklassen städtische Flächen, Feuchtgebiete sowie Wälder erreicht. Diese Ergebnisse sind vor allem auf Einschränkungen in der Mikrowellenfernerkundung zurückzuführen. Landwirtschaftliche Flächen wurden nur durchschnittlich disaggregiert. Dies ist vor allem durch Defizite des in der Studie verwendeten hydrologischen Modells erklärbar.

Ausgehend von den obengenannten Ergebnissen sind die folgenden Punkte für zukünftige Forschungen zu formulieren.

Erstens sollte eine Überprüfung der Disaggregierungsmethode am gleichen Untersuchungsgebiet für anderen Zeitraum und unter Verwendung anderer Datensätze durchgeführt werden. Hierbei sind zwei Forschungsrichtungen zu empfehlen: 1) die Abschätzung der Referenzdaten basierend auf anderen Eingangsdaten (z.B. Niederschlagsdaten) und 2) die Verwendung anderer Fernerkundungsdaten. Mögliche Satellitensysteme hierfür wären das *Advanced Scatterometer* (ASCAT) an Bord des MetOp-Satelliten, welcher 2006 gestartet wurde sowie der *Soil Moisture and Ocean Salinity* (SMOS), welche voraussichtlich 2008 gestartet wird (EUROPEAN SPACE AGENCY, 2007).

Zweitens ist die Überprüfung der Disaggregierungsmethode an einem anderen Untersuchungsgebiet notwendig. Hiermit könnte die Frage geklärt werden, ob die ermittelten primären Kontrollfaktoren, Landbedeckung und Bodengruppe, auch in anderen Gebieten das gefundene Erklärungspotential besitzen.

Drittens wird die Anwendung eines mesoskaligen hydrologischen Modells, in welchem die Bodensäule in horizontal aufeinanderfolgende Bodenschichten untergliedert wird, empfohlen. Hierbei sollte eine obere Bodenschicht von 5 cm implementiert werden. Dies ist korrespondierend zur gemessenen Bodenschicht des Satellitensensors. Die Abschätzung des Bodenwassergehaltes mittels hydrologischer Modellierung dieser Schicht ermöglicht den direkten Vergleich der real erfassten Bodenschicht mit Referenzdaten. Eine solche Untersuchung könnte des Weiteren zu einer Optimierung des abgeleiteten SWI_{ERS} führen.

Der vierte Forschungsbereich umfasst die Integration der disaggregierten Bodenwasserzeitreihen in die mesoskaligen hydrologische Modellierung. Die Studie zeigt, dass die fernerkundlichen Daten einen entscheidenden Informationsgewinn für die hydrologische Modellierung darstellen können. Speziell in Gebieten mit keiner oder unzureichender Infrastruktur können diese als Validierungsinstrument dienen, mit denen Modellergebnisse einer besseren Qualitätsanalyse unterzogen werden können. Mit der Entwicklung von geeigneten Methoden können die Information zum Bodenwasserhaushalt aus Satellitendaten einen wichtigen Beitrag in der Modellparametrisierung und Modellkalibrierung als auch deren Bewertung liefern und somit zu einer Verbesserung der simulierten Niederschlags-Abfluss Beziehung führen. Die Daten können damit, als hochwertiges Instrument zu einem verbesserten regionalen Wassermanagement führen.

CHAPTER 1

INTRODUCTION

Water management authorities observe, manage and regulate surface water and groundwater resources. In semi-arid areas, this task is particularly aggravated by imbalances between parts of regions with water surplus versus parts of regions with water deficiency, as well as by the highly temporal variability of year to year and seasonal rainfall. Due to these natural conditions, water authorities benefit from applying hydrological models to predict rainfall runoff relationships in any given region with some confidence. Unfortunately, most semi-arid catchments lack hydrologic data, a basic underlying requirement for hydrological model applications, so their use to gain understanding of hydrologic conditions is severely impacted. In addition, due to difficulties in obtaining sufficient and accurate data, the model calibration and -validation procedures are often technically unsatisfactory.

Researchers have examined the possibility of transferring knowledge from more robust models to other catchments having similar characteristics as the observed one. However, due to the individual characteristics of every catchment, the transfer of model results from one catchment to another often is difficult. In order to overcome this problem, other sources of information have to be used, and other validation tools have to be developed. Remote sensing techniques are a potentially useful tool because they operate over wide areas

with temporal resolution of several days, thereby overcoming the problem of having sparse *in-situ* measurements.

The key underlying basis of this study is the fact that coarsely resolved data contain valuable information to bridge this scale related gap between local *in-situ* measurements and the spatial data demands for hydrological model validation and parameterization.

An area of focus in current remote sensing research involves the quantification of soil water conditions from space. Researchers have focused on the derivation of the surface soil water content from microwave data, because the microwave signals are independent of cloud cover and can penetrate depending upon the wavelength into the soil column up to a few centimeters. One class of microwave instruments offering the possibility to derive soil water information involves the use of scatterometers. A global remotely sensed soil water dataset based on microwaves was derived from the European Remote Sensing Satellite (ERS) scatterometer. However, because the satellite wavelength can only penetrate the upper few centimeters of the soil column, the root zone soil water content has to be estimated. The dataset used in this study estimates the root zone soil water, based on the surface soil moisture information by applying a simple infiltration model. The comparison of this dataset with field measurements in the semi-arid Duero catchment in Spain revealed quite good agreement between the two different estimation methods. The drawback, however, of the remotely sensed dataset is its spatial resolution of 50 km. This is problematic for hydrological characterization purposes, because models generally require more highly resolved data.

Therefore, the overall goal of this study is the assessment and evaluation of the macro-scale root zone soil water estimates for purposes of regional hydrological modeling applications. The study will focus on the following: 1) evaluation of the influence of landscape parameters (soil, land cover, topography, and geology) between local and regional scales, and 2) the use of this information to develop a method to disaggregate the macro-scale root zone soil water estimate over a range of various scales. Due to the lack of sufficient field data available in this study, regional hydrological modeling is applied. This thereby provides the meso-scale soil water areal distribution. Because the spatial soil moisture distribution depends on landscape characteristics such as land cover, soil type, topography and geology, the distributed physically based

modeling system J2000 has been applied. The application of this model ensures a more process oriented representation of soil water distribution.

The meso-scale soil water time series were then used to disaggregate the macro-scale soil water estimates. A downscaling scheme based on a statistical method thereby was developed. The present work has the following contributions for the scientific community:

- The development of a downscaling method that translates large scale remote sensed data into meso-scale distributed soil moisture data.
- The determination of key landscape parameters that affect soil moisture distribution at the respective scale (macro-scale = 50 km, meso-scale = \varnothing 0.7 km²) and their incorporation into the downscaling method.
- The application and verification of the developed method on model dependencies.
- The evaluation of the applicability of the macro-scale remotely sensed data for regional hydrological modeling

The evaluation and use of low spatial resolution scatterometer data gives a better understanding of the weaknesses and strengths of both the hydrological model and the remotely sensed dataset results. This study makes an important contribution to the application of future remote sensing applications for hydrological purposes. For example, these techniques could be used with the data from the Advanced Scatterometer (ASCAT). This is a similar technical instrument to the ERS-scatterometer and is onboard the Meteorological Operational satellite (MetOp)-satellite, launched in October 2006.

The present study is divided in the following chapters: Chapter 2 gives an overview on the current state of the art in both remote sensing of soil moisture and in hydrological modeling. It outlines the technical challenges for the derivation of the soil water content from space and the different approaches to model soil moisture. Chapter 3 introduces the study area, the Great Letaba catchment in South Africa. It also gives an overview of the data used. Chapter 4 explains the methodological approach used in this study. Chapter 5 presents the results of the applied rainfall runoff modeling approach. This chapter describes the downscaling method that was derived and the results from

applying it to this case. In the last chapter, Chapter 6, the study is summarized and recommendations made for future research.

CHAPTER 2

RESEARCH REVIEW

For developing a downscaling method, reference data at a smaller scale are required. So far, soil moisture information can be obtained from three sources. First, ground based measurements provide soil moisture information as a point measurement but at spatial distributions that are limited. Second, remote sensing techniques offer the possibility to obtain soil moisture information over various space and time scales. However, only macro-scale remote sensing techniques succeed in derivation of soil moisture information for routine application. Third, rainfall runoff models estimate soil moisture as an element of their hydrological cycle whereas the accuracy of soil moisture generation depends on model structure and model input data. As a result of the locally restricted availability of ground based measurements and the inability of remote sensing to achieve meso-scale soil moisture, hydrological modeling offers the only possibility to obtain soil moisture information at a smaller scale over an area of 50 km.

To set the context for the study, the current state of the art in a few areas has to be reviewed. Given the importance of soil moisture in hydrological modeling, a discussion of soil moisture versus soil water will follow, which will be important for the study in order to derive the corresponding variables for downscaling. Secondly, the current state of the art in remotely sensed soil moisture retrieval will be presented. An important part is dedicated to the

fundamentals on microwave remote sensing to delineate limitations of this technique. Also the reference macro-scale soil water index will be discussed for understanding the methods for its retrieval and the evaluation of its boundaries. Thirdly, an introduction to hydrological models will be given. Here, different model types with a particular view on the soil water representation will be presented and an argument will be presented for using a particular model type in the study. The fourth point in this section deals with the existing downscaling and up scaling procedures. Based on this literature review, the appropriate downscaling method will be determined.

2.1 Soil Moisture in the Hydrological Cycle

The Earth's water is always in movement as pictured in the global water cycle shown in *Figure 2-1*. Only 0.001 % of the world total water reserves which accounts for 0.05 % of the fresh water reserves (DINGMAN, 2002:P.55) are stored as soil moisture. Yet, soil moisture still plays an important role in distributing the water.

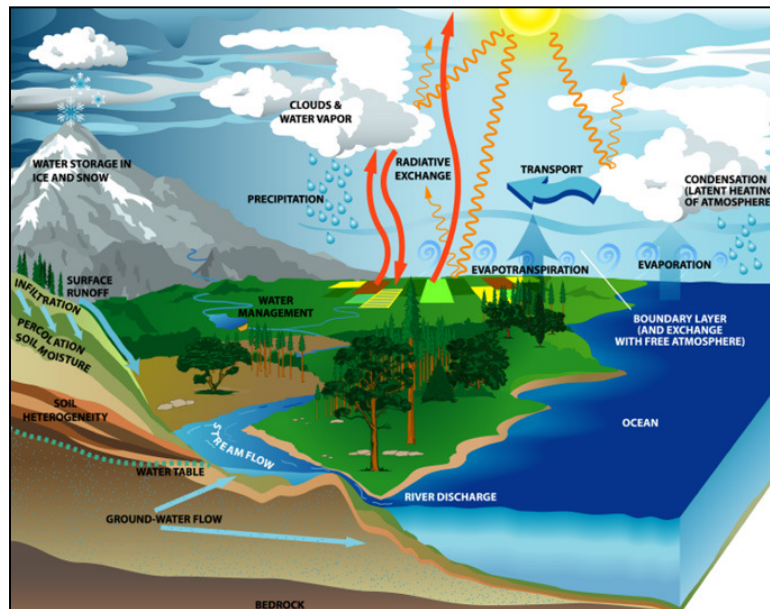


Figure 2-1: The Global Water Cycle (Source: ENTIN, HOUSER ET AL.(2007:P.9))

Especially, in the following fields and for the mentioned processes, soil moisture is an important factor:

1) in atmospheric circulation (WALKER AND HOUSER, 2004), as well as near-surface atmospheric dynamics, soil moisture influences energy and mass transfer across the landscape boundary (MOHANTY, SKAGGS ET AL., 2000; ARORA AND BOER, 2003; FINDELL AND ELTAHIR, 2003);

2) in water resources management, for instance in flood protection and drought monitoring (DE MICHELE AND SALVADORI, 2002; VERDIN AND KLAVER, 2002; WU, GELLER ET AL., 2002);

3) in agricultural management, by defining appropriate irrigation amounts and intervals (HANSON, ORLOFF ET AL., 2000);

4) in soil science it is a key parameter in determining potential land slides and erosion (E.G. FERNÁNDEZ, VEGA ET AL., 2004); and

5) in plant biology, soil moisture is the key factor for plant water stress (VEIHMEYER AND HENDRICKSON, 1950).

2.1.1 Definition of Soil Moisture

In the literature, “soil moisture” is also referred to as “soil water”. Also different science communities use the same word but with different meaning. For instance, soil science refers to soil moisture as the water content between field capacity and wilting point, whereas in remote sensing it is often the entire water in the soil column that is defined by the term soil moisture. In the following section the soil moisture term is evaluated according to soil science to obtain a better distinction between remotely sensed soil moisture and soil moisture as defined by soil science.

The soil medium can be described as a “three- phase system” (HILLEL, 1980:P.6) consisting of liquid, gaseous and solid phases. The solid phase is represented by the soil matter (the sum of the mineral matter and the organic matter) and amounts about to 50 % of the entire soil column (HILLEL, 1980:P.6). The other 50 %, the pore space, is subdivided into the gaseous- (the soil atmosphere) and the liquid phase (the soil water)-with variable proportions. The term soil water defines the total amount of water within the soil column (SCHEFFER AND SCHACHTSCHABEL, 2002). The soil water can be divided in its components shown in *Figure 2-2*.

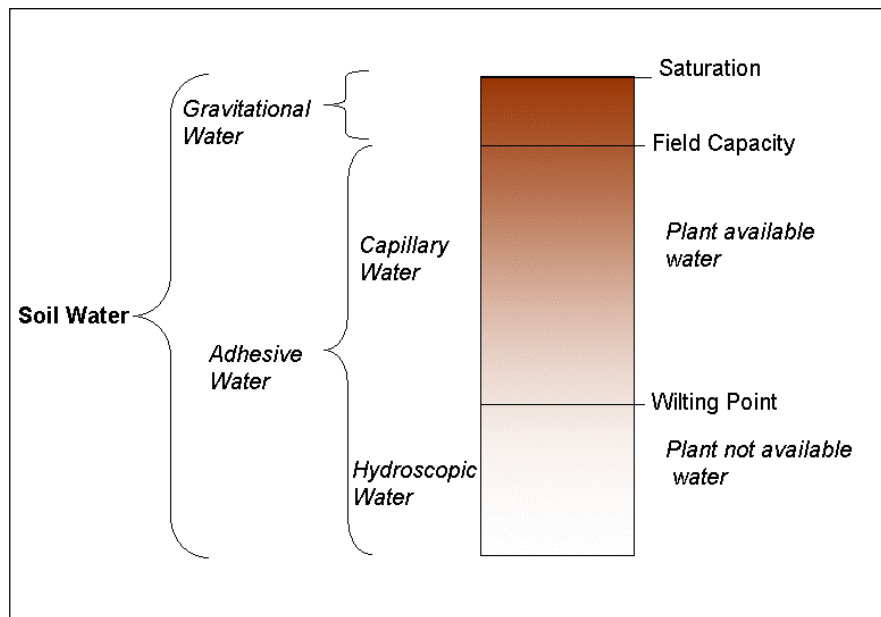


Figure 2-2: Soil Water and its Components (modified after Donahue, Miller et al (1983:p.171))

As shown in the figure above the soil water can be held due to different forces (FOTH, 1990:P.55FF).

The plant available water is held between a pressure range of $pF = 1.8$ and $pF = 4.2$ (SCHEFFER AND SCHACHTSCHABEL, 2002). This water runs in the capillary of the soil and is held due to the forces of cohesion. However, the forces of tension increase with decreasing pore diameter (SCHEFFER AND SCHACHTSCHABEL, 2002:P.210), so that at permanent wilting point this water moves so little that plants are not able to absorb that water. This wilting point marks the “largest water content of a soil at which indicator plants, growing in this soil, wilt and fail to recover when placed in a humid chamber” (TOLK, 2003:P.927). The wilting point corresponds to a water potential at $pF = 4.2$ (SCHEFFER AND SCHACHTSCHABEL, 2002). The soil water below wilting point, is retained by the strongest force, the molecular force of elements, is called the hydroscopic water and is immobile and therefore unavailable to plants. This water can only be removed through heating (FOTH, 1990:P.55).

The upper boundary of the capillary water reservoir is described by the field capacity. The water at field capacity is held against $pF = 1.8$ and this point describes the “greatest amount of water that a soil can hold, or store under conditions of complete wetting followed by free drainage” (DONAHUE, MILLER ET AL., 1983:P.170). Water held at pressure potential higher than $pF=1.8$ drains only by the forces of gravity. It is therefore free within the soil pores. This water

is called the gravitational water and stays up to one or two days in the soil. According to SCHEFFER AND SCHACHTSCHABEL (2002:P.209) soil moisture defines the water kept against the forces of gravity, which corresponds to the sum of hydroscopic and capillary water.

Based on the argumentation above, in the following section the term soil water content will refer to remotely sensed data and the term soil moisture to the soil science based method.

2.1.2 Calculation of Soil Moisture

Soil moisture can be expressed as the ratio of water to soil by mass or volume (HILLEL, 1980:P.58) and is calculated using the following equations:

1. Gravimetric water content

$$w = \frac{M_w}{M_s} \quad \text{Equation 2-1}$$

The gravimetric soil moisture content (w) is calculated using the mass of a soil package under wet conditions (M_w) in relation to the dry soil mass (M_s).

2. Volumetric soil moisture content

$$\theta = \frac{V_w}{V_t} \quad \text{Equation 2-2}$$

The volumetric soil moisture content (θ) defines the depth of water per unit depth of soil. It is calculated using the water volume (V_w) in relation to the total soil volume (V_t).

These two equations are related to each other through the bulk density ρ . The bulk density defines the ratio of the dried soil mass to the total soil volume. The following equation allows the transformation from gravimetric water (w) to volumetric water content (θ) (HILLEL, 1980:P.59).

$$\theta = w * \frac{\rho_{soil}}{\rho_{water}} \quad \text{Equation 2-3}$$

2.2 Estimation of the Soil Water Content and its Monitoring

The water content of the soil column can be determined using three different approaches: 1) *in-situ* measurements 2) remote sensing techniques and 3) application of a land surface model. In-situ measurements, such as gravimetric (HILLEL, 1980), nuclear (OBHODJAS, SUDAC ET AL., 2004), electromagnetic (SCHEFFER AND SCHACHTSCHABEL, 2002) or the tensiometer (DONAHUE, MILLER ET AL., 1983:P.180) techniques estimate the soil moisture content at a point scale. Instrumentation of large areas using in-situ measurements, however, is not possible due to high instrumentation costs and the need for good infrastructure. The determination of soil water content over large areas can only be achieved using remote sensing technique and/or land surface modeling. In the following sections both concepts will be explained and advantages and disadvantages will be specified.

2.2.1 Estimation of the Soil Water Content using Remote Sensing Techniques

In 1974, ULABY (1974: AS CITED IN DOBSON AND ULABY, 1998) published the results of his investigation on using microwave instruments for the retrieval of soil water. Since then the remote sensing community has been working on measuring soil water from space using different techniques (DOBSON AND ULABY, 1998:P. 407), with microwave applications yielding the most promising results. This is not only because the microwave signal is able to penetrate into the soil but also due to the fact that the signal does not suffer from cloud cover interference and is independent from solar illumination. It is therefore possible to take measurements at any time (LEWIS, 1998:P.616). The acquisition of soil water information using the microwave sensing technique is possible because the backscattering coefficient of the emitted radar signal depends, in addition to surface roughness and vegetation, on the moisture content (ULABY, DOBSON ET AL., 1981; WANG, QI ET AL., 2004) of the penetrated surface body. Based on these results, research has been carried out to identify how parameters such as the wavelength of the radar signal or incidence angle are affecting the measurement of the soil water content from space and to determine the most suitable sensor configuration for this task (DOBSON AND ULABY, 1998). The first part of this section introduces the possible microwave techniques to retrieve soil

water information and the second part will provide the fundamentals of active microwave remote sensing.

2.2.1.1 Microwave Techniques for Soil Water Retrieval

Microwave remote sensing encompasses both active and passive means to measure soil water information from space. Whereas passive microwave instruments measure the naturally emitted radiation of objects on earth, active microwave instruments send their own microwave radiation and measure a reflected signal. In the following section both techniques will be introduced and their advantages and disadvantages discussed.

Passive Techniques

Passive microwave instruments, such as the Special Sensor Microwave Imager (SSM/I), measure the emitted soil brightness temperature which depends on the soil water content (NJOKU AND ENTEKHABI, 1996:P.102). The emission of soil corresponds to a brightness variation of 90 Kelvin (NJOKU AND ENTEKHABI, 1996:P.102). However, the brightness temperature is also affected by soil surface roughness, vegetation cover, surface and surface heterogeneity, which are limiting factors for accurate soil water retrieval (HENDERSON AND LEWIS, 1998).

JACKSON, LE VINE ET AL. (1999) examined the data from the passive L-Band electronically scanned thinned array radiometer (ESTAR) over the area of the Southern Great Plain Experiment (SGP97) for one month. With their applied retrieval algorithm they have been able to measure soil moisture values with an error level of 3 %. BURKE AND SIMMONDS (2001) coupled a physically based soil water and energy balance model with a microwave emission model and retrieved soil moisture with an error of 3-4 %.

In comparison to active instruments, passive microwaves are less affected by soil roughness and vegetation COVER (ENGMAN AND CHAUHAN, 1995:P.194; NJOKU AND ENTEKHABI, 1996). On the other hand, measurements of passive instruments were not available operationally until 2003 with the launch of the Advance Microwave Scanning Radiometer (AMSR-E) (MORAN, MCELROY ET AL., 2006), which is limited the coverage and temporal resolution. Therefore, in recent years, more effort has been taken to retrieve soil water information from measurements taken by active microwave instruments.

Active Techniques

The most important active microwave instruments in the remote sensing domain are the Synthetic Aperture Radar (SAR), altimeter and the scatterometer (CRACKNELL AND HAYES, 2007:P.129). Whereas the altimeter is used for measuring and surveying the shape of the Earth, SAR as well the scatterometer are promising techniques in order to retrieve soil water content from space. The application of SAR-satellite systems offers the possibility to achieve soil moisture in a high spatial resolution of 10 m to 100 m (MORAN, MCELROY ET AL., 2006:P.92), which was intensively researched in various studies such as ZRIBI AND DECHAMBRE (2002) , MORAN, HYMER ET AL. (2002) and LE HEGARAT-MASCLE, ZRIBI ET AL (2002).

MORAN, HYMER ET AL. (2002), for instance, examined the possibility of ERS-SAR data for agricultural purposes at a test site in Arizona, USA. The authors found that the backscatter coefficient was sensitive to tillage, vegetation density as well as surface soil moisture. Using additional optical Landsat-Thematic Mapper (TM) data they were able to discriminate between vegetation and soil information in the backscattered signal.

Despite the promising results, the SAR-techniques for soil water retrieval still face unsolved problems, which is why, as of today no operational algorithm exists (MORAN, MCELROY ET AL., 2006). An evaluation of the capability of SAR-instruments for such purposes has been conducted by SATALINO, MATTIA ET AL. (2002) who examined SAR-data over bare soil fields. One major source of error in the soil water retrieval was found to lie in the SAR-configuration, which was also confirmed by (KERR, 2007). The SAR-design leads to speckle effects which make it difficult to determine soil water content. Also, SATALINO, MATTIA ET AL. (2002) found that variations in surface roughness are influencing the backscatter coefficient and therefore the soil water detection. They suggest retrieving not more than two soil moisture classes (dry and wet) by an application of ERS-SAR. LE HEGARAT- MASCLE, ZRIBI ET AL. (2002) tested their method over three different test sites for the development of an operational method to use SAR-data. They found changes in surface roughness due to agricultural activity, which resulted in a high soil water bias. Therefore, they suggest using retrieved soil water values as relative but not as absolute values. Another drawback of SAR-data is because of the trade off between high spatial resolution and high temporal resolution. Due to the high spatial

resolution, SAR-systems lag high temporal resolution (KERR, 2007) of approximately 30 days. This is a major disadvantage of soil water datasets based on SAR-data for water management purposes.

An instrument, which has a different technical design but is able to retrieve soil water, is the scatterometer (WAGNER, 1998; BLUMBERG, FREILIKHER ET AL., 2000). This instrument was originally built to measure wind speed and wind direction over oceans. However, its feasibility for soil water retrieval is questioned due to a number of influences on the signal, which will be introduced in the following section.

2.2.1.2 Fundamentals of Active Microwave Remote Sensing

The received microwave signal is influenced by various parameters, such as the dielectric constant of the reflecting material, vegetation structure and moisture content of the illuminated area. This section will give an overview of factors influencing the backscattered signal and the difficulty of retrieving soil water information from that signal.

The Dielectric Constant Dependence on Soil Water Content

A major factor influencing the backscatter signal is the dielectric constant (ULABY, DOBSON ET AL., 1981:P.92). The dielectric constant describes the electrical characteristics of different materials (KRAUS AND SCHNEIDER, 1988:P.174). Therefore it is necessary to understand the dielectric behaviors of soil materials.

This dielectric behavior of soils is very complex (DOBSON, ULABY ET AL., 1985:P.35) because soil consists of the three components mentioned before: soil particles, water and air (SCHEFFER AND SCHACHTSCHABEL, 2002). The dielectric constant therefore is influenced by “soil bulk density (compaction), soil composition (particle size distribution and mineralogy), the volume fraction of soil water components, the salinity of the soil solution, and temperature” (DOBSON, ULABY ET AL., 1985:P.35). ULABY, DUBOIS ET AL. (1996) found that the dependency of the dielectric constant on moisture actually increases with increasing moisture content. They found that for dry soils it is predominately the soil type, especially the bulk density that determines the dielectric constant. When the moisture content increases, the response to soil type becomes weaker than the response to moisture content. The observed differences of the dielectric

constant between dry and wet soil conditions correspond to a backscattering range of about six to eight decibel (dB) (DOBSON AND ULABY, 1998:P.416). Additionally, it was shown that the dielectric constant is influenced by temperature (DOBSON AND ULABY, 1998:P.412). In the narrow temperature range between 0° C and the soil starting to freeze, the dielectric constant shows a stronger relationship to temperature than to soil moisture.

Penetration Depth

Microwave signals are able to penetrate through vegetation and the upper soil layer (CAMPBELL, 2007:P.213). The penetration depth describes “the thickness of the top surface layer of the soil medium governing the backscatter observed by a radar system” (ULABY, DUBOIS ET AL., 1996:P.71). This depth, however, depends on surface roughness, incidence angle, moisture content as well as wavelength (ULABY, DUBOIS ET AL., 1996; CAMPBELL, 2007). An increasing moisture content decreases the penetration depth tremendously (ULABY, DUBOIS ET AL., 1996). An example is given in ULABY, DUBOIS ET AL. (1996:P.69), who investigated the L-Band penetration depth. With an increase of soil moisture content from 1 to 40 % the signal depth dampens from 1 m down to 0.06 m.

The penetration depth increases additionally with a decrease in frequency, as stated in WEGMÜLLER, MÄTZLER ET AL. (1989). For C-Band, the estimated penetration depth ranges between 0.5-2 cm (SCHMUGGE, 1983: AS CITED IN WAGNER, LEMOINE ET AL., 1999B), whereas in WAGNER, SCIPAL ET AL. (2003) a penetration depth for the C-Band scatterometer of 5 cm is found. The L-Band signal can penetrate about 4 to 5 cm (KERR, 2007) into the soil.

The Backscatter Coefficient from Bare Soil Surfaces

The intensity of the backscattering signal is influenced by surface roughness, vegetation structure and density as well as technical parameters such as incidence angle and frequency (DOBSON AND ULABY, 1998). The most important parameter for describing the backscattering from bare soil surfaces is the surface roughness. The surface roughness determines the direction in which the transmitted radar signal will be reflected. In the case of a slight roughness, one part of the signal will be reflected back to the antenna and the other part will be reflected away from it (WAGNER, 1998:P.23). With an increasing surface

roughness the diffuse scattered portion of the signal increases which also increases the portion scattered back to the sensor (WAGNER, 1998:P.23).

Several models have been developed in order to describe the surface roughness. Every model is based on various assumptions and, therefore can only be applied under certain conditions. For instance, the small perturbation method shows good model results for horizontal-horizontal (HH)-polarized signals with an incidence angle up to 60° (DOBSON AND ULABY, 1998:P.418) but overestimates when applied to vertical-vertical (VV) polarization. The best model results, according to DOBSON AND ULABY (1998), have been achieved with the semi-empirical model.

The Backscatter Coefficient from Vegetated Surfaces

In the case of vegetated surfaces the backscattering signal is influenced by the backscattering contribution of bare soil, the direct backscattering of the vegetated surfaces, the two-way attenuation of the vegetation, and the mixed backscattering which includes vegetation elements as well as ground surface elements (DOBSON AND ULABY, 1998:P.426). Additionally, the structure of vegetation, in particular of branches and leaves controls the intensity of the backscattered signal. Also, similar to the soil backscattering the backscatter coefficient increases with an increasing vegetation water content (HENDERSON AND LEWIS, 1998; NJOKU AND CHAN, 2005).

In terms of soil moisture retrieval, the interactions between the signal and the vegetation are a problem. Therefore, research has been carried out to determine the extent to which the microwave signal is influenced by vegetation effects (SCHMULLIUS AND FURRER (1992), LEE, BURKE ET AL. (2002) AND NJOKU AND CHAN (2005)). The possibility of microwave signals transmitting through vegetation increases with frequency, incidence angle and less biomass density (ENGMAN AND CHAUHAN, 1995:P.194; DOBSON AND ULABY, 1998:P.426). Studies have revealed that the L-Band is the most unaffected wavelength in terms of its vegetation influence for soil moisture retrieval (KERR, 2007). The retrieval of soil moisture using C-Band is possible but the vegetation effects should not be ignored (TACONET, VIDAL-MADJAR ET AL., 1996; KERR, 2007). However, using L-Band for soil moisture retrieval at a similar spatial resolution as C-Band requires huge technical effort (KERR, 2007).

Studies, especially of measurements of C-Band scatterometers have been conducted on how to reduce the vegetation influence within the C-Band and to select the soil water information within the mixed signal. Its feasibility for soil water retrieval depends on the scatterometers technical design. Scatterometers use different incidence angles and, as stated in WOODHOUSE AND HOEKMAN (2000), the vegetation influence is highest at larger angles. WOODHOUSE AND HOEKMAN (2000) have chosen four test sites in Spain (Ciudad Real, Murcia, Zaragoza and San Sebastian) to retrieve soil water information using data from the scatterometer onboard of ERS-1 captured between 1992 and 1995. However, the research community has been and is skeptical of the capability of the scatterometer to measure soil water (KERR, 2007). FRISON, MOUGIN ET AL. (2000) compared the ERS-windscatterometer and Special Sensor Microwave/Imager (SSM/I) data for vegetation monitoring over a Sahelian region in Mali. The authors examined the backscatter behavior at an incidence angle of 45° and found a relationship between the backscatter signal and the herbaceous biomass. In the previous study, FRISON AND MOUGIN (1996) found agreements between the wind-scatterometer data and vegetation types, especially in regions with dense vegetation, such as the tropics. Also, SCHMULLIUS AND FURRER (1992) analyzed the three C-Band polarizations (HH, HV and VV) for their feasibility of soil water retrieval at an incidence angle of 23°. They found a high influence of vegetation on the C-Band but there was also a dependence on the polarization. The result was that HH-polarization is more significant for soil water changes, whereas the HV- and VV- polarizations react more to the surface wetness of the vegetation cover.

Despite the skepticism and disadvantages, the first global soil water product has been derived from the ERS-scatterometer (SCIPAL, 2002). The retrieval of soil water from the scatterometer will be explained in the following section.

2.2.1.3 The ERS Macro-Scale Soil Water Estimates

This section will provide an overview on the investigated macro-scale soil water product derived from the ERS-scatterometer. The ERS-scatterometer was onboard of the ERS-1 and 2 satellites, both having the exact same technical design. The ERS-1 satellite was launched in 1991 and was followed by the

launch of ERS-2 in 1995. As of today, ERS-2 is still in operation (EUROPEAN SPACE AGENCY, 2008).

The ERS-scatterometer features three antennas which are looking in different directions: one antenna faces forward, one antenna backwards and the third antenna looks vertical downwards (WOODHOUSE AND HOEKMAN, 2000). The incidence angle of every antenna is variable. The incidence angle ranges from 18° to 47° for the downward looking antenna, and from 25° to 59° for the backwards and forwards looking antennae (WAGNER, LEMOINE ET AL., 1999A:P.938) The ERS-windscatterometer works at C-Band Frequency (5.3 GHz) with a vertical (VV) polarization. The beam of each of the antennas scans a 500 km strip on the Earth's surface crossways to the flight track. The temporal resolution of the microwave instrument is three to four days with a spatial resolution of approximately 50 km (FRISON, MOUGIN ET AL., 2000:P.1794).

Revealing the Vegetation Cover Effects from the Scatterometer Data

As discussed in *Section 2.2.1.2*, the surface backscattering is very complex and one of the most influential parameters is vegetation cover. Therefore, the vegetation has to be extracted in order to extract soil moisture from the backscattering signal.

As shown in ULABY, BATLIVALA ET AL. (1978), the intensity of the vegetation influence increases with the incidence angle due to an increasing volume scattering of the vegetation cover. However, the vegetation contribution to the backscattered signal stays similar over larger ranges of incidence angles (WAGNER, LEMOINE ET AL., 1999A:P.940).

In order to detect the vegetation influence on the ERS-scatterometer data WAGNER, LEMOINE ET AL.(1999A) analyzed the backscattered signal with Normalized Difference Vegetation Index (NDVI) scenes from Advanced Very High Resolution Radiometer (AVHRR) images over the Iberian Peninsula. One of their findings was that the backscattering coefficient showed a higher temporal variability than the NDVI, whereas the NDVI has been seen as a greenness indicator rather than a wetness parameter for vegetation canopy (WAGNER, LEMOINE ET AL., 1999A:P.940). The authors followed the concept of finding an incidence angle at which the vegetation contribution to the backscatter signal is mainly constant and backscatter changes are affected by changes of surface soil water. The authors succeed and found the lowest

vegetation influence under wet soil conditions at an incidence angle of 40° and for dry soil conditions at an incidence angle of 25° (WAGNER, LEMOINE ET AL., 1999A:P.941-942).

These two incidence angles were later used for a determination of a seasonal vegetation signal, which then was eliminated from the overall backscattered signal. For dry soil moisture conditions, the vegetated portion on the backscattered signal was determined to range from 1.5 to 2.5 dB depending on the status of vegetation growth (WAGNER, 1998:P.53). For wet soil moisture conditions the vegetation influence was very low. Through the determination of the relationship of the backscatter coefficient between different incidence angles, the backscatter coefficient at an incidence angle 40° is calculated. In their analyses WAGNER, LEMOINE ET AL. (1999A) also revealed that temporal changes in the backscatter signal at an average incidence angle of 40° are caused by the moisture status of the surface layer rather than by vegetation.

The Retrieval of the Surface Soil Water Content

The determination of the surface soil water content (m_s) is based on a change detection approach (WAGNER, 1998; SCIPAL, WAGNER ET AL., 2002). The developed algorithm (WAGNER, LEMOINE ET AL., 1999A; WAGNER, LEMOINE ET AL., 1999B; WAGNER, NOLL ET AL., 1999) relates the actual measured value $\sigma^0(40,t)$ to the lowest $\sigma_{dry}^0(40,t)$ and highest values $\sigma_{wet}^0(40,t)$ of the respective time series. The soil water content m_s is then determined according to the following equation (WAGNER, LEMOINE ET AL., 1999B:P.195)

$$m_s = \frac{\sigma^0(40,t) - \sigma_{dry}^0(40,t)}{\sigma_{wet}^0(40,t) - \sigma_{dry}^0(40,t)} \quad \text{Equation 2-4}$$

This equation can only be applied under the condition of a non frozen and non snow covered soil. The achieved surface water values (m_s) represent a relative topsoil soil water value (<5 cm) (WAGNER, SCIPAL ET AL., 2003) of a bare soil or only sparse covered part of a pixel such as agricultural land or grassland. The two backscatter parameters, $\sigma_{dry}^0(40,t)$ and $\sigma_{wet}^0(40,t)$ are characterizing dry and wet soil water conditions. These two boundary values are assumed to characterize wilting point ($\sigma_{dry}^0(40,t)$) and field capacity ($\sigma_{wet}^0(40,t)$). This

assumption can be made because of the processed time period of 1992 to 2000, in which it is most likely that measurements under dry and wet soil water conditions were taken.

This algorithm can also not be applied in desert and wetland areas. In order to solve the problem, a specific correction method has been applied for arid regions but not for wetlands (SCIPAL, 2002). In wetland areas the derived soil water content is constantly underestimated.

The Calculation of the Root Zone Soil Water Content

The scatterometer can only measure the surface soil water content. To retrieve the profile soil water content, a simple two layer soil infiltration model has been used (WAGNER, LEMOINE ET AL., 1999B:P.196). This model divides the soil profile into the top layer, representing the layer scanned by the satellite and the bottom layer, the “reservoir” (WAGNER, LEMOINE ET AL., 1999B:P.196). The authors assume that the reservoir is only influenced by the water flow of the top layer and shows no interactions with the surrounding environment (WAGNER, 1998). Processes such as transpiration, groundwater recharge, lateral flow as well as upward fluxes are neglected. The developed model describes the soil water content of the bottom layer by the past events in the upper layer whereas the most recent events have a higher priority. The consequential trend indicator ERS-Soil Water Index (SWI_{ERS}) is calculated as follows (WAGNER, LEMOINE ET AL., 1999B:P.197):

$$SWI_{ERS}(t) = \frac{\sum_i m_s(t_i) e^{-\frac{t-t_i}{T_L}}}{\sum_i e^{-\frac{t-t_i}{T_L}}} \quad \text{for } t_i \leq t \quad \text{Equation 2-5}$$

m_s = saturation of the surface layer

T_L = characteristic time length

t = time

The crucial parameter in this equation is the determination of the characteristic time length T_L , which is connected to the hydraulic conductivity

of the soil. According to WAGNER (1998:P.72) the parameter T_L increases with an increasing length of the reservoir, and reduces with a decreasing soil hydraulic conductivity. The characteristic time length has been determined according to different climatic conditions. In tropical climates T_L amounts ten days, whereas in Mediterranean and humid continental climates T_L equals twenty days (WAGNER, 1998).

The calculation of the SWI_{ERS} is restricted to the availability of an adequate amount of surface soil water measurements (m_s). For the case that T_L equals twenty, the necessary amount therefore, is at least one measurement of the surface soil water in the time frame of twenty days and at least three measurements within a timeframe of 100 days (WAGNER, 1998:P.72).

In conclusion, the calculation of the SWI_{ERS} is a low pass filter which reduces the influence of higher frequency (RICHARDS AND XIUPING, 2006:P. 115-118). Therefore, the image information or in this case the root zone soil water content is smoother than the surface soil water time series.

Validation of the Macro-Scale Soil Water Estimates

The validation of scatterometer derived soil moisture was carried out through several studies at local and large scale. At the local scale, SCIPAL (2002) compared over 45.000 soil moisture measurements from 372 stations worldwide were compared to the remotely sensed datasets. The results showed an average error range of 5-6 vol. % (SCIPAL, 2002:P.114). In a more detailed analysis the remotely sensed data were evaluated with soil moisture field measurements from the REMEDHUS network (CEBALLOS, MARTÍNEZ-FERNÁNDEZ ET AL., 2002; CEBALLOS, SCIPAL ET AL., 2005). All stations of the REMEDHUS network are situated within one scatterometer pixel. For comparison all in-situ measurements were averaged and afterwards a regression analysis was carried out. The coefficient of determination amounted to 0.74 with a mean square error of 2.2 vol. % (CEBALLOS, SCIPAL ET AL., 2005). The validation at global scale was accomplished by WAGNER, SCIPAL ET AL. (2003). The remotely sensed data was compared to precipitation data and global modeled soil moisture. The result showed a reasonable agreement between the two datasets for tropical and temperate climates whereas less satisfactory results were observed over steppe and desert climates.

FONTAINE, LOUVET ET AL. (2007) applied the SWI_{ERS} to derive fluctuations in rainfall, soil moisture and heat fluxes in West Africa. The study showed that the pattern in annual, as well as inter seasonal, cycles in soil water content could be explained by the pattern in rainfall.

The results of the mentioned studies showed that the SWI_{ERS} could provide interesting information on the root zone soil water content that was not available previously. It could, therefore, be a valuable tool for hydrological modeling.

2.2.2 Soil Moisture Generation in Land Surface Modeling

Land surface models help to understand and describe the natural system processes. The models also help to study interactions between components of the hydrological cycle. Since 1966, when the first watershed model, the Stanford Watershed Model, was developed by Crawford and Linsley (SINGH, 1995) the number of hydrological models has been increased. Land surface models have been developed for different purposes, input data, and scales. This section analyses 1) the current models available and 2) evaluates the available approaches in order to model soil moisture generation.

2.2.2.1 Classification of Models

One requirement of the study is to develop a downscaling scheme taking all landscape parameters into account. Therefore, the hydrological model used has to simulate soil moisture using these landscape characteristics. The available model types will be introduced in the following section and evaluated according to the purpose of the study in order to select the appropriate model.

According to SINGH (1995:P.6) hydrological models can be distinguished according to their 1) process description, 2) their time and space scale and 3) their representation of spatial variability.

Firstly, the two classic categories of hydrological models are deterministic and stochastic. Deterministic models can be further distinguished depending on whether the description is empirical, conceptual or more physically based (REFSGAARD, 1996:P.28): Empirical models are based on a mathematical description of the relationship between input and output (REFSGAARD, 1996:P.28). Conceptual models use semi-empirically equations based on the underlying physical processes (REFSGAARD, 1996:P.29). These

models are characterized by two points: first, they include feedbacks between the model components and second, this model type includes a threshold which activates or inactivates model components (DOOGE AND O' KANE, 2003:P.2). The last group, physically based models, describe hydrological processes using “governing continuum (partial differential) equations” (REFSGAARD, 1996:P.30). Stochastic models, however, are based on long term time series analysis for which the relationship between input and output is determined (REFSGAARD, 1996:P.30). Classical statistical techniques for a determination of that relationship can be the Monte Carlo Method (REFSGAARD, 1996:P.31) or autoregressive moving average (YEVJEVIEH, 1987).

Secondly, models can be distinguished according to the represented spatial scale. There are three scales according to SINGH (1995:P.9): small (>100 km²), medium-sized (100 to 1000 km²) and large watershed (>1000 km²) models.

Thirdly, hydrological models can be classified according to their representation of spatial variability. A distinction can be made between the lumped and distributed modeling approach. Lumped models do not account for spatial variations, the catchment is considered to be a single model entity and therefore only a single model parameter set is applied representing the entire catchment (BEVEN, 2001B:P.18). The processes are mostly described using simplified hydraulic laws or are based on empirical-algebraic equations (SINGH, 1995:P.6). The tank model (SUGAWARA, 1995) and the Stanford model (CRAWFORD AND LINSLEY, 1966: AS CITED IN REFSGAARD, 1996) are examples of the lumped modeling approaches. The distributed modeling approach, however, accounts for spatial variability in the process description, input data and watershed characteristics (SINGH, 1995:P.8). Distributed models make hydrological predictions “by discretizing the catchment into a large number of elements or grid squares and solving the equations for the state variable associating with every element grid square” (BEVEN, 2001B:P.18). In reality, distributed models still often follow the lumped modeling concept but on scale of the model entities (BEVEN, 2001B). Examples for distributed models are Precipitation-Runoff-Modelling System (PRMS) (LEAVESLEY, LICHTY ET AL., 1983), J2000 (KRAUSE, 2001) and TOPMODEL (BEVEN AND KIRKBY, 1979).

Based on this summary of models, the distributed process oriented models would be more suitable to account for a spatially explicit representation

of natural processes and landscape characterization and should therefore be applied in the present study.

2.2.2.2 Determination of Soil Moisture Using Land Surface Modeling

As part of the hydrologic cycle, hydrological models take care of soil moisture accounting. However, hydrological models are developed to analyze a specific problem, which is reflected in its model structure (SINGH, 1995). In the following section the four existing concepts to describe soil moisture generation will be explained and later evaluated for their applicability in the study.

Soil Storage as Single Storage

The single storage, known as the single bucket method, is the simplest approach for modeling soil moisture generation (IRANNEJAD AND SHAO, 2002:P.179). According to IRANNEJAD AND SHAO (2002:179) the soil moisture storage in the single bucket is defined by the upper and lower boundary. The upper boundary, saturation, is set to field capacity and the lower boundary is the wilting point. Internal flows within the bucket are neglected.

MANABE (1969) introduced this approach to atmospheric science by integrating surface hydrology into a general circulation model (GCM). He introduced a single soil layer with 1 m depth in which vegetation roots can be included, for representing interactions between land surface and soil. Instead of using the field capacity as an upper boundary, he used the fixed value of 15 cm water in the soil column for generating runoff. Another example of a bucket model is given in GUSWA, CELIA ET AL. (2002). The model uses a volume balance equation over the plant root zone. In this example the bucket loses water through evapotranspiration and leakage as a function of the soil saturation.

The simple bucket soil approach is often applied in large scale models, such as the Water Balance Model (WBM) by VÖRÖSMATRY, MOORE ET AL. (1989).

The Force-Storage Model (Based on Irannejad and Shao, 2002: Section 5.3.2)

The force-storage model improves upon of the single bucket model by implementing a thin top-layer. This approach to model soil water was introduced by DEARDORFF (1977: AS CITED IN IRANNEJAD AND SHAO, 2002). According to IRANNEJAD AND SHAO (2002) the top layer is driven by the forces of the boundary layer between the atmosphere and land surface. Upward fluxes

from the deeper soil layer to the surface layer are taken into account through moisture diffusion from the lower soil layer (IRANNEJAD AND SHAO, 2002:181-182). DEARDORFF (1977: AS CITED IN IRANNEJAD AND SHAO, 2002) also introduced a vegetation layer on top of the soil layers in order to account for interception and evaporation for the vegetated surface.

Vertical Distinction of the Soil Column into Two or More Soil Layers

The application of a vertically layered distinction of the soil column is one of the most common concepts in hydrology. The soil column can be divided into two or more layers. There are two different concepts in determining water flow between the different soil layers. The first concept handles the different soil layers as buckets in which the soil water cascades into the lower zones when field capacity in the upper zones is reached (IRANNEJAD AND SHAO, 2002:P.180). Modifications of this approach can be found in the PRMS-Model (LEAVESLEY, LICHTY ET AL., 1983).

The second concept, a more advanced way to model soil moisture transfer between the soil layers, is the application of numerical solutions of the Richards Equation (GUSWA, CELIA ET AL., 2002; IRANNEJAD AND SHAO, 2002). The Richards Equation describes the vertical water movement in unsaturated soil in a three dimensional system (DINGMAN, 2002:P.249). It is a non-linear differential equation with specific boundaries and conditions (SUMMER, 2000:P.A-98). The equation can only be solved under very limited conditions and often no solution is found (SUMMER, 2000:P.A-98). Therefore, the equation had to be simplified. Attempts have been made by PHILIP (1957; 1969: BOTH AS CITED IN DINGMAN, 2002:P. 250-251) and SWARTZENDRUBER (1997: AS CITED IN DINGMAN, 2002:P. 250-251).

The advantage of applying the vertical distinction of the soil column is its improved simulation of the interactions between atmosphere and land surface and therefore a better representation of soil humidity, temperature and evapotranspiration (LEAVESLEY, LICHTY ET AL., 1983; GUSWA, CELIA ET AL., 2002; IRANNEJAD AND SHAO, 2002). It also allows the drying of the upper soil layer and therefore leads to a reduction of evaporation (SNELGROVE, 2002).

Distinction of the Soil Layer into the Specific Pore Storages

The fourth concept divides the soil column into specific pore storages (KRAUSE, 2001) to account for different runoff processes (BEVEN AND KIRKBY, 1979).

BEVEN AND KIRKBY (1979:P.44-45) analyzed four different ways runoff can occur: (1) overland flow due to rainfall rate exceeding the infiltration rate over the entire catchment (Horton overland flow) (HORTON, 1933; AS CITED IN BEVEN AND KIRKBY, 1979); (2) the same situation as (1) but only on parts of the catchment; (3) overland flow due to soil saturation (saturation overland flow) (DUNNE AND BLACK, 1970; AS CITED IN BEVEN AND KIRKBY, 1979); and (4) subsurface flow in saturated and unsaturated soil. BEVEN AND KIRKBY (1979), therefore divided the soil column into the interception depression storage, the near-surface infiltration storage and the subsurface soil water storage. The concept of BEVEN AND KIRKBY (1979) was also applied in the WaSiM-Model by SCHULLA AND JASPER (1998). KRAUSE (2001) took this concept and developed the soil module for the J2000 model.

In summary, the different concepts of soil water generation are evaluated for their applicability within the project. The first two concepts neglect processes such as up- and downward soil water movement within the soil column, which are important for soil water generation (SCHEFFER AND SCHACHTSCHABEL, 2002). The third concept, the distinction of the soil column into vertical layers, would be similar to the two layered model of the SWIERS. The fourth concept, however, takes physical soil parameters into consideration and represents, therefore, a realistic generation of soil moisture, which is an important requirement of the study. Therefore, a model, described in *Section 3.2.1*, has been applied that implements the fourth concept.

2.3 On Temporal and Spatial Scaling of Soil Moisture

As a “hierarchical organization of the geographical world” (MARCEAU, 1999:P.2) the scale concept has been widely accepted and analyzed amongst scientists of different fields such as remote sensing (QUATTROCHI AND GOODCHILD, 1997) and hydrology (BLÖSCHL, 1996). The scale concept was created to overcome the problem that results made at one scale cannot be

transferred to another scale (BLÖSCHL, 1996). Scale defines „the spatial dimensions at which entities, patterns, and processes can be observed and characterized“ (MARCEAU, 1999:P.3). BLÖSCHL (1996) went one step further and differentiated between the scale of natural processes (BLÖSCHL, 1996:P.73), the scale of measurements, which are constrained by the measurement technique applied and the modeling scale. The process scales is the only scale describing natural events, whereas the measurement and modeling scale are referring to artificial scales.

BLÖSCHL (1996:P.73) defines the measurement scale with a triplet consisting of extent, spacing and support. According to the same author, extent describes the spatial coverage of the dataset, spacing determines the space between two measurement points and the support refers to the “integration volume (time) of one sample” (BLÖSCHL, 1996:P.73). This triplet can also be applied to the modeling scale (WESTERN AND BLÖSCHL, 1999).

In order to apply the scale triplet, the different scales have to be defined first. The following table describes the scales ranges in hydrology according to BECKER (1992) in which the scale definitions after BLÖSCHL (1996) have been added.

Table 2-1: Scale Ranges in hydrology (modified after Becker (1992:p. 19) and Blöschl (1996))

MAIN SCALE	TRANSITION SCALE	CHARACTERISTIC		SCALE ACCORDING TO BLÖSCHL (1996)
		LENGTH	AREA	
Macro-	-	> 100 km	> 10 ⁴ km ²	Regional
	Lower Macro-scale	30 to 100 km	10 ³ to 10 ⁴ km ²	
Meso-	Upper Meso-scale	10 to 30 km	10 ² to 10 ³ km ²	Catchment
	-	1 to 10 km	1 to 10 ² km ²	
	Lower Meso-scale	0.1 to 1 km	0.1 to 1 km ²	
Micro-	Upper Micro-scale	30 to 100 m	0,001 to 0,1 km ²	Hillslope
	-	> 30 m	>0,001 km ²	Local

In order to change scales, information has to be transferred from one scale to another (MARCEAU, 1999:P.4). This process can be described by one of two scaling methods: up scaling and downscaling. Up scaling describes the transition of information from a smaller scale to a higher scale whereas

downscaling is defined as disaggregation of spatial information with a change from macro-scale or meso-scale to a lower scale (BECKER, 1992). The transformation from one scale to another “requires an understanding of the complex hierarchical organization of the geographic world where different patterns and processes are linked to specific scales of observation, and where transitions across scales are based on geographically meaningful rules“ (MARCEAU, 1999:P.4). Therefore, the next section focuses on scale dependencies of the soil moisture variability.

2.3.1 Scale Dependent Spatial and Temporal Distribution of Soil Moisture Variability

Soil moisture is a highly variable parameter in space and time (FAMIGLIETTI, DEVEREAUX ET AL., 1999; MARTINEZ, HANCOCK ET AL., 2007). The determination of soil moisture variability derived from different scales was investigated in several studies such as GRAYSON, WESTERN ET AL. (1997), PETERS-LIDARD, PAN ET AL. (2001) and MERZ AND PLATE (1997). The finding of these studies was that soil moisture variability is driven by a number of parameters, such as vegetation, soil type, topography and meteorological patterns, where the importance of each of these parameters decreases or increases depending on scale.

In general, the greatest knowledge about soil moisture distribution has been achieved in laboratory work or through experiments and observation in the field. These results provided a general understanding of the governing processes in soil moisture distribution at micro-scale. Due to technical limitations, knowledge of soil moisture distribution on the meso- or macro-scale is restricted. Here, geoinformatics and remote sensing have to be used in order to determine soil moisture distribution (VAN OEVELEN, 1998:P.511).

At the micro-scale, the soil moisture pattern is influenced by topography (WESTERN, GRAYSON ET AL., 1999; SVETLICHNYI, PLOTNITSKIY ET AL., 2003). SVETLICHNYI, PLOTNITSKIY ET AL. (2003) analyzed with topography parameters can be used to describe soil moisture pattern. They found that the slope morphometry, which is a combination of aspect, gradient, profile and plan slope showed the highest influence on the spatial soil moisture variability. The importance of topography was initially indicated by BEVEN AND KIRKBY (1979), who introduced the topography index for analyzing soil moisture variability.

Other parameters were determined by MOHANTY ET AL. (2004) by analyzing the distribution within and between four field sites in the Walnut Creek watershed. They found that the soil moisture patterns were influenced by vegetation, in particular the portion of the soil covered by vegetation. The corn plants analyzed had a higher leaf area index (LAI) than soybeans. This led to a reduction of soil evaporation and therefore to a higher soil moisture under crop vegetation (JACOBS, MOHANTY ET AL., 2004:P.440). In the same study, MOHANTY ET AL. (2004) determined topography, cropping practice and soil properties (e.g. sand content) as additional driving parameters in spatial soil moisture distribution. The influence of agricultural practices was also identified by FAMIGLIETTI, DEVEREAUX ET AL (1999). In the Tarrawarra catchment, WESTERN, GRAYSON ET AL. (1999) indicated a dependency of spatial distribution on the initial soil moisture content. Under low soil saturation the soil moisture pattern was randomly distributed, whereas under high saturation the soil moisture pattern was controlled by topography.

At the meso-scale, topography remains the main factor in driving the spatial pattern but only up to a specific medium scale. WESTERN, GRAYSON ET AL. (1999) analyzed the depiction of soil moisture patterns using terrain indices. They found that the wetness index of BEVEN AND KIRKBY (1979) only represents the soil moisture distribution up to the catchment scale. An application on higher scales resulted in unrealistic spatial patterns. Other parameters were identified as being the driving factors for soil moisture distribution. In their study MARTINEZ, HANCOCK ET AL. (2007) differentiated key driving parameters between near-surface soil moisture and root zone soil moisture. They found that near-surface soil moisture is primarily influenced by aspect whereas the root zone soil moisture is driven by slope gradient, elevation and soil type (MARTINEZ, HANCOCK ET AL., 2007:P.14). Additionally, BARDOSSY AND LEHMANN (1998) identified vegetation and soil properties as governing factors in their test area of the Weihersbach in Germany. They also studied the influence of the initial soil moisture distribution and determined it to be a key parameter. According to a study of VAN OEVELEN (1998) geomorphological features can be added to this list. Furthermore, studies also indicated a dependence on climatic conditions (GRAYSON, WESTERN ET AL., 1997; WESTERN, GRAYSON ET AL., 1999; WILSON, WESTERN ET AL., 2005). These authors identified preferred states of soil moisture: first, the wet state dominated by topography and second, the dry

state governed mainly by soil properties (soil texture) and the local terrain. These differences are caused by seasonal changes in the precipitation–evaporation relationship (GRAYSON, WESTERN ET AL., 1997).

On the macro-scale, the driving factors change. Results of studies, such as BLÖSCHL (1996) showed the influence of atmospheric effects on soil moisture variability as a main factor. This finding was confirmed by GÓMEZ-PLAZA, ALVAREZ-ROGEL ET AL. (2000:P.1267) who demonstrated a higher soil moisture distribution during the wet period than during the dry period.

It can be concluded, that spatial patterns of soil moisture are scale dependent. VINNIKOV, ROBOCK ET AL. (1996) and ENTIN, ROBOCK ET AL. (2000) introduced a two-scale concept: on meso-scale the patterns are driven by vegetation, soil type, root structure and topography whereas on large scale the variability is caused mainly through climatic conditions. Thus, soil moisture variation at a scale higher than 500 km is most likely caused by precipitation and evapotranspiration. This result was also verified by JACKSON, LE VINE ET AL. (1999) who determined rainfall at regional scale as the driving factor. Here, also the temporal scale should be analyzed. VINNIKOV, ROBOCK ET AL. (1996) defined a temporal scale of three months at macro-scale. The study was extended by ENTIN, ROBOCK ET AL. (2000), who analyzed soil moisture time series from the available archives for Illinois and Iowa in the United States, as well as data from Russia, Mongolia and China. They also distinguished between the upper soil layer (10 cm) and the root zone soil layer (1 m depth). The derived time scale for the 10 cm layer was less than two months and approximately two months for the 1 m layer. However, the results were achieved using soil moisture time series from grassland and agricultural sites and a transformation of those results to other vegetation types has to be researched (ENTIN, ROBOCK ET AL., 2000).

Based on these results, the conclusion can be made, that the spatial resolution of scatterometer derived soil water estimates is able to provide soil water variability driven by atmospheric effects (SCIPAL, WAGNER ET AL., 2003).

2.3.2 The Up- and Downscaling Process

To transfer information, such as soil moisture, from a higher scale to a lower resolution or vice versa, up scaling and downscaling procedures have to be applied.

The process of up scaling consists of two steps. In the first step the distribution of information at smaller scale (BLÖSCHL AND SIVAPALAN, 1995:P.18), meaning the determination of characteristics of heterogeneity (WU AND LI, 2006:P.26), is analyzed. Hydrological parameters, such as precipitation or evapotranspiration, are often only available for specific points because those measurements can only be achieved on point scale. In order to retrieve spatial information, these point measurements have to be interpolated (BLÖSCHL AND SIVAPALAN, 1995; BIERKENS, FINKE ET AL., 2000; WU AND LI, 2006). The second step in up scaling involves the aggregation of the information to the larger scale (BLÖSCHL AND SIVAPALAN, 1995; WU AND LI, 2006).

The reverse procedure, called downscaling, also involves two steps: disaggregation and singling out. Disaggregating aims to reconstruct the variations at a specific scale under the assumption that the values at the larger scale are the average of the values at the smaller scale (BIERKENS, FINKE ET AL., 2000:P.111) by using auxiliary information (WU AND LI, 2006). To downscale information, there are three disaggregation approaches: deterministic, conditional stochastic and unconditional stochastic (BIERKENS, FINKE ET AL., 2000). In the deterministic approach, the average value at the larger scale is known and there is only one solution in order to determine the variation at smaller scale (BIERKENS, FINKE ET AL., 2000). The conditional stochastic problem also assumes that the average value is known but that there are multiple functions describing the temporal and spatial distribution on a finer scale (BIERKENS, FINKE ET AL., 2000). In the case of the unconditional stochastic problem, the average value at the larger scale is not exactly known (BIERKENS, FINKE ET AL., 2000). The distribution at finer scale is described through different models. In the second step of downscaling, the so called singling out, the known pattern are assigned to the smaller scale (BLÖSCHL AND SIVAPALAN, 1995:P.19) and therefore connects the values between the two interested scales.

2.3.2.1 Upscaling methods

The first step in the upscaling procedure mentioned above is distribution of information, which is basically an interpolation of information over space (BLÖSCHL AND SIVAPALAN, 1995:P.19). Several interpolation techniques have been analyzed for various hydrological parameters and scales (VIRDEE AND KOTTEGODA, 1984; GOOVAERTS, 2000; LIN AND CHEN, 2004). The traditional

problem in hydrological modeling is the point measurement of climatologic parameters such as temperature, precipitation and humidity and the need for areal information. Common methods to interpolate these point measurements are kriging, and inverse distance, as well as spline interpolation (WACKERNAGEL, 1995; KITANIDIS, 1997; WEBSTER AND OLIVER, 2001).

In the second step the information will be aggregated to the higher scale. Here, two issues have to be analyzed (BLÖSCHL AND SIVAPALAN, 1995:P.21): First, the dominant processes at the respective scales have to be analyzed and second, an appropriate aggregation rule has to be chosen to describe adequately the distribution pattern at higher scale.

The study carried out by DE LANNOY, HOUSER ET AL. (2007) analyzed six statistically based upscaling methods: the absolute mean difference, the relative mean difference, linear relationship, the cumulative distribution function (cdf) matching, transfer function in frequency domain and the autoregressive moving average filter (ARMA) model. These methods have been evaluated in terms of their applicability to predict mean soil moisture over the investigated study area. In their study, the best results were found by applying the linear relationship and the cdf-matching methods. Furthermore, they examined the possibility of finding a representative soil moisture measurement station for representing different soil moisture depths. Unfortunately, the authors were not able to determine one or several probes that fit for all soil layers. This leads to the conclusion that the soil moisture distribution in different layers is driven by different parameters. As a result of their study, the authors suggest that, if a representative point measurement is used, the applied transfer function has to be chosen carefully.

CROW, RYU ET AL. (2005) examined the uncertainty of upscaling soil moisture using only field observations, only model predictions or a combination of both by applying a linear relationship. The best results were made using a two-step upscaling approach. First, determine a representative station using the time stability method (VACHAUD, PASSERAT DE SILANS ET AL., 1985) to upscale the point measurements to field scale. And second, apply the model-based approach in order to determine the soil moisture at footprint-scale.

2.3.2.2 *Downscaling Methods*

Traditionally downscaling methods were used in the fields of climatology and meteorology to obtain regional precipitation or other climatological information (HEWITSON AND CRANE, 1996; PEGRAM AND CLOTHIER, 2001; HUTH, 2002) or model outputs (ZORITA AND VON STORCH, 1999; MACKAY, CHANDLER ET AL., 2001) on smaller scale. The availability of macro-scale soil water estimates encouraged researchers such as REICHLE, ENTEKHABI ET AL. (2001), PELLENQ, KALMA ET AL. (2003) and KIM AND BARROS (2002A) to explore methods to use these datasets in regional hydrological modeling, either for validation or calibration purposes or even as input datasets. For the successful application of a downscaling method it is necessary to determine the relationship between the large scale and local scale characteristics.

For example, REICHLE, ENTEKHABI ET AL. (2001) investigated the possibility of achieving small resolved soil water information from passive, lower resolution, microwave measurements using data assimilation techniques for interpolation and extrapolation of remotely sensed data. The applied downscaling method for estimating the soil water content at smaller scale was based on micrometeorological data, soil texture and land cover inputs.

An other approach was carried out by CHARPENTIER AND GROFFMAN (1992), who examined the soil water distribution within a remote sensing pixel in Kansas. One of the findings was that the remotely sensed soil water captured the spatial soil water distribution better under wet condition than under dry conditions. BURKE AND SIMMONDS (2003) compared microwave brightness temperature to modeled soil moisture data using MICRO-SWEAT. In their research, they found an influence of the vegetation water content on the accuracy of soil water retrieval. The error increased for dense vegetation types.

BINDLISH AND BARROS (2002) examined the downscaling potential of electronically scanned thinned array radiometer (ESTAR) images from 200 to 40 m to determine the temporal and spatial variability of soil water content in the Little Washita catchment. The key finding was that the sub-pixel soil water variability is strongly related to soil hydraulic properties. These result were taken by KIM AND BARROS (2002A) who went one step further. They successfully disaggregated macro-scale soil water information from 10 km to 1 km using a fractal interpolation scheme and ancillary data, such as soil texture and

vegetation water content. Also PELLENQ, KALMA ET AL. (2003) developed a downscaling method. They established their downscaling algorithm by applying the simple Soil Vegetation Atmosphere Transfer (SVAT) model coupled with TOPMODEL. The soil moisture information at catchment scale was determined using a simple relationship between mean quantities of topography and soil depth. The findings were compared to soil moisture measurements taken in the catchment and the results were very promising.

These studies showed that meso-scale soil water information can be estimated from low resolution data. However, the applied downscaling approaches are based on individual relationships which depend on local constraints. For instance, the approach of KIM AND BARROS (2002A) did not consider topography as an important factor for soil moisture variability at all. For an exact scientific development of a scale concept, based on the results above, a combination of all driving parameters that influence spatial and temporal variability is recommended. In addition, the concept of distributed response units (FLÜGEL, 1995; FLÜGEL, 1996), which is more process oriented than the raster based concepts used in most studies, could help in the development of a more generic downscaling method which is less dependent on local constraints of the test sites.

A very promising approach was examined by WAGNER, PATHE ET AL. (SUBMITTED). The authors investigated the possibility of describing the relationship between local and regional backscatter information of the microwave signal of Environmental Satellite (ENVISAT) Advanced Synthetic Aperture Radar (ASAR) as a linear approach. The authors found, that the implemented scaling parameter can be described as function of soil moisture properties, vegetation and topography since the backscatter coefficient is very sensitive to these parameters. In a previous studies by CROW, RYU ET AL. (2005) and DE LANNOY, HOUSER ET AL. (2007) a linear relationship has been already used to up scale soil moisture information.

2.4 Research Needs

Based on the review of the literature, the following research needs can be derived, which are addressed in this study:

How can the relationship between macro-scale and meso-scale soil water distribution be described?

In the literature review, different downscaling approaches, such as statistical, fractal and linear regression, were highlighted. However, some of these downscaling schemes were applied to the microwave signals, which are determined by landscape parameters such as surface and vegetation roughness, soil water content and topography. Other downscaling schemes do not account for all parameters driving the spatial distribution of soil water. In this study, the question to be answered is if such a downscaling algorithm can be applied to process driven soil water time series.

What are the driving variables controlling the scaling parameter to downscale the macro-scale soil water product?

The discussion on spatial soil water distribution showed that the driving parameter changes when the scale changes. On the macro-scale it is the climatic parameters, especially precipitation and evapotranspiration that determine the spatial distribution whereas, on the meso-scale, topography, vegetation cover and soil properties are the important parameters. At the micro-scale more local parameters such as slope morphometry, amount of vegetation cover on top of the soil influence the soil distribution. This leads to the question to what extent these parameters can be used to downscale the macro-scale soil water estimates.

What are the limitations for the downscaling method?

There are limitations to the remotely sensed soil water dataset. For instance, in densely vegetated areas the microwave signal can not penetrate into the soil column, and therefore no information on the actual soil water content can be derived.

On the other hand, hydrological models are developed for certain research questions and, therefore, have their own limitations. Also, hydrological models depend highly on calibration parameters, which have to be determined. A change in the calibration parameters might influence the downscaling method. This leads to a two fold limitation that has to be evaluated.

CHAPTER 3

SCIENTIFIC OBJECTIVES AND METHODICAL APPROACH

The overall goal of this work is the Evaluation of the ERS-remotely sensed soil water estimates for an application in regional hydrological modeling. Here fore, the macro-scale soil water estimates have to be transferred to a smaller scale. To accomplish such a scale transfer the development of an appropriate downscaling scheme is necessary. Therefore, the cornerstone of this work is the **development of a downscaling scheme for application of the macro-scale soil water estimates in meso-scale hydrological modeling.**

To accomplish this goal, reference data are needed. An estimation of soil moisture using in-situ measurements on spatial scale of the remotely sensed soil water estimates is not possible. Therefore, other sources of information have to be used. Here, hydrological modeling offers a possibility to retrieve meso-scale soil water distribution. In hydrological modeling, the soil water content will be achieved as part of the water cycle calculation with high spatial and temporal resolution. The so resulting simulated soil water time series will be compared to the macro-scale soil water estimates and later used to derive the downscaling method. To achieve the research goal the study is into the following three research objectives:

- Application of a distributed hydrological model to estimate the spatial soil water distribution and the factors influencing this distribution
- Evaluation of the influence of landscape parameters (soil, land cover, topography and geology) on the macro-scale soil water estimates (SWI_{ERS}) and using this information for
- Development of a downscaling method for the macro-scale soil water estimates for an application on various scales.

For the realization of the overall goal of the work and the three specific objectives the following three methodical steps were followed, shown in the flowchart figure. The three steps and its proposed methods a more described in detail in the following sections.

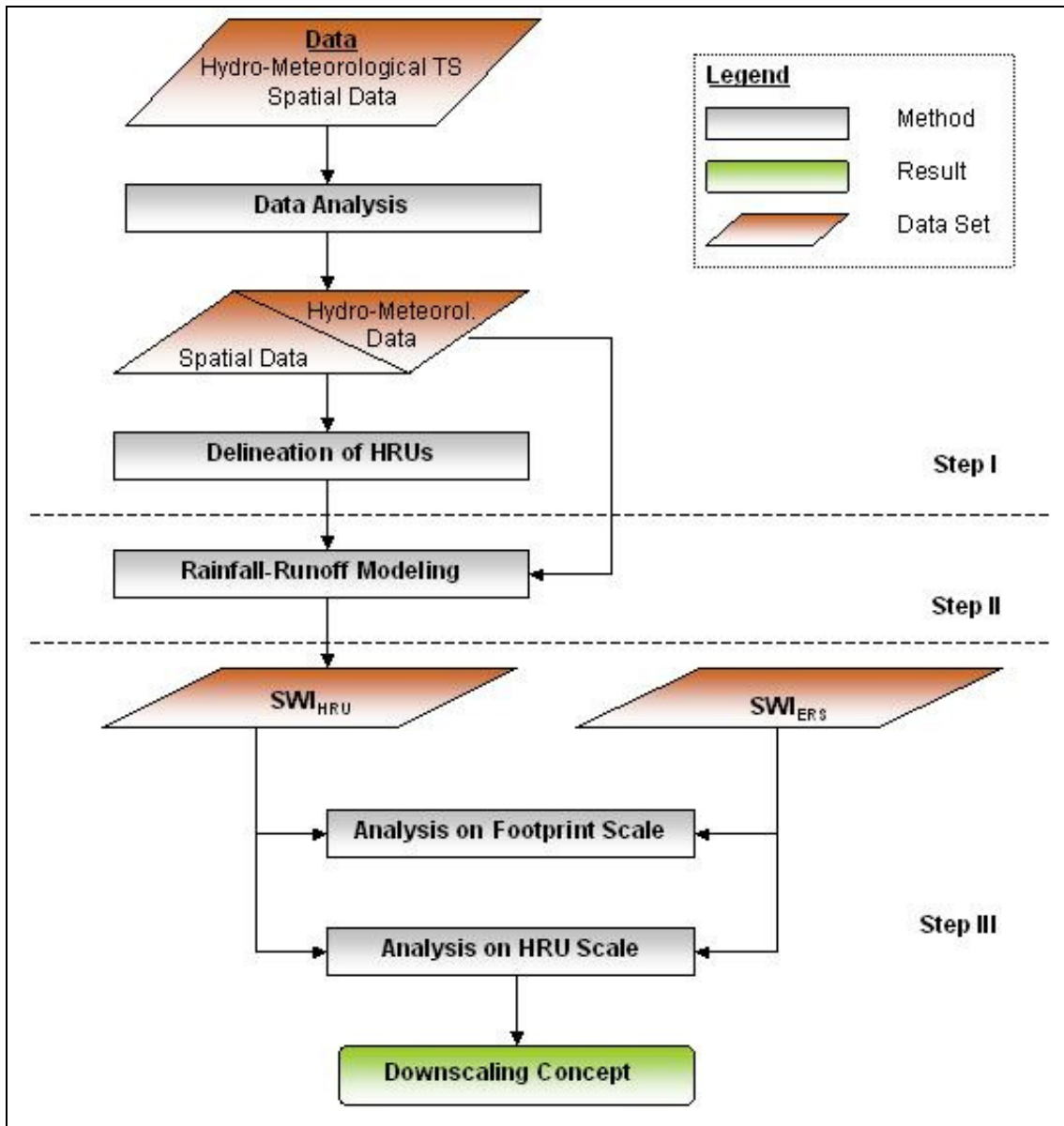


Figure 3-1: Flowchart of the Methodological Approach

3.1 Step I: Hydrological System Analysis and Delineation of Hydrological Response Units

3.1.1 Hydrological System Analysis

The hydrological system analysis is the base for the delineation of the Hydrological response units (HRUs) and the calibration of the distributed hydrological model J2000. Initially, the hydrological system analysis studies the interactions of the landscape parameters soil, water, vegetation and climate in order to understand the system response to rainfall and therefore the

generation of the respective hydrological response. Also, the examination of the hydro-meteorological time series using data analysis methods for changes in hydrological system response is an important preparation for the rainfall-runoff modeling of the catchment.

3.1.1.1 Data Analysis of Hydro-Meteorological Time Series

The quality of the model output depends directly on the input data (BEVEN, 2001B). Hydrological models are driven, in part, by hydro-meteorological data, which contains daily field observations. The resulting time series are never perfect and the data contains data errors (BEVEN, 2001B). The data errors are divided into systematic errors and random errors. The first group contains errors which affect the measuring instrument systematically (BEVEN, 2001B) and result in a constant measurement bias. These errors can be caused, for instance, by false calibration of the instrument. Random errors, on the other hand, are caused by randomly occurring factors, such as interference of the automatic recording by animals. To achieve good modeling results it is crucial to control for data quality.

Rainfall Data

Rainfall data are measured as point observations and there are several potential sources of data errors associated with those measurements (DINGMAN, 2002:P.114). The design of rain gauges can lead to a standard error between 3 to 30 % of the total annual measured rainfall sum (DINGMAN, 2002:P.115). These data errors can be corrected using an approach presented by RICHTER (1995). Rainfall time series might also include missing values. Here, DINGMAN (2002:P.115-117) suggests the following methods for data filling: station average method, normal ratio method, inverse distance weighting, regression analysis or the most common technique: the double mass curve between two stations.

Runoff Data

The discharge observed at the runoff station is an integrated value over the entire catchment. In a hydrological model, the data is used for calibration of simulated runoff against observed runoff. Therefore, it is necessary to check runoff data for homogeneity and inconsistency (BEVEN, 2001B). The most common technique, in case of available data at a nearby station, is the double

mass curve (BEVEN, 2001B). The double mass analysis compares two neighboring measuring stations by the plotting of accumulated volumes. Changes in the runoff records will be visible in slope changes compared to the reference line.

This analysis gives information on missing values or changes in the catchment affecting the measured runoff. Another technique to check for data errors is the statistical analysis of low flows and high flows as suggested in DEUTSCHER VERBAND FÜR WASSERWIRTSCHAFT UND KULTURBAU (1983; 1999). The resulting data was used to calculate the annual and monthly average runoff and to establish the rainfall runoff relationship.

Additional Datasets

The time series data on wind speed, humidity, temperature as well as the time series of the macro-scale soil water product was checked for homogeneity and consistence using the aforementioned methods for rainfall and runoff data analysis. Missing values were filled by applying regression analysis.

3.1.1.2 Spatial Data Modeling

Hydrological models require spatial information of the hydro-meteorological information. The hydro-meteorological time series used, however, contain measurements at point scale. For a spatial representation of these parameters the missing information has to be interpolated. Here, several methods exist such as kriging, Thiessen Polygons, linear regression and inverse distance weighting (IDW) (WACKERNAGEL, 1995; KITANIDIS, 1997; WEBSTER AND OLIVER, 2001).

Regionalization of the hydro-meteorological datasets is accomplished by the preprocessing module in J2000 and is based on the inverse distance weighting approach (KRAUSE, 2001). The regionalization consists of several steps (JAMS; KRAUSE, 2001): First, the linear regression is applied to determine the relationship between station measurements and the respective station elevation. In the second step, the numbers of stations next to each HRU is determined, whereas the user defines the number of stations necessary to take into account. Then the distance between the found stations and each HRU is calculated. To account for the difference in the distance between HRU and station, the application of a user defined weighting factor weightings the

distances. In the third step, the final weighting factor for the hydrometric station is calculated applying an inverse distance weighting method. In the last step, the actual data values were calculated under consideration of the weighted values of step 3 and the elevation factors of step 1. For more detailed information on the regionalization algorithm in J2000 refer to KRAUSE (2001) and JAMS (JAMS).

Another important step in this framework is to check the spatial data for missing values. Particularly important is the digital elevation model (DEM), which is one of the most important datasets, because it will be used for the delineation of the stream network, catchment boundaries and topographic parameters such as slope, aspect, flow direction and flow accumulation. The DEM can be derived from remote sensing imagery, such as SAR Interferometry (LUDWIG, HELLWICH ET AL., 2000) or from the Shuttle Radar Topography Mission (SRTM) (U.S. GEOLOGICAL SURVEY EROS DATA CENTER AND NASA, 2007). The SRTM-DEM, in particular, often contains voids which have to be filled for a hydrological application (KÄÄB, 2005; GROHMAN, KROENUNG ET AL., 2006).

3.1.2 Delineation of Hydrological Response Units

The rainfall-runoff relationship of a catchment is determined by the following characteristics: topography, vegetation cover, land cover, soils, climate and geology (BEVEN, 2001B:P.179). To account for a realistic representation of the catchment characteristics, the model used should be fully distributed. This type of model is difficult to apply because the model demands highly spatially distributed input information of the landscape parameters, which cannot be measured at the requested resolution (BEVEN, 2001B; BLÖSCHL, 2005). Therefore, the attempt has been made to define model entities that show a “hydrological similarity” (BEVEN, 2001B:P.179), which can be defined using one of the following three approaches. The first, the concept of Aggregated Simulation Area (ASA) has been applied in the SLURP (Semi-distributed Land Use-based Runoff Processes) model (KITE, 1995). This concept involves aggregating simulation areas which are heterogeneous in their land cover and elevation; however, the distribution of these parameters within the respective entity is known. These ASAs have the requirement of contributing runoff to a stream channel and, therefore, act as sub catchments (KITE, 1995). The second

approach, the **Representative Elementary Area (REA)** (WOOD, SIVAPALAN ET AL., 1990) defines minimal areas in which the spatial heterogeneity of hydrological variables such as infiltration, evaporation, and runoff are unimportant. The distribution of these variables within the areas is represented by a probability function. The third concept, the **Hydrological Response Unit (HRU)**, was introduced by LEAVESLEY, LICHTY ET AL. (1983) as model entities in the Precipitation Runoff Modelling System (PRMS). HRUs are characterized as homogenous areas with respect to their hydrological response (LEAVESLEY, LICHTY ET AL., 1983:P.9). This approach was extent by FLÜGEL (1995, 1996) who defined HRUs as areas with common in “climate, land use and underlying pedo-topo-geological conditions” (FLÜGEL, 1995:P.426). The delineation of HRUs involves the definition of classification criteria, which are based on hydrological system analysis (FLÜGEL, 2000). The concept of HRUs has been tested and applied in several studies as an integrated regionalization tool (BONGARTZ, 2001; KRAUSE, 2001; MÄRKER, 2001; KRAUSE, 2002; FINK, KRAUSE ET AL., 2007; SCHEFFLER, BÄSE ET AL., 2007; SCHEFFLER, KRAUSE ET AL., 2007).

It can be concluded that the concepts of HRUs are the only modeling entities that consider all landscape parameters important in hydrological processes. Therefore, the HRU-approach has been applied in this study and is explained in the following section.

Conceptual Approach of the Hydrological Response Units

The HRU concept, according to FLÜGEL (1995; 1996), is based on the representation of the catchment heterogeneity in the form of entities showing a similar or equal system response.

The landscape parameters of geology, soil, vegetation and climate are strongly interacting to each other. The soil is formed from bedrock material through various weathering and erosion processes. Climate conditions determine the intensity of these various processes and, therefore, the types of soil formed. Soil formation and distribution is also determined by the topography controlling the accumulation of soil material and the water movement within and on top of the soil column. The natural vegetation depends on climate, relief and soil type. A specific combination of geology, soil, relief, vegetation and climate characteristics, therefore, generates a specific system response.

The HRUs divide the catchment into areas with similar or equal geology-soil-relief-vegetation and climate combinations. These entities are delineated based on detailed hydrological system analyses in a Geographical Information System (GIS) (FLÜGEL, 1995; 1996). Based on the results of the hydrological system analysis the GIS datasets are reclassified, aggregated and overlaid in a step-by-step procedure. To ensure the hydrological flow between HRUs and to the stream network, the flow routing is determined (STAUDENRAUSCH, 2001, JAMS; KRAUSE, 2002). As a result, the derived HRUs represent topologically connected lumped model entities. These entities act as model input for the rainfall-runoff simulation of the study area.

3.2 Step II: Rainfall-Runoff Modeling with J2000

To obtain the above stated study goal, the meso-scale distribution of soil moisture has to be estimated. Due to the lack of in-situ measurements covering the entire ERS-scatterometer footprint area, the meso-scale soil water distribution is simulated. For this purpose, the distributed hydrological model has been applied. The delineated HRUs serve as spatial modeling entities in the model. The following section gives an introduction in the model design but also the steps of the modeling process (*Figure 3-2*) such as input data preparation (*Section 3.2.2*), parameterization and calibration (*Section 3.2.3*) are described.

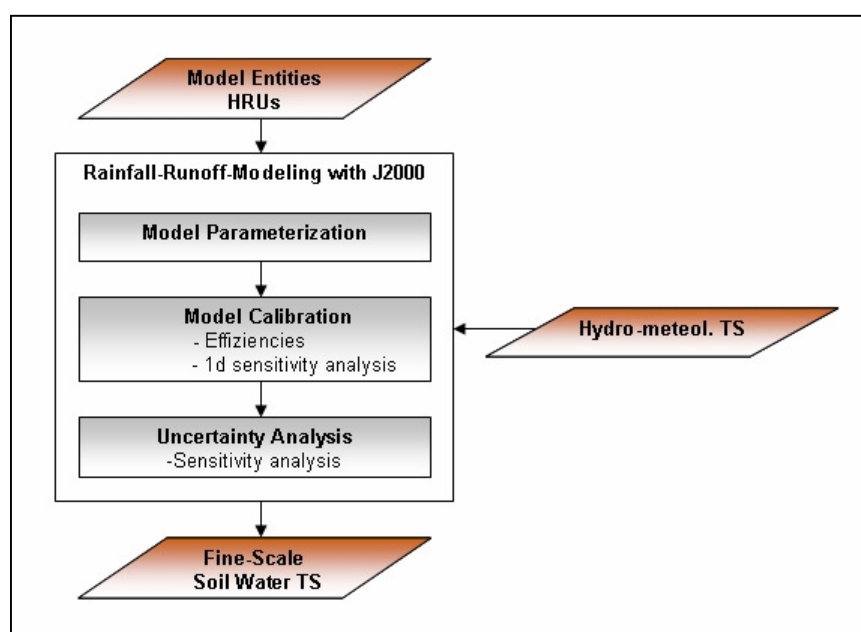


Figure 3-2: Flowchart Methodological Steps in the Rainfall-Runoff Modeling

3.2.1 Modular Design of J2000

The model used for this study was the distributed, process oriented, modeling system J2000 (KRAUSE, 2001). The structure of the model is shown in Figure 3-3. The modeling system has been successfully applied in catchments of between 2 and 6000 km² in Europe (KRAUSE, 2001). Additionally the model was applied in the semi-arid catchments of the Tsitsa River (BÄSE, HELMSCHROT ET AL., 2006) as well as the Great Letaba (SCHEFFLER, BÄSE ET AL., 2007) in South Africa.

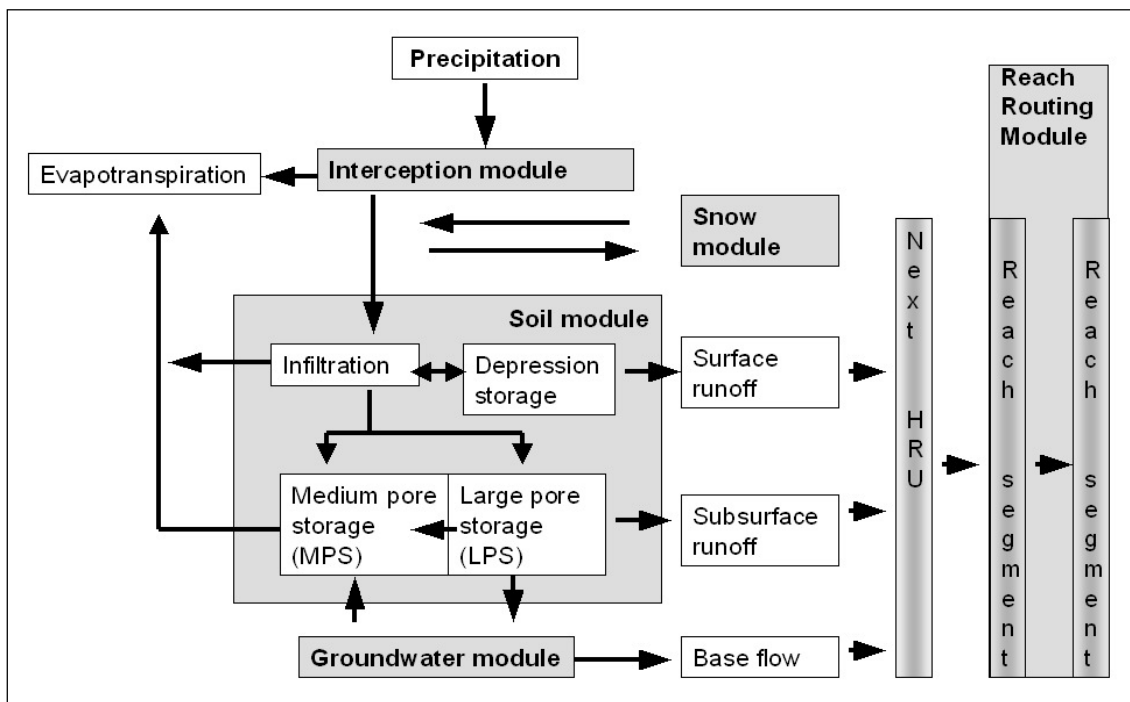


Figure 3-3: The Modeling System J2000 (modified from Krause (2001:p.74 and p.89) and Bäse (2005:p.25))

As shown in the figure, the modeling system is divided into process modules such as the interception, snow, soil water, and ground water modules as well as the reach routing module.

For every model entity (HRU), the surface runoff and interflow are calculated in the soil module while the fast and slow base flow components are calculated in the groundwater module. Afterwards, the simulated values of all the runoff components are routed to the adjacent HRUs and added to the respective storages. This process is repeated until a stream segment is reached. Within the reach segment the water is transported to the catchment outlet.

The Soil Water Module (based on Krause (2001) and JAMS (JAMS))

The soil module separates the soil layer into medium pore storage and large pore storage. The medium pore storage represents pores with a diameter of 0.2 to 50 μm . The large pore storage represents pore diameters over 50 μm . The fine pore storage is neglected. In addition to these pore storages, there is the depression storage which mainly generates surface runoff and is defined through the terrain. In areas where the slope is higher than 5° , the available storage is reduced by 50 %. Depending on the empirically calculated infiltration rate water infiltrates into the soil storages or is routed to the depression storage.

The actual infiltration (*Inf*) rate for every time step is dependent on the current soil saturation and the user-defined maximum infiltration rate. In order to take into account different infiltration scenarios depending on precipitation generation, three different infiltration scenarios have been developed: summer infiltration, winter infiltration and snow infiltration.

The actual infiltration rate is calculated using the following equation;

$$Inf = (1 - soil_{sat}) * inf_{max} \quad \text{Equation 3-1}$$

The actual soil saturation ($soil_{sat}$) is derived according to the following equation.

$$soil_{sat} = \frac{MPS_{act} + LPS_{act}}{MPS_{max} + LPS_{max}} \quad \text{Equation 3-2}$$

If the precipitation amount is higher than the actual infiltration rate, the water is stored temporarily in the depression storage. The infiltrated precipitation water is transported into the pore storages whereas the saturation of the medium pore storage determines how much water can infiltrate.

The medium pore storage acts like a sponge in which water is held more strongly with decreasing saturation. This behavior reflects the natural forces in the soil column. The inflow in the medium pore storage is calculated using *Equation 3-3*. The calibration parameter (*soilDistMPSLPS*) determines how much water infiltrates into the medium pore storage. If the parameter is set close to zero more water infiltrates into large pore storage.

$$MPS_{inflow} = inf * (1 - e^{\frac{-1 * soilDistMPSLPS}{\frac{MPS_{act}}{MPS_{max}}}}) \quad \text{Equation 3-3}$$

The reduction of the medium pore storage is forced by evapotranspiration. The forces of evapotranspiration are depending on the saturation of the medium pore storage. The evapotranspiration increases with increasing saturation.

The residual infiltration water is transported into the large pore storage.

$$LPS_{inflow} = inf - MPS_{inflow} \quad \text{Equation 3-4}$$

The outflow of this storage is determined by the moisture conditions, according to the following equation:

$$LPS_{outflow} = (soil_{sat})^{SoilOutLPS} - LPS_{act} \quad \text{Equation 3-5}$$

The water in the large pore storage gets distributed to lateral flow component (*inter*) and percolation (*perc*). The amount of water that is distributed to each of these processes is dependent on the calibration parameter (*soilLatVerDist*) and the surface slope (*slope*), as highlighted in the following equations:

$$perc = LPS_{out} * (1 - \tan(slope) * soilLatVerDist) \quad \text{Equation 3-6}$$

$$inter = LPS_{out} * (\tan(slope) * soilLatVerDist) \quad \text{Equation 3-7}$$

The water movement between large pores and medium pores is represented using the following equation:

$$LPS2MPS = LPS_{act} * (1 - e^{\frac{-soilDiffMPSLPS}{\frac{MPS_{act}}{MPS_{max}}}}) \quad \text{Equation 3-8}$$

in which the parameter *soilDiffMPSLPS* determines the fraction of water distribution.

The flow of the direct surface ($\text{runoff}_{\text{direct}}$) and subsurface ($\text{runoff}_{\text{subsurface}}$) runoff can be delayed by using adjustment parameters, in which are described the following equations.

$$\text{runoff}_{\text{direct}} = \frac{1}{\text{soilconcRD1}} * \text{RD1} \quad \text{Equation 3-9}$$

$$\text{runoff}_{\text{subsurface}} = \frac{1}{\text{soilconcRD2}} * \text{RD2} \quad \text{Equation 3-10}$$

A more detailed description of the soil water module can be found in KRAUSE (2001).

3.2.2 Input Data Preparation

The model J2000 requires the following data files, shown in the following table.

Table 3-1: Data Input Files in J2000

DESCRIPTION	UNITS
Absolute Humidity	g/cm ³
Relative Humidity	%
Observed Runoff	m ³ /s
Observed Rainfall	mm
Sunshine Duration	H
Maximum Daily Temperature	°C
Minimum Daily Temperature	°C
Mean Daily Temperature	°C
Wind Speed	m/s

The needed daily mean temperature was not provided by the South African Weather Service, hence it was calculated as the average of the maximum (T_{max}) and minimum (T_{min}) daily temperature.

Also, the model requires the absolute humidity as an input parameter dataset. The dataset, therefore, has been calculated in several steps, depicted in the following equations:

1. Calculation of the saturation vapor pressure e_s (DINGMAN, 2002:P.586)

$$e_s(T) = 6.1078 * e^{\frac{17.3 * T}{T + 237.3}} \quad [\text{hPa}] \quad \text{Equation 3-11}$$

2. Calculation of the maximum humidity with T as mean air temperature and the computed values for e_s

$$R_m(T) = e_s * \frac{216.7}{T + 273.15} \quad \left[\frac{g}{cm^3} \right] \quad \text{Equation 3-12}$$

3. Calculation of the absolute humidity (R_a) by taking relative humidity R_u and maximum humidity R_m into account.

$$R_a(T) = R_m * \frac{R_u}{100} \quad \left[\frac{g}{cm^3} \right] \quad \text{Equation 3-13}$$

All data files (*Table 3-1*) were transformed into ASCII- format. In addition to the actual data values, J2000 requires information on geographical location as well as the elevation of the station. The geographical location for the stations was derived using ArcMAP 9.1 (ESRI, 2003). In case of missing elevation data, that information was taken from the available digital elevation model (SRTM 2004).

3.2.3 Model Parameterization and Calibration

The hydrological model J2000 requires parameter input files in order to describe the natural characteristics. These parameter values were obtained from literature and are described in *Section 5.2.1*. Additionally, the model J2000 contains 30 direct model parameters: four parameters in the groundwater module, fifteen parameters in the soil module (lumped approach), eight snow module parameters, one reach routing parameter and two interception parameters, shown in *Appendix A*. The table in *Appendix A* does not include the snow parameters because the snow module was not applied in the study area of Great Letaba River.

The goal of model calibration is a satisfactory fit between simulated and observed variables (REFSGAARD AND STORM, 1996:P.42). Therefore these parameters have to be adjusted. This is necessary for three reasons as stated in BLÖSCHL (2005): First, the hydrological models are based on empirical equations which are depended on catchment characteristics. Second, model boundaries are mostly poorly defined. The model calibration adjusts input errors such as measurement errors. Third, landscape parameters such as soil, vegetation,

geology and topography are highly variable in space, and the knowledge of their real occurrences as well as physical characteristics is limited. Here, parameter adjustment accounts for unknown parameters and characteristics.

According to REFSGAARD AND STORM (1996:P.47), three approaches can be used to calibrate hydrological models: 1) manual adjustment using “trial and error”, 2) automatic model calibration, and 3) a combination of 1) and 2). The “trial and error” method requires expert knowledge about the model structure and involves a lot of time because the manual assessment it requires a larger number of number runs (REFSGAARD AND STORM, 1996:P.47). The automatic model calibration, however, is much faster and less subjective than the manual method (REFSGAARD AND STORM, 1996:P.47). The drawback of the automatic parameter adjustment is the evaluation of the model fit depending only on the objective function, which can lead to a wrong model solution. In order to account for the catchment characteristics and decrease the time effort, a combination of both methods is recommended (REFSGAARD AND STORM, 1996:P.48). In this study, the automatic parameter adjustment was used to define sensitive parameters and parameter ranges and afterward the model was calibrated using the “trial and error” method.

3.2.3.1 Automatic Parameter Estimation using Sensitivity Analysis

Sensitivity analysis is an important tool in hydrological modeling. Especially during the model design and model calibration phase, sensitivity analysis provides a better understanding of the relationship between model parameters and model processes (MCCUEN, 1973). It allows the identification of sensitive parameters influencing the model output (BAHREMAND AND DE SMEDT, 2008:P.2).

BÄSE (2005) analyzed the parameter sensitivity in J2000 using one dimensional parameter analysis Monte Carlo and Latin-Hypercube Method in the Wilde Gera Catchment, Germany. The author reported the following sensitive parameters influencing high peak flow: *gwCapRise*, *soilPolRed*, *soilOutLPS*, *soilLatVertDist*, *soilrecRD1*, *soilrecRD2*, *soilmaxPerc*, *soiMaxlInfSummer* as well as *soiMaxlInfWinter*. In terms of base flow, all parameters in the groundwater module as well as in the soil water modules with the exception of *IP >80*, *IP <80* and *SoilMaxDPS*, were determined as sensitive parameters. BÄSE (2005) also examined parameter interactions and

determined three direct parameter interactions: *coldContFac* and *groundFac*, *tempFac* and *groundFac* as well as *soilDistMPSLPS* and *soilDiffMPSLPS*. A more detailed description can be found in BÄSE (2005:P.57).

For determination of sensitive parameters and sensitive parameter ranges in the Great Letaba catchment, first the one dimensional sensitivity analysis in J2000 has been applied. Here, the reaction of the model output to one specific parameter change is analyzed. The reaction was then evaluated using objective functions: Nash-Sutcliffe-Efficiency (NaS) (NASH AND SUTCLIFFE, 1970), logarithmic Nash-Sutcliffe Efficiency (log. NaS), absolute volume error (AVE) and the coefficient of determination (R^2).

Nash- Sutcliffe Efficiency

The Nash-Sutcliffe Efficiency (NaS) (NASH AND SUTCLIFFE, 1970) is used in hydrological models to determine the goodness of fit between the modeled and observed runoff. The NaS is calculated as follows:

$$\text{NaS} = 1 - \frac{\sum_{i=1}^n ((Q_{obs})_i - (Q_{sim})_i)^2}{\sum_{i=1}^n ((Q_{obs})_i - (\bar{Q}_{obs}))^2} \quad \text{Equation 3-14}$$

with Q_{obs} representing the observed runoff value and Q_{sim} the modeled runoff value at time i , \bar{Q}_{obs} defines the observed mean runoff for the given time period. The range of the NaS lies between $-\infty$ and 1; a NaS of 1, therefore, confirms a perfect fit. As stated in KRAUSE, BOYLE ET AL. (2005:P.90), the disadvantage of the NaS is an insensitivity to model over- and under predictions, especially in periods of low flow. The authors suggest using the NaS with logarithmic values.

Logarithmic Nash Sutcliffe Efficiency

The calculation of the logarithmic Nash-Sutcliffe Efficiency (log. NaS) is carried out as follows:

$$\text{log. NaS} = 1 - \frac{\sum_{i=1}^n (\log(Q_{obs})_i - \log(Q_{sim})_i)^2}{\sum_{i=1}^n (\log(Q_{obs})_i - \log(\bar{Q}_{obs}))^2} \quad \text{Equation 3-15}$$

The influence of the low flow values is stronger than in the NaS calculation due to the logarithmic values of \bar{Q}_{obs} , Q_{obs} and Q_{sim} . This leads to a higher sensitivity to over and under estimation of the observed runoff during low flow conditions (KRAUSE, BOYLE ET AL., 2005:P.91).

The Absolute Volume Error

The AVE estimates the difference between the predicted runoff volume (Q_{sim}) and the observed runoff volume (Q_{obs}) over a given time period. The AVE is calculated as follows:

$$AVE = \sum_{i=1}^n (Q_{sim})_i - \sum_{i=1}^n (Q_{obs})_i \quad \text{Equation 3-16}$$

The crucial identification of a good fit between the two outputs was the visual comparison of the observed and simulated runoff. In the second step, the “trial and error” method was used to determine final parameter values which acted as baseline values for the estimation of uncertainty.

3.2.3.2 Prediction of Model Uncertainty

The achieved model calibration will contain uncertainty because it is not feasible to represent the model boundary conditions as a true reflectance of nature and also input data still contain error (BEVEN, 2001B:P.217). To estimate the uncertainty range, the sensitivity index (SI) according to FENTIE, MARSH ET AL. (2005) has been calculated. The SI determines the influence of the parameter change in relationship to the model output and is calculated as follows:

$$SI = \frac{\partial Y}{\partial X} \quad \text{Equation 3-17}$$

In which δY defines the relative change in the model output in comparison to the baseline output and δX defines the relative parameter change from the baseline values.

3.3 Step III: Analysis of the Macro-Scale Soil Water Estimates with the Simulated Soil Water Time Series

The achieved soil water time series (*Section 3.2*) were then assessed and evaluated at two scales: first at the footprint scale and second at HRU-scale. The evaluation of these datasets on footprint scale will identify difference and similarities on reflecting soil water generation in the catchment. This analysis will provide the base for the meso-scale analysis. Here, the goal is to find a relationship describing the connection between the remotely sensed data and the simulated soil water data.

3.3.1 Retrieving the Catchment Area Covered by one ERS-Scatterometer Footprint

To develop the downscaling scheme, the area covered by the scatterometer footprint was determined. The ERS-scatterometer features three antennae which measure the backscattered signal of each antenna beam in 19 nodes being 25 km apart from each other (BARTALIS, 2005). Each of these nodes contains the backscattered information integrated over an area of approximately 50 km diameter (BARTALIS, 2005). The flight route of the ERS-satellite is not stable in terms of its geographical location. To assign the measurements to permanent coordinates, a fixed grid with a resolution of 25x25 km² was determined. The transfer of measurements to the fixed orbit was done by applying spatial averaging in terms of a Hamming window (HAMMING AND JUNGE, 1987) with a side width of 36 km (WAGNER, 1998). This window side width was chosen with respect to the orbit grid. A minimum of three orbit measurements are required in order to carry out the spatial weighting. Therefore, each point of the fixed grid contains a spatially averaged value of the closest satellite measurements representing a measurement integrated over 50 km diameter. To derive the integrated area of each scatterometer footprint a circle of 25 km radius was used. The scatterometer footprint covers an area of about 1963 km².

3.3.2 Delineation of the HRU-Soil Water Index (SWI_{HRU})

According to *Section 2.2.1.3*, the SWI_{ERS} is derived using a change detection method, taking the highest and lowest ever measured value for the

soil water content. Therefore, the SWI_{ERS} describes the soil water content of the soil column as a value between zero and one. The macro-scale soil water index is also described as the soil moisture status between wilting point and field capacity, where the highest value of the SWI_{ERS} -time series is defined as field capacity and the lowest value as the moisture status at wilting point. However, this argumentation raises questions regarding the representation of wilting point and field capacity.

The saturation of the soil to field capacity does not mean that no further water infiltration is possible. The grand size pores are still able to store water, so that saturation above field capacity is possible. This fact was shown by KAMARA AND HAQUE (1987), who examined the moisture content in a Verticisol toposequence in Ethiopia and found soil saturations above field capacity. In an other study, carried out by GABRIELLE AND BORIES (1999), found that field capacity and infiltration rate are not unique parameters. These parameters depend on the soil depth and time scale chosen for the study (GABRIELLE AND BORIES, 1999:P.143). Based on the results of these studies it can be argued that the highest remotely measured soil moisture values do not necessarily represent the moisture status at field capacity. It is even more likely that this value represents a moisture status above field capacity.

Similar observation can be made with regard to the wilting point. ARCHER, HESS ET AL. (2002) studied a field site in south-eastern Spain and they found that the soil moisture was dropping down to wilting point during the dry season. Similar results have been made by KINCAID, GARDNER ET AL. (1964). They observed that soil moisture can drop below wilting point in the first approx. 15 cm of the soil column, at a test site in the Walnut Gulch Experimental Catchment.

Based on this argumentation, it is questionable that the highest and lowest measured moisture value of the surface soil moisture time series reflects field capacity and wilting point respectively. Therefore, for the comparison of the simulated and remotely sensed soil water time series the water content of the entire soil column and its storages from the model has been taken into account. The time series of the model J2000 had to be normalized using the following equation:

$$sw_{act} = FPS_{act} + MPS_{act} + LPS_{act} \quad \text{Equation 3-18}$$

$$SWI_{HRU} = \frac{sw_{act} - sw_{min}}{sw_{max} - sw_{min}} \quad \text{Equation 3-19}$$

First, the daily actual water content of the entire soil column (sw_{act}) was calculated by summing the water amount stored of the three storages: fine pore storage (FPS_{act}), medium pore storage (MPS_{act}) and large pore storage (LPS_{act}). The fine pore storage acts hereby as a constant, derived from the soil parameters of the FOOD AND AGRICULTURE ORGANIZATION OF THE UNITED NATIONS (FAO) (2003). In the second step, the highest (sw_{max}) and lowest (sw_{min}) value of the respective model time period was determined. To calculate the modeled soil water index (SWI_{HRU}), the actual soil water content (sw_{act}) was then put into relationship to the highest (sw_{max}) and lowest (sw_{min}) soil water content. Also the temporal resolution had to be adjusted. The SWI_{ERS} is calculated for every 10th day within a month. For comparison, the corresponding day has been extracted from the time series of the SWI_{HRU} .

3.3.3 Procedures for Evaluation of the Time Series at Footprint Scale

The comparison on the footprint scale will provide insight on the overall evolution of the time series at this scale. The modeling results for each HRU were used to calculate the area average. Here, the HRUs contribution is weighted according to the area covered within the footprint. The resulting average time series were compared to the SWI_{ERS} . Later, the decomposition of the time series into its trend and seasonal is used to analyze similarities and variations of trend in the time series components.

3.3.3.1 Decomposition of Time Series

In time series the observations made are arranged chronologically (HIPEL AND MCLEOD, 1994:P.63). The time series analysis examines these datasets and tries to find typical behaviors and trends (ASSENMACHER, 1998:P.195). Time series can be divided into three components: 1) trend component, 2) cyclical trend or seasonal component and 3) a random component (ASSENMACHER, 1998:P.197).

For the decomposition of time series two techniques can be used: nonparametric tests and parametric test (HIPEL AND MCLEOD, 1994). The parametric tests consider the absolute values and therefore the results are

affected by data distribution. The nonparametric tests, on the other side, use relative values or ranks and ignore the magnitude of observations (HIPEL AND MCLEOD, 1994:P.854). As a result, these tests might not provide information of the magnitude of the trend. For the decomposition of environmental data, however, time series nonparametric regression techniques are recommended because environmental data, such as data on water quality contain more information, which affects the application of parametric tests (HIRSCH AND SLACK, 1984: AS CITED IN HIPEL AND MCLEOD, 1994).

In this study, the decomposition of the time series into the seasonal and trend components has been carried out using the “stl”-Function (CLEVELAND, CLEVELAND ET AL., 1990) provided in the statistical software R (R DEVELOPMENT CORE TEAM, 2008). This function uses a nonparametric function in form of the local regression technique in order to predict the estimates in trend.

3.3.3.2 Agreement Criteria

The agreement between the two time series SWI_{ERS} and SWI_{HRU} in each component, had been evaluated using the coefficient of determination (R^2) (ROGERSON, 2006), bias as well as the root mean square error (RMSE). The later ones are described in the following sections.

Bias

The bias (WAGNER, SCIPAL ET AL., 2003) determines the difference in the soil water content between the satellite derived values (SWI_{ERS}) and the modeled content (SWI_{HRU}). The value n describes the number of time steps in the analysis.

$$bias = 1 - \frac{\sum_{i=1}^n (SWI_{ERS})_i - (SWI_{HRU})_i}{n} \quad \text{Equation 3-20}$$

The Root Mean Square Error

The RMSE defines the average magnitude of the error. A value of zero would describe the perfect fit between the two analyzed variables.

$$RMSE = \sqrt{\frac{\sum_{i=1}^n ((SWI_{ERS})_i - (SWI_{HRU})_i)^2}{n}}$$

Equation 3-21

3.3.3.3 Procedures for Evaluation of the Time Series at HRU Scale

Based on the findings of the authors CROW, RYU ET AL. (2005), DE LANNOY, HOUSER ET AL. (2007) and WAGNER, PATHE ET AL. (SUBMITTED) a linear regression was used in this study as a base for developing of the downscaling approach. However, the preliminary analysis, described in *Section 5.3.3*, reveals that precipitation is an important predictor in the model and has to be taken into account. Therefore, the applied model *Equation 3-23* includes the sum of the precipitation between two ERS-observations (*Equation 3-22*) as an independent variable. Also, a further analysis of the resulting distribution of the scaling parameters within all possible landscape parameter combinations will determine the range of uncertainty according to the respective class properties.

$$P_{sum(HRU)} = \sum_{i=1}^n P_{d(HRU)}$$

Equation 3-22

$$SWI_{HRU} = m_1 * SWI_{ERS} + m_2 * P_{sum(HRU)} + d$$

Equation 3-23

- $P_{d(HRU)}$ = Daily precipitation of the specific HRU in mm
- $P_{sum(HRU)}$ = Precipitation sum between two SWI_{ERS} calculations of the specific HRU
- n = Number of days between two SWI_{ERS} calculations
- m_1 = Regression coefficient for SWI_{ERS} variable for a specific HRU
- m_2 = Regression coefficients for P_{sum} variable for a specific HRU
- SWI_{ERS} = ERS-Soil water index in %
- SWI_{HRU} = J2000-Soil water index of a specific HRU in %
- d = Intercept (point of intersection of the plane with the y-axis)

For every HRU an estimation of the specific multiple regression parameters m_1 , m_2 and d has been carried out. The factors m_1 , m_2 and d are calculated based on least-squares multiple regressions according to the following equations *Equation 3-25* to *Equation 3-27*.

$$\Delta SWI_{ERS} = SWI_{ERSi} - \overline{SWI_{ERS}} \quad \text{Equation 3-24}$$

$$\Delta SWI_{HRU} = SWI_{HRUi} - \overline{SWI_{HRU}}$$

$$\Delta P_{sum} = P_{sumi} - \overline{P_{sum}}$$

$$m_1 = \frac{\sum_{i=1}^n [(\Delta SWI_{ERS}) * (\Delta SWI_{HRU})] * \sum_{i=1}^n \Delta P_{sum} - \sum_{i=1}^n [(\Delta P_{sum}) * \Delta SWI_{HRU}] * \sum_{i=1}^n [(\Delta SWI_{ERS}) * (\Delta P_{sum})]}{\sum_{i=1}^n (\Delta SWI_{ERS})^2 * \sum_{i=1}^n (\Delta P_{sum})^2 - (\sum_{i=1}^n [(\Delta SWI_{ERS}) * (\Delta P_{sum})])^2}$$

Equation 3-25

$$m_2 = \frac{\sum_{i=1}^n [(\Delta P_{sum}) * (\Delta SWI_{HRU})] * \sum_{i=1}^n \Delta SWI_{ERS} - \sum_{i=1}^n [(SWI_{ERS}) * \Delta SWI_{HRU}] * \sum_{i=1}^n [(\Delta SWI_{ERS}) * (\Delta P_{sum})]}{\sum_{i=1}^n (\Delta SWI_{ERS})^2 * \sum_{i=1}^n (\Delta P_{sum})^2 - (\sum_{i=1}^n [(\Delta SWI_{ERS}) * (\Delta P_{sum})])^2}$$

Equation 3-26

$$d = \overline{SWI_{HRU}} - m_1 * \overline{SWI_{ERS}} - m_2 * \overline{P_{sum}} \quad \text{Equation 3-27}$$

It is assumed that the regression parameters m_1 , m_2 and d can be described as functions of landscape parameter combinations (land cover, soil, slope, aspect and geology). For example, HRUs characterized by woodland over a soil with clay content between 10-25 % on a north facing hillside sloping between 5-15 ° will have different m_1 , m_2 and d parameters than a HRU with the same landscape parameters but covered by forest instead of woodland. Therefore, after calculation of the HRU specific regression parameters their dependency on the landscape parameter combinations was analyzed. For this purpose the corresponding value ranges of m_1 , m_2 and d values for all possible landscape parameter combinations (classes) were statistically evaluated using measures of descriptive statistics. To reduce the influence of outliers in describing the class properties the median and quintiles were used as decision criteria. Afterwards, the class corresponding medians of m_1 , m_2 and d were used to evaluate and validate the downscaling success of the macro-scale soil water estimates using the simulated time series of the second modeling time period. The coefficient of determination acted as quality criteria of the downscaling success and the derivation of the adequate regression parameters m_1 , m_2 and d for the possible landscape parameter combinations.

CHAPTER 4

STUDY AREA AND DATA BASE

The study area chosen had to fulfill certain requirements due to the constraints of the satellite technique. The transmitted signal of the satellite is not able to penetrate dense vegetation, such as forest. The SWI_{ERS} also cannot be derived in deserts, wetland areas and areas with permafrost. Since anthropogenic infrastructures also interfere with the backscattered signal, the goal was to find areas that primarily exhibit natural characteristic and have low anthropogenic influence.

Since a hydrological modeling was used to derive meso-scale soil water distribution, the study area should have data of sufficient quality and quantity to run the model.

The study area chosen was the Great Letaba River in South Africa. The catchment of the Great Letaba encompasses the quaternary catchments B81A-J and it is located in the north eastern part of the Northern Province of South Africa (*Figure 4-1*). The study area covers about 4,700 km² at the river gauge Letaba Ranch (23°39'29''S, 31°03'00''E) (DEPARTMENT OF WATER AFFAIRS AND FORESTRY, 2007). The catchment itself lies approximately between 23°20' S and 24°5' S latitude and 29°53' E and 31°03' E longitude. The altitude of this region ranges from 330 m above sea level at the catchment outlet to up to 2120 m above sea level at the foothills of the Great Escarpment (U.S. GEOLOGICAL SURVEY, 2003). Only one major city, Tzaneen, is located within the catchment.

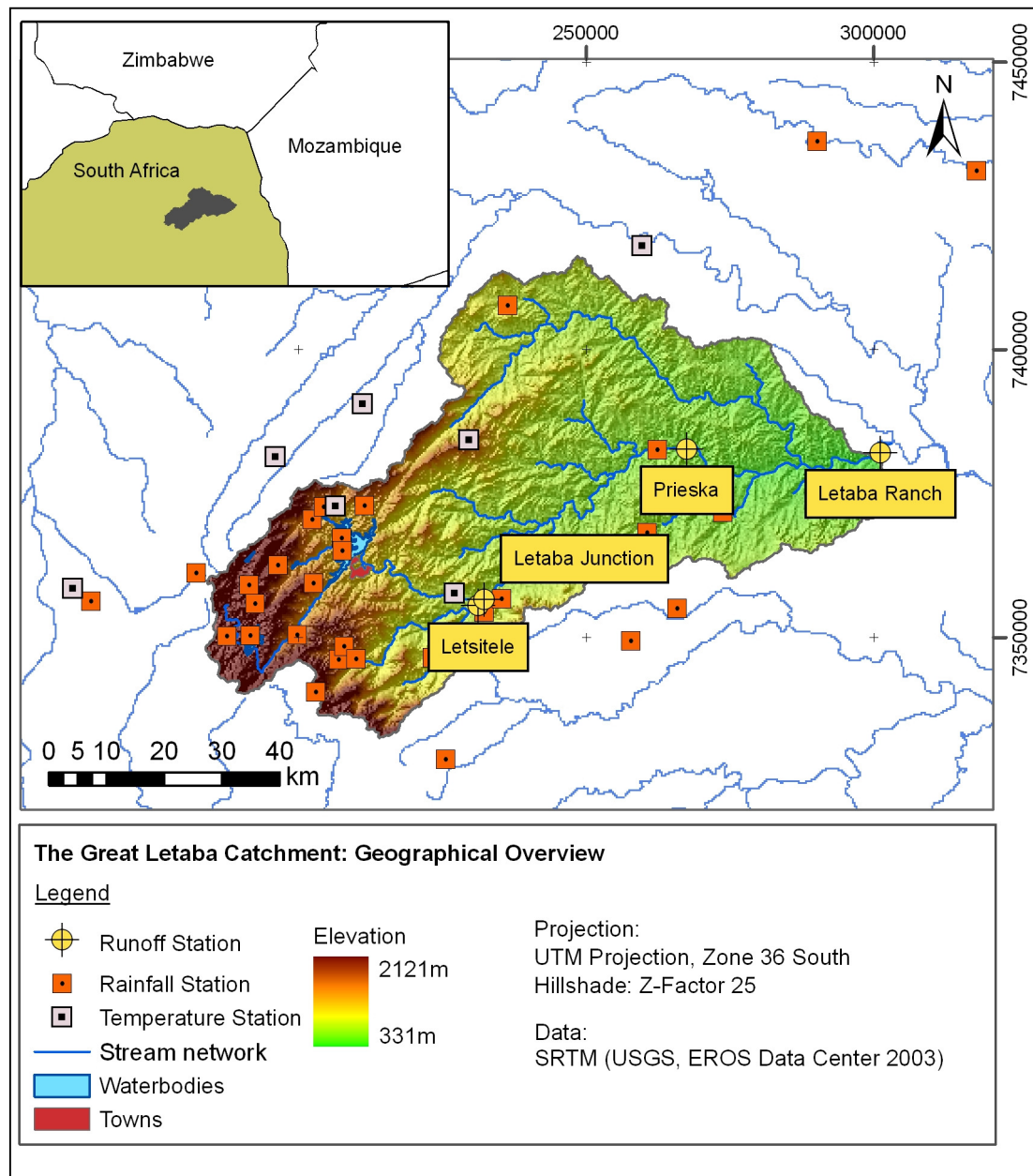


Figure 4-1: Geographic Location of the Study Area

4.1 Study Area

4.1.1 Climate

The major part of the Great Letaba catchment lie in the Bsh-climate zone according to the Köppen-Geiger Classification (GEIGER, 1961: AS CITED IN KOTTEK, GRIESER ET AL., 2006). This zone is characterized by a dry to semi-arid savanna climate, defined as having three to five months when precipitation exceeds evapotranspiration (LAUER AND FRANKENBERG, 1992). The mean annual

precipitation (MAP) amounts to approximately 760 mm (SCHEFFLER, KRAUSE ET AL., 2007). This value is based on the analysis of the 35 rainfall stations (available from 1980-1999) located within and outside of the catchment and using an inverse distance weighting method for interpolation (SHEPARD, 1968). *Figure 4-2* shows the spatial distribution of the MAP over the catchment.

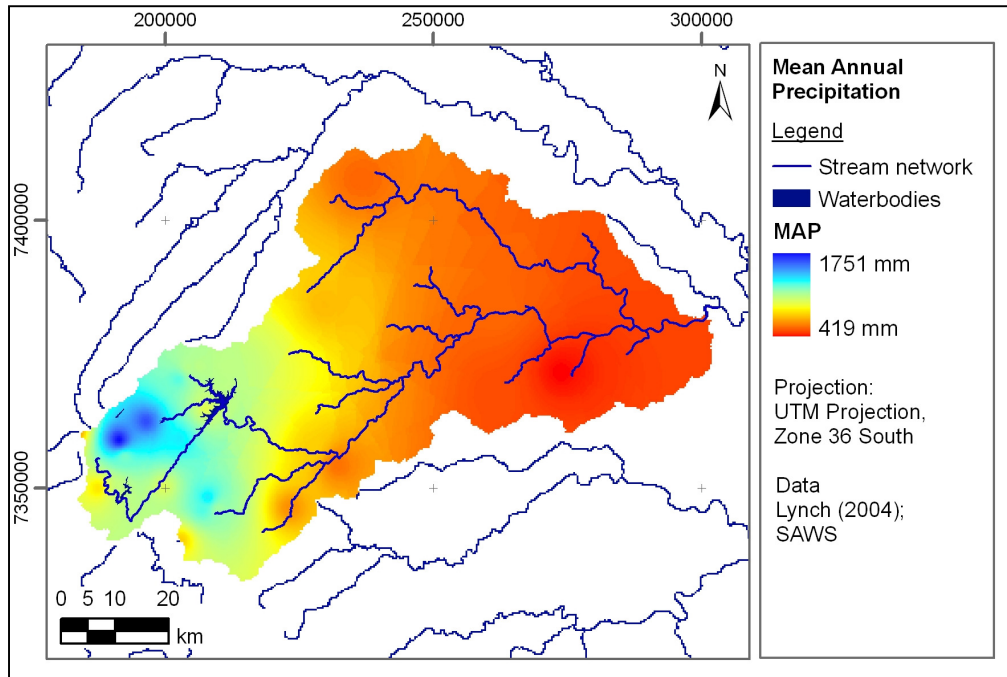


Figure 4-2: Spatial Distribution of the Yearly Rainfall Amount in the Catchment of the Great Letaba Derived from Inverse Distance Weighting Interpolation

The MAP ranges from 1751 mm in the mountainous area in the western part to approximately 419 mm in the eastern part of the catchment. According to TYPSON (1987:P.6) most of the summer rainfall is of convective origin. In addition to the high spatial distribution, the rainfall shows a high seasonality with a precipitation peak in the summer (between October and March), in which over 80 % of the annual rainfall is measured (TYPSON, 1987:P.1-2). As stated in SCHULZE, MAHARAJ ET AL. (1997:P.41-56), for the Northern Province the average value for the percentage of summer rainfall on MAP is 92 %, peaking in January (with December a close second monthly rainfall) (*Figure 4-3*). This value is approximately the same for the Great Letaba catchment in which over 85 % of precipitation occurs in the summer period and with a slight delay of its peak to February.

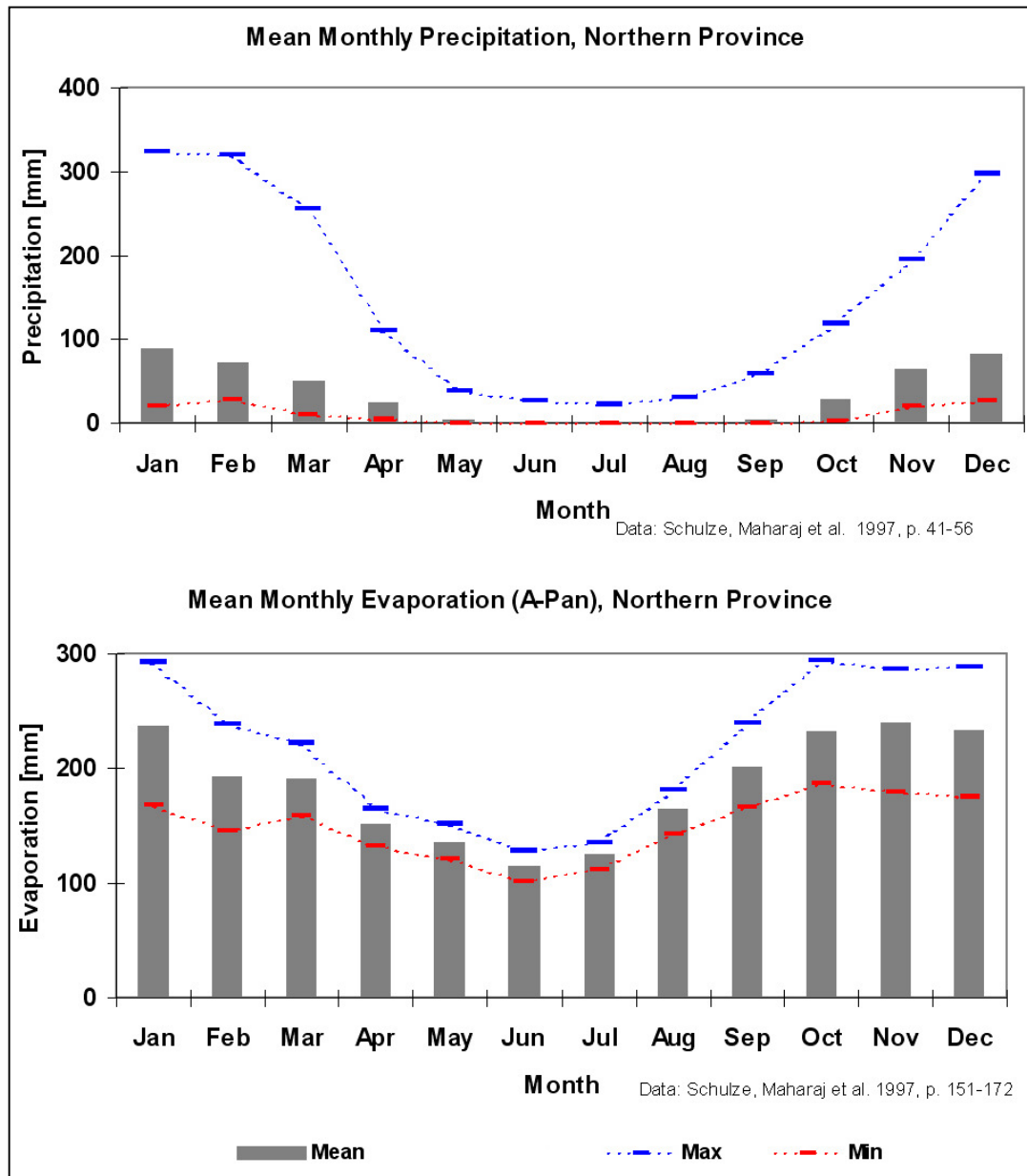


Figure 4-3: Monthly Mean Precipitation and Evaporation in the Northern Province (Data Source: Schulze, Maharaj et al. 1997)

The annual potential evaporation rate for Northern Province lays between 1787 and 2219 mm (A-Pan-Technique) (SCHULZE, MAHARAJ ET AL., 1997:P.152-172). Its seasonal distribution is shown in Figure 4-3. The highest evaporation rates are reached in early summer, i.e. November. During the winter time, the evaporation rate drops down to a mean of 125 mm. These values are also confirmed through a study carried out by MCKENZIE AND CRAIG (1999) in which the authors determined the evaporation rate for South Africa also using the A-Pan Method. Their analysis had a higher spatial distribution and values for the study area could be derived. The net evaporation in the

mountainous area reaches between 1000 to 1300 mm, whereas in the eastern part the net evaporation reaches between 1300 to 1600 mm. The highest net evaporation was estimated for the central part with values between 1600 and 1900 mm (MCKENZIE AND CRAIG, 1999:P.6-5)

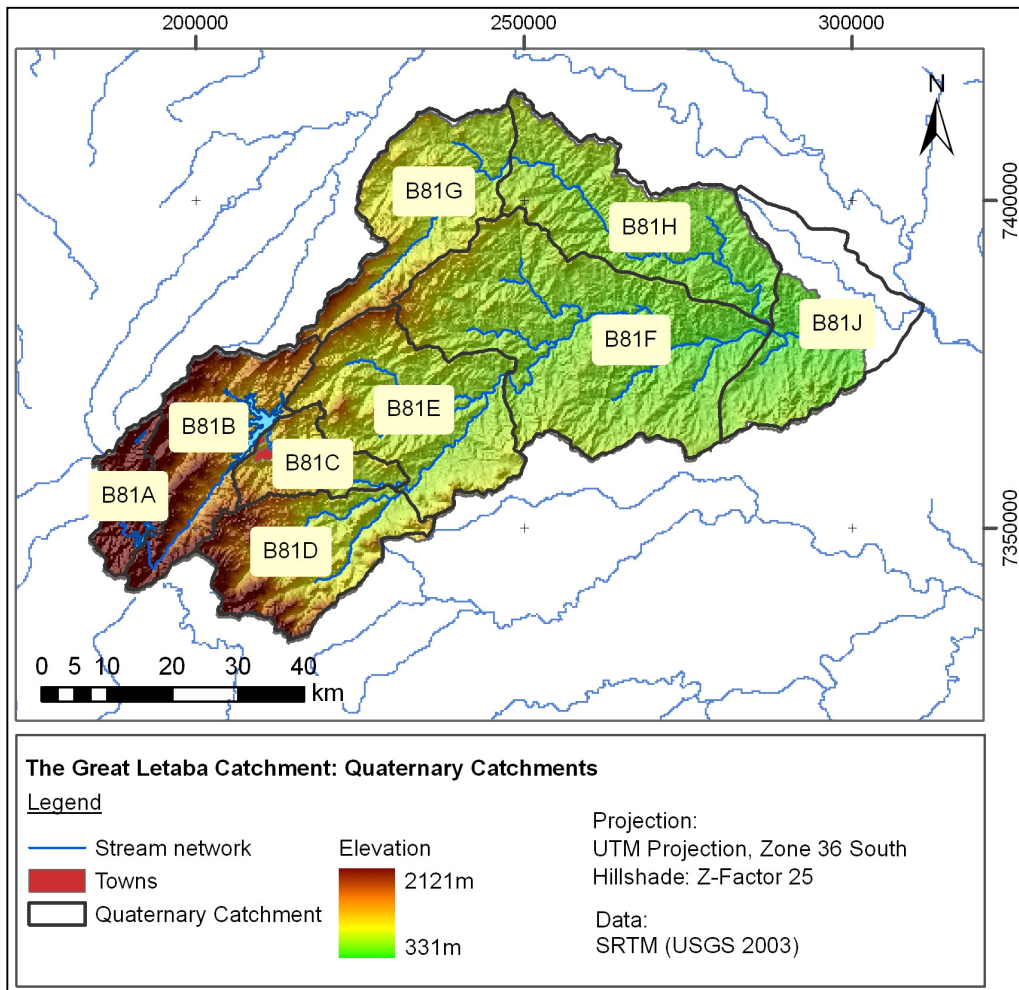
In the Northern Province, the temperature ranges from an average minimum of 9° C (SCHULZE, MAHARAJ ET AL., 1997:P.93-98) during the winter time to an average maximum of 28.1° C (SCHULZE, MAHARAJ ET AL., 1997:P.93-98) in summer.

4.1.2 Runoff and Water balance

The Great Letaba River is a tributary of the Olifants River, one of the most important rivers in southern Africa. The most important tributaries in the Great Letaba catchment are the Molototsi, Thabina and Letsitele.

Dams and weirs were installed along the Great Letaba River to compensate for the limited water resources, caused by the high spatial and temporal variation of rainfall (DEPARTMENT OF WATER AFFAIRS AND FORESTRY AND DIRECTORATE: NATIONAL WATER RESOURCE PLANNING (NORTH), 2004). The most important dams are the Tzaneen Dam with a capacity of 157.6 million m³, the Ebenezer Dam with a capacity of 70 million m³ and the Magoebaskloof Dam with a capacity of 4.91 million m³ (DEPARTMENT OF WATER AFFAIRS AND FORESTRY AND DIRECTORATE: NATIONAL WATER RESOURCE PLANNING (NORTH), 2004: APPENDIX F). The dams are for domestic, industrial and irrigation purposes. In addition there are four schemes to transfer water out of the Great Letaba catchment. In 2000, about 10.7 million m³ water were transported into the surrounding catchments (DEPARTMENT OF WATER AFFAIRS AND FORESTRY, 2003A).

As discussed above, semi-arid environments are characterized by highly spatially distributed rainfall events which result in an accordingly high spatial distribution of runoff generation (HERALD, 1989:P.4), expressed also in variability of the runoff-rainfall coefficient (RRC) within the different quaternary catchments, shown in the figure below.



QUATERNARY CATCHMENT (B81X)	MAP [MM]	MAR [MM]	RRC [%]
A	1194	378	32.0
B	1163	323	28.0
C	880	83	9.0
D	832	141	17.0
E	667	44	7.0
F	544	16	3.0
G	627	31	5.0
H	510	11	2.0
J	502	9.4	2.0
B 81	684	77	11.0

Figure 4-4: Location of the Quaternary Catchments and Runoff-Rainfall Coefficients for the Quaternary Catchments (Data Source: Midgeley, Pitman et al. (1994a: Appendix 8.6); Midgeley, Pitman et al. (1994b), Pitman and Middleton (1994)

Figure 4-4 shows a reduction of precipitation going from west to east and corresponding to a reduction of the mean annual runoff (MAR). Whereas in the

western part of the catchment (Quaternary catchment: B81A/B) approximately 30 % of the precipitation contributes to runoff, in the eastern part of the catchment only 2 % of the precipitation is measured as runoff. As shown in the table, on average only 77 mm of 684 mm measured precipitation is contributing to runoff. This corresponds to a RRC of 11 %. The majority of the precipitation water is used in evapotranspiration processes. MCKENZIE & CRAIG (1999) calculated evaporation losses for two flow rate scenarios for the Orange River in South Africa. For a flow release of 50 m³/s about 575 million m³/a (=18.23 m³/s – own calculation) water is evaporated (MCKENZIE AND CRAIG, 1999:7-2). This number corresponds to 36 % of the annual flow. In the second scenario, a flow rate of 400 m³/s resulted in evaporation losses of 989 million m³/a (= 31.36m³/s – own calculation) (MCKENZIE AND CRAIG, 1999:P.7-2), which corresponds to 7.8 % of the annual flow.

4.1.3 Geology

The geological formation of the Great Letaba catchment took place in the precambrian era (DU TOIT AND HAUGHTON, 1954; VEGTER, 1995) whereas the headwater region of the Great Letaba catchment has been formed through the Drakensberg activities during the proterozoic period and is thereby younger than the rest of the catchment.

Granite and diorite entities form the steep foothills of the Drakensberg Escarpment. The eastern part of the catchment is characterized by gneisses and granitoids (VEGTER, 2003:P.I) which show a higher potential for weathering and lead to a undulated surface.

The Great Letaba has its source in the foothills. In the mountainous area the Great Letaba shows a very interesting river course. According to OBST AND KAYSER (1949:P.105) the headwater river stream consists of two parts: first the river shows a meandering river course following a North-South-Line, and second, turning in the East-North-East direction and deeply carving into the material. OBST AND KAYSER (1949:P.105) found indication that the Great Letaba River was twice cutting back on itself through the mountains, followed by a connecting with an older river stream.

4.1.4 Soil

Soil formation depends on various factors such as geological bedrock, climate, overlaying vegetation, topography as well as groundwater (SCHEFFER AND SCHACHTSCHABEL, 2002:P.439).

The following map (Figure 4-5) shows the distribution of soil types based on the World Reference Base of Soil (WRB) classification (FAO, ISRIC ET AL., 1998) in the catchment of the Great Letaba River.

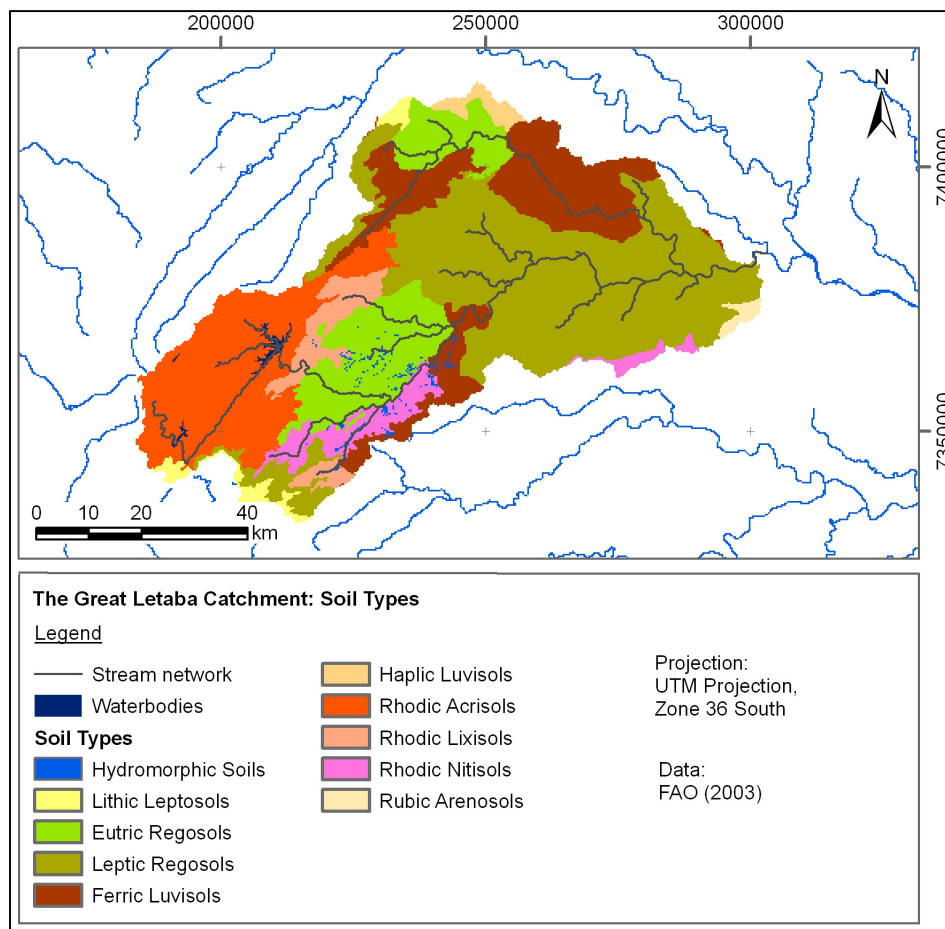


Figure 4-5: The WRB- Soil Types in the Catchment of the Great Letaba River

Rhodic Acrisols are found in the headwater of the Great Letaba River. This area is characterized by high rainfall amounts which have formed this deeply weathered soil type in that area. The Acrisols are characterized by “a higher clay content in the subsoil than in the topsoil” (FAO, ISRIC ET AL., 2006:P.67) due to leaching of the clay from the topsoil into the subsoil. The deep weathering also determined the low base saturation (FAO, ISRIC ET AL., 2006:P.67). Also found in the headwater are Lixisols, which have similar

characteristics as Acrisols. This soil type also shows weathering processes that lead to a higher clay content in the subsoil than in the topsoil. In comparison, Lixisols show a higher base saturation, which results in higher fertility and greater use for agriculture, including crops such as bananas and maize (FAO AND UNESCO, 1977:P. 208). Following the river stream downwards, Rhodic Nitisol developed, which is deeply weathered and characterized by a deep reddish color (FAO, ISRIC ET AL., 2006:P.87). According to the same source, this soil type develops over intermediate to basic parent material and is also found in more humid climates. In high elevations and steep areas Leptosols are found. This soil type is an azonal soil which only develops shallowly and is characteristic of mountainous areas (FAO, ISRIC ET AL., 2006:P.84). The Regosol is the most dominant soil in the catchment. This soil type is most commonly found in arid regions (FAO, ISRIC ET AL., 2006:P.92) and is characterized by a low water holding capacity and has been irrigated to be used for agricultural needs (FAO, ISRIC ET AL., 2006:P.92). The soil found in the area of the catchment outlet, the Arenosol, is also a poor soil for agricultural use. It has been developed over sand deposits and therefore contains a high sand percentage.

4.1.5 Land Cover and Land Use

The natural vegetation of the Great Letaba basin spans over the following Acocks Veld Types (ACOCKS, 1988; SCHULZE AND PIKE, 2004): the Inland Tropical Forest and the Tropical Bush Savanna. In order to derive the actual land cover, the National Land Cover (NLC) of South Africa (CSIR AND ARC, 2005) has been analyzed. This dataset includes 48 land cover classes. These classes are grouped according to *Section 5.2.1.1* and shown in *Figure 4-6*.

The high elevated (> 650 m asl.) areas are dominated by forests, especially monocultures of eucalyptus, pine and acacia. The lower elevations are characterized by savanna vegetation (bush- and woodland) which is interspersed by agriculture mainly along the river course. The intensive agriculture, however, leads to the problem of extensive soil exposure. Thus, in combination with the climatic conditions, these areas are affected by soil erosion.

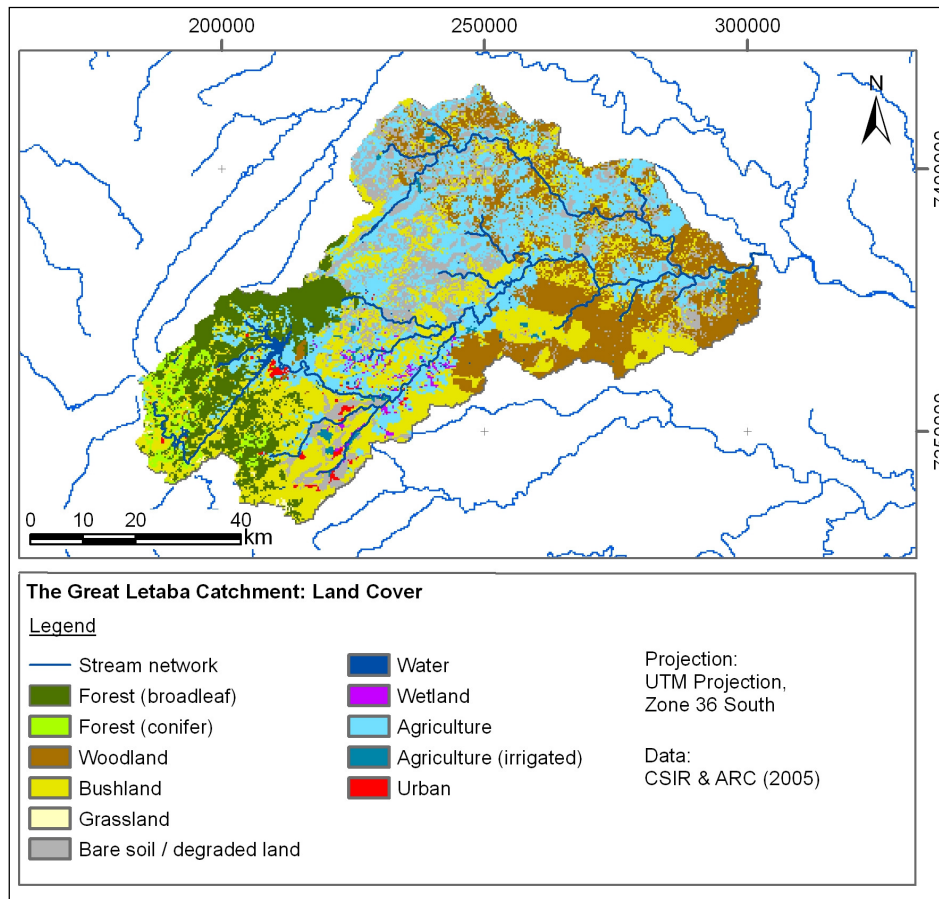


Figure 4-6: Reclassified Land Cover of the Great Letaba Catchment

Afforestation occurred in the high rainfall areas, located in the upper parts, of the Great Letaba catchment (DEPARTMENT OF WATER AFFAIRS AND FORESTRY AND DIRECTORATE: NATIONAL WATER RESOURCE PLANNING (NORTH), 2004). These activities resulted in monocultures of pine and eucalyptus; both are alien plants in South Africa (RICHARDSON AND VAN WILGEN, 2004). Those plantations had an impact on the natural environment. The plantation of eucalyptus, for instance, reduced the freshwater supply to the rivers due to its higher water demand (RICHARDSON AND VAN WILGEN, 2004:P.49). The DEPARTMENT OF WATER AFFAIRS AND FORESTRY AND DIRECTORATE: NATIONAL WATER RESOURCE PLANNING (NORTH) (2004) estimated the stream flow reduction due to afforestation to be 35 million m³ in the Great Letaba catchment.

Another important characteristic of the Great Letaba catchment is its importance for South African agriculture production. Due to the high annual variation of rainfall the crops have to be irrigated. The most common techniques in the area of the Great Letaba are flood irrigation, sprinkler and

micro systems (VAN VUUREN, JORDAAN ET AL., 2003:TABLE P. 3-25). Irrigation farming occurs perennially with a maxima in mid-summer (January / February) and mid- winter (July / August) (VAN VUUREN, JORDAAN ET AL., 2003:P.3-24). According to CSIR and ARC (2005) about 9 % of the agricultural area is under irrigation using about 161.9 million m³ water in 2000 (DEPARTMENT OF WATER AFFAIRS AND FORESTRY AND DIRECTORATE: NATIONAL WATER RESOURCE PLANNING (NORTH), 2004).

4.2 Data Base

4.2.1 Hydro-meteorological time series

For rainfall-runoff modeling of the Great Letaba River catchment the following daily hydro-meteorological time series have been used as input data.

4.2.1.1 Rainfall Data

The rainfall data used has been extracted from the rainfall database for southern Africa (LYNCH, 2004). This database contains rainfall observation between 1950 and 1999 from more than 12000 stations. The available stations in the catchment as well as in the surrounding areas were extracted and the proportion of patched values was analyzed. From that database 35 stations within and surrounding the catchment were extracted (*Appendix B*). For eight stations the amount of interpolated data is higher than 50 %. In a first model approach these stations were not used as model input. The model results, however, showed an under-simulation of runoff events. Therefore, the rainfall data from the neglected stations were compared with available runoff data. After an experiment to model the catchment with all 35 rainfall data the simulation improved, which indicated that the originally excluded stations were a good source of data. According to LYNCH (2004) the filling algorithm was based on a long term relationship (1903 to 2000). Within this time frame the stations had measurements for at least 57 % which corresponds to 55 years of data. Therefore, it can be assumed that the patched data are a good estimate of the actual rainfall amount and can be used in this study. The resulting rainfall network density amounts approximately seven stations per 1000 km².

4.2.1.2 *Temperature Data*

There were two data sources used for the temperature data (*Table 4-1*): 1) data were provided by the South African Weather Service (SAWS) and 2) data were extracted from the temperature database of SCHULZE AND MAHARAJ (2004) which contains daily minimum and maximum temperature data for the time period 1950 to 2000.

Table 4-1: Available Stations with Temperature Measurements

NUMBER	STATION NAME	START	END	LON	LAT	ELEVATION	SOURCE
0677802_BX	Pietersburg	1992	2004	29.45	-23.87	1250	SAWS
0678291_A	Pietersburg	1950	2000	29.40	-23.51	1295	Database
0679009_A	Goedgelegen	1950	2000	30.1	-23.39	753	Database
0679194_A	Duiwelskloo	1950	2000	30.7	-23.44	808	Database
0679274_W	Koedoesrivi	1950	2000	30.10	-23.34	732	Database
0679562_A	Letaba Letsitele	1950	2000	30.19	-23.52	520	Database
0679608_W	Modjadji	1950	2000	30.21	-23.38	975	Database
0681722_W	Mopani	1950	2000	31.25	-23.32	330	Database
0682141_W	Letaba	1950	2000	31.35	23.51	240	Database
0724260_W	Giyani	1950	2000	30.39	-23.20	472	Database
7220991_W	Mara	1992	2004	28.33	-24.90	897	SAWS
5895941_W	Warmbad	1992	2004	29.57	-23.15	1143	SAWS

The data extracted from the database are data which had been already filled. The percentage of filled data for the time frame between 1993 and 1999 is shown in *Table 4-2*. With the exception of the Letaba and Giyani stations, the percentage of filled data is below 10 % for the respective time frame.

Table 4-2: Percentage of Filled Minimum and Maximum Data from Lynch (2004)

STATION NUMBER	STATION NAME	% FILLED MAX TEMP	% FILLED MIN TEMP
0678291_A	Pietersburg	6	6
0679009_A	Goedgelegen	2	4
0679194_A	Duiwelskloo	2	7
0679274_W	Koedoesrivi	4	4
0679562_A	Letaba Letsitele	3	5
0679608_W	Modjadji	6	7
0681722_W	Mopani	6	7
0682141_W	Letaba	100	100
0724260_W	Giyani	8	11

For three stations Pietersburg, Warmbad and Mara data from both sources were available. Here, the difference between filled data (database value) and measured value (SAWS-value) was estimated and a quality analysis of the data base had been carried out (*Section 5.1.1*). This analysis showed that the filled data are a good estimated of the actual measured temperature.

4.2.1.3 *Additional Climatological Parameters*

The additional climatological parameters (wind speed, sunshine duration and relative humidity) were provided by the SAWS. Despite the existence of the Pietersburg station, measurements for these parameters within and in the area surrounding the catchment were not available or incomplete. Therefore, measurements of the Mara, Warmbad and Messina hydrometric stations, located up to 200 km away from the catchment, were taken into account, as shown in the following table.

Table 4-3: Additional Climatological Parameters

STATION NUMBER	STATION NAME	START RECORD	END RECORD	LON	LAT	ELEVATION	MEASURED PARAMETER
0677502_BX	Pietersburg	1993	2004	29.45	-23.87	1226	Rhum Wind
7220991_W	Mara	1993	2004	28.33	-24.90	897	Rhum
5895941_W	Warmbad	1993	2004	29.57	-23.15	1143	Rhum Sun
0809706_X	Messina	1993	2004	29.90	-22.27	525	Sun

The relative humidity was measured at three stations (Pietersburg, Warmbad and Mara). Two stations (Warmbad and Messina) recorded sunshine duration and only one station (Pietersburg) provided wind speed measurements.

4.2.1.4 *Runoff Data*

The runoff data was provided by the online database of the Department of Water Affairs and Forestry in South Africa (DEPARTMENT OF WATER AFFAIRS AND FORESTRY, 2003D). The catchment outlet is the hydrometric station B8h008 (Letaba Ranch), which went into operation in September 1959 (DEPARTMENT OF WATER AFFAIRS AND FORESTRY, 2003D) and has been delivering automatic

recordings since 1965. The structure, which is shown in *Figure 4-7*, is comprised of two sharp crested notches with gauging capacity of 0.585m (VILJOEN, 2006). The stage discharge relationship was updated two times during the operational period: in October 1986 and October 2002 (DEPARTMENT OF WATER AFFAIRS AND FORESTRY, 2003D).



Figure 4-7: The Gauging Station Letaba Ranch (Photo: Scheffler, March 2006)

4.2.2 Spatial Datasets (GIS-Datasets)

The J2000 modeling system uses distributed model entities as input. These entities are based on the concept of the HRUs (FLÜGEL, 1995; FLÜGEL, 1996) using GIS-datasets of land cover, soil, geology as well as a DEM. The datasets used in this study are summarized in *Table 4-4*. The shuttle radar topography mission (SRTM) dataset (U.S. GEOLOGICAL SURVEY EROS DATA CENTER AND NASA, 2007) provided information on topography parameters such as elevation, slope and aspect. Additionally, it was used to delineate the stream network, catchment borders and sub catchments. Information on soil type was derived from the Soil and Terrain Database for Southern Africa (FAO, 2003). This database contains vector datasets of this area; it also gives information on soil texture for the soil types in Southern Africa. The geological information was provided by the Department of Water Affairs and Forestry in form of a vector dataset of the hydrogeological maps (DEPARTMENT OF WATER

AFFAIRS AND FORESTRY, 2002; DEPARTMENT OF WATER AFFAIRS AND FORESTRY, 2003C; DEPARTMENT OF WATER AFFAIRS AND FORESTRY, 2003B). The land cover parameters (vegetation type, vegetation height) were obtained using the National Land Cover dataset of South Africa 2000 (CSIR AND ARC, 2005).

Table 4-4: GIS-datasets for the HRU-delineation

DATA-SET	DESCRIPTION	FORMAT	RES	SOURCE	MODEL-PARAMETER
DEM	Shuttle Radar Topography Mission (SRTM)	Raster	90m ²	US Geological Survey (2003, 2007)	Elevation Aspect Slope Stream network
Geology	Hydrogeol. Maps (Messina, Polokwane, Phalaborwa)	Vector	1:500.000	DWAF (2002, 2003)	Bed rock characteristics, Storage Capacity,
Soil	Soil and Terrain Database for Southern Africa	Vector	1:2Mill.	FAO 2003	Soil Texture
Land Cover	National Land cover (NLC) South Africa 2000	Raster	320 m ²	CSIR AND ARC (2005)	Vegetation Type, Rooting depth, Vegetation height

For the HRU delineation, all datasets should have the same spatial resolution as well as projection. Therefore, all datasets were transformed into the UTM-Projection, Zone 36 South with a spatial resolution of 100 m. Datasets, having a coarser spatial resolution, such as soil information, land cover, and geology have been resampled in ArcGIS 9.1 (ESRI, 2003) using the nearest neighborhood method.

4.2.3 The Remotely Sensed Soil Water Dataset

The remotely sensed soil water dataset, ERS-Soil Water Index (SWI_{ERS}), was derived from the ERS 1/2 and was provided by the Institute for Photogrammetry and Remote Sensing (IPF) at the Technical University Vienna. The dataset span a time frame from 1992 to 2000 and contains information on the soil water within the soil column with 10 day resolution.

CHAPTER 5

RESULTS AND DISCUSSION

In this chapter, the results of the study will be presented. The chapter is divided into three sections. First, in the data analysis section (*Section 5.1.1*), the input data will be checked for missing values as well as for plausibility. Subsequently, a system analysis will be carried out to investigate the data for indications of an influence on the hydrological response. Second, the conclusion drawn from this analysis will be used for the model calibration and validation (*Section 5.2*). The modeling outputs will also be investigated for their sensitivity to parameter changes. The conclusions will later be used to assess the downscaling results.

Third, to compare the meso-scale soil water time series with the macro-scale soil water time series, the area under investigation had to be determined (*Section 5.3.1*). After doing so, the model entities lying in this area of interest are averaged using the area weight, and then compared to the macro-scale soil water time series (*Section 5.3.2*). In this step, similarities and variations in long term (trend) and short term (seasonal) soil moisture will be highlighted. This analysis will give an insight on the evolution of the time series and therefore information on future behavior can be drawn. Based on these results, the downscaling scheme will be developed using the meso-scale soil water time series by applying a multiple regression model using precipitation and macro-

scale soil water time series as independent variables. The results will be presented in *Section 5.3*.

5.1 System Analysis and Delineation of Hydrological Response Units

5.1.1 Data Analysis and System Analysis

5.1.1.1 Rainfall Data Analysis

As documented in *Section 4.2.1.1*, the rainfall data needed in this study were collected by LYNCH (2004). Thirty five rainfall stations (*Figure 4-1*) in and surrounding the catchment area were extracted from this database and used in this study. As discussed in *Section 4.2.1.1*, the author filled the data using a combination of algorithms such as inverse distance weighting, expectation maximization algorithm, median ratio method and monthly infilling technique (LYNCH, 2004).

For each station the long term monthly and yearly statistical parameters mean, median, minimum, maximum and standard deviation were calculated for the time frame from 1980 to 1999 and summarized in *Appendix C*. The long term mean annual precipitation (MAP) amounts to between 416 and 1751 mm with a standard deviation ranging from 124 mm to 517 mm. The regression analysis reveals a very strong positive relationship between the standard deviation and the mean values ($R^2 = 0.90$). In other words, the year-to-year variability increases with an increasing MAP.

5.1.1.2 Runoff Data Analysis

The double mass approach, explained in 3.2.2, has been applied to analyze the runoff observation between stations along the Great Letaba River stream. *Figure 5-1* shows the double mass–analysis between the runoff stations Letaba Ranch and Prieska as well as Letsitele and Letaba Junction, whose locations are shown *Figure 4-1*.

The left hand side of *Figure 5-1* shows the double mass curve between the catchment outlet (Letaba Ranch) and the Prieska station, located approximately 43 km upstream from the Letaba Ranch station. On the right hand side of the figure, the double mass curve between the Letsitele and the Letaba Junction stations is illustrated. The Letsitele measuring station records the discharge of the Letsitele River, a tributary to the Great Letaba River. The Letaba Junction runoff station lays about 0.5 km before the Letsitele River joins the Great Letaba River. The two runoff stations are approximately 1.5 km apart from each other, shown in *Figure 4-1*.

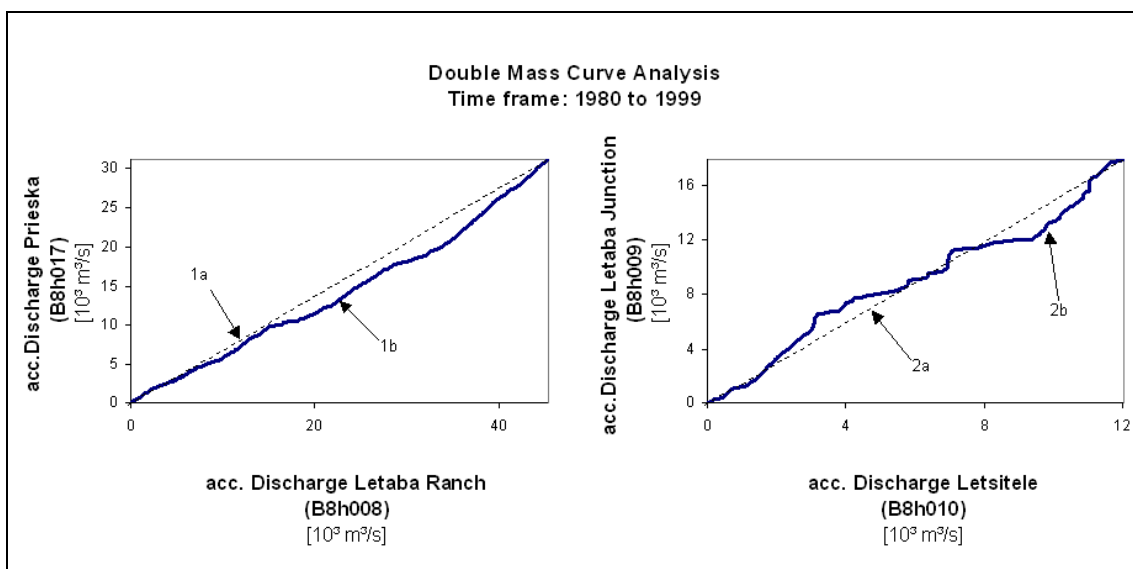


Figure 5-1: Double Mass Curve Analysis in the Great Letaba Catchment

Recall that the double mass curve analysis plots accumulated discharge recorded at the two sites. Under ordinary circumstances, the downstream site will record more water, but the relationship between the two sites should be linear. The double mass curve on the left side of *Figure 5-1*, shows that runoff relationship between the two station had been changed, and “more” runoff has been recorded at the outlet station (Great Letaba Ranch) than at the upstream station (Prieska) within the 1980 to 1999 time frame. The first 1/6 of the curve, covering the time period January 1980 to February 1982, is characterized by a nearly diagonal gradient to the dashed line (perfect fit). After that the curve bends towards the Great Letaba Ranch station, indicating more discharge has been recorded at this station (flag 1a). In February 1988 the curve shows nearly parallel gradient again until March 1992. At this point the double mass curve bends again toward the outlet station (flag 1b) with the “peak” by November

1996 and follows up to a parallel gradient again. The comparison of this curve with the MAP-data indicates that these characteristics could be explained by anthropogenic influences on the river discharge. The first section marks the time period until the end of 1982, characterized by an above average mean annual precipitation (MAP) (*Figure 5-2*). The years from 1982 to 1996, with the exception of two years 1985 and 1988 are characterized by low precipitation, whereas the years from 1996 to 1999 show above average MAP. Given the intensive agricultural activities in this catchment, the changes in slope can be explained by water uptake along the river before the Prieska station, especially during the years with low precipitation (1982 to 1996). The Great Letaba Ranch station measures the of the main channel of the Great Letaba River system and the Malotsi River, a river stream tributary that is only minor affected by irrigation (DEPARTMENT OF WATER AFFAIRS AND FORESTRY AND DIRECTORATE: NATIONAL WATER RESOURCE PLANNING (NORTH), 2004).

This argument of anthropogenic impacts on the stream flow volume is supported by the analysis of the second double mass curve on the right hand side of *Figure 5-1*. In this figure two bends are shown (flag 2a and 2b). The first bend (flag 2a) covers the time frame February 1981 to September 1988, indicating “less” recorded discharge at Letaba Junction. During this period the recorded precipitation was below average. The lower recorded discharge during that time period would be a sign of restricted water supply through the dams located upstream. The opposite situation has been illustrated in flag 2b. Here, “more” discharge has been measured at the Letaba Junction. The year 1996 marks the beginning of a time period of above average MAP. A comparison with allocation data from the dam located upstream, the Tzaneen dam, showed that the water supply from the dam was not restricted anymore and water was transferred into the river stream.

This double mass analysis indicates intensive anthropogenic regulation of the discharge. The discharge in the river stream is especially ruled by the major dams, Ebenezer dam and Tzaneen dam, located in the headwater of the catchment. To reduce the anthropogenic influence in the rainfall-runoff modeling, the catchment area of the dams was not taken into model calibration. The amount of water supplied in the river stream from the dams was used as an input dataset in J2000.

5.1.1.3 Temporal Relationship between Rainfall and Runoff in the Great Letaba River

The hydrological modeling of the catchment of Great Letaba River requires an understanding of the natural as well as anthropogenic influences on the runoff generation as shown in the preceding analysis. The rainfall-runoff interaction analysis was carried out for a longer time period (1980-1999) than in the actual study (1993-1999). This was done to gain more information on the system. The investigation focuses on the annual, seasonal and daily temporal scale.

Figure 5-2 compares the long term mean annual precipitation (blue bars) to the annual runoff sum (blue line), as well as the variation from the 20 years average for rainfall (blue filled bars) and runoff (blue unfilled bars).

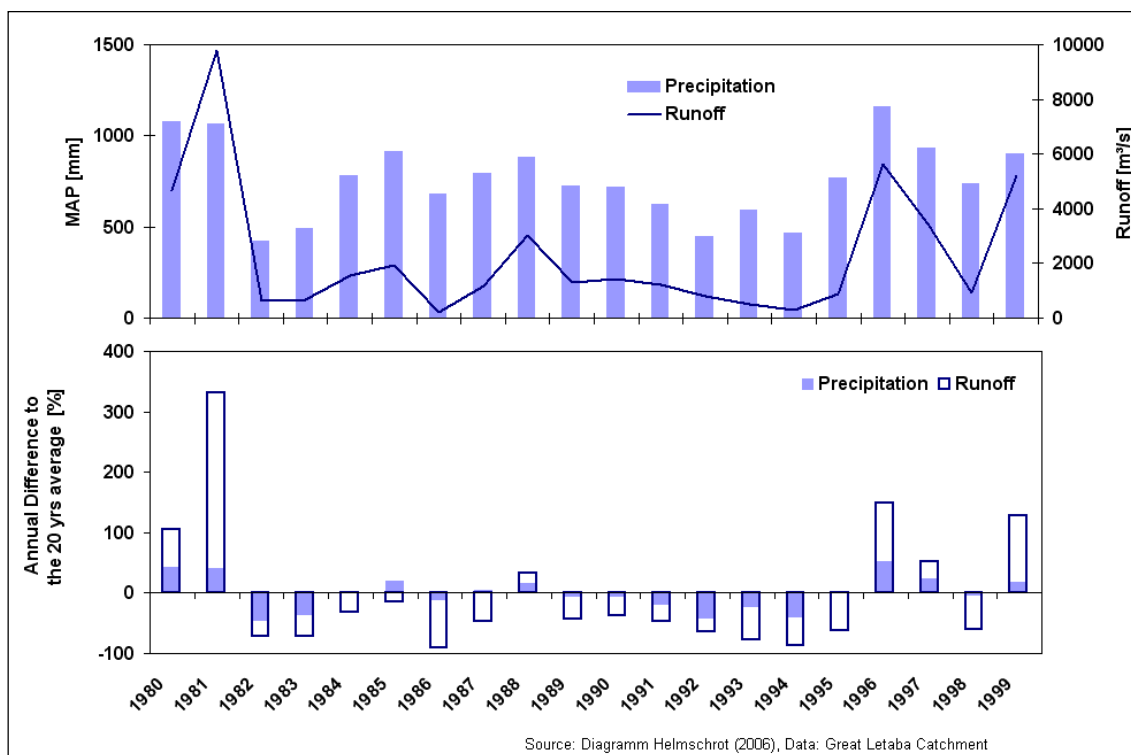


Figure 5-2: Long term (20 years) Evaluation of Precipitation and Runoff

The figure shows that the years 1980, 1981, 1985, 1988, 1996, 1997 and 1999 are characterized with rainfall above the 20 years average whereas in the years 1982, 1983, 1986, 1991-1994 MAP-values below average have been recorded. The years 1984, 1989, 1990, 1995 and 1998 are characterized with a MAP approximately on average. Comparing this with the recorded runoff it is shown that the runoff follows the precipitation dynamics. However, there are

some exceptions, which reflect the anthropogenic influence and the high water demand in this region. For example, in 1995 the MAP-annual rainfall is roughly on average, whereas the mean annual runoff (MAR) runoff was 61 % below average. Data from the DWAF on the actual water allocation of the Tzaneen dam shows that no water has been released from the dam. It can be assumed, therefore, that water was still taken from the river stream. Similar situations, in which the MAR was measured below under MAP can be found in the years 1985, 1989, 1990, 1995 and 1998.

In the next step, the seasonal variability has been studied. The Great Letaba catchment lies in the semi-arid climate zone with a strong distinction between the dry and wet seasons, as illustrated in *Figure 5-3*.

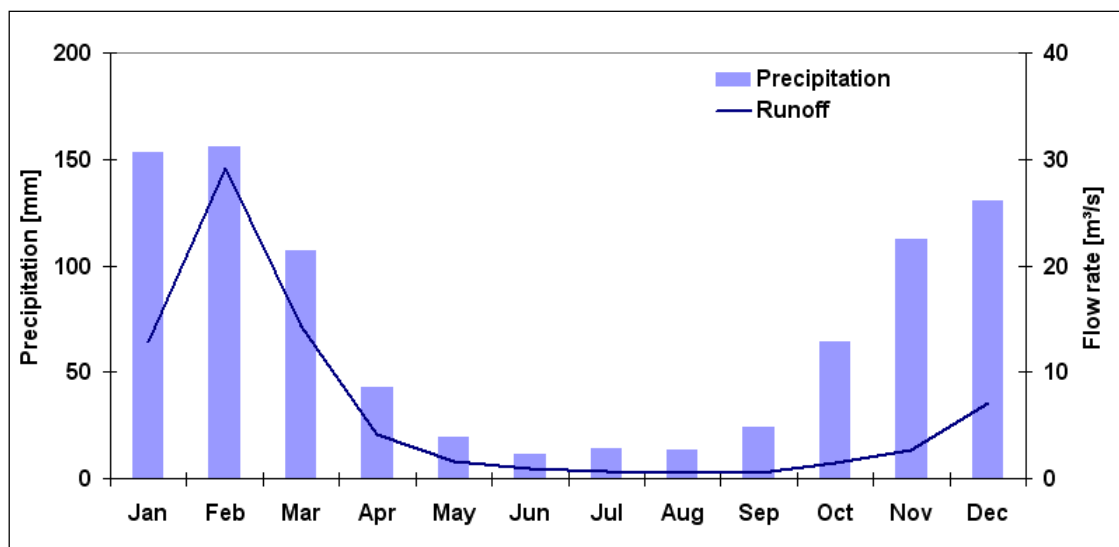


Figure 5-3: The 20 years Monthly Average of Precipitation and Runoff

Figure 5-3 compares the average monthly values of the runoff rate (black line) at the outlet of the catchment and the observed precipitation (grey bars). The picture is based on data from 1980 to 1999.

As shown in the figure, the temporal variability in rainfall amount varies between the dry and wet periods. In the wet period (October to March) about 723 mm, corresponding to 85 % of the annual rainfall, are recorded. In the dry season (April to September) the measured monthly rainfall amounts to less than 50 mm, whereas during June to August only 12 to 14 mm precipitation are documented. The high temporal variability is also reflected in the runoff, as shown in the differences between the low flow and high flow seasons (*Figure 5-3*). During the dry season, the average monthly flow rate falls under 1 m³/s. It also possible for the river to run dry and no runoff is observed. The wet season,

however, is characterized by high discharge values with a runoff peak in February corresponding to the precipitation peak.

In the following examination, the daily flows were analyzed. The daily flow varies depending on natural process behavior and natural extraction (evapotranspiration) as well as due to human influence (water extraction for irrigation purposes) along the river.

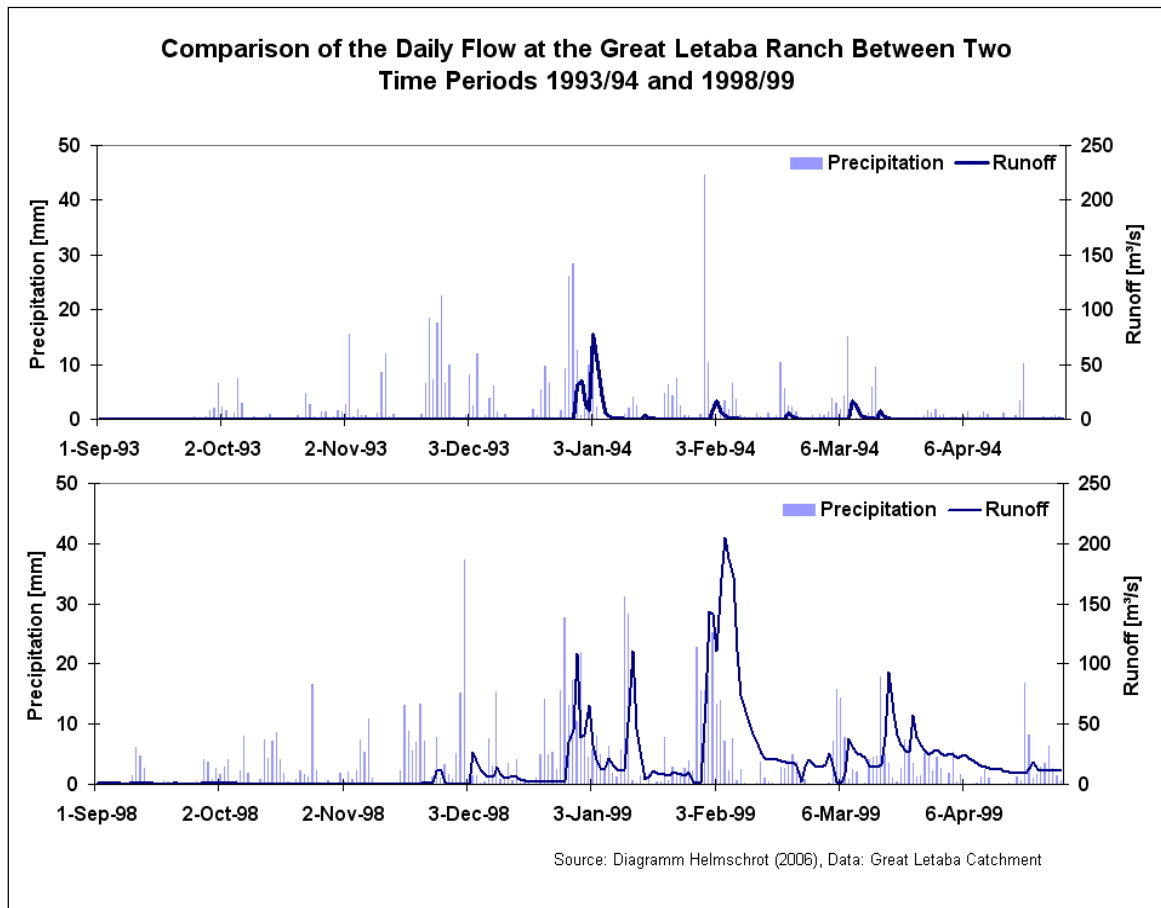


Figure 5-4: Comparison of the Daily Flow at the Great Letaba Ranch Between Two Time Periods 1993/94 and 1998/99

The figure shows daily runoff in comparison to daily rainfall for two time periods: the first figure is from the summer of 1993/94, representing a relatively “dry” year, and the second figure is from the summer of 1998/99, illustrating a “wet” year. In the wet year the runoff response to rainfall occurs earlier than in the dry year. During the wet year the first runoff occurs at the beginning of December. In the dry year, however, no discharge was observed until the end of December. This analysis indicates that the runoff might be generated due to accumulated precipitation between 300 and 350 mm.

5.1.1.4 *Analysis of the Additional Datasets*

Temperature

As shown in *Section 4.2.1.2*, the temperature estimates were taken from 12 stations within and surrounding the catchment and come from two data sources (*Figure 4-1, Table 4-1*). For three stations (Pietersburg, Warmbad and Mara) data from both data sources were available. Here, a regression analysis between the two datasets has been carried out. The calculated coefficient of determination amounted to between $R^2 = 0.97$ to $R^2 = 0.98$. The difference between filled data (database value) and measured value (SAWS-value) was estimated. It showed that for over 83 % of the filled values the difference to the actual value amounted to $\pm 3^\circ\text{C}$, whereas over 50 % of these were in the range of $\pm 1^\circ\text{C}$. These results justify taking the database with the filled data values as an input into the modeling. Also, the missing values within the SAWS-time series (Warmbad = 8 days, Mara = 1 day, Pietersburg= 4 months) were filled with the values from the database.

The data were used to calculate the mean monthly temperature for the timeframe of 1993 to 1999¹. The calculated mean temperature in the area of the Great Letaba catchment amounts to 19.5°C with the lowest mean temperatures in July with 14.6°C and the highest mean temperatures in December with 22.9°C . The minimum annual temperature reaches from 7.1°C in July to 18.7°C in January and the maximum annual temperature amounts to between 23°C in July to 29.7°C in January.

Humidity, Wind Speed and Sunshine Duration

Measurements at 8 am, 2 pm and 8 pm were available for humidity and wind speed. The daily mean average was calculated by averaging over these measurements. The mean values were calculated if at least two measurements of the specific day were available. If only one measurement during the day was available, this value has been compared the monthly mean value and its standard deviation. If the measured value was lying within the range of the standard deviation, the value was taken as a daily measurement. Otherwise that value was set as a missing value. The missing values were then filled using

¹ This calculation of the mean values is based on a simple average calculation. Due to their location, the stations Mara and Warmbad were not taken into account.

a regression analysis with a station nearby. Because wind speed is a chaotic component and has a local dependency, stations with a distance over 100 km from each other were not used to fill the missing values. Due to these requirements, only the Pietersburg station was used as input data for wind speed in the modelling system. For relative humidity the measurements of the Pietersburg, Mara and Warmbad stations were used as input data. For these stations the absolute humidity was calculated using *Equation 3-11* to *Equation 3-13*.

For sunshine duration only data measured outside of the catchment were available. After analyzing the missing values and carrying out regression analysis, the data of the Warmbad and Messina stations were used. For these time series only 2.3 % of the data were missing, which were filled using nearby stations.

Preparation of Macro-Scale Soil Water Index

The scatterometer derived soil water data were checked for missing values and one single missing value was found in the time series of the footprint ID393. To fill this value, the linear regression analysis between the time series of ID393 and ID394 as well as ID393 and ID376 was carried out. The resulting coefficient of determination (R^2) ranged from $R^2 = 0.94$ (ID 376) to $R^2 = 0.97$ (ID 394). Due to the higher R^2 between ID393 and ID394, the missing value was filled using the following linear relationship

$$SWI_{ID393} = 1.02 * SWI_{ID394} + 2.1 \quad \text{Equation 5-1}$$

5.1.1.5 Summary of the Data Analysis

In summary, the data were checked for missing values, and reliability. The data analysis reveals the hydrometric time series are fitting together and therefore will provide a sufficient database for direct input to the hydrologic model. The data analysis also showed an intensive anthropogenic influence on observed runoff data over the time period of the investigation.

Here, the following conclusions can be made. An intensive water infrastructure can be found in the headwater of the Great Letaba River. The analysis of rainfall and runoff data revealed that the time period from 1981 to

1988 was described by water shortage, since the double mass analysis revealed that the relationship between accumulated runoff changed. A comparison of water release data from Tzaneen dam with the double mass analysis indicate the time period from 1992 to 1996 as a time under water restriction. This changes in 1996 with the start of a period with above average MAP and the restriction on water supply was reversed. This was also seen in the double mass analysis by observing more water in the main channel. However, the second double mass analysis reveals intensive water uptake within the middle part of the river stream.

The anthropogenic influence has to be accounted for in the hydrological modeling. The catchment of the Tzaneen dam will be excluded during this procedure to reduce the influence of the dams on the model calibration. Since there are no data available to determine the actual water uptake along the river and the hydrological model does not take irrigation farming or water uptake into account, it will be expected that the modeled runoff simulation will overestimate some events.

5.1.2 Spatial Datasets

Table 4-4 shows the datasets used to delineate the HRUs used in the model. In order to achieve a common spatial resolution the raster datasets, land cover and the DEM, were resampled to 100 m. The vector datasets, the soil data and the geology dataset, were converted into raster files with a resolution of 100 m by applying the nearest neighbor method. All GIS-data files were then transformed into the UTM Projection, Zone 36 South.

The DEM delineated from the SRTM-data (U.S. GEOLOGICAL SURVEY EROS DATA CENTER AND NASA, 2007) was used to derive topographical parameters such as aspect and slope. Therefore, the dataset had to first be prepared and sinks had to be filled (KÄÄB, 2005; GROHMAN, KROENUNG ET AL., 2006) with the “fill” routine implemented in ArcInfo within ArcGIS Desktop 9.1 (ESRI, 2003). Afterwards, flow direction and flow accumulation were delineated in ArcInfo within ArcGIS Desktop 9.1 (ESRI, 2003). An accumulation threshold of 1000 cells was used for the delineation of the stream network. The resulting stream network was compared visually to the available topographic maps and corrected if necessary. Afterwards, the sub catchments were delineated using the ArcHydro-Tools (MAIDMENT, 2003) for ArcGIS Desktop. The location of

available hydrometric stations was corrected so that the runoff stations were located on the delineated stream network. As a result, 17 sub catchments with sizes from 104 to 619 km² were delineated.

The hydro-meteorological time series (*Table 4-1, Table 4-3, Appendix B*) are representing measurements at point scale. To obtain spatial information for these hydro-meteorological parameters, the measurements had to spatially generalized using the IDW- method implemented in J2000 (KRAUSE 2001) described in *Section 3.1.1.2*.

5.1.3 Delineation of Hydrological Response Units

The delineation of the HRUs consists of several steps, as shown in *Figure 5-5*. In the first step the individual GIS-datasets will be reclassified according to their hydrological significance. Then the prepared datasets will be overlaid on one another and, if necessary, reclassified again. Afterwards, small polygons under a certain threshold will be aggregated into neighboring polygons. Finally, the flow routing (topology) will be delineated for this final dataset and the resulting HRUs will act as model entities in the hydrological model. The following sections give a more detailed description of these steps.

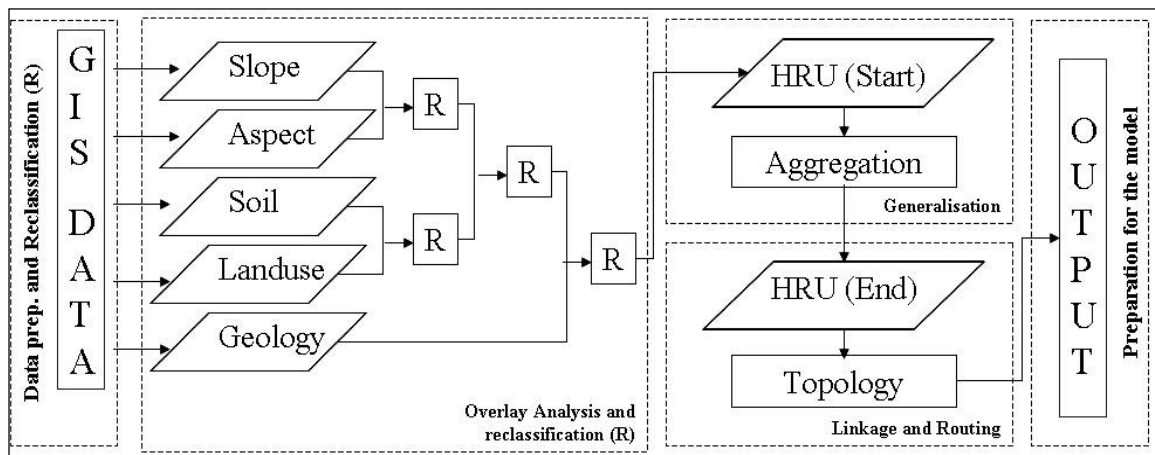


Figure 5-5: Flow-chart of the Delineation of HRUs (modified after Bäse, Helmschrot et al. (2006))

Data Preparation and Reclassification

The first step of the HRU-delineation involves data preparation and reclassification of the GIS-datasets. This is necessary to meet the requirements for the hydrological model (KRAUSE, 2001:P. 140). The single values of the

topography, slope, aspect, geology, soil and land cover datasets are reclassified according to their hydrological importance to reduce the number of HRUs.

The slope values were grouped into the following classes: low slope areas (0-5°), medium slope areas (5- 15°) and high slope areas (>15°) according to the work of BONGARTZ (2001). For the aspect, classes modified from BONGARTZ (2001) and HELMSCHROT (2006) have been used, as shown in *Table 5-1*.

Table 5-1: Classification of Aspect

CLASS	DESCRIPTION	ASPECT IN °
1	North	337.5 – 360; 0-22.5
	Northeast	22.5- 67.5
	Northwest	292.5 – 337.5
2	Southeast	112.5 – 157.5
	South	157.5 – 202.5
	Southwest	202.5- 247.5
3	West	247.5 – 292.5
	East	67.5 – 112.5

As discussed in *Section 2.3*, one of the most important factors for soil moisture generation is the soil texture, namely the particle composition of sand, silt and clay. The studies carried out by SALVE AND ALLEN-DIAZ (2001) showed a positive correlation between the clay content and the soil moisture content. Soils are dominated by clay particles that mainly show a coherent arrangement, which allows shrinking and swelling processes to take place (SCHEFFER AND SCHACHTSCHABEL, 2002:P.201). The swelling process leads to a reduction of the coarse pores and an increase of the amount of medium and fine pores in which water is stored (SCHEFFER AND SCHACHTSCHABEL, 2002:P.217). In the opposite process, shrinking, the stored water is slowly released to the surrounding area. Based on these findings the soil was grouped according to its clay content. After analyzing the available texture data of the soil dataset (FAO, 2003), the following classes were delineated.

Table 5-2: Classification of the Soil Types

SOIL GROUP	CLAY CONTENT[%]	FAO SOIL TYPES
1	<10	Rubic Arenosol
2	10-25	Lithic Leptosols Eutric Regosols Leptic Regosols
3	>25	Rhodic Acrisols Ferric Luvisols Haplic Luvisols Rhodic Lixisols Rhodic Nitisols
4	-	Wetland Soil

The first group describes the soil class with a very low clay content (below 10 %), accompanied with a low water holding capacity. The only soil type present in this group is the Arenosol, which is characterized by a sand content of up to 90 % (FAO, 2003). The second group summarizes soils with clay content between 10 and 25 %, including the Leptosol and Regosol soil types. The third group contains all the soil types with clay content more than 25 %. In this group the Lixisole, Acrisole, Nitisole and Luvisole types are included. The last group has been created because of the specific hydrological dynamics of wetland soils.

The land cover information was grouped into land cover classes, shown in *Table 5-3*. Distinction between the major land cover classes was made based on vegetation characteristics, such as vegetation height, rooting depth, leaf area index and stomata resistance. Smallholding urban areas were group to the surrounding land cover class. The field work showed that these areas are only mud hut with a small sealing of the soil, as shown in *Figure 5-6*.



Figure 5-6: Example of a Smallholding Area in South Africa (Photo: Scheffler, 2006)

Table 5-3: Classification of the Land Cover Classes (Source: CSIR and ARC (2005))

LAND COVER CLASS	LAND COVER CLASSES	DESCRIPTION
Broadleaf forest	1, 8, 10, 11, 12	Indigenous Forest and Forest Plantations of Acacia, Eucalyptus and others
Conifer forest	9	Forest Plantations (Pine)
Woodland	2, 39	Forest & Woodland; Smallholding Urban Area in Woodland Area
Bushland	0, 3, 4, 40, 41	Thicket & Bushland, Shrubland, Smallholding Urban Area in Bushland and Shrubland Areas
Grassland	5, 6, 7, 42	Herbland, Grassland (un- and improvement), Smallholding Urban Area Grassland
Bare soil and rocks	15,16,17,18,19,20,21, 22,36,37,38,47,48,49	Degraded Land (areas with low vegetation cover) Area of townships, Mineries
Water	13	Water
Wetland	14	Wetland
Agriculture	24,25,27,28,23,26,29	Agricultural Land (Cultivated and Uncultivated)
Urban Area	30,33,35,43,44,45,46 31,32,34	Urban Land (commercial, residential, Build-up)

The available geology information was grouped into only two classes, shown in *Table 5-4*. This is due to the fact that in the Great Letaba basin the underground material does not play an important role in runoff dynamics. As a

result, base flow does not contribute to the mean annual runoff in major parts of the catchment (VEGTER, 1995). It is only in the mountainous area, in the western part of the catchment, that the base flow contribution can reach up to 50 % (VEGTER, 1995: FIGURE 6).

Table 5-4: 1. Step of the Geology Classification

CLASS	DESCRIPTION	DWAF-CODE
1	Igneous Rocks Mafic / ultramafic intrusive rocks (dolerite, diabase, diorite, gabbro, dunite, pryoxenite, norite, anthrosite, hornblendite, carbonatite)	50
	Igneous Rocks Acid/ Intermediate, Alkaline intrusive rocks (various granitoide)	51
	Igneous Rocks Mafic/ ultramafic extrusive rocks	52
	Igneous Rocks Acid / intermediate/ alkaline extrusive rocks	53
	Metamorphic Rocks Predominately meta-argillaceous rocks (slate, phyllite, meta-pelite, schist, serperntine amphibolite, hornfels)	54
	Metamorphic Rocks Predominately meta-arenaceous rocks (quartzite, gneiss, migmatite, granuite)	55
	Metamorphic Rocks Predominately gneissoid rocks with xenoliths and undifferentiated metamorphic rocks	57
2	Sedimentary, Igneous and metamorphic rocks Undifferentiated rock and various mixed lithogies	58

The depth of the weathering layer is influenced by the topography, mainly by the slope. To take this control factor into account, the two geology classes were later further subdivided. For HRUs with slope values over 5° the weathering layer was determined to be at a depth of 2.5 m, leading to the following geology classes:

Table 5-5: 2. Step of the Geology Classification

GEOLOGY CLASS	DESCRIPTION
1	Fracture-bedrock aquifers with a weathering layer of 15 m depth
2	Sedimentary aquifers with a weathering layer of 15 m depth
3	Fracture-bedrock aquifers with a weathering layer of 2.5 m depth
4	Sedimentary aquifers with a weathering layer of 2.5 m depth

Overlay Analysis and Reclassification

The overlay of the GIS-datasets was carried out in successive steps as shown in *Figure 5-5*. The first overlay (aspect and slope) build Topography-Complex (TC) entities. Here, the number of classes was reduced by eliminating the aspect in classes with a slope $< 5^\circ$ due to the similar radiation input as flat surface (SCHULZE, MAHARAJ ET AL., 1997).

In a second overlay the Vegetation-Soil-Complexes (VSC) were created by overlaying soil and land cover. Classes with a pixel amount below 1000, which corresponds to 0.21 % of the catchment area, were added to a class with similar natural characteristics (e.g. grassland to bushland, woodland to broadleaf forest). After the reclassification of the VSC, the resulting VSC were overlaid with the TC. In this step, two major reclassification processes were undertaken: 1) Agriculture classes with slopes over 15° were transformed to bushland. The same procedure was applied to wetlands. Additionally about 3 % of the bushland area had been transformed to woodland with the same soil group, because the soil characteristics were set to a higher priority. In the last aggregation step, in woodland and forest classes with a slope below 5° , the east / west aspects have been transformed to a north aspect. SCHULZE, MAHARAJ ET AL. (1997:P.29-30) analyzed the solar radiation on different slopes and aspects. Their finding was that with a slope below 5° the radiation amount for North, NE/NW, as well as E/W facing aspects were comparable, whereas SE/SW and South facing aspects with the same slope showed a much higher radiation input. This has only been applied to areas with dense vegetation, such as woodland and forest. In the last step of the successive overlay processes the resulting Topography-Soil-Vegetation Complexes were overlaid with the geology groups. The reclassification process was done using the same parameter as before: The reclassification was only carried out with classes amounting to less than 1000 pixels. As a result of the generalization process 31830 HRUs were defined for the Great Letaba Catchment.

Generalization and Delineation of Linkage and Routing

After finishing the knowledge based aggregation, the resulting entities were overlaid with the sub catchments. The smallest polygons with an area below 10 Pixels ($<0.1 \text{ km}^2$), were then eliminated using the Dissolve Adjacent Polygons 1.7 Extension (JENNESS, 2005) in ArcView 3.0 (ESRI, 1997) with the

following options: 1) dissolve into polygon with longest adjacent border and 2) dissolve if polygons share a common border. A requirement for the polygon aggregation was that only polygons within the same sub catchment were eliminated, thereby ensuring that no water flow occurs across the watershed borders. The 31830 HRUs were generalized to 8051 HRU-Polygons and used as model entities for the J2000 model. The physical characteristics were assigned using the majority function for land cover, soil and geology. For elevation, slope and aspect mean values were calculated using the Landscape Management Analyst Extension (HURVITZ, LAST ACCESS 2007) for ArcView 3.0. The so resulted model entities cover the catchment of the Great Letaba River and same parts of its surrounding area. This was necessary because the scatterometer footprints are extend over the catchment boarder and in the further analysis the entire footprint area will be under investigation.

5.2 Rainfall–Runoff Modeling using J2000

5.2.1 Model Parameterization

The model requires separate parameter files for land cover, soil and ground water. Each land cover class consists of 23 land use parameters, each soil class of 24 soil parameters and each groundwater class of 4 groundwater parameters. The parameter values were taken from literature values and are explained in more detail in the following sections.

5.2.1.1 Land Cover Information

The J2000 model calculates the daily evapotranspiration rate based on the Penman-Monteith approach (MONTEITH, 1975). This approach estimates the evapotranspiration in the canopy layer using several vegetation parameters such as leaf area index (LAI), stomata resistance, rooting depth, and vegetation height. This information was retrieved from literature values, shown in *Table 5-6* for land cover classes. According to SCHULZE AND PIKE (2004) the vegetation growing period in this region of South Africa occurs between October and February. In the simulation of the rainfall-runoff dynamics the months September and March act as transition periods between the growing season and the season with no vegetation growth.

Table 5-6: Parameters of the Land Cover Classes for the Soil Water and Evapotranspiration Module

LAND COVER CLASS	ALB [-]	MAXIMUM BULK SURFACE CONDUCTANCE						LAI		EFFECTIVE HEIGHT		RD [DM]
		[SM-1]						[-]		[M]		
		1	2	3	4	5	6	D1	D2	D1	D2	
		7	8	9	10	11	12	D3	D4	D3	D4	
Forest (deciduous)	0.2	135	135	138	141	141	141	3	1.5	15	10	18
		141	141	138	135	135	135	1.5	3	10	15	
Forest (broadleaf)	0.12	140	140	160	179	179	179	3.5	2.7	10	10	14
		179	179	160	140	140	140	2.7	3.5	10	10	
Woodland	0.14	181	181	190	198	198	198	3	1	5	2	12
		198	198	190	181	181	181	1	3	2	5	
Bushland	0.18	170	170	205	240	240	240	3	0.5	3	1	10
		240	240	205	170	170	170	0.5	3	1	3	
Grassland	0.24	150	150	200	250	250	250	1.5	0.5	1	0.5	8
		250	250	200	150	150	150	0.5	1.5	0.5	1	
Bare soil and sparse vegetation	0.1	140	140	155	170	170	170	1	1	0.6	0.3	10
		170	170	155	140	140	140	1	1	0.3	0.6	
Water	0.06	20	20	20	20	20	20	1	1	0.1	0.1	0
		20	20	20	20	20	20	1	1	0.1	0.1	
Wetland	0.2	55	55	67	80	80	80	3	1.5	2	1	10
		80	80	70	55	55	55	1.5	3	1	2	
Agriculture	0.18	90	90	105	120	120	120	3	1	2	1.5	15
		120	120	105	90	90	90	1	3	2	1.5	
Urban areas	0.1	90	90	90	90	90	90	1	1	5	5	2
		90	90	90	90	90	90	1	1	5	5	

(The values in the table above are taken from: Matthews (1984: as cited in Center for Environmental Remote Sensing Chiba University, 2006), Koerner (1995), Kelliher, Leuning et al. (1995), CSIR and ARC (2005), Schulze (1995), Canadell, Jackson et al. (1996), Breuer and Frede (2003), Schenk and Jackson (2002), Krause (2001), Kim and Lee (2004))

5.2.1.2 Information on Soil Data

The soil information was taken from the Soil and Terrain Database for Southern Africa (SOTERSAF). That database contains field measurements with information on soil type and its texture. Several measurements are available for each soil type. The database unfortunately did not contain any field probe within the study area. To achieve representative soil texture characteristics for the soil types found in the study area, the available soil texture information was averaged according to the soil type and later the values for each soil type were

averaged according to the soil groups. The field capacity and air capacity parameters were derived from ARBEITSGRUPPE BODEN (1994) and AD-HOC ARBEITSGRUPPE BODEN AND SPONAGEL, H. (2005) assuming a soil density of four to five for the top soil horizon and a soil density of three for the lower horizons.

Table 5-7: Parameters of the Soil Classes for the Soil Water Module

SG	D [CM]	AC [MM]	AVAILABLE FIELD CAPACITY												
			[MM/DM]												
			1	2	3	4	5	6	7	8	9	10	11	12	13
			14	15	16	17	18	19	20	21	22	23	24	25	26
1	125	212.5	13.5	13.5	18.5	18.5	18.5	18.5	18.5	18.5	18.5	18.5	18.5	18.5	-
			-	-	-	-	-	-	-	-	-	-	-	-	-
2	139	150	14.5	21	21	21	21	20.5	20.5	20.5	20.5	20.5	20.5	20.5	20.5
			-	-	-	-	-	-	-	-	-	-	-	-	-
3	254	129.8	12	12	21.5	21.5	21.5	21.5	21.5	21.5	21.5	21.5	21.5	21.5	21.5
			21.5	21.5	21.5	21.5	21.5	21.5	21.5	21.5	21.5	21.5	21.5	21.5	21.5
4	110	59.0	55	55	55	55	55	21.5	21.5	21.5	21.5	21.5	21.5	-	-
			-	-	-	-	-	-	-	-	-	-	-	-	-

In addition to these input soil parameters, J2000 has two parameters to adapt the field capacity and air capacity. The available field capacity defines the upper boundary water available to plants. The parameter values shown in the table above are mean values for each of these soil classes. The hydrological modeling with the initial values showed a tremendous overestimation by the model which could not be explained by the aforementioned water uptake along the river. To reduce this overestimation, the field capacity values were adapted by a factor of 1.5. However, in the sensitivity analysis this value was changed and the results and consequences analyzed.

5.2.1.3 *Information on Geology Data*

In the groundwater module the base flow components are divided into the fast (RG1) and the slow base flow (RG2) component. For each base flow component the module requires to define the maximum storage capacity (RG1_{max}, RG2_{max}) and a coefficient determining the retention time (RG1_K, RG2_K). The applied coefficients are shown in the table below.

Table 5-8: Parameters of the Geology classes for the Groundwater Module

GEOLOGY CLASS	RG1 MAX	RG2 MAX	RG1_K	RG2_K
1	1000	1200	8	250
2	2500	2000	14	100
3	40	600	8	250
4	125	1000	14	100

(The values in the table above modified from: Davis and DeWiest (1966), Krause (2001), Vegter (2003)).

The parameters $RG1_{max}$ and $RG2_{max}$ were calculated using the suggested calculation method after KRAUSE (2001:P.157).

5.2.2 Modeling Results

Semi-arid areas are characterized by a strong seasonal rainfall accompanied by high evapotranspiration rates. The soil water content can drop tremendously, especially during the dry season. ARCHER, HESS ET AL. (2002) studied a field site in southeastern Spain and they found that the soil moisture was dropping down to the wilting point during the dry season. Therefore, the parameters of the soil water module and groundwater module within J2000 were set for depletion of the medium pore storage and by doing so to have a better representation of the soil water generation.

The runoff-precipitation simulation of the Great Letaba River has been carried out for the time frame between 1993 and 1999 in which February 1993 to September 1997 was used as a calibration period and October 1997 to December 1999 as a validation period. The simulation results are presented in the following figure.

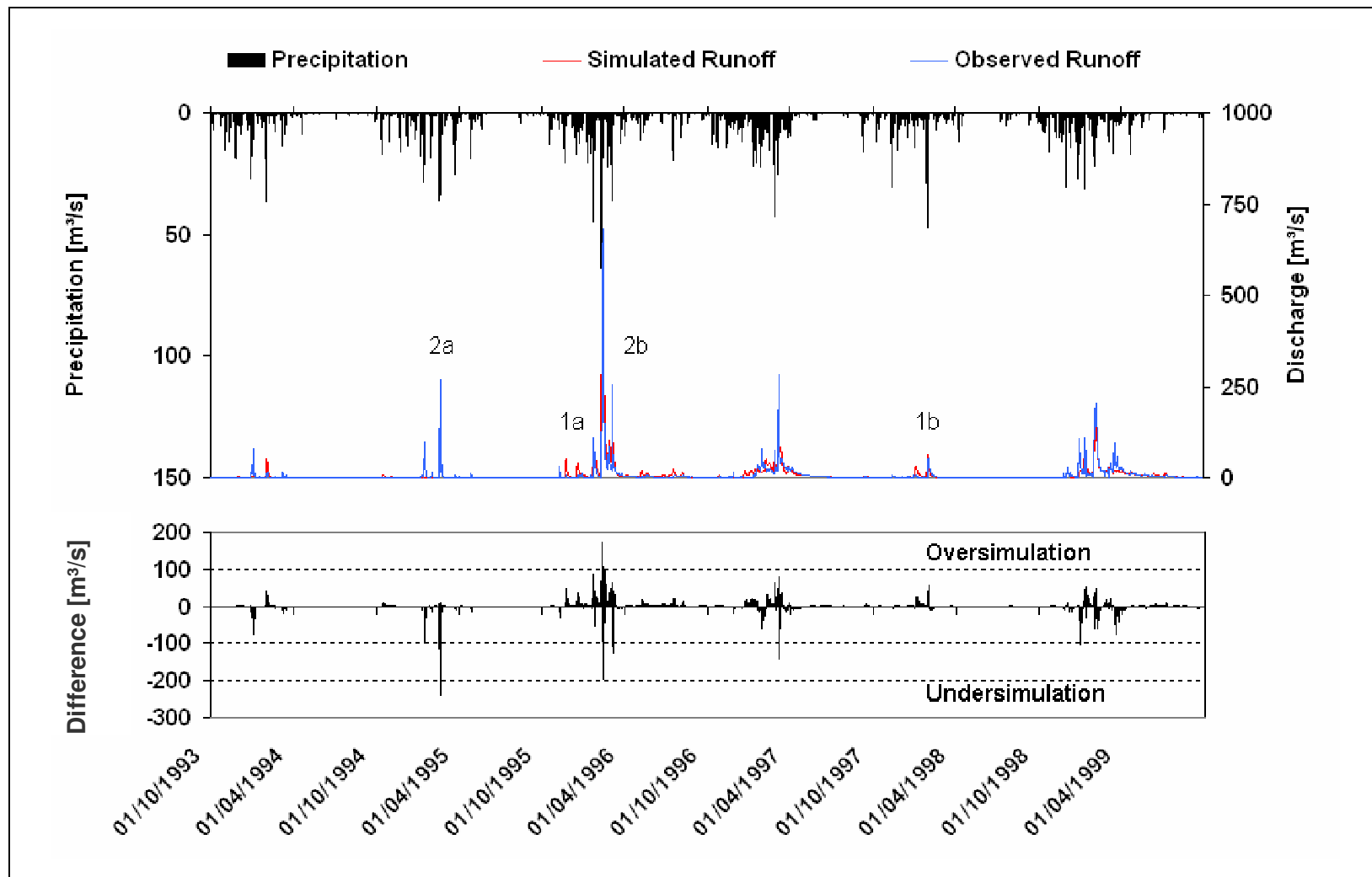


Figure 5-7: Simulated Hydrological Dynamics with the Distributed Model J2000, Great Letaba River Catchment (Without Catchment of the Tzaneen Dam)

The simulated hydrological dynamics (blue line) are shown in comparison to the observed runoff (red line) in the upper figure. The black columns reflect the daily catchment precipitation. The lower figure displays the difference between observed and simulated runoff and highlights over- and under simulation. The figure illustrates that the J2000 model is able to predict the runoff dynamics of the Great Letaba River.

Table 5-9: Efficiency Criteria for the Simulation

TIME PERIOD	EFFICIENCY CRITERIA			
	NAS	LOG. NAS	R ²	AVE [M ³ /s]
1993-1997 (Calibration)	0.80	0.36	0.81	1653
1997-1999 (Validation)	0.77	0.62	0.77	169

With the exception of the log NaS value (log NaS = 0.36), the efficiencies in Table 5-9 show a good model fit. However, as discussed in SCHEFFLER, BÄSE ET AL. (2007), the first half of the calibration period (1993 to 1995) was below MAP. This period was characterized by seasonal dry periods up to seven months in which no runoff was measured. This seasonality of the observed river runoff was not simulated by the model. The validation period, however, shows a very good value of the log. NaS (log. NaS = 0.62). During this period the river never runs dry, mainly as a result of higher precipitation during the years 1996 to 1999 in comparison to the time period 1992 to 1995. However, regardless of better model efficiencies some overall modeling problems remain:

1) Over prediction of single events

The representation of single events, such as the over-prediction of the observed runoff at the beginning of the summer 1995/96 (flag 1a, Figure 5-7) is deficient. Analysis of the precipitation data showed that a precipitation event in the headwater of the Letsitele River, a tributary of the Great Letaba River, was the main cause of the runoff event. This was also confirmed through measured runoff data at the Letsitele gauge station. Examination of the runoff data along the course of the Great Letaba River showed that the runoff continuously decreased because of evaporation losses (MCKENZIE AND CRAIG, 1999) and water extraction due to irrigation (DEPARTMENT OF WATER AFFAIRS AND FORESTRY, 2003A; DEPARTMENT OF WATER AFFAIRS AND FORESTRY AND

DIRECTORATE: NATIONAL WATER RESOURCE PLANNING (NORTH), 2004). Both of these factors are not yet considered in J2000. The hydrological dynamics of the Great Letaba River is mainly influenced by irrigation farming and dams, which were built for this purpose. Due to the low precipitation that characterized the 1988 to 1995 time period (*Figure 5-2*) it can be assumed that the dams along the river course contained only a limited amount of water at this time. The runoff reduction at the beginning of the rainy season 1995/96 can be partially explained through backfilling of the dams. Flag (1b) in *Figure 5-7* shows a similar situation for which it is assumed that the runoff reduction has been caused by water extraction along the river course.

2) Under prediction of single events

The modeling results showed an under simulation of single events during the rainy season e.g. in the year 1994/95 (flag 2a, *Figure 5-7*). In order to clarify that under simulation, data from runoff stations along the river were analyzed. The analysis of these data showed that the runoff has its source in the area between the catchment outlet and the Letsitele river station. Also, a comparison of the six stations in this 3000 km² expanse showed that precipitation had been recorded in this area but the total amount of these events can not explain the observed runoff. Therefore, it can be argued that the density of precipitation stations in this area is not able to measure local precipitation events and leads to the conclusion that the precipitation can be underestimated. Flag 2b in *Figure 5-7* refers to similar situations for which an underestimation of the precipitation might cause the under prediction of the runoff by the model.

Verification of the Modeling Results

Table 5-10 shows the calculated water budget components for the modeled time period from 1993 to 1999.

Table 5-10: Water Budget Components for the Entire Modeled Period (1993 to 1999)

YEAR	P [MM]	PET [MM]	AET [MM]	Δ STOR [MM]	Q _{SIM} [MM]	Q _{OBS} [MM]
1993/94	507	1585	498	3	6	7
1994/95	596	1590	592	-1	6	14
1995/96	1046	1359	861	49	135	104
1996/97	808	1398	774	-39	73	64
1997/98	478	1634	473	-10	15	11
1998/99	856	1408	817	-41	80	87
Mean	638	1496	596	-3	45	50
Max	1046	1634	861	49	135	104
Min	478	1359	473	-41	6	7
Median	702	1496	682	-6	44	39
STD	224	120	169	33	52	43

The calculated evapotranspiration values range between 473 mm and 861 mm and, in conjunction with rainfall amounts between 478 mm to 1046 mm, which results in an evapotranspiration/rainfall ratio of 82 to 99 %. In other words, between 82 % and 99 % of the rainfall water is evapotranspired. Similar ranges for the percentage of water evapotranspired were achieved by SCHOEMAN, MATLAWA ET AL. (2002). They calculated the evapotranspiration as part of the water balance equation for different test sites in the Mpumalanga–Province, located south of the catchment used in this study. They achieved values showing that between 45 and 100 % of the precipitation water was evapotranspired.

Also, the estimated potential evapotranspiration was compared to estimated potential evapotranspiration values found IN SCHULZE, MAHARAJ ET AL. (1997). The values of 1359 mm to 1634 mm for the entire modeled period are within the estimated range of 1250 and 1899 mm for the Northern Province.

5.2.3 Sensitivity Analysis

The sensitivity analysis was carried out to determine the parameters influencing the model outputs. The parameter values, found during the calibration phase, were increased and decreased by 5 and 10 %. The differences in the model output have been calculated. The applied parameter values are shown in the following table.

Table 5-11: Parameter Values for Sensitivity Analysis

MODULE	ANALYZED PARAMETER	PARAMETER CHANGES IN %				
		-10	-5	0	+5	+10
Soil Water	SoilMaxDPS	2.7	2.85	3	3.15	3.3
	InfSummer	18	19	20	21	22
	InfWinter	49.5	52.25	55	57.75	60.5
	soilDistMPSLPS	1.8	1.9	2.0	2.1	2.2
	SoilDiffMPSLPS	0.45	0.475	0.5	0.525	0.55
	SoilOutLPS	0.36	0.38	0.4	0.42	0.44
	SoilLatVertLPS	0.45	0.475	0.5	0.525	0.55
	SoilMaxPerc	2.7	2.85	3	3.15	3.3
	soilconcRD1	1.53	1.615	1.7	1.785	1.87
	soilconcRD2	1.8	1.9	2.0	2.1	2.2
	FCAdaptation	1.35	1.425	1.5	1.575	1.65
	ACAdaptation	1.35	1.425	1.5	1.575	1.65
Ground- water	gwdistRG1RG2	0.81	0.855	0.9	0.945	0.99
	gwfacRG1	1.35	1.425	1.5	1.575	1.65
	gwfacRG2	6.66	7.03	7.4	7.77	8.14
	gwCapRise	0.009	0.0095	0.01	0.0015	0.02
Reach Routing	TA	9.9	10.45	11	11.55	12.1

The Sensitivity Index (SI) (Equation 3-17), a measure of the change in model output for a given change in model parameter, has been calculated for two model outputs: 1) the simulated runoff and 2) the modeled soil water amount (sum of actual soil water amount in the large pore storage and the medium pore storage). The following figure illustrates the results for parameters affecting the soil water module.

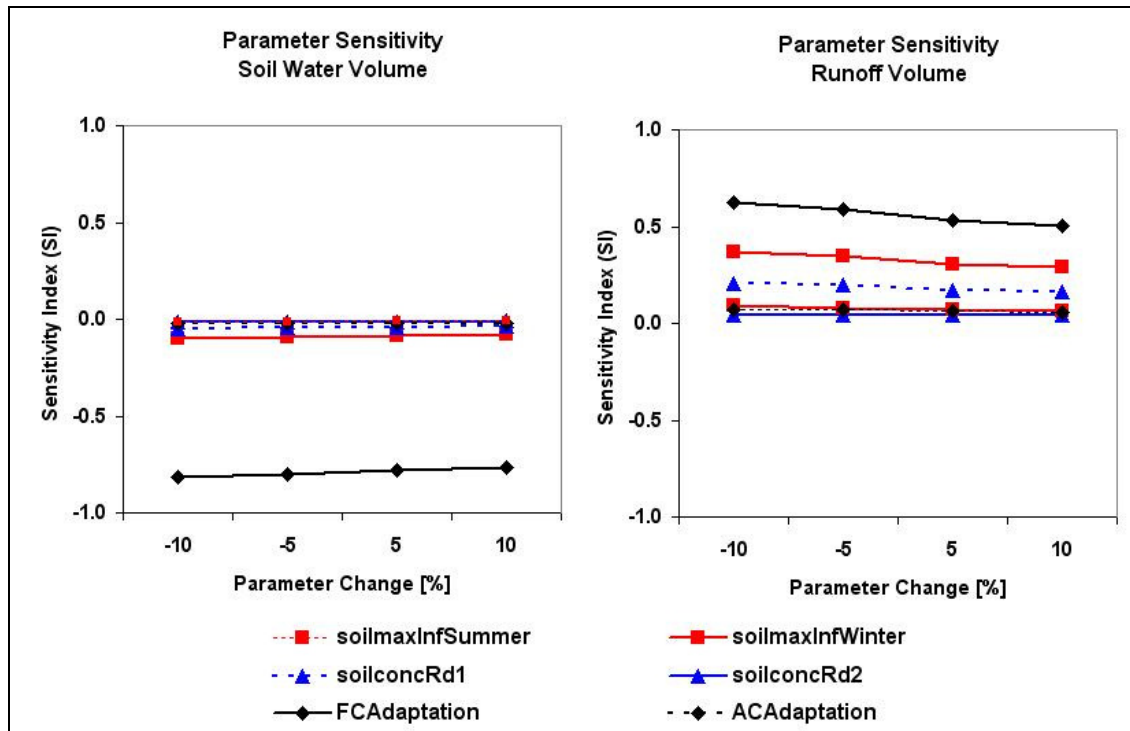


Figure 5-8: Sensitivity Index for the Parameter of the Soil Water Module in Regard to Simulated Runoff and Simulated Soil Water Volume

In the case of $SI = 0$, the model output is not sensitive to the parameter increase. A value of SI below zero illustrates a decreasing volume of model output as the parameter increases, whereas value higher than zero showing an increasing model volume with the parameter increase (FENTIE, MARSH ET AL., 2005:P. 1143). The higher the absolute values of SI, the higher the sensitivity of the model output to the respective parameter (FENTIE, MARSH ET AL., 2005:P.1143).

In Figure 5-8 only the soil parameters *soilInfWinter*, *soilInfSummer*, *soilconcRd1*, *soilconcRd2*, *FCAdaptation* and *ACAdaptation* are shown because the values for the parameters *soilMaxDPS*, *soilDistMPSLPS*, *soilDiffMPSLPS*, *soiloutLPS*, *soilLatVertLPS* and *soilMaxPerc* are close to zero. In Appendix D and E, a summary of the actual SI-values can be found. As expected, the parameter changes have a different effect on the analyzed model outputs. The parameter increase results in increasing observed runoff, whereas the soil water amount decreases. The actual sensitive parameters are mostly the same for both model outputs.

For both model outputs investigated the most sensitive parameter is the soil module parameter *FCAdaptation*. Additionally, for the runoff output the parameters *soilInfWinter* ($SI=0.29$ to 0.37) and the *soilconcRD1* ($SI=0.16$ to 0.21)

are significant. The soil water is also slightly sensitive to the *soilInfWinter* parameter (SI=0.04 to 0.05).

Figure 5-9 illustrates the effects of parameter changes in the groundwater module on the soil water and runoff volume. The most sensitive parameter for both model outputs is the *gwRG1RG2dist* with SI = 0.02 for the soil water and SI = 0.2 for the runoff. The modeled soil water and runoff volume are insensitive to the other parameters.

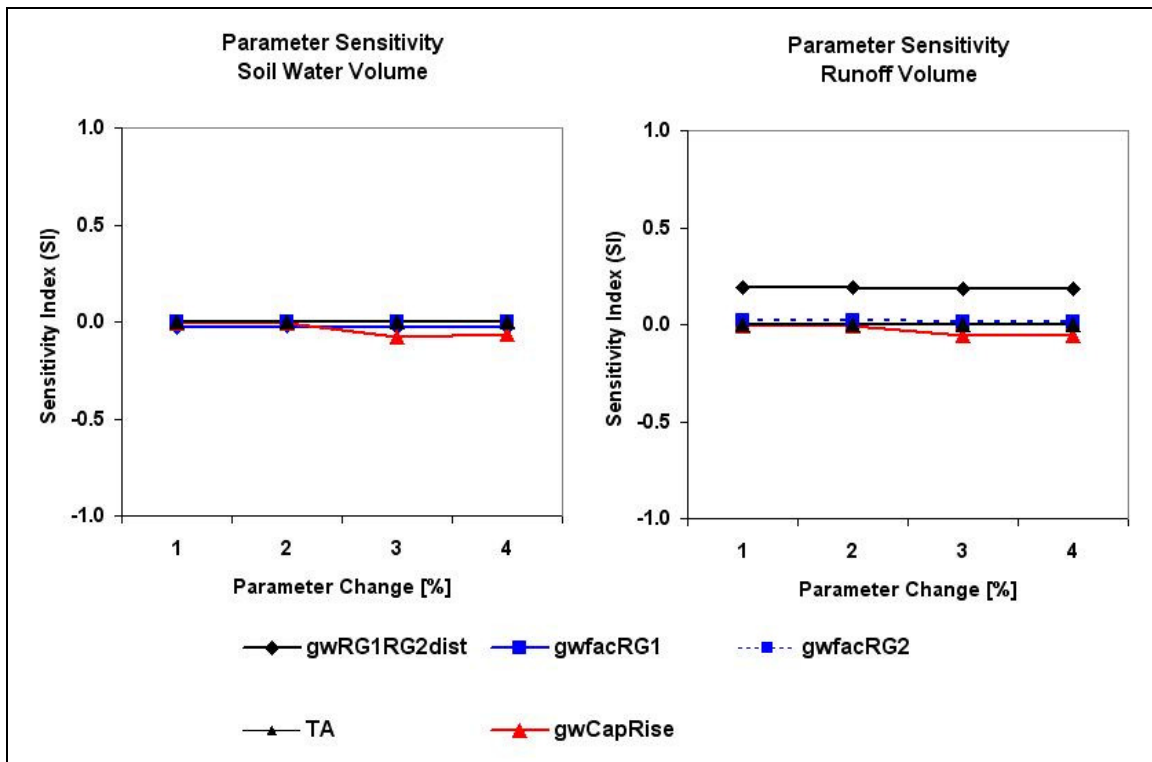


Figure 5-9: Sensitivity Index for the Parameter of the Ground Water Module in Regard to Simulated Runoff and Simulated Soil Water Volume

In summary, the sensitivity analysis indicates that the parameter *FCAdapation* has the greatest effect on both model outputs. In Figure 5-10 the influence of a 10 % parameter increase and decrease is pictured.

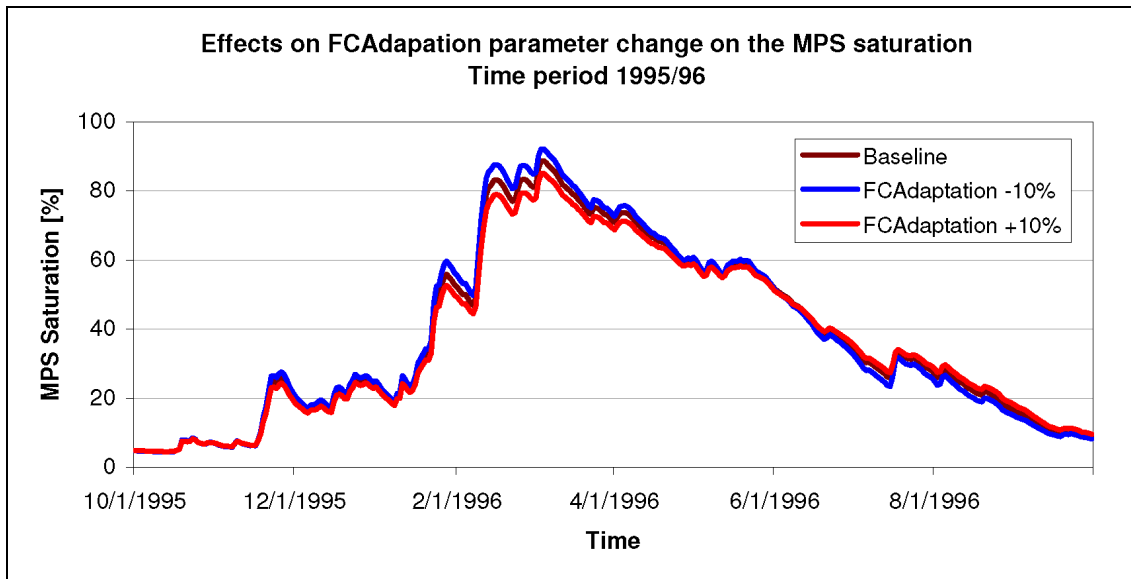


Figure 5-10: Effects of Changes in FCAdaptation Parameter to the MPS-Saturation Output, Time Period 1995/96

The figure shows variations in the saturation of the medium pore storages during the summer of 1995/96. A decrease of the parameter by 10 % leads to a higher saturation during the summer time whereas an increase of 10 % results in a lower saturation. This behavior turns in the transition period from summer to winter. Here, a reduction of the parameter results in less saturation in the medium pore storage and a higher saturation in the case of a parameter increase. This can be explained by the evapotranspiration algorithm applied in the model. The evapotranspiration rate depends on the soil saturation. In case of the parameter increase less water is stored as soil water in the soil column, which reduces the available water for evapotranspiration processes.

These variations in the soil water amount will be taken into account in the following investigation to determine if such parameter changes will influence the relationship between the remotely sensed soil water dataset and the simulated time series.

5.3 Assessment and Evaluation of the Macro-Scale Soil Water Estimates

The assessment and evaluation analysis is based on the J2000 modeling results from October 1993 to September 1997. The period from October 1997 to September 1999 will act as a validation period for the results.

5.3.1 Delineation and Characterization of the ERS-Scatterometer Footprints in the Catchment

In the catchment of the Great Letaba River three ERS-scatterometer footprints are located as shown in *Figure 5-11*. For the comparison of the scatterometer derived soil water content with the modeled soil moisture, the area covered by the scatterometer footprint was determined. As explained in *Section 3.3.1*, one scatterometer footprint covers an area of about 1963 km² (BARTALIS, 2005). To derive the integrated area of each scatterometer footprint a circle of 50 km diameter was used. The three footprints cover different parts of the catchment. The summary of the landscape parameters is given in *Table 5-12*.

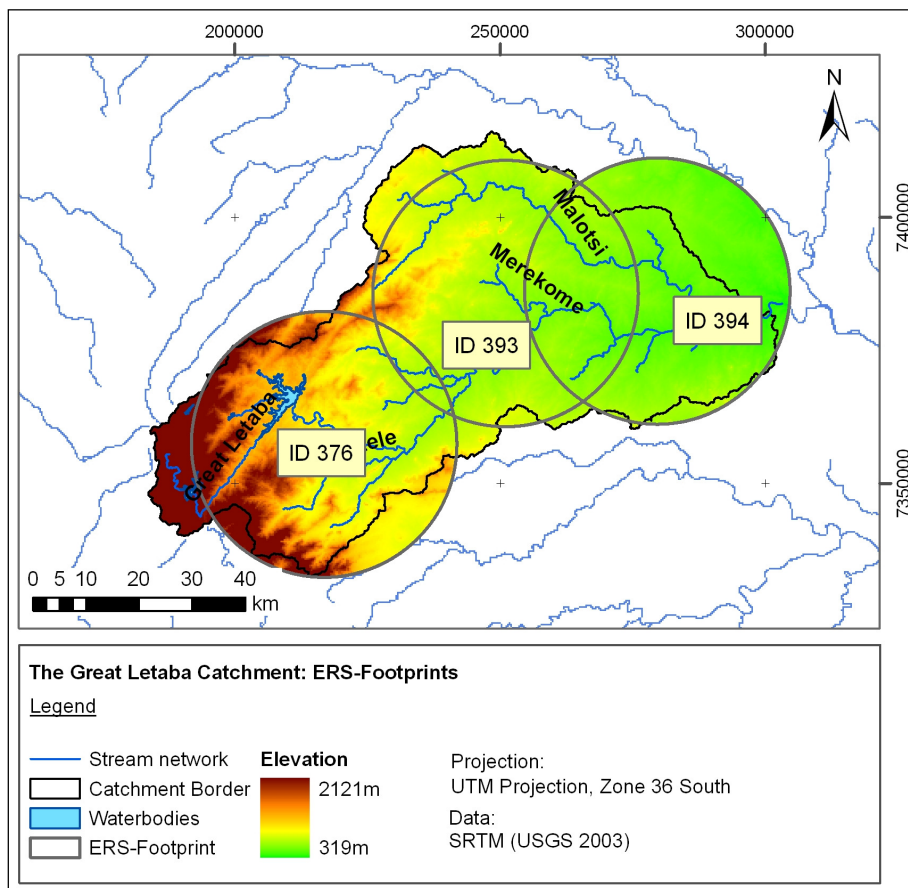


Figure 5-11: ERS-Scatterometer Footprints in the Great Letaba Catchment

Table 5-12: Description of the Landscape Characteristics of Each Footprint

PARAMETER	PARAMETER SUBCLASS	ID376	ID393	ID394
Land Cover Class	Forest (Deciduous)	26.7	-	-
	Forest (Broadleaf)	2.0	-	-
	Woodland	0.5	23.9	41.1
	Bushland	35.2	21.2	17.5
	Grassland	0.8	-	-
	Bare soil and sparse vegetation	10.9	18.4	12.3
	Water	1.7	0.4	0.4
	Wetland	1.3	0.099	-
	Agriculture	19.5	36.0	28.7
	Urban areas	1.4	0.001	-
Soil Group	C: <10 %	-	-	1.4
	C: 10-25 %	33.3	66.3	54.7
	C.25 %	65.4	33.6	43.9
	Wetland Soil	1.3	0.1	-
Slope Class	0-5°	48.2	93.4	99.6
	5-15°	35.9	5.8	0.399
	>15°	15.9	0.8	0.001
Geology Class	1	44.5	91.8	93.5
	2	4.2	1.699	6.4
	3	44.8	6.5	0.2
	4	6.5	0.001	0.1

The three footprints are characterized by different vegetation, soil distribution, and geology, as well as topography. The footprint ID376, located in the mountainous western part of the catchment, has slope values higher than 5° for more than 50 % of the footprint area. This higher elevation (500 m to 2121 m) of the footprint is represented mainly by the main vegetation types: Bushland (35.2 %) as well as forest (28.7 %) where soils with high clay content (>25 %) dominate. The footprints located in the center and eastern parts of the catchment (ID393 and ID394) are dominated by relief with low slope ranges. The main vegetation changes from a bushland (23.9 %)-woodland (21.2 %)-plant community influenced landscape in the center to plant community dominated by woodland (41.1 %) and lesser bushland (17.5 %) in the east. Additionally, agriculture plays an important role in both footprints due to the low elevation (<500 m) for the most parts of the footprints. The major area of the grid points is represented by soils having medium clay content (10-25 %).

The HRUs lying with each footprint were extracted (1733 HRUs (ID394) to 3711 HRUs) whereas HRU characterized as water were not taken into account. For every extracted HRUs, the modeled soil water index (SWI_{HRU}) has been calculated according to *Equation 3-18* with an adjusted temporal resolution as described in *Section 3.3.2*.

5.3.2 Comparison of Remotely Sensed Soil Water and Modeled Soil Water Time Series at Footprint Scale

To compare the SWI_{HRU} and SWI_{ERS} time series at footprint scale (50 km), the SWI_{HRU} was averaged over all HRUs lying within each respective footprint (*Figure 5-11*) and taking the area weight into account. The result was the area weighted average $\overline{SWI_{HRU}}$.

Figure 5-12 shows the SWI_{ERS} (blue line) compared to the area-weighted $\overline{SWI_{HRU}}$ (red line) for each of the three ERS-footprints for the time frame between 1993 and 1997. In the figure the footprints are sorted from the river source to the outlet, starting with ID376 located in the western part and finishing with ID394 in the eastern part of the catchment. *Figure 5-12* shows similar dynamics between the analyzed model-concepts, which is also reflected by the coefficient of determination (R^2) summarized in *Table 5-13*.

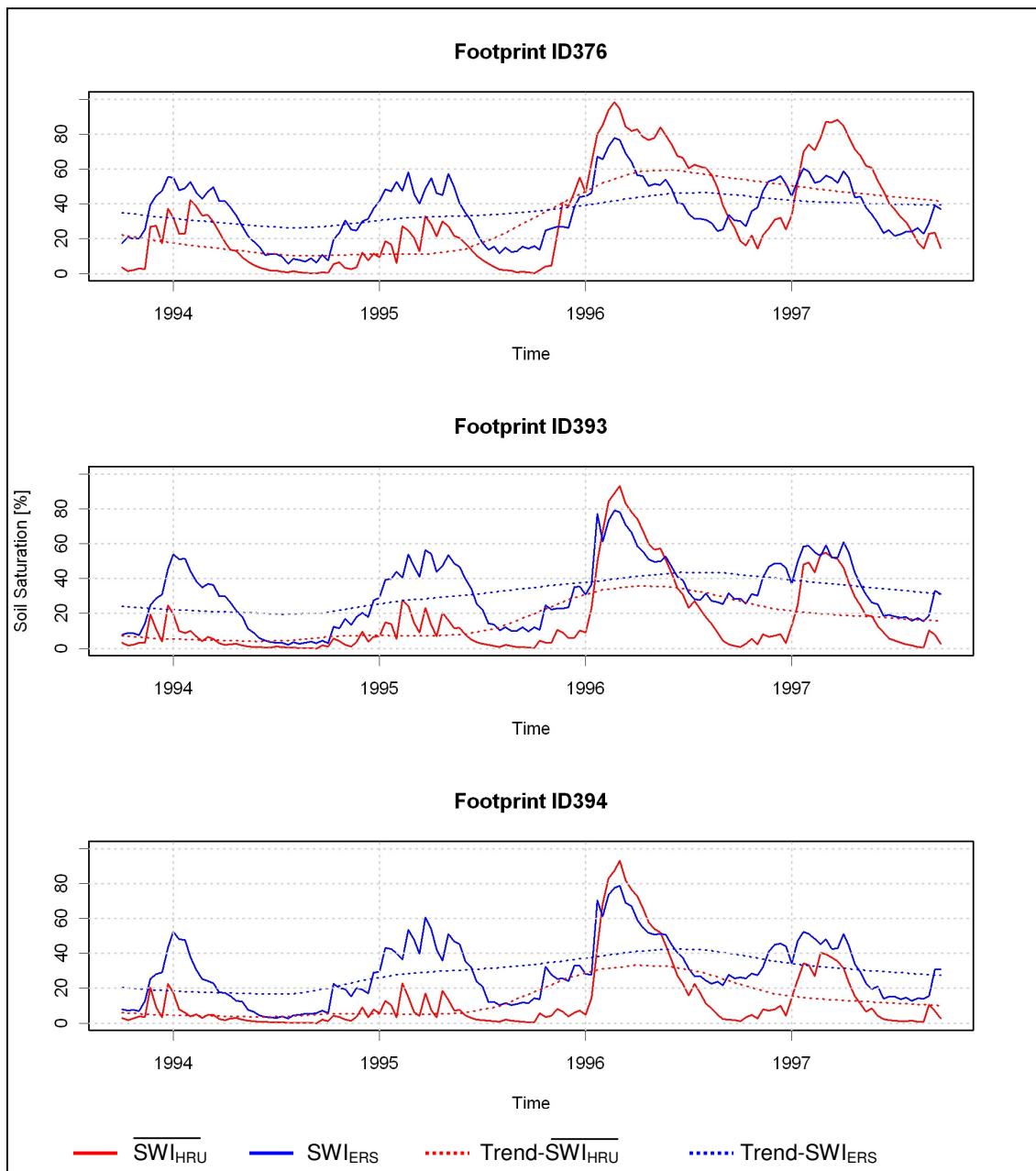


Figure 5-12: Time Series with Trend Components of the \overline{SWI}_{HRU} and the SWI_{ERS} for Each Footprint for the time frame 1993 to 1997

Table 5-13: Summary of Coefficients of Comparison

Coefficient	ID376	ID393	ID394
R ²	0.53	0.62	0.60
Bias	4.0	15.4	15.9

The coefficient of determination ranges between 0.53 for ID376 and 0.62 for ID393. These values can be interpreted that between 53 % and 62 % of \overline{SWI}_{HRU} (y) variability can be explained by the variability in the SWI_{ERS} (x). The corresponding x-y-plots are illustrated in Figure 5-13 with the \overline{SWI}_{HRU} on the y-axis and SWI_{ERS} on the x-axis. The dashed black line highlights the regression

line representing the relationship between the two variables. Similar results have been found by VISCHEL, PEGRAM ET AL. (2007) who compared the ERS-data to model results of TOPKAPI.

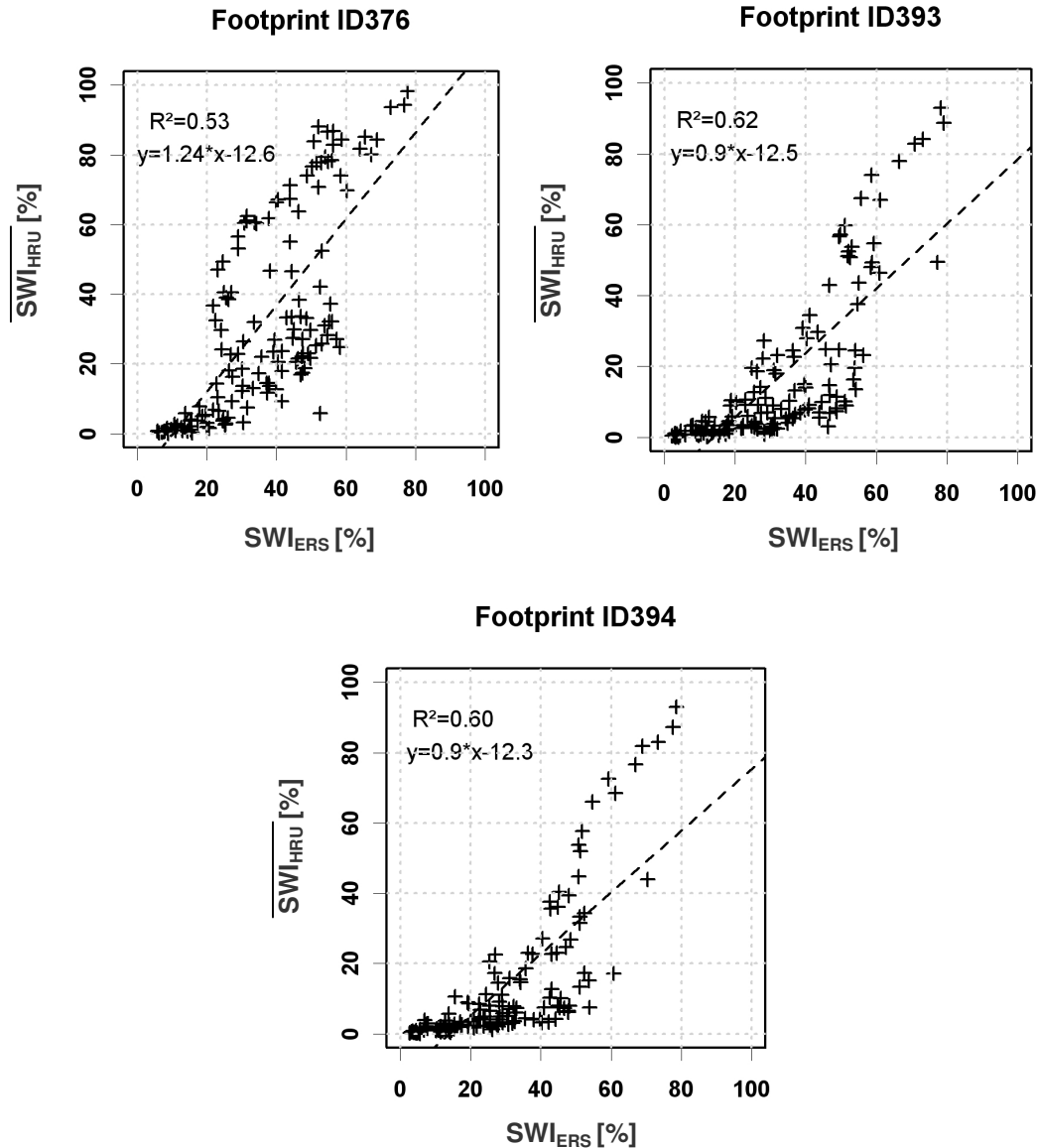


Figure 5-13: X-Y-Plots \overline{SWI}_{HRU} and SWI_{ERS} for Each Footprint

The plots reveal a two-fold relationship between the analyzed variables. When \overline{SWI}_{HRU} -soil water values are below 40 % saturation an increase in the values of SWI_{ERS} is associated with a smaller increase in the \overline{SWI}_{HRU} values. For \overline{SWI}_{HRU} -soil water values over 40 % this observation is reversed: An increase of SWI_{ERS} -values is now connected to larger increase in \overline{SWI}_{HRU} -values.

This two-fold relationship might be traced back to the “observed” volumes. The SWI_{ERS} is based on surface soil water measurements whereas the

\overline{SWI}_{HRU} was derived from the saturation of the entire soil column. The volume of the surface layer is smaller than the soil column volume. In case of low soil water saturation, the same input will result in a stronger saturation change for the surface volume than for the entire soil volume.

Table 5-13 highlights differences between the footprints in their coefficients of determination. This might be caused to some extent by the variability in land cover and especially in differences in land cover density. As discussed above, the scatterometer cannot penetrate into dense vegetation cover such as forests (LEWIS, 1998). As documented in *Table 5-12* footprint ID376 is mainly characterized by forest, bushland and agriculture, whereas footprint ID393 and ID394 are covered mainly by savanna vegetation and agriculture.

Figure 5-12 also shows that the \overline{SWI}_{HRU} mostly predicts lower values than the SWI_{ERS} . This is also reflected by the bias (WAGNER, SCIPAL ET AL., 2003; 2007) with values between 4.0 and 15.9, summarized in *Table 5-13*. This wide range might be caused by the conceptual formulation of the SWI_{ERS} . According to WAGNER (1998), the calculation of the SWI_{ERS} only depends on the water content of the surface soil layer. Interactions with the surrounding environment such as transpiration, lateral flow as well as upward fluxes are neglected. These processes, however, are important processes for soil water generation in semi-arid areas.

The first process, transpiration, leads to a reduction of soil water up to several decimeters in the soil column in which the surface layer plays a special role. The soil saturation, especially the soil surface saturation controls the beginning of plant growth. ARCHER, HESS ET AL. (2002) examined different savannah species in Spain. They found a relationship between plant growth and the surface soil moisture content. Additionally, the authors documented soil drying of up to 2 m due to evapotranspiration processes (ARCHER, HESS ET AL., 2002). The second process leading to a reduction of the soil water content in semi-arid areas are upward soil fluxes documented in particular under bare-soil conditions (WYTHERS, LAUENROTH ET AL., 1999). They found the greatest decrease in moisture occurs in the first centimeters independent of soil properties. The third processes, the lateral sub surface flow can not be neglected in semi-arid areas. UHLENBROOK, WENNINGER ET AL. (2005) observed lateral flow processes in the semi-arid Weatherley catchment in South Africa. On their experimental site, they documented macro pores leading the precipitation

water through the surface layer which responded in a drying of the surface layer within 12 hours after a heavy rainfall event.

These processes lead to a decrease of saturation in the subsurface layer as well as the entire soil column and, therefore, have to be accounted for. The processes are implemented in J2000 but not accounted for in deriving the ERS-scatterometer index, which explains the occurrence of the bias. The difference in the range of the bias between the footprints might be explained by the conceptual calculation of the \overline{SWI}_{HRU} . As explained above, the footprint ID376 is characterized by forest, bushland and agriculture whereas the footprints ID393 and ID394 show savannah vegetation. \overline{SWI}_{HRU} was calculated taking all HRUs, except for HRUs characterized by water, into account but the microwave signal can not penetrate dense vegetation such as forest (HENDERSON AND LEWIS, 1998). Forests reduce the soil water stress (CAYLOR, SHUGART ET AL., 2005) by conserving water and providing a more balanced water regime. The consideration of HRUs characterized by forest leads to a higher \overline{SWI}_{HRU} and the reduction of the bias between \overline{SWI}_{HRU} and SWI_{ERS} .

After analyzing the entire time series as one element, in the next step, the time series components have been analyzed. The investigation of the time series in detail will increase the knowledge about the evaluation of the soil water over time and will give insight into the seasonal behavior of soil water in semi-arid areas. The comparison of each of the \overline{SWI}_{HRU} and SWI_{ERS} components will indicate further similarities as well as variances in observations.

Decomposition of the Time Series

Each time series contains a long term trend, a seasonal component and a random component (ASSENMACHER, 1998). The trend component describes the long term movement over the analyzed time period. The seasonal component describes the short term variation due to seasonal weather patterns such as summer and winter. The random component is an unpredictable error caused by factors such as local weather conditions at a given time.

The SWI_{ERS} and \overline{SWI}_{HRU} time series were portioned into their trend and seasonal components using the *stl*-function (CLEVELAND, CLEVELAND ET AL., 1990) which are compared and analyzed in the following sections.

Trend Component

The trend component was calculated for the time frame October 1993 to September 1997, shown in *Figure 5-12*. The red line highlights the \overline{SWI}_{HRU} time series, its trend component is illustrated with a dashed red line. The blue line describes the SWI_{ERS} time series with the trend component picture by the dashed blue line.

Both the SWI_{ERS} and \overline{SWI}_{HRU} data series reveal a similar trend behavior, also reflected in the R^2 -values ranging from $R^2=0.79$ (ID394) to $R^2=0.94$ (ID376) shown in *Table 5-14*. The trend curve is corresponding to the annual measured rainfall. After a period of low annual precipitation in the years 1993 to 1995, in 1996 the annual precipitation was greater than the long term average. The observed precipitation in 1997 was close to the long term MAP. The trend curves decrease from the beginning in October 1993 until the middle of the year 1994. In the beginning of the 1994/95 rainy season the curves increase smoothly which increases more strongly by the beginning of the 1995/96 rainy season and peaks in the middle of the year 1996.

Table 5-14: Summary of the Comparison between the \overline{SWI}_{HRU} and SWI_{ERS} Trend Components

	\overline{SWI}_{HRU} [%]			SWI_{ERS} [%]			TIME LAG (IN 10DAYS TIME STEPS)	R^2
	MIN	MAX	RANGE	MIN	MAX	RANGE		
ID 376	10.4	59.6	49.2	26.20	46.5	20.3	6	0.94
ID 393	4.0	35.9	31.9	19.6	43.6	24.0	8	0.87
ID 394	3.5	33.2	29.7	16.8	42.6	25.8	5	0.79

The comparison, however, of the SWI_{ERS} and \overline{SWI}_{HRU} trend curves exhibits differences in magnitude. The range of values for the \overline{SWI}_{HRU} trend curve amounts to between 29.7 (ID376) and 49.2 (ID394) percent whereas the SWI_{ERS} curve ranges only from 20.3 (ID376) to 25.8 (ID376) percent (*Table 5-14*). An analysis also shows a time lag between the SWI_{ERS} and the \overline{SWI}_{HRU} peak of five to eight time steps which approximately correspond to 50 to 80 days.

As explained above, the SWI_{ERS} is an integrated value based on the surface soil water amount. For this reason, in the beginning of the rainy season the SWI_{ERS} shows higher saturation values than the \overline{SWI}_{HRU} , which is an integrative measurement that also takes the dry lower soil into account. This also explains the earlier peak of SWI_{ERS} by the end of January whereas the

\overline{SWI}_{HRU} peaks in mid February. In the transition period (April to June) the time series are a fit to each other. During June to October the SWI_{ERS} predicts lower values. After a certain time of wetting the surface soil layer, the water infiltrates deeper in the soil and the surface soil layer dries out, which results in higher \overline{SWI}_{HRU} values than SWI_{ERS} .

Seasonal Component

In the second, step the seasonal component of the \overline{SWI}_{HRU} and SWI_{ERS} time series have been analyzed. The *Figure 5-14* illustrates the seasonal component of the SWI_{ERS} and the \overline{SWI}_{HRU} time series by plotting the soil saturation percentage for each footprint.

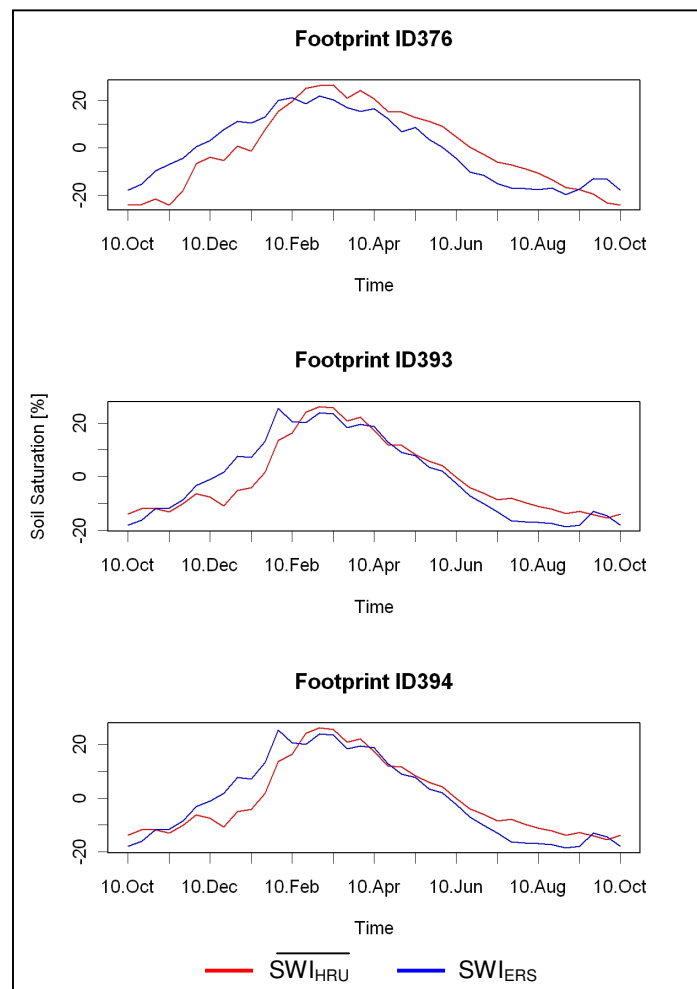


Figure 5-14: Seasonal Analysis Between 1993 and 1997 for Each Footprint

The overall picture shows that the seasonal components of the SWI_{ERS} and \overline{SWI}_{HRU} are similar to each other. This is also highlighted in *Table 5-15* by

comparing the range values and the coefficients of determination for the seasonal components of the two indices.

Table 5-15: Summary of the Comparison between the Seasonal Components \overline{SWI}_{HRU} and SWI_{ERS}

	\overline{SWI}_{HRU} [%]			SWI_{ERS} [%]			R^2
	MIN	MAX	RANGE	MIN	MAX	RANGE	
ID 376	-24.2	26.5	50.7	-19.7	21.9	41.6	0.74
ID 393	-15.4	26.2	41.6	-18.5	25.4	43.9	0.85
ID 394	-12.0	22.6	34.6	-16.6	24.02	40.2	0.81

The seasonal component follows the seasonal precipitation dynamics with a peak in February, though the SWI_{ERS} peaks about 30 days earlier than the \overline{SWI}_{HRU} . Also, the SWI_{ERS} seasonal component of the footprint ID393 and ID394 is characterized by a double peak with a primary maximum by the end of January and the second maximum by the end of February. Differences in the curve evaluation are obvious, in particular during the transition periods: between the dry and wet season (September/October) and from wet to dry season (March/April). In all footprints the SWI_{ERS} rises earlier than the \overline{SWI}_{HRU} . These variations in the seasonal component might also be caused by differences in the observed soil water volumes of SWI_{ERS} and \overline{SWI}_{HRU} . With the beginning of the rainy season, the surface layer gets wet, resulting in higher saturation of SWI_{ERS} . After a certain period in which the surface layer gets wet, the water infiltrates into the underlying soil column, resulting in rising \overline{SWI}_{HRU} values. This also explains the earlier peak of SWI_{ERS} by the end of January whereas the \overline{SWI}_{HRU} peaks at the end of February. In the transition period (April to June) the surface layer dries out. By the end of June the surface layer is nearly dry whereas water is still available in lower parts of the soil compartments. This results in higher \overline{SWI}_{HRU} values between June and October. The footprint ID376, however, depicts lower SWI_{ERS} values than \overline{SWI}_{HRU} during April to September. An explanation here might again be the conceptual calculation of the \overline{SWI}_{HRU} , taking HRUs with forest cover into account. The forest vegetation delays the drying out of the surface layer, which would result in higher \overline{SWI}_{HRU} values.

In summary, the analysis shows that significant similarities in the evaluation of the soil water over time can be found, which indicates that the macro-scale soil water estimates contains valuable information on soil water

content. The similarities in the trend component, as well as in the seasonal component, are very promising results that justify taking this analysis further and comparing the macro-scale soil water estimates to the meso-scale distribution. The analysis also showed that the absolute values can not be used in the analysis due to differences in observed volumes, which results in a bias of up to 16 %.

5.3.3 Development of the Downscaling Scheme

As described in *Section 3.3.3.3*, a multiple linear regression approach, *Equation 3-23*, was used to downscale the macro-scale soil water estimates. The preliminary analysis showed that precipitation had to be included into the downscaling model. The hypothesis is that the regression parameters m_1 , m_2 and d (*Equation 3-25 to Equation 3-27*) can act as scaling parameters, which can be described as a function of combinations of the landscape parameters: land cover, soil, slope, aspect and geology. The derivation of the scaling parameters will be carried out using the simulation period from October 1993 to September 1997 and will be validated using the simulation period from October 1997 to September 1999.

The Importance of Precipitation

A single linear regression analysis with the SWI_{ERS} as the independent and the SWI_{HRU} as the dependent variables has been applied. The resulting R^2 , regression coefficient m and the intercept value d were plotted to analyze their spatial distribution. The spatial distribution indicated that the regression was influenced by the mean annual precipitation (MAP). The overlay of the regression coefficient with the MAP-map, experimentally for footprint ID376, showed that HRUs with MAP over 850 mm result in a regression coefficient higher than 1, whereas HRUs characterized by MAP under 850 mm had regression coefficients under 1. The hypothesis of the precipitation influence was verified by adding precipitation as an independent parameter into a multiple linear regression model (*Equation 3-23*). The multiple regression analysis was carried out with the `lm`-function within the R-Software (R DEVELOPMENT CORE TEAM, 2008). The function includes a T-Test, analyzing the distribution of the sample mean and assesses the statistical significance between two samples (ROGERSON, 2006) and the associated p-values, to provide a

measure for significance of the respective predictor. The null hypothesis states that the analyzed variable, in this case precipitation, does not influence the dependent variable (SWI_{HRU}). The associated p-value defines the probability to wrongly reject the null hypothesis in the case that the null hypothesis is true (ROGERSON, 2006). If the p-value is equal to or less than the significance level the null hypothesis can be rejected. For the analysis of the importance of precipitation as an exploratory variable in the model, p-values higher than the significance level (in this case over 0.05) indicate that P_{sum} does not explain the dependent variable SWI_{HRU} in the applied model whereas p-values equal or less than 0.05 point to a statistical significance of precipitation. The analysis revealed that precipitation is a significant predictor in the model for 34.8 % (ID376) to 58.8 % (ID394) of the HRUs. These findings agree with studies by VINNIKOV, ROBOCK ET AL. (1996), JACKSON, LE VINE ET AL. (1999) AND ENTIN, ROBOCK ET AL. (2000) who have shown that precipitation is a driving parameter in spatial distribution of soil water on a larger scale. Also as stated in SCIPAL, WAGNER ET AL. (2003), the SWI_{ERS} does provide information on soil moisture variability which is driven by precipitation. This is strengthened by the results found here. The analysis shows that whether P_{sum} is statistically significant in the regression equation depends on landscape parameters, especially land cover. The land cover classes bushland, woodland and forest are primarily the ones influenced by P_{sum} rather than wetland, urban, bare soil and sparsely vegetated areas. This can be traced back to the fact that in bushland, woodland and forests the effectiveness of precipitation on the actual soil moisture content is higher than for the wetland, urban and bare soil and sparse vegetated areas.

Therefore, precipitation is an important variable in the applied regression model and can not be neglected in the further data analysis. Subsequent analysis extends the downscaling model by including precipitation as an independent variable by applying the model defined in *Equation 3-23*.

Spatial Distribution of the Regression Parameters

The spatial distribution of the regression parameters was again plotted, including the additional precipitation parameter, to investigate the assumption that different landscape parameter combinations result in a variation in the relationship between the SWI_{ERS} and modeled SWI_{HRU} . The following figures show the spatial variability within the footprint ID376 of the regression

coefficient m_1 and m_2 , the intercept d and the coefficient of determination (R^2). The figures for the footprints ID393 and ID394 are in *Appendix F to M*.

Figure 5-15 illustrates the spatial distribution of R^2 -coefficients. The figure reveals that the R^2 -values are spatially variable within the footprint. For the majority of HRUs R^2 lays between 0.4 and 0.6, highlighted in greenish colors in *Figure 5-15*. R^2 -values over 0.60, plotted in yellow to orange colors, can be found isolated primarily in the southern half of the footprint. The first hypothesis was that this distribution of R^2 might be explained by landscape parameter characteristics, in particular by the land cover. Forest and woodland vegetation does occur in the east and the northern part of the footprint, whereas agriculture and bushland dominate in the south. The analysis of the R^2 -range of the land cover classes revealed a high distribution of R^2 -values, indicating that other landscape parameters such as soil group, aspect, slope and geology might help to explain this distribution.

Figure 5-16 illustrates the spatial variability of the regression coefficient m_1 between the SWI_{HRU} and the macro-scale soil water time series (SWI_{ERS}). Areas with a regression coefficient higher than 1 are those where a change in the SWI_{ERS} corresponds to a stronger change in saturation by the hydrological model. Areas having a regression coefficient under 1, represent regions where a change to the SWI_{ERS} saturation corresponds to a smaller amount of change in the soil moisture calculated by the hydrological model. HRUs showing an m_1 -value higher than 1 are pictured in blue to blue-green color in *Figure 5-16*. These areas are mainly located in the western half of the footprint whereas HRUs characterized by regression coefficients less than 1 (highlighted with a green to red coloration) are in the southeastern part of the footprint. This distribution has been overlaid with the land cover and soil information. This analysis indicates that these parameters might be responsible for the spatial distribution. Forests over very clayed soils can be found in the western part of the footprint corresponding to values below 1, whereas in the southern part (values >1) it is agricultural areas, bushland and areas with bare soil and sparse vegetation over soils with medium clay content (10 to 25 % clay content) that are dominant.

Similar results are found for the regression parameters m_2 and d . *Figure 5-17* shows the regression coefficients m_2 for P_{sum} for every HRU. The figure shows distinctive spatial patterns for this parameter. In the northern as well as in the western part of the footprint, which are dominated by forests, the m_2 -

values range from -0.2 to 0. In the southern part of the footprint the m_2 -values reach from 0 up to 0.5, especially in the south to southeastern part of the footprint, where values up to 0.5 can be found.

The intercept of each HRU, pictured in *Figure 5-18* defines the intersection point of the plane with the y-axis. The figure shows that the intercept value ranges from -25 to 20 and is also spatially distributed. The picture shows a decrease in the intercept values from west to east. Intercepts equal or higher than zero are found in the very western part, dominated by dense forests, as well as isolated HRUs in the southeastern part of the footprint. The eastern part of the footprint, agricultural and bushland area, has intercept values below -5, though intercept values between -15 and -20 can be found in the eastern part of the footprint.

These figures highlight the spatial variability of the regression parameters m_1 , m_2 and d , indicating that these empirical values might be dependent upon specific landscape parameter combinations. In the next step this dependency will be investigated and the specific m_1 , m_2 and d parameters for the respective landscape parameter combinations derived.

Multiple Linear Regression: Coefficient of Determination (R^2) at HRU-Scale (Time Period: 1993-1997)
Footprint ID376

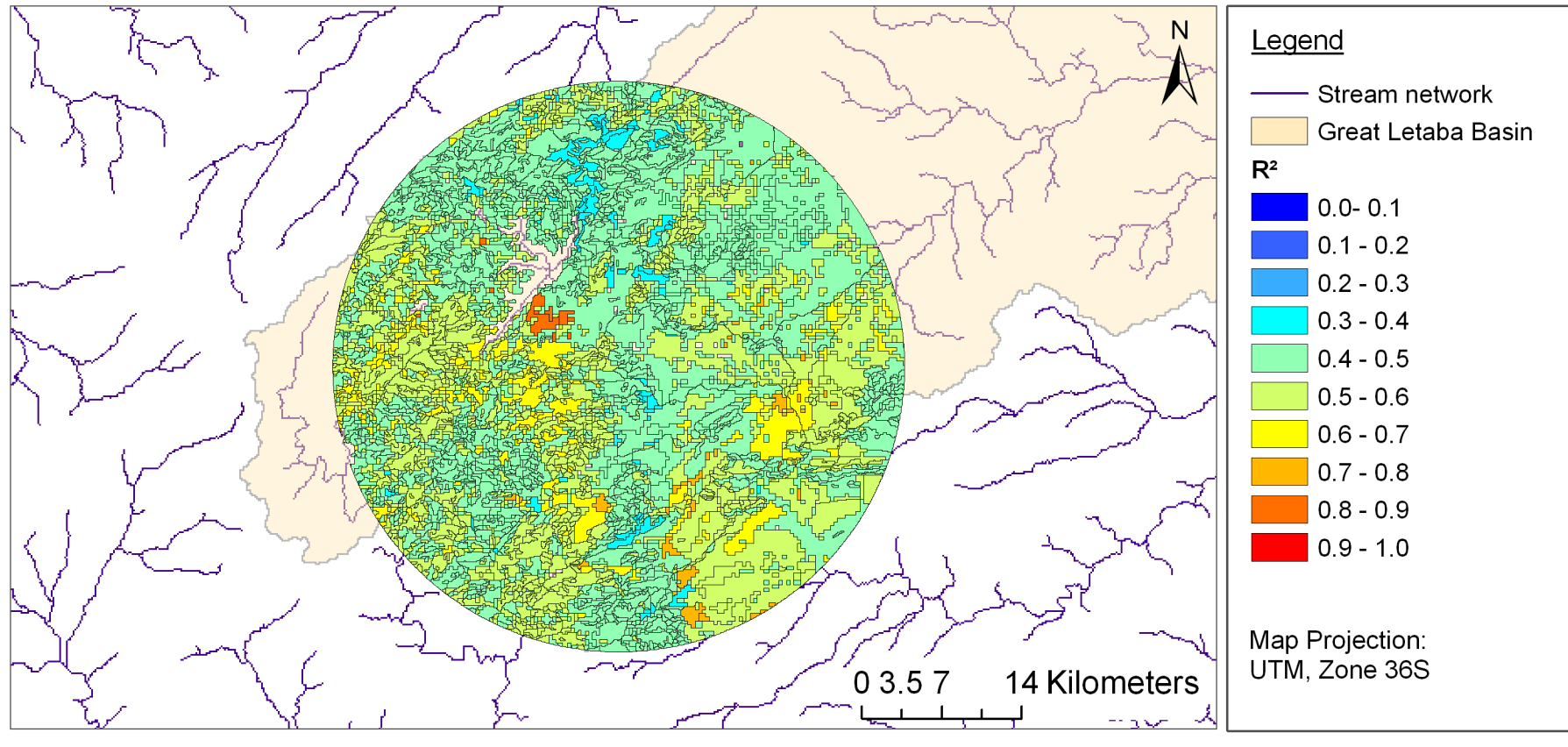


Figure 5-15: Multiple Linear Regression: Spatial Variability of the Coefficient of Determination, Footprint ID376

Multiple Linear Regression: Regression Coefficient m_1 at HRU-Scale (Time Period: 1993-1997)
Footprint ID376

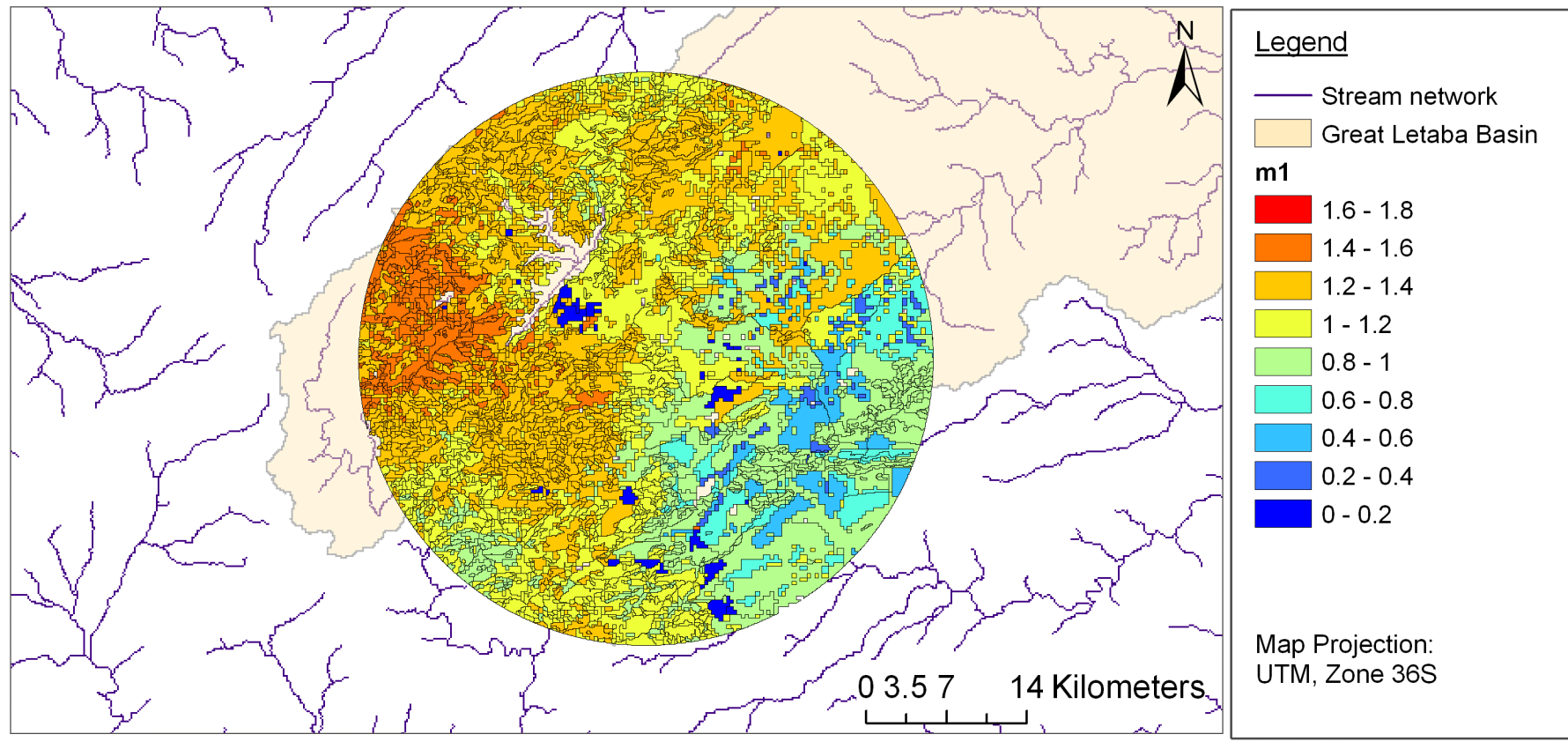


Figure 5-16: Multiple Linear Regression: Spatial Variability of the Regression Coefficient m_1 , Footprint ID376

Multiple Linear Regression: Regression Coefficient m_2 at HRU-Scale (Time Period: 1993-1997)
Footprint ID376

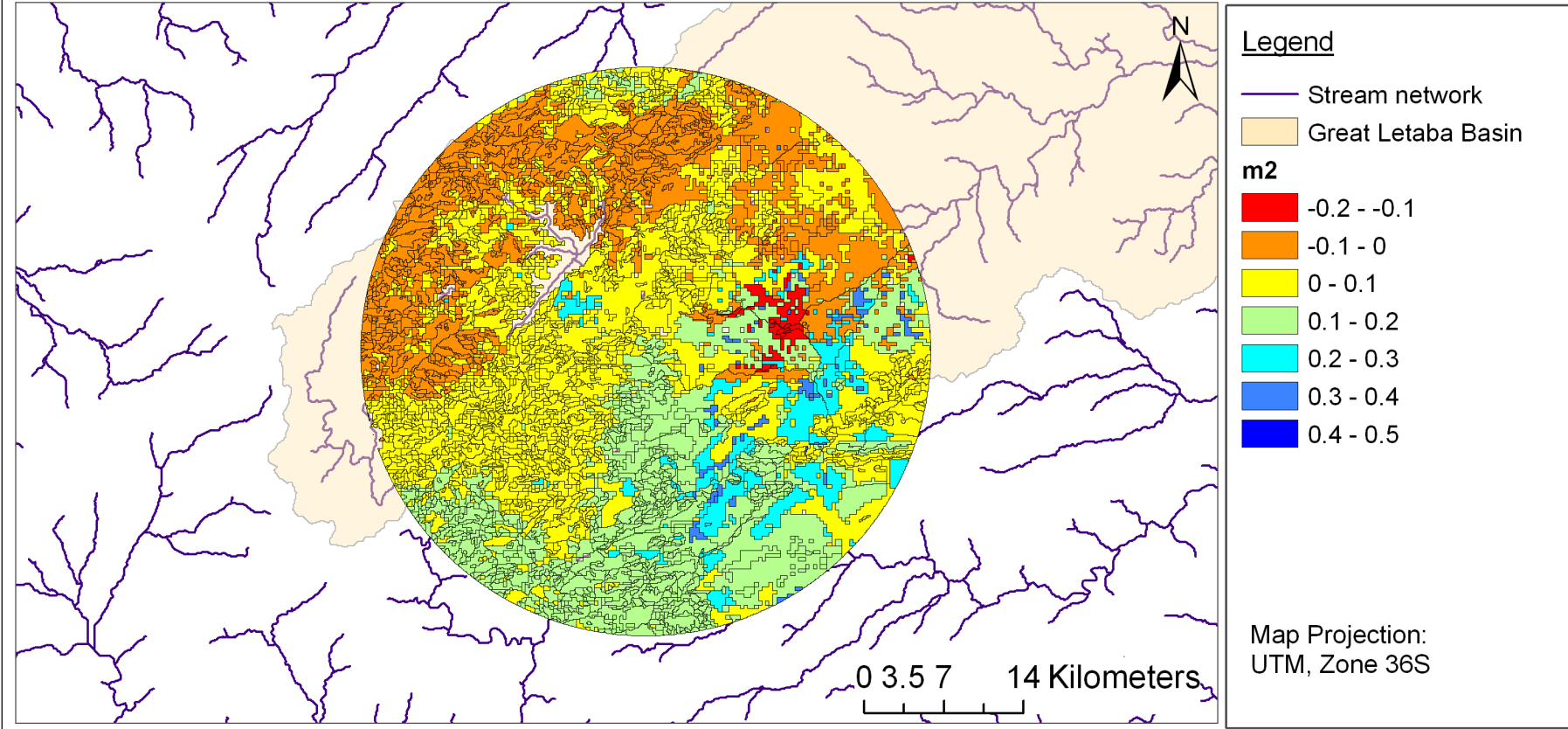


Figure 5-17: Multiple Linear Regression: Spatial Variability of the Regression Coefficient m_2 , Footprint ID376

Multiple Linear Regression: Intercept (d) at HRU-Scale (Time Period: 1993-1997)
Footprint ID376

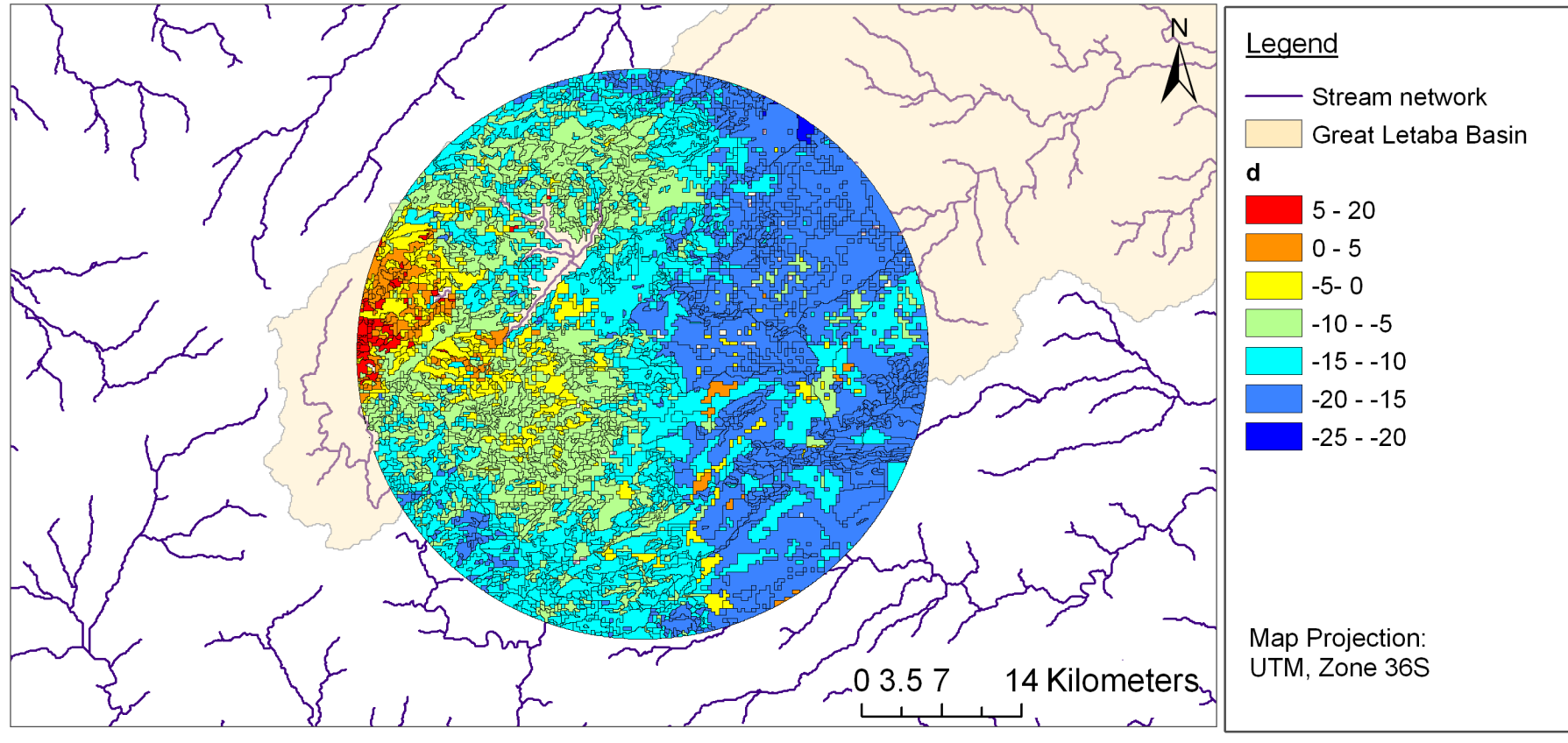


Figure 5-18: Multiple Linear Regression: Spatial Variability of the Intercept, Footprint ID376

Determination of Landscape Specific Downscaling Parameters

Taking the results of the analysis carried out before, the hypothesis will be tested that the spatial distribution of the model parameters m_1 , m_2 and d might be driven by landscape parameter combinations. HRUs with similar or equal landscape parameter combinations will have similar model parameters. To verify this hypothesis, the model parameters are statistically evaluated using measures of descriptive statistics. The measures chosen are median and quintiles, to reduce the influence of outliers on the results (HOFFMANN AND RÖDEL, 2004:P.17-20). The 20th (1st quintile) and 80th (4th quintile) percentile of the distribution were used in this study, to make sure that more than 50 % of the values are taken into the analysis. The values of the upper and lower quintile will be used to distinguish between the different combinations and to determine specific parameter distributions.

The model parameters were analyzed stepwise. First, the upper and lower quintiles as well as median were calculated for every possible combination of land cover and soil group. Land cover and soil group were chosen due to their direct impact on soil water. The soil group, based on clay content, influences the amount of stored water within the soil column. Land cover controls various processes such as evapotranspiration and, therefore, affects the soil water content. Also, vegetation can reduce soil water losses. Second, the analysis was extended to include the slope. The sloping of a hillside influences runoff generation and therefore impacts the soil water content. In the third step, the aspect of an area was taken as a parameter into the analysis. The aspect of an area determines the radiation input and consequentially the evapotranspiration. In the last step, the geology was added as a fifth parameter into the analysis.

For each of the respective landscape parameter combinations:

- I.) Land cover and soil group (LCS) (20 classes) ,
- II.) Land cover , soil group and slope (LCSS) (45 classes),
- III.) Land cover , soil group, slope and aspect (LCSSA) (113 classes),
- IV.) Land cover, soil group, slope, aspect and geology (LCSSAG) (213 classes),

the median for each possible combination (class) was calculated and if feasible regrouped. For the resulting classes the quintiles and median of the

respective distribution were calculated. For the following analysis, 22 HRUs characterized with agriculture on a hillside sloping over 15° were excluded (equaling 0.08 % of the modeled area). These areas are an artifact of applying the majority function after eliminating the small polygons.

Results for Downscaling using Land Cover and Soil Group

For the first landscape parameter combination LCS, the scaling parameters m_1 , m_2 and d were grouped according to the all available combinations of the soil group with land cover. The achieved parameters are summarized in *Table 5-16*.

Table 5-16: Scaling Parameters for the Land Cover and Soil Groups

Regression coefficient m_1

	SG1			SG2			SG3			WETLAND			MiSc		
	LQ	UQ	MD	LQ	UQ	MD	LQ	UQ	MD	LQ	UQ	MD	LQ	UQ	MD
Urban Area													0.00	0.12	0.06
Broadleaf Forest				0.98	1.16	1.10	1.21	1.37	1.29						
Conifer Forest				1.03	1.14	1.11	1.23	1.45	1.37						
Woodland	1.02	1.02	1.02	0.81	0.99	0.90	0.73	0.91	0.82						
Bushland	1.03	1.03	1.03	0.91	1.26	1.10	0.83	1.36	1.02						
Grassland				1.00	1.18	1.07									
Bare Soil	0.74	0.75	0.75	0.67	1.06	0.76	0.62	1.02	0.70						
Agriculture	0.78	0.78	0.78	0.60	1.04	0.82	0.55	1.13	0.99						
Wetland										0.25	0.39	0.30			

Regression coefficient m_2

	SG1			SG2			SG3			WETLAND			MiSc		
	LQ	UQ	MD	LQ	UQ	MD	LQ	UQ	MD	LQ	UQ	MD	LQ	UQ	MD
Urban Area													0.25	0.31	0.29
Broadleaf Forest				0.09	0.12	0.10	-0.02	0.03	-0.01						
Conifer Forest				0.09	0.11	0.10	-0.01	0.07	0.01						
Woodland	0.00	0.00	0.00	0.02	0.11	0.06	0.06	0.15	0.12						
Bushland	0.01	0.01	0.01	0.00	0.12	0.07	0.03	0.13	0.08						
Grassland				0.15	0.18	0.16									
Bare Soil	0.14	0.15	0.15	0.09	0.18	0.14	0.13	0.22	0.18						
Agriculture	0.13	0.13	0.13	0.03	0.19	0.09	0.03	0.23	0.08						
Wetland										0.26	0.32	0.30			

Table 5-16 (continued): Scaling Parameters for the Land Cover and Soil Groups

Intercept d

	SG1			SG2			SG3			WETLAND			MiSc		
	LQ	UQ	MD	LQ	UQ	MD	LQ	UQ	MD	LQ	UQ	MD	LQ	UQ	MD
Urban Area													-3.0	0.4	-1.1
Broadleaf Forest				-14.3	-10.2	-12.6	-10.1	-5.1	-8.7						
Conifer Forest				-13.3	-10.1	-11.7	-8.7	2.3	-5.6						
Woodland	-13.0	-12.8	-12.9	-13.1	-12.5	-12.9	-13.2	-12.0	-12.6						
Bushland	-10.9	-10.9	-10.9	-14.1	-10.9	-12.6	-14.3	-7.4	-12.3						
Grassland				-16.4	-11.8	-14.5									
Bare Soil	-11.9	-11.8	-11.9	-14.0	-11.0	-11.9	-13.8	-10.6	-11.5						
Agriculture	-12.8	-12.8	-12.8	-15.8	-10.3	-13.3	-14.5	-8.9	-12.8						
Wetland										-8.6	-4.5	-6.3			

MiSc=miscellaneous, grey background = based on a small number of events

For the downscaling, the parameter m_1 and m_2 and d are contributing together as input variables in the downscaling model. Therefore, for each land cover class, the arrangement of all three parameters was analyzed. The wetland and urban areas have, with the exception of m_2 , very distinctive parameters and could be clearly separated from the other LCS-groups. The range of m_1 , m_2 and d values of the other groups overlap one another and no strong separation between the parameter values could be derived. For instance, take the m_1 and m_2 -parameters of the two forest types on soil group 2. Here the median of m_1 and m_2 are similar or only by 0.01 different from one another, with the range of the conifer forest a little bit narrower than for the broadleaf forest. The clear distinction was observed in the intercept values. The parameters for the LCS-groups woodland, bushland, bare soil and sparse vegetation as well as agriculture on top of soil group 1, are highlighted by a grey background in Table 5-16, are derived from a very small HRU number (<5 HRUs). The representation of achieved parameters for the particular LCS-group is therefore questionable.

The median values of m_1 , m_2 and d for the different classes (combinations of land cover and soil type) were then used as input parameters in Equation 3-23 to downscale again the macro-scale soil water estimates for the time period October 1993 to September 1997 but now with the before grouped scaling parameter. The resulting soil water time series was compared to the simulated soil water time series with J2000 (Section 5.2.2). The correlation between the two times series was used to evaluate the performance of the

downscaling model. For this landscape parameter combination the R^2 -distribution was plotted in *Figure 5-19* for each footprint as a relative frequency histogram.

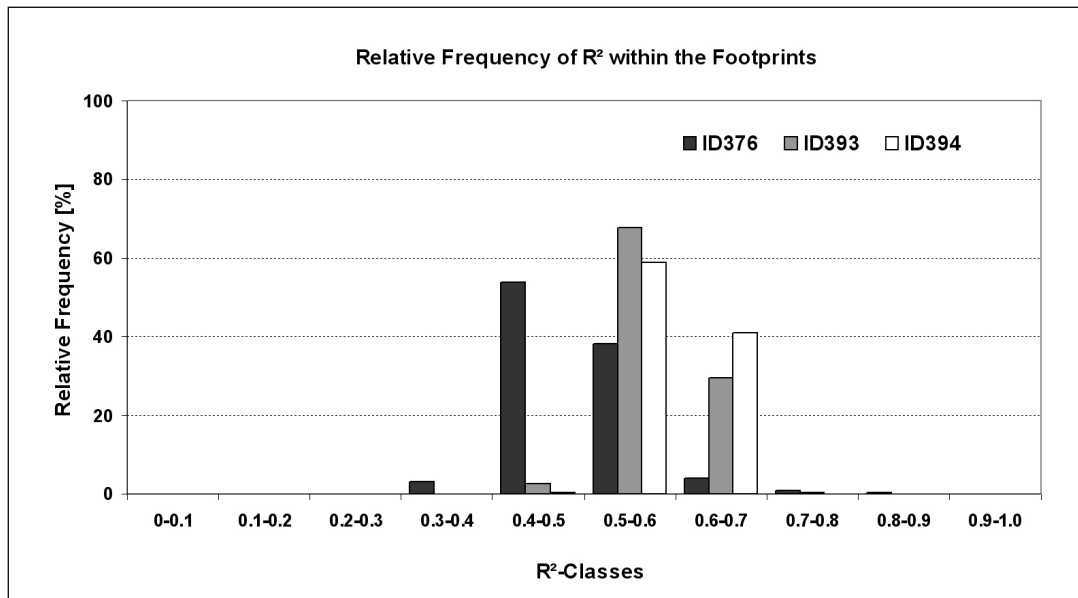


Figure 5-19: Relative Frequency of the R^2 -values for Each Footprint Achieved with the LCS-Scaling Parameters

The figure reveals that 43.2 % (ID376) to 99.7 % (ID394) of the HRUs within the respective footprint received a R^2 -value higher than 0.5. The analysis of areas with low R^2 -values ($R^2 < 0.5$) show that they are, for the most parts, forest (broadleaf and conifer) on top of soil group 3 as well as agricultural areas on top of soil group 3. Therefore, in the next step, the slope, aspect and geology parameters will be taken into account and the result will be analysed.

Effect of Slope, Aspect and Geology

In the next step the scaling parameters according to land cover, soil group and slope (LCSS) have been derived and applied in the downscaling model. The resulting R^2 -values were subtracted from the previous R^2 -values and HRUs with an increase ($\Delta R^2 > 0.01$) were extracted and their landscape parameter combination was analyzed.

An R^2 -improvement of higher than 0.01 were seen in 6 % (ID376), 9 % (ID393) and 8 % (ID394) of the HRUs. However, the SWI_{ERS} is an integrated signal over the entire footprint area. It is, therefore, assumed that classes covering a larger area have more impact on the signal than classes with low

footprint coverage. In order to account for this, the area weight of the improved LCSS-class was taken into account. The analysis shows that only the agricultural LCS-class on top of soil group 2 and 3 shows a significant improvement of R^2 , covering between 7 % (ID376) to 21 % (ID394) of the respective footprint. In conclusion, the consideration of slope in the grouping of scaling parameters only improved the results for agricultural areas. For the other LCS classes the improvement was below 0.01 and therefore not significant.

In the next step, the scaling parameters were differentiated according to land cover, soil group, slope and aspect. Here the same procedure was applied as above. Here, a further improvement was achieved for 0.2 % (ID394) to 5.3 % (ID393) of the respective footprint area. This improvement was mainly observed in agriculture areas with soil group 2 and 3, whereas no improvement in the areas covered with forest was observed.

The last step, the improvement of applying the scaling parameter for the land cover, soil group, slope, aspect and geology (LCSSAG)-combinations was analyzed. The application of these parameter resulted in an R^2 -improvement for 0.5 % (ID393) to 1.6 % (ID394) of the footprint area. The examination of the respective LCSSAG-classes did not reveal an improvement in a specific class.

Discussion of the Downscaling Results

The results show that in the case study of the Great Letaba catchment geology does not significantly improve the results. Only up to 1.6 % of the footprint area show an increase of R^2 by at least 0.01. This weak influence could be explained by the minor influence of underlying geology formation on the rainfall-runoff generation in that area. For the Great Letaba catchment, the landscape parameters of land cover and soil group are the driving parameters to predict the meso-scale soil water distribution. This agrees with the findings of KIM AND BARROS (2002B) who disaggregated soil water information based on a fractional interpolation scheme and used soil texture and vegetation water content as additional data. In the present study, instead of vegetation water content, the actual land cover class has been used which is connected to the vegetation water content.

An adding of the topography parameters slope and aspect as additional landscape parameters helped to improve the R^2 -values and therefore the

explained variability of SWI_{HRU} with SWI_{ERS} and P_{sum} only for agricultural areas with the soil group 2 and 3. The additional topography information needed for agricultural land might be explained by the studies of FAMIGLIETTI, DEVEREAUX ET AL. (1999) and MOHANTY, SKAGGS ET AL. (2000) who identified an influence of agricultural practice on soil moisture distribution. Parameters determining tillage operations are, for instance, slope and stone cover of the agricultural field (GOE, 1999). Also, agricultural land is affected by crop rotation, which might result in variations of the signal contributions into the integral remotely sensed signal.

In the case of the forested areas, the downscaling method showed only weak success. The reasons can be found in the constraints of the microwave remote sensing. As discussed in *Section 2.2.1.2* the transmitted microwave signal can not penetrate dense vegetation such as forests. The microwave can only penetrate into the soil in areas with clear cuts in the forest. The integrated ERS-signal, therefore, contains no, or only minor, information on the soil water content under this vegetation cover, which constraints the application of the downscaling model in these areas.

Downscaling Results with the Resulting Scaling Parameters

The downscaling was carried out for the timeframe October 1997 to September 1999 using the scaling parameter based on the land cover and soil combination (*Table 5-16*) with the exception of agricultural areas for which the following parameter were applied (*Table 5-17*). The resulting time series were than compared to the modeled SWI_{HRU} time series.

Table 5-17: Scaling Parameters for Agricultural Land under Consideration of the Specific Soil, Slope and Aspect Group

	SG	SLOPE	ASPECT	M1			M2			D		
				LQ	UQ	MD	LQ	UQ	MD	LQ	UQ	MD
Agriculture	2	<5°	N	0.57	0.95	0.70	0.05	0.21	0.15	-14.68	-9.81	-11.84
			E/W	0.63	1.05	0.84	0.01	0.19	0.08	-15.01	-10.60	-13.43
			S	0.54	1.03	0.75	0.02	0.23	0.11	-14.31	-9.21	-12.61
		5°-15°	N	0.95	1.10	1.04	0.03	0.08	0.05	-16.42	-13.53	-14.32
			E/W	0.84	1.11	1.02	0.02	0.13	0.04	-16.92	-12.07	-14.03
			S	0.86	1.12	1.03	0.03	0.16	0.06	-16.56	-13.88	-14.45
	3	<5°	N	0.49	1.06	0.74	0.06	0.24	0.15	-14.06	-8.35	-11.90
			E/W	0.49	1.05	0.64	0.05	0.25	0.19	-13.81	-8.08	-11.18
			S	0.47	0.93	0.69	0.07	0.25	0.19	-12.92	-7.85	-11.29
		5°-15°	N	1.03	1.19	1.11	0.03	0.09	0.06	-14.67	-12.77	-13.87
			E/W	1.04	1.17	1.12	0.00	0.07	0.04	-14.63	-12.25	-13.44
			S	1.04	1.15	1.11	0.02	0.08	0.06	-14.83	-13.33	-14.02

As a quality criterion, the coefficient of determination between the two time series was calculated and its spatial distribution was analyzed. The resulting R²-distributions are plotted in Figure 5-20 to Figure 5-22.

The figures show the spatial distribution of the R²-values within the respective footprints. In general, the downscaling of the macro-scale root zone soil water estimates resulted in R²-values between R² = 0.03 and R² = 0.87 with between 66.2 % (ID376) and 94.9 % (ID394) of the respective footprint area achieving R²-values higher than 0.5 (Table 5-18).

Downscaling: Coefficient of Determination (R^2) for the Time Period 1997-1999
Footprint ID376

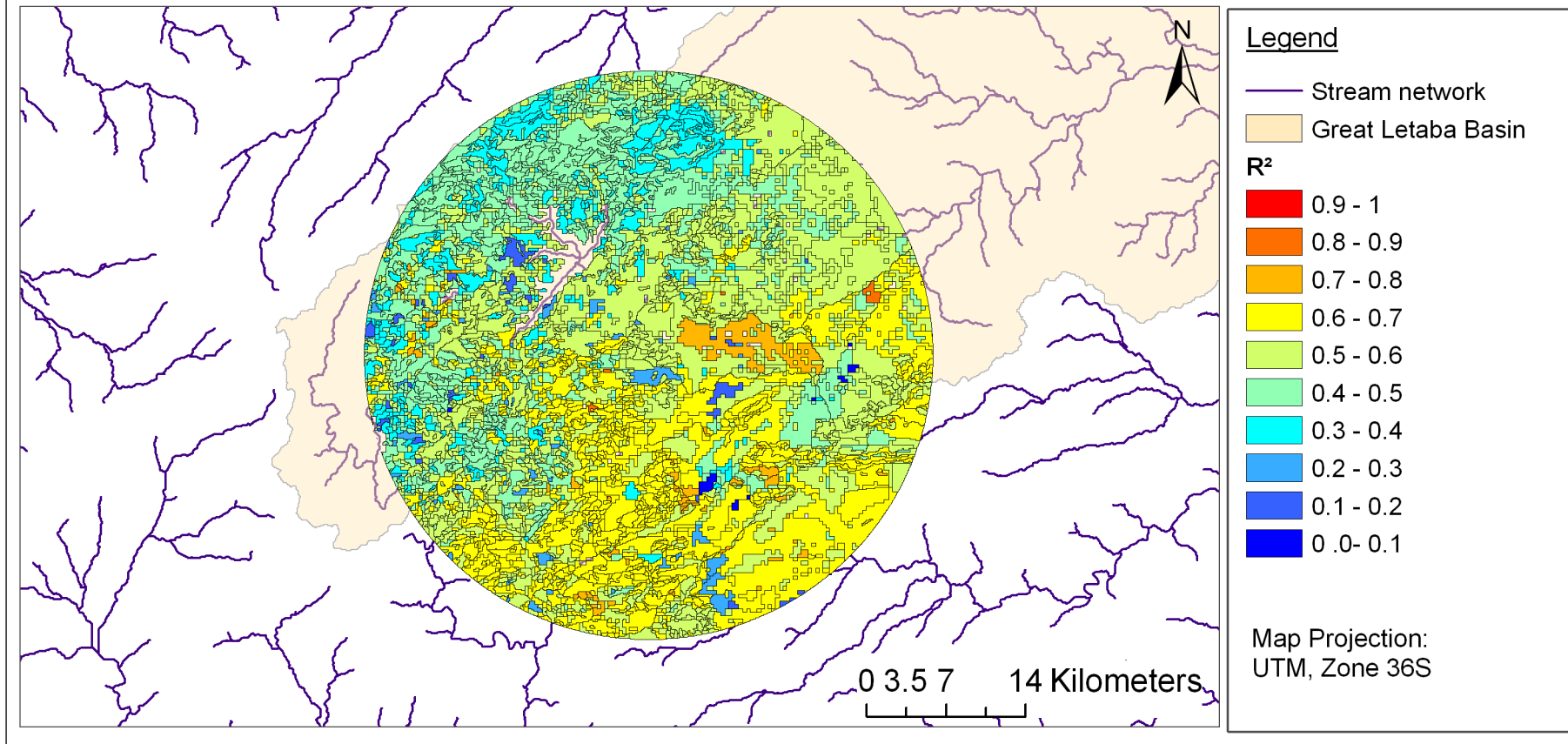


Figure 5-20: R^2 -Spatial Distribution for the Downscaling, (Timeframe 1997 to 1999), Footprint ID376

Downscaling: Coefficient of Determination (R^2) for the Time Period 1997-1999
Footprint ID393

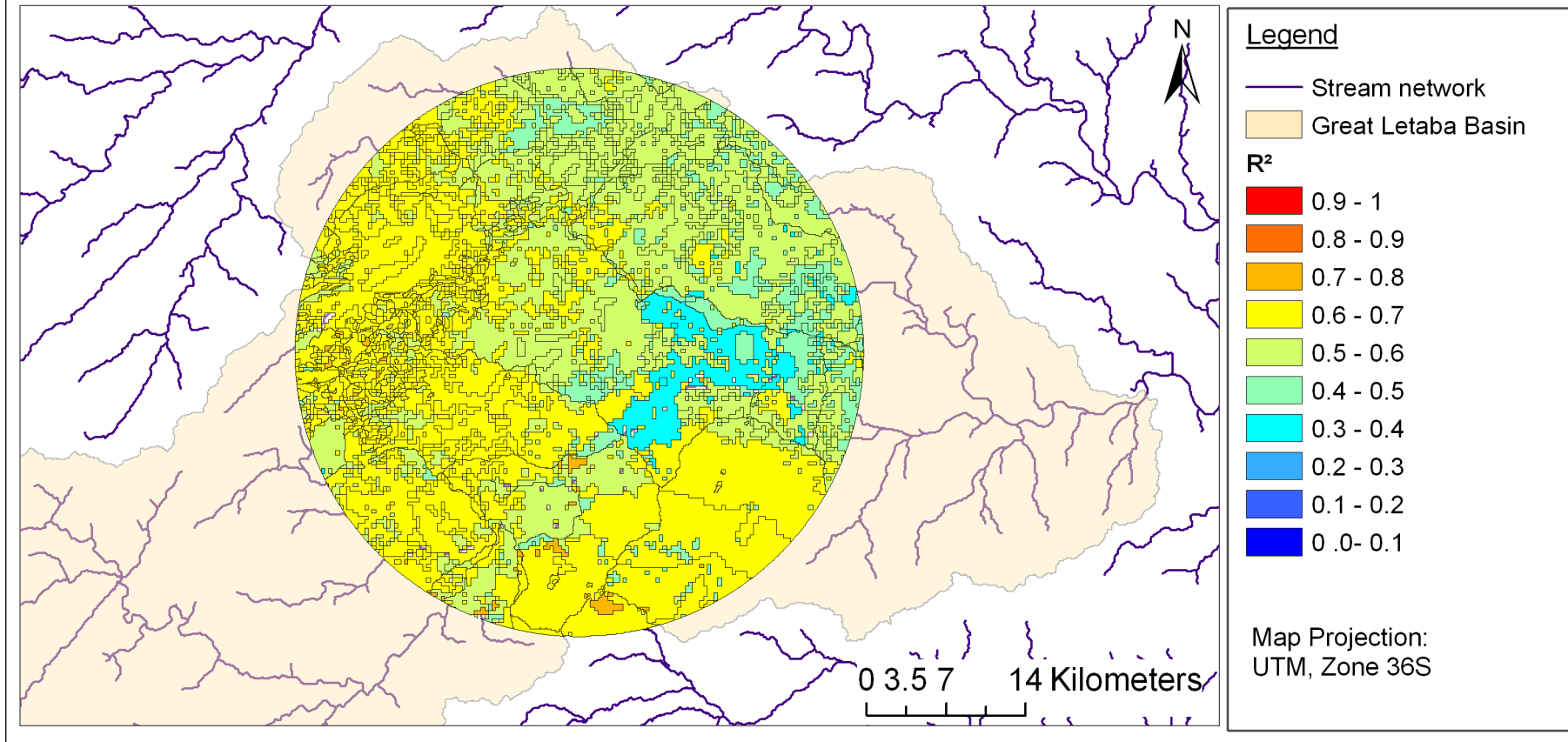


Figure 5-21: R^2 -Spatial Distribution for the Downscaling (Timeframe 1997 to 1999), Footprint ID393

Downscaling: Coefficient of Determination (R^2) for the Time Period 1997-1999
Footprint ID394

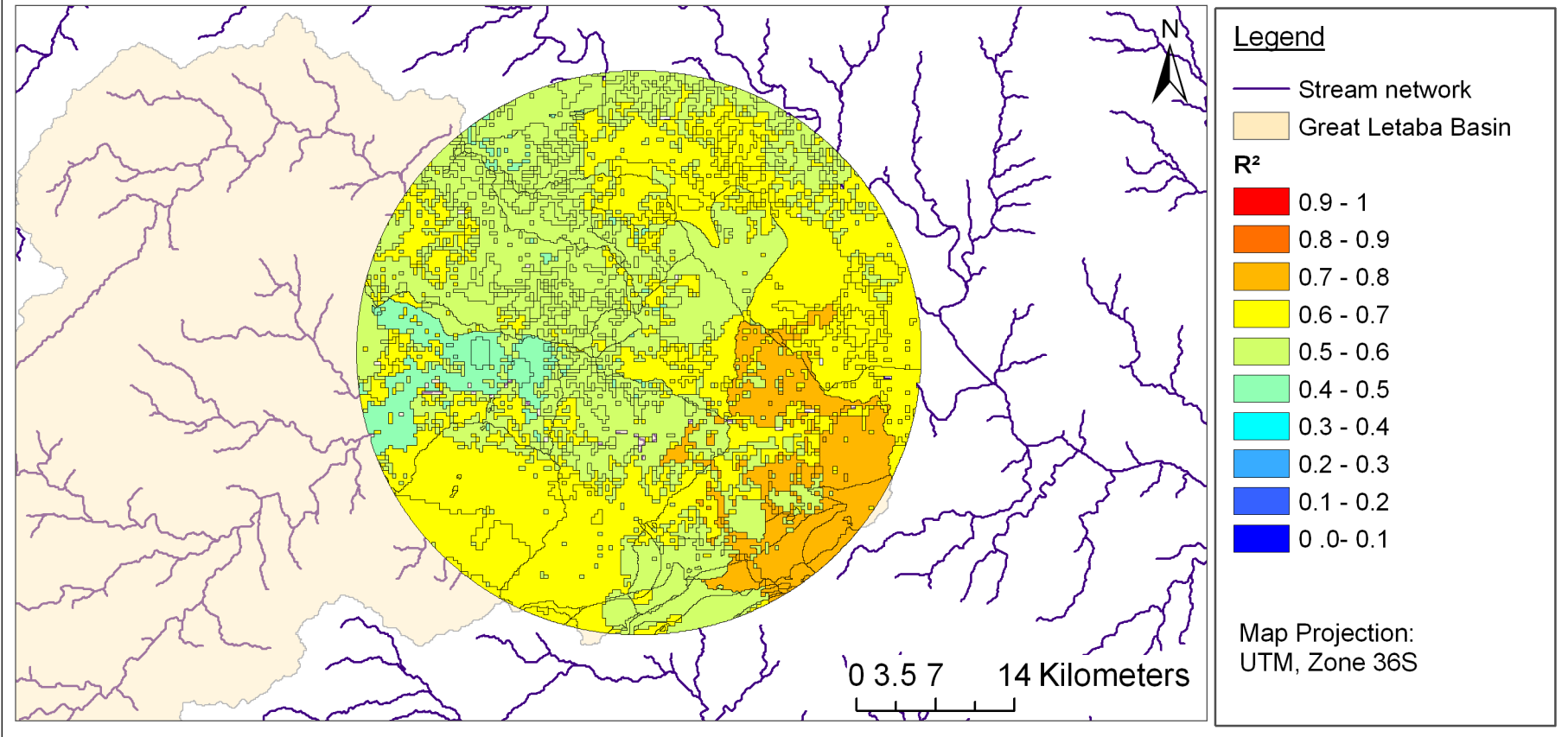


Figure 5-22: R^2 -Spatial Distribution for the Downscaling, (Timeframe 1997 to 1999), Footprint ID394

Table 5-18:HRU-Amount and its Respective Footprint Area of HRUs achieving R^2 over 0.5

	$R^2 > 0.5$	
	AMOUNT HRUs	% FOOTPRINT AREA
ID376	62.6 %	66.2 %
ID393	85.9 %	86.4 %
ID394	96.0 %	94.9 %

As illustrated in Table 5-18, parts of the footprints show R^2 -values under 0.5, especially in the footprint ID376 where values below $R^2=0.5$ were calculated for about 34 % of the area. The spatial distribution of R^2 -values indicates that some land cover classes achieve better downscaling results than others. About 28.7 % of the footprint area of ID376 is covered by forest whereas savanna vegetation (bushland and woodland) are the major land cover classes for the footprints ID393 and ID394, (Table 5-12) which indicates that dense vegetated areas show low R^2 -values. This was analyzed by plotting the lower quintile, upper quintile as well as the median for every land cover class. The results are summarized in Table 5-19.

Table 5-19: Statistical Summary of the R^2 -values for the Land Cover Classes

	R^2 -DISTRIBUTION					
	LQ	UQ	MD	MIN	MAX	MEAN
Deciduous Forest	0.39	0.51	0.44	0.09	0.76	0.45
Conifer Forest	0.39	0.55	0.48	0.15	0.70	0.46
Woodland	0.57	0.66	0.61	0.36	0.74	0.61
Bushland	0.53	0.65	0.59	0.20	0.84	0.59
Grassland	0.63	0.70	0.65	0.37	0.73	0.65
Bare soil and Sparse Vegetated Areas	0.52	0.64	0.56	0.28	0.75	0.57
Wetland	0.43	0.53	0.48	0.37	0.80	0.50
Agriculture	0.49	0.63	0.56	0.18	0.87	0.55
Urban Areas	0.15	0.39	0.25	0.04	0.59	0.27

The table above shows differences in the achieved R^2 -values between the land cover classes. Urban areas, for instance, resulted in R^2 -values between 0.04 and 0.59, whereas 60 % of the HRUs are lying between 0.15 and 0.39. Also for forest areas, deciduous and conifer, R^2 -values reached only between 0.09 and 0.76, respectively 0.15 to 0.70, in which 60 % of the HRUs are within the range of 0.39 and 0.51 and 0.55 respectively. Land cover classes with R^2 -values between

0.56 and 0.65 in median, are woodland, bushland, grassland and bare soil and sparse vegetated areas. Agricultural areas ranged from 0.18 to 0.87, but the majority, 60 % of the HRUs, are ranged from $R^2 = 0.49$ to $R^2 = 0.63$ but as shown in *Figure 5-21* and *Figure 5-22* some areas reach values below this range and highlighted with light blue coloring.

The difference in the explained variability of SWI_{HRU} with P_{sum} and SWI_{ERS} might be explained by the application of two different concepts: 1) the remotely sensed approach and 2) the hydrological model. As discussed in *Section 2.2.1*, the ERS-scatterometer can not penetrate dense vegetation such as forest but also in impervious areas the soil water content can not be predicted (WAGNER, LEMOINE ET AL., 1999A; WAGNER, LEMOINE ET AL., 1999B; WAGNER, NOLL ET AL., 1999). It is therefore predicted that in those areas the macro-scale soil water estimates does not contain information and the downscaling of those areas is of a minimal success. The resulting small R^2 -values of HRUs characterized by urban and forest vegetation is, therefore, not surprising. Wetland areas are also difficult to measure with the ERS-scatterometer (SCIPAL, 2002). For areas with bushland, woodland, agriculture bare soil, sparse vegetation and grassland, high R^2 -values have been achieved. Here, the transmitted signals can penetrated into the surface soil layer due to low vegetation cover or open vegetation areas and the integrated ERS-signal does contains soil water information on those areas. The results agree with the findings of WAGNER, PATHE ET AL. (SUBMITTED) who also achieved good downscaling results for cropland and herbaceous areas.

Also, on the side of the applied hydrological model, limits occur that reduce the explanatory power of the downscaling scheme. In the model applied, irrigation is not implemented in the model structure. About 9 % of the agricultural area in the Great Letaba river is temporally or permanently under irrigation (CSIR AND ARC, 2005), which affects the remotely sensed signal. As a result, a difference evolves between the modeled and disaggregated time series especially in these areas.

Despite the limitations of the applied procedure discussed, the results achieved are very positive, indicating that the model is able to disaggregated soil water dynamics in the Great Letaba River. In the next section, the influence of the applied hydrological model will analyzed. Therefore, the scaling

parameter will be calculated based on the variation of the model output resulting from the sensitivity analysis.

5.3.4 Impact of Model Calibration Parameter on the Downscaling Parameters

The downscaling scheme described above is based on meso-scale soil water time series derived from the rainfall-runoff modeling using the J2000 hydrological modeling system. The resulting soil water time series are, therefore, a result of the calibration of J2000. The sensitivity analysis identified the *FCAdaptation* parameter as having the largest influence on the soil water output. An important question to answer is how much this specific model calibration parameter impacts the m_1 , m_2 and d downscaling parameters.

To assess this influence the calibration parameter *FCAdaptation* was changed by +/- 10 %. The resulting soil water time series were then used to recalculate the m_1 , m_2 and d downscaling parameters. The first test, the reduction of *FCAdaptation* by 10 %, results in a decrease of the soil water storage and the second test, the increase of *FCAdaptation* by 10 %, results in an increase of the soil water storage.

For each land cover and soil group combination the scaling parameters were calculated for the two test cases and compared to the former values achieved with the baseline J2000 model output. For the forest, bushland, woodland, bare soil and sparse vegetated surfaces, and wetland land cover classes the calculated maximum difference between the median of the baseline and the test runs amounted to +/- 6.2 % for the m_1 and m_2 parameters and +/- 8.6 % for the intercept.

The direction of change was also analyzed. The decrease of *FCAdaptation* resulted in a decline of the m_2 parameter by 4.3 % for the aforementioned land cover classes. The increase of *FCAdaptation* resulted in an increase of the m_2 parameter by 6.2 %. Parameters m_1 and d showed the opposite behavior. Here an increase of the maximum soil water storage resulted in a decrease of the scaling parameters m_1 and d of about 5 % whereas a decrease of the soil water storage showed an increase of the scaling parameters of up to 8.6 %.

For two land cover soil groups, however, these model parameter changes resulted in larger variations of the downscaling parameters. First, for agricultural land on soil group 2 with a hillside slope lower 5°, as well as

agricultural land on soil group 3 with a hillside slope between 5° and 15°, the parameter adaptation resulted in changes of the scaling parameters up to 50 %. A possible explanation could be the missing consideration of irrigation by the J2000 modeling system, which is common practice for this land cover soil group combination. A second explanation might be the low number of samples (below 50 HRUs), especially for all HRUs characterized by the soil group 1. Here high variations of the scaling parameters could be observed as a result of the parameter variation. Because of the absolute low number of samples it is very likely that these classes could not produce a stable distribution, which results in higher variations of the scaling parameters.

In summary, the analysis showed that the downscaling parameters are changing when they are based on different model calibration parameters. In particular, the parameters influencing the simulated soil water storage will alter the scaling parameters and therefore influence the relationship between the macro-scale and meso-scale soil water time series. This analysis, therefore, gives an indication of variation in the prediction range of the developed downscaling scheme, which can be quantified as less than 10 %. However, considering the assumptions made and considering the fact that the applied modeling system is able to reflect hydrological processes in this area, the resulting variations are acceptable. For further studies, an a priori estimation of model calibration parameters based on “stable” landscape characteristics, such as topography, might result in more generic model calibration parameter sets. This would then lead to more stable downscaling parameters and therefore to a reduction of uncertainty

CHAPTER 6

SUMMARY, CONCLUSIONS AND FUTURE RESEARCH

6.1 Summary and Conclusions

The goal of the presented study was the **development of a downscaling scheme for application of the macro-scale soil water estimates in meso-scale hydrological modelling**. To achieve this goal three main objectives were addressed: I) application of a distributed hydrological model to estimate the spatial soil water distribution and the factors influencing this distribution, II) evaluation of the influence of landscape parameters (soil, land cover, topography, geology) on the macro-scale soil water estimates and, using this information, III) the development of a method for disaggregating macro-scale soil water estimates.

For the realization of the overall goal of the work and the three specific objectives, the conceptual and methodical approach of this study was based on the following aspects: a) data analyses and integrated systems analysis; b) estimation of meso-scale soil water distribution by establishing the rainfall-runoff relationship using a hydrological model; and c) evaluation of the relationship between macro-scale and meso-scale soil water distribution.

The area used as a case study was the Great Letaba River catchment (ca. 4.700 km²), a tributary of the Olifants River in South Africa. This area was

chosen, due to constraints in the microwave techniques, in the inability of penetrating dense vegetation cover, such as forests, while also covering a large enough catchment size to include at least three scatterometer grid points. A database was established for this area incorporating land cover, soil, geology, a digital elevation model, hydrometric data (runoff) and meteorological data such as humidity, wind speed and air temperature time series. The database then was used in the integrated systems analysis. This resultant analysis indicated that the hydrological response of the Great Letaba River is influenced by hydrometric infrastructure. Two major dams and several small dams were built within the catchment to ensure water availability for daily use as well as the extensive application of irrigation water for farming. This infrastructure was not taken into account in the modeling approach by calibrating the model without taking the catchment of the dams into account.

For a process oriented estimation of the meso-scale soil water distribution, the concept of HRUs was applied. These HRUs were then used as model entities in the process oriented modular J2000 modeling system. The model estimates the soil water content of the soil column as a component of the water balance.

The modeling system was able to predict the hydrological processes using the available data in an acceptable manner for the Great Letaba River catchment, despite the problems of representing the observed runoff by the model due to: 1) uncertain inputs and model validation resulting from incomplete and inaccurate hydro-meteorological data and 2) unknown water allocation along the stream channel.

The model performance was evaluated by the comparison of observed and simulated runoff as well as with the comparison of the modeled evapotranspiration with theoretical values published in the literature. Considering that the parameters of the water balance (precipitation as an input variable, evapotranspiration as an output) compared favorably with values found in literature and the observed and simulated runoffs were comparable, it can be assumed that the soil moisture is adequately accounted for. However, the modeling still includes “room for improvement” that is discussed further in the next section.

As a next step, the variable for comparison had to be identified. The SWI_{ERS} variable is described as the soil water content between wilting point and

field capacity. However, research has indicated that, in semi-arid areas, the soil water content can drop below wilting point and saturation above field capacity is possible. In order to overcome this problem, the simulated soil water index (SWI_{HRU}) has been calculated, taking the soil water content of the three pore storage components (large pore storage, medium pore storage and fine pore storage) into account.

The resultant time series values were compared to the macro-scale soil water estimates at a footprint scale. The analyses indicated considerable similarities in the evaluation of the soil water over time. This indicates that the macro-scale soil water estimates contain valuable information on soil water content. The similarities in the time trend data series, as well as in the seasonal component, are very promising results that justify extending this analysis to develop a downscaling scheme for the macro-scale soil water estimates.

The overall downscaling concept is based on a linear regression approach that indicated encouraging results in previous studies (CROW, RYU ET AL., 2005; DE LANNOY, HOUSER ET AL., 2007; WAGNER, PATHE ET AL., SUBMITTED). In a preliminary analysis, precipitation was determined to be an important parameter. To take this parameter into account, the conceptual downscaling approach was transformed into a multiple linear regression approach. The included scaling parameters determined by the regression model were found to be related to the landscape characteristics. With the exception of agricultural areas, the combination of land cover and soil group can be used to derive the scaling parameters. For agricultural areas, the consideration of the specific topography group, slope and aspect in this case study improved the downscaling results.

The resulting scaling parameters were applied on the time period of 1997 through 1999 and the results evaluated accordingly. For grassland, bushland, woodland and bare soil and sparse vegetation land cover classes, it was found that the downscaling model achieved very good results. Wetland areas and urban areas exhibited unsatisfactory results, that are primarily caused by satellite limitations. Specifically, the transmitted signal cannot penetrate dense vegetation, impervious areas as well as water. The downscaling results for agricultural areas are moderate; this condition might be explained by model limitations. The integrated systems analysis indicated that some parts of agricultural areas in the catchment are currently under irrigation. This form of

water resources management could not be included in the modeling structure and therefore was not accounted for.

These results are very promising, despite the underlying uncertainties inherent in both concepts, model results vs. macro-scale estimates. From the model standpoint, uncertainties occur in the uncertain input data, anthropogenic influence and the lack of including irrigation use in the model structure. In addition, the analysis indicated that the scaling parameters are dependent on the calibration model parameters, which increase the uncertainties of the resulting scaling parameters. In the case of the macro-scale soil water estimates, uncertainties occur in the conceptual approach of the SWI_{ERS} based on the simple infiltration model as well as the definition of the index and the inability of microwave to penetrate dense vegetation, impervious areas and water.

Hence, further research should be conducted (see next section). Taking these uncertainties into account, the results are very promising and justify further research to downscale macro-scale soil water estimates. The main contributions to this field can be summarized by answering the following research questions.

Which characteristics of the macro-scale soil water estimates are important for their application in meso-scale hydrological modeling?

The results of this study show that both concepts, hydrological modeling and remotely sensed soil water estimates, reveal large similarities in predicting the soil water distribution over time. This analysis also exhibited variations in the prediction of the actual soil water values. These differences can be explained by the difference in the observed soil water volumes. The remotely sensed soil water estimates are based on the surface soil water content, whereas the simulated soil water time series are based on the root zone soil water content. From this it can be concluded that the macro-scale soil water estimates can act as a data source on dynamics of the soil water content for meso-scale hydrological modeling.

What downscaling method can be applied to describe the relationship between macro-scale and meso-scale soil water distribution?

The study confirms results published BY CROW, RYU ET AL. (2005), DE LANNOY, HOUSER ET AL. (2007) and WAGNER, PATHE ET AL. (SUBMITTED), in which the relationship between macro-scale and meso-scale soil water is described by a linear relationship. The study also shows that precipitation acts as a control factor and has to be included in the downscaling scheme. The study showed that the meso-scale soil water distribution can be described as a multivariable linear regression function of the macro-scale soil water values and the regional measured precipitation.

What are the driving variables controlling the scaling parameters used to downscale the macro-scale soil water estimates and how can they be used to explain meso-scale soil water distribution?

The results of this study show that land cover and soil group are suitable parameters to derive regression parameters to explain the meso-scale soil water distribution. For the most part, a very good downscaling result has been achieved using these parameters. The addition of the slope and aspect parameters only improved the results slightly for agricultural areas. The study indicates that the simulated modeled time series is not a complete description of the soil water distribution, because the effects of irrigation processes in the catchment were not modeled. Geology was not found to be an important parameter describing the meso-scale soil water distribution in the Great Letaba River catchment.

Which areas can be disaggregated with the macro-scale soil water product and with what level of success?

The downscaling model developed has been applied in the Great Letaba River catchment for the time period from 1997 through 1999. The downscaling model was able to predict the meso-scale soil water distribution and indicate the differences among the various applicable land cover classes. Very good downscaling results were achieved for the woodland, bushland, grassland, bare soil and sparsely vegetated areas land cover classes. For agricultural areas, the applied model generated only moderately acceptable results, which might be mainly caused by limitations in the applied model structure. The downscaling

scheme resulted in completely unsatisfactory results only for urban areas, wetlands and forest classes. In these cases, the limitations of the applied satellite technique were a significant factor.

6.2 Future Research

This study presents very promising results for downscaling macro-scale soil water data. However, uncertainties still exist, from which key areas for further research can be derived.

First, a validation of the downscaling method should be conducted in the same study area but for a different time frame and with different input data. Two directions for research are recommended: 1) the estimation of meso-scale soil water time series based on different input data, such as precipitation information derived from radar. Such datasets would help to characterize the areal rainfall patterns more accurately. Also, data on the actual water uptake would ensure a more certain and acceptable model calibration; 2) application of different macro-scale soil water data. Possible datasets could be data from the Advanced Scatterometer (ASCAT) onboard the MetOp-Satellite launched in 2006 or the Soil Moisture and Ocean Salinity (SMOS), expected to launch in 2008 (EUROPEAN SPACE AGENCY, 2007).

Second, the proposed method needs to be applied to other catchments. Specifically, two kinds of study areas are recommended to be analyzed: 1) study areas with similar catchment characteristics will give an indication of the dependency of the study on the specific catchment characteristics. There is a need to validate the findings in other areas that are similar to the area used to develop the method; 2) the proposed method has to be applied to areas with different natural characteristics. Such an analysis would give an indication of applicability of the method under various climatic and natural conditions.

Third is the application of a hydrological model with a vertical subsurface profile layer. The ERS-scatterometer penetrates only into the upper (< 5 cm) (WAGNER, SCIPAL ET AL., 2003) surface soil layer and the applied simple infiltration model component introduces considerable uncertainty. The hydrological modeling of the soil water distribution in the upper soil layer and its comparison with the remotely sensed measurements would help in the following ways: 1) to understand the applicability of the assumed infiltration

model for the ERS-scatterometer measurements and 2) to give further insight for SWI_{ERS} model improvement. Also it would help to establish a better relationship between the meso-scale and macro-scale distribution.

This would also be helpful for a fourth area for future research, establishing a method for integrating macro-scale remotely sensed data, such as the SWI_{ERS}-data, in meso-scale hydrological models. The study shows that the remotely sensed datasets contain valuable information which could help to improve meso-scale hydrological models. In particular, in areas with no or only limited hydrometric infrastructure, these data could act a validation tool. Modeling results could be evaluated using an additional data source. With the development of appropriate methods, the remotely sensed data could serve as an important data source in model parameterization and model calibration. In this way, remotely sensed soil water data provides a valuable tool for water resources management.

REFERENCES

- Acocks, J. P. H. (1988). *Veld Types of South Africa* (3rd. ed.): Botanical Research Institute, South Africa.
- Ad-hoc Arbeitsgruppe Boden, & Sponagel, H. (2005). *Bodenkundliche Kartieranleitung* (5.th ed.). Hannover: Bundesanstalt für Geowissenschaften und Rohstoffe in Zusammenarbeit mit den Staatlichen Geologischen Diensten.
- Arbeitsgruppe Boden. (1994). *Bodenkundliche Kartieranleitung* (4.th ed.). Hannover: Bundesanstalt für Geowissenschaften und Rohstoffe in Zusammenarbeit mit den Staatlichen Geologischen Diensten.
- Archer, N., Hess, T., & Quinton, J. (2002). The Water Balance of Two Semi-Arid Shrubs on Abandoned Land in South-Eastern Spain after Cold Season Rainfall. *Hydrology and Earth System Sciences*, 6(5), 913-926.
- Arora, V. K., & Boer, G. J. (2003). *The Temporal Variability of Soil Moisture and Surface Hydrological Quantities* (No. Report No. 33): CAS/JSC WGNE Research Activities in Atmospheric and Oceanic Modelling
- Assenmacher, W. (1998). *Deskriptive Statistik* (2nd ed.). Berlin: Springer Verlag.
- Bahremand, A., & De Smedt, F. (2008). Distributed Hydrological Modeling and Sensitivity Analysis in Torysa Watershed, Slovakia. *Water Resources Management*, 22(3), 393-408.
- Bardossy, A., & Lehmann, W. (1998). Spatial Distribution of Soil Moisture in a Small Catchment. Part 1: Geostatistical Analysis. *Journal of Hydrology*, 206(1-2), 1-15.
- Bartalis, Z. (2005). *Selection of Resampling Procedure*. Vienna: Vienna University of Technology Institute for Photogrammetry and Remote Sensing (IPF).
- Bäse, F. (2005). *Beurteilung Der Parametersensitivität und der Vorhersagesicherheit am Beispiel Des Hydrologischen Modells J2000*. Friedrich-Schiller Universität Jena, Jena.

- Bäse, F., Helmschrot, J., Müller-Schmied, H., & Flügel, W.-A. (2006, 4.-6. Oktober 2006). *The Impact of Land Use Change on the Hydrological Dynamic of the Semiarid Tsitsa Catchment in South Africa*. Paper presented at the 2nd Göttinger GIS and Remote Sensing Days, Göttingen, Deutschland.
- Becker, A. (1992). Methodische Aspekte der Regionalisierung. In H.-B. Kleeberg (Ed.), *Regionalisierung in der Hydrologie: Ergebnisse von Rundgesprächen der Deutschen Forschungsgemeinschaft* (pp. 16-32). Weinheim: VCH Verlagsgesellschaft mbH.
- Beven, K., & Kirkby, M. (1979). A Physically-Based, Variable Contributing Area Model of Basin Hydrology. *Hydrological Sciences Bulletin*, 24(11), 43-69.
- Beven, K. (2001a). How Far Can We Go in Distributed Hydrological Modelling? *Hydrology and Earth System Sciences*, 5(1), 1-12.
- Beven, K. (2001b). *Rainfall-Runoff Modelling*. Chichester [a.o.]: John Wiley & Sons.
- Bierkens, M. F. P., Finke, P. A., & Willigen, P. d. (2000). *Upscaling and Downscaling Methods for Environmental Research*. Dordrecht; Boston: Kluwer Academic Publishers.
- Bindlish, R., & Barros, A. P. (2002). Subpixel Variability of Remotely Sensed Soil Moisture: An Intercomparison Study of SAR and ESTAR. *IEEE Transaction on Geoscience and Remote Sensing*, 40(2), 326-337.
- Blöschl, G., & Sivapalan, M. (1995). Scale Issues in Hydrological Modelling: A Review. In J. Kalma & M. Sivapalan (Eds.), *Scale Issues in Hydrological Modelling* (pp. 9-48). New York: John Wiley & Sons.
- Blöschl, G. (1996). *Scale and Scaling in Hydrology*. Wien: Technische Universität Wien
- Blöschl, G. (2005). Rainfall-Runoff Modeling of Ungauged Catchments. *Encyclopedia of Hydrological Sciences*.
- Blumberg, D. G., Freilikher, V., Lyalko, I. V., Vulfson, L. D., Kotlyar, A. L., Shevchenko, V. N., et al. (2000). Soil Moisture (Water-Content) Assessment by an Airborne Scatterometer: The Chernobyl Disaster Area and the Negev Desert. *Remote Sensing of Environment*, 71(3), 309-319.
- Bongartz, K. (2001). *Untersuchung Unterschiedlicher Flächendiskretisierungs- und Modellierungskonzepte für die Hydrologische Modellierung am Beispiel Thüringer Vorfluter* Friedrich-Schiller-Universität Jena, Jena.

-
- Breuer, L., & Frede, H. (2003). Plapada - an Online Plant Parameter Data Drill for Eco-Hydrological Modelling Approaches, (Online Database). Retrieved 31.05.2006: <http://www.uni-giessen.de/~gh1461/plapada/plapada.html>.
- Burke, E. J., & Simmonds, L. P. (2001). A Simple Parameterisation for Retrieving Soil Moisture from Passive Microwave Data. *Hydrology and Earth System Sciences*, 5(1), 39–48.
- Burke, E. J., & Simmonds, L. P. (2003). Effects of Sub-Pixel Heterogeneity on the Retrieval of Soil Moisture from Passive Microwave Radiometry. *International Journal of Remote Sensing*, 24(10), 2085–2104.
- Campbell, J. B. (2007). *Introduction to Remote Sensing* (4th ed.). New York, London: The Guilford Press.
- Canadell, J., Jackson, R. B., Ehleringer, J. R., Mooney, H. A., Sala, E., & Schulze, E.-D. (1996). Maximum Rooting Depths of Vegetation Types at the Global Scale. *Oecologia*, 108(4), 583-595.
- Caylor, K. K., Shugart, H. H., & Rodriguez-Iturbe, I. (2005). Tree Canopy Effects on Simulated Water Stress in Southern African Savannas. *Ecosystems*, 8(1), 17–32.
- Ceballos, A., Martínez-Fernández, J., Santos, F., & Alonso, P. (2002). Soil Water Behaviour of Sandy Soils under Semi-Arid Conditions in the Duero Basin (Spain). *Journal of Arid Environment*, 51(4), 501-519.
- Ceballos, A., Scipal, K., Wagner, W., & Martínez-Fernández, J. (2005). Validation of ERS Scatterometer-Derived Soil Moisture Data in the Central Part of the Duero Basin, Spain. *Hydrological Processes*, 19(8), 1549-1566.
- Center for Environmental Remote Sensing Chiba University. (2006). Matthews Seasonal Albedo, (Online Database). Retrieved 30.05.2006: <http://dbx.cr.chiba-u.jp/gdes/Albedo/matthews1984.html>
- Charpentier, M. A., & Groffman, P. M. (1992). Soil Moisture Variability within Remote Sensing Pixels. *Journal of Geophysical Research*, D17, 97, 18987-18995.
- Cleveland, W. S. (1979). Robust Locally Weighted Regression and Smoothing Scatterplots. *Journal of the American Statistical Association* 74(368), 829-836.
- Cleveland, R. B., Cleveland, W. S., McRae, J. E., & Terpenning, I. (1990). Stl: A Seasonal-Trend Decomposition Procedure Based on Loess. *Journal of Official Statistics*, 6(1), 3-73.
-

- Cracknell, A. P., & Hayes, L. (2007). *Introduction to Remote Sensing* (2nd ed.). Boca Raton CRC Press Taylor & Francis Group.
- Crawford, N. H., & Linsley, R. K. (1966). *Digital Simulation in Hydrology: Stanford Watershed Model Iv* (No. Technical Report 39). Palo Alto: Dept. of Civil Engineering, Stanford University, California.
- Crow, W. T., Ryu, D., & Famiglietti, J. S. (2005). Upscaling of Field-Scale Soil Moisture Measurements Using Distributed Land Surface Modeling. *Advances in Water Resources*, 28(1), 1-14.
- CSIR, & ARC. (2005). National Land Cover 2000 South Africa, Version 2005. Raster-Data Set. Pretoria: Council for Scientific and Industrial Research and Agricultural Research Council.
- Davis, S. N., & DeWiest, R. J. M. (1966). *Hydrogeology*. New York [a.o.]: Wiley.
- De Lannoy, G. J. M., Houser, P. R., Verhoest, N. E. C., Pauwels, V. R. N., & Gish, T. J. (2007). Upscaling of Point Soil Moisture Measurements to Field Averages at the Ope3 Test Site. *Journal of Hydrology*, 343 (1-2), 1-11.
- De Michele, C., & Salvadori, G. (2002). On the Derived Flood Frequency Distribution: Analytical Formulation and the Influence of Antecedent Soil Moisture Condition. *Journal of Hydrology*, 262(1), 245-258.
- Deardorff, J. W. (1977). A Parameterization of Ground-Surface Moisture Content for Use in Atmosphere Prediction Models. *Journal of Applied Meteorology*, 16(1), 567-594.
- Department of Water Affairs and Forestry (Cartographer). (2002). *Messina 2127*
- Department of Water Affairs and Forestry. (2003a). *National Water Resource Strategy: South Africa's Water Situation and Strategies to Balance Supply and Demand: Luvuvhu and Letaba Wma* (No. WMA 02/000/00/0203). Pretoria, South Africa: Department of Water Affairs and Forestry, South Africa.
- Department of Water Affairs and Forestry (Cartographer). (2003b). *Phalaborwa 2330*
- Department of Water Affairs and Forestry (Cartographer). (2003c). *Polokwane 2326*
- Department of Water Affairs and Forestry, S. A. (2003d). Hydrological Information System (Online Database). Retrieved 10.10. 2006, from Department of Water Affairs and Forestry, South Africa: <http://www.dwaf.gov.za/hydrology/cgi-bin/his/cgihis.exe/station>

- Department of Water Affairs and Forestry, & Directorate: National Water Resource Planning (North). (2004). *Internal Strategic Perspective: Luvuvhu/Letaba Water Management Area* Pretoria, South Africa: Department of Water Affairs and Forestry.
- Department of Water Affairs and Forestry. (2007). Groot Letaba Water Development Project - Home. Retrieved 6-12-2007, 2007, from <http://www.dwaf.gov.za/Projects/GrootLetaba/default.asp>
- Deutscher Verband für Wasserwirtschaft und Kulturbau. (1983). *Niedrigwasseranalyse -Teil 1: Statistische Untersuchung des Niedrigwasser-Abflusses*. Hamburg: Paul Parey.
- Deutscher Verband für Wasserwirtschaft und Kulturbau. (1999). *Statistische Analyse von Hochwasserabflüssen*. Hamburg: Paul Parey.
- Dingman, L. S. (2002). *Physical Hydrology*. Upper Saddle River: Prentice- Hall Inc.
- Dobson, M., Ulaby, F. T., T., H. M., & El- Rayes, M. A. (1985). Microwave Dielectric Behavior of Wet Soil – Part Ii: Dielectric Mixing Models. *IEEE Transaction on Geoscience and Remote Sensing*, GE- 23(1), 35-46.
- Dobson, C. M., & Ulaby, F. T. (1998). Mapping Soil Moisture Distribution with Imaging Radar. In F. M. Henderson & A. J. Lewis (Eds.), *Principles and Applications of Imaging Radar (Manual of Remote Sensing, Volume 2)* (3rd ed., Vol. 2nd, pp. 407-433). New York [a.o.]: John Wiley & Sons.
- Donahue, R. L., Miller, R. W., & Shickluna, J. C. (1983). *Soils : An Introduction to Soils and Plant Growth* (5th ed.). Englewood Cliffs, N.J.: Prentice-Hall.
- Dooge, J. C. I., & O' Kane, P. J. (2003). *Deterministic Methods in System Hydrology*. Lisse: Swets & Zeitlingers Publishers.
- Du Toit, A. L., & Haughton, S. H. (Eds.). (1954). *The Geology of South Africa* (3 ed.). Edinburgh: Oliver and Boyd.
- Dunne, T., & Black, R. D. (1970). Partial Area Contributions to Storm Runoff in a Small New England Watershed. *Water Resources Research*, 6(5), 1296-1311.
- Engman, E. T., & Chauhan, N. (1995). Status of Microwave Soil Moisture Measurements with Remote Sensing. *Remote Sensing of Environment*, 51(1), 189-198.
- Entin, J. K., Robock, A., Vinnikov, K. Y., Hollinger, S. E., Liu, S., & Namkhai, A. (2000). Temporal and Spatial Scales of Observed Soil Moisture Variation in the Extratropics. *Journal of Geophysical Research*, 105(D9), 11865-11877.

- Entin, J. K., Houser, P. R., Schiffer, R. A., Schlosser, A. C., Lapenta, W. M., Rossow, W. B., et al. (2007). A NASA Earth Science Implementation Plan for Energy and Water Cycle Research: Predicting Energy and Water Cycle Consequences of Earth System Variability and Change. Unpublished Draft. National Aeronautics and Space Administration (NASA).
- ESRI. (1997). ArcView 3.0. Redlands, CA, USA: ESRI.
- ESRI. (2003). ArcGIS Desktop 9.1. Redlands, CA, USA: ESRI.
- European Space Agency. (2007). Programs in Progress. *ESA Bulletin*, 132(November), 70-83.
- European Space Agency. (2008). Missions- Earth Observations- ERS. Retrieved 22. January, 2008, from <http://earth.esa.int/ers/>
- Famiglietti, J., Devereaux, J. A., Laymon, C. A., Tsegaye, T., Houser, P. R., Jackson, T. J., et al. (1999). Ground-Based Investigation of Soil Moisture Variability within Remote Sensing Footprints During the Southern Great Plains 1997 (Sgp97) Hydrology Experiment. *Water Resources Research*, 35(6), 1839-1851.
- FAO, & UNESCO. (1977). *Africa* (Vol. 6). Paris: UNESCO.
- FAO, ISRIC, & ISSS. (1998). *World Reference Base for Soil Resources* (No. 84). Rome: FAO.
- FAO. (2003). *Soil and Terrain Database for Southern Africa*. Rome: FAO.
- FAO, ISRIC, & ISSS. (2006). *World Reference Base for Soil Resources 2006: A Framework for International Classification, Correlation and Communication* (No. 103). Rome: FAO.
- Fentie, B., Marsh, N., & Steven, A. (2005). *Sensitivity Analysis of a Catchment Scale Sediment Generation and Transport Model*. Paper presented at the MODSIM.
- Fernández, C., Vega, J. A., Gras, J. M., Fonturbel, T., Cuiñas, P., Dambrine, E., et al. (2004). Soil Erosion after Eucalyptus Globulus Clearcutting: Differences between Logging Slash Disposal Treatments. *Forest Ecology and Management*, 195(1-2), 85-95.
- Findell, K. L., & Eltahir, E. A. B. (2003). Atmospheric Controls on Soil Moisture–Boundary Layer Interactions. Part II: Feedbacks within the Continental United States. *Journal of Hydrometeorology*, 4(3), 570-583.

- Fink, M., Krause, P., Kralisch, S., Bende-Michl, U., & Flügel, W.-A. (2007). Development and Application of the Modelling System J2000-S for the EU-Water Framework Directive. *Advances in Geosciences*, 11, 123–130.
- Flügel, W.-A. (1995). Delineating Hydrological Response Units by Geographical Information System Analyses for Regional Hydrological Modelling Using PRMS/MMS in the Drainage Basin of the River Broel, Germany. *Hydrological Processes*, 9(3-4), 423–436.
- Flügel, W.-A. (1996). Hydrological Response Units (HRU's) as Modelling Entities for Hydrological River Basin Simulation and Their Methodological Potential for Modelling Complex Environmental Process Systems. - Results from the Sieg Catchment *Die Erde*, 127, 43-62.
- Flügel, W.-A. (2000). Systembezogene Entwicklung Regionaler Hydrologischer Modellsysteme. *Wasser & Boden*, 52(3), 14-17.
- Fontaine, B., Louvet, S., & Roucou, P. (2007). Fluctuations in Annual Cycles and Inter-Seasonal Memory in West Africa: Rainfall, Soil Moisture and Heat Fluxes. *Theoretical and Applied Climatology*, 88(1-2), 57-70.
- Foth, H. D. (1990). *Fundamentals of Soil Science* (8th ed.). New York: Wiley.
- Frison, P. L., & Mougin, E. (1996). Use of ERS-1 Wind Scatterometer Data over Land Surface. *IEEE Transaction on Geoscience and Remote Sensing*, 34(2).
- Frison, P. L., Mougin, E., & Jarlan, L. (2000). Comparison of ERS Wind-Scatterometer and SSM/I Data for Sahelian Vegetation Monitoring. *IEEE Transaction on Geoscience and Remote Sensing*, 38(4), 1794-1803.
- Gabrielle, B., & Bories, S. (1999). Theoretical Appraisal of Field-Capacity Based Infiltration Models and Their Scale Parameters. *Transport in Porous Media*, 35, 129–147.
- Geiger, R. (Cartographer). (1961). *Köppen-Geiger / Klima Der Erde*
- Goe, M. R. (1999). Influence of Slope and Stone Cover on Tillage Operations in the Ethiopian Highlands. *Soil and Tillage Research*, 49(4), 289-300.
- Gómez-Plaza, A., Alvarez-Rogel, J., Albaladejo, J., & Castillo, V. M. (2000). Spatial Patterns and Temporal Stability of Soil Moisture across a Range of Scale in a Semi-Arid Environment. *Hydrological Processes*, 14(7), 1261-1277.
- Goovaerts, P. (2000). Geostatistical Approaches for Incorporating Elevation into the Spatial Interpolation of Rainfall. *Journal of Hydrology*, 228(1-2), 113-129.

- Grayson, R. B., Western, A. W., & Chiew, F. H. S. (1997). Preferred States in Spatial Soil Moisture Patterns: Local and Nonlocal Controls. *Water Resources Research*, 33(12), 2897-2908.
- Grohman, G., Kroenung, G., & Strebeck, J. (2006). Filling SRTM Voids: The Delta Surface Fill Method. *Photogrammetric Engineering & Remote Sensing*, 72(3), 213-216.
- Guswa, A., Celia, M. A., & Rodriguez-Iturbe, I. (2002). Models of Soil Moisture Dynamics in Ecohydrology: A Comparative Study. *Water Resources Research*, 38(9), 255-268.
- Hamming, R. W., & Junge, H.-D. (1987). *Digitale Filter* (H.-D. Junge, Trans. 1th German edition of the 2nd edition ed.). Weinheim [u.a.]: VCH.
- Hanson, B. R., Orloff, S., & Peters, D. (2000). Monitoring Soil Moisture Helps Refine Irrigation Management. *California Agriculture*, 54(3), 38-42.
- Helmschrot, J. (2006). *An Integrated, Landscape-Based Approach to Model the Formation and Hydrological Functioning of Wetlands in Semiarid Headwater Catchments of the Umzimvubu River, South Africa*. Göttingen: Sierke Verlag.
- Henderson, F. M., & Lewis, A. J. (1998). *Principles and Applications of Imaging Radar (Manual of Remote Sensing, Volume 2)* (3rd ed. Vol. 2nd). New York [a.o.]: John Wiley & Sons.
- Herald, J. R. (1989). *An Assessment of Some Statistical Techniques for Hydrological Modelling in Semiarid Areas* (No. WRC Report no. 138/3/89). Pretoria, South Africa: Water Research Commission by the Hydrological Research Unit, Rhodes University.
- Hewitson, B. C., & Crane, R. G. (1996). Climate Downscaling: Techniques and Application. *Climate Research*, 7, 85-95.
- Hillel, D. (1980). *Introduction to Soil Physics*. San Diego [a.o.]: Academic Press.
- Hipel, K. W., & McLeod, A. I. (1994). *Time Series Modelling of Water Resources and Environmental Systems*. Amsterdam, Lausanne, New York, Oxford, Shannon, Tokyo: Elsevier Science.
- Hirsch, R. M., & Slack, J. R. (1984). A Nonparametric Trend Test for Seasonal Data with Serial Dependence. *Water Resources Research*, 20(6), 727-784.
- Hoffmann, T., & Rödel, R. (2004). *Leitfaden für die Statistische Auswertung Geographischer Daten*. Greifswald: Geographisches Institut, Ernst-Moritz-Arndt-Universität Greifswald.

-
- Horton, R. E. (1933). The Role of Infiltration in the Hydrologic Cycle. *American Geophysical Union Transactions*, 14, 446-460.
- Hurvitz, P. (last access 2007). The Landscape Management Analyst Extension. Seattle: University of Washington, USA.
- Huth, R. (2002). Statistical Downscaling of Daily Temperature in Central Europe. *Journal of Climate*, 15(3), 1731-1742.
- Irannejad, P., & Shao, Y. (2002). Land Surface Processes. In G. Peng, L. M. Leslie & Y. Shao (Eds.), *Environmental Modelling and Prediction* (pp. 173-214). Berlin: Springer.
- Jackson, T. J., Le Vine, D. M., Hsu, A. Y., Oldak, A., Starks, P. J., Swift, C. T., et al. (1999). Soil Moisture Mapping at Regional Scales Using Microwave Radiometry: The Southern Great Plains Hydrology Experiment. *IEEE Transaction on Geoscience and Remote Sensing*, 37(5), 2136- 2150.
- Jacobs, J. M., Mohanty, B. P., Hsu, E.-C., & Miller, D. (2004). Smex02: Field Scale Variability, Time Stability and Similarity of Soil Moisture. *Remote Sensing of Environment*, 92(4), 436-446.
- JAMS. Jena Adaptable Modeling System Wikipage. Retrieved 15. November, 2007, from <http://jams.uni-jena.de/jamswiki/index.php/Hauptseite>
- Jenness, J. (2005). Dissolve Adjacent Polygons (Diss_Adjac.Avx) Extension for Arcview 3.X, Version 1.7 Flagstaff, AZ, USA: Jenness Enterprises.
- Kääb, A. (2005). Combination of SRTM3 and Repeat Aster Data for Deriving Alpine Glacier Flow Velocities in the Bhutan Himalaya. *Remote Sensing of Environment*, 94(4), 463-474.
- Kamara, C. S., & Haque, I. (1987). Soil Moisture Storage Along a Toposequence in Ethiopian Vertisols. In S. C. Jutzi, I. Haque, J. McIntire & J. E. S. Stares (Eds.), *Management of Vertisols in Sub-Saharan Africa- Proceedings of a Conference Held at Ilca, Addis Ababa, Ethiopia, 31 August-4 September 1987*. ILCA, Addis Ababa.
- Kelliher, F. M., Leuning, R., Raupach, M. R., & Schulze, E.-D. (1995). Maximum Conductances for Evaporation from Global Vegetation Types. *Agricultural and Forest Meteorology*, 73(1), 1-16.
- Kerr, Y. H. (2007). Soil Moisture from Space: Where Are We? *Hydrogeology Journal*, 15(1), 117-120.
-

- Kim, G., & Barros, A. P. (2002a). Downscaling of Remotely Sensed Soil Moisture with a Modified Fractal Interpolation Method Using Contraction Mapping and Ancillary Data. *Remote Sensing of Environment*, 83(3), 400-413.
- Kim, G., & Barros, A. P. (2002b). Space–Time Characterization of Soil Moisture from Passive Microwave Remotely Sensed Imagery and Ancillary Data. *Remote Sensing of Environment*, 81(2), 393-403.
- Kim, S.-H., K., & Lee, K.-S. (2004). *Quality Assessment of Global MODIS LAI Product for the Regional Scale Applications* Paper presented at the ISPRS.
- Kincaid, D. R., Gardner, J. L., & Schreiber, H. A. (1964). Soil and Vegetation Parameters Affecting Infiltration under Semiarid Conditions. *Bulletin of the International Association of Scientific Hydrology* 65, 440–453.
- Kitanidis, P. K. (1997). *Introduction to Geostatistics*. Cambridge: Cambridge University Press.
- Kite, G. W. (1995). Scaling of Input Data for Macroscale Hydrological Modelling *Water Resources Research*, 31(11), 2769-2781.
- Körner, C. (1995). Leaf Diffusive Conductance in the Major Vegetation Types of the Globe. In E. Schulz & M. Caldwell (Eds.), *Ecophysiology of Photosynthesis* (2nd. ed., Vol. 100, pp. 463-490). Berlin, Germany: Springer.
- Kottek, M., Grieser, J., Beck, C., Rudolf, B., & Rubel, F. (2006). World Map of the Köppen-Geiger Climate Classification Updated. *Meteorologische Zeitschrift* 15, 259-263.
- Kraus, K., & Schneider, W. (1988). *Fernerkundung Band 1: Physikalische Grundlagen und Aufnahmetechniken*. Bonn: Dümmler Verlag.
- Krause, P. (2001). *Das Hydrologische Modellsystem J2000- Beschreibung und Anwendung in großen Flussgebieten* (Vol. Band 29). Jülich: Forschungszentrum Jülich.
- Krause, P. (2002). Quantifying the Impact of Land Use Changes on the Water Balance of Large Catchments Using the J2000 Model. *Physics and Chemistry of the Earth*, 27, 663-673.
- Krause, P., Boyle, D. P., & Bäse, F. (2005). Comparison of Different Efficiency Criteria for Hydrological Model Assessment. *Advances in Geosciences*, 5, 89–97.

-
- Lauer, W., & Frankenberg, P. (1992). Erde-Klima. In C. Diercke (Ed.), *Diercke Weltatlas*. Braunschweig: Westermann.
- Le Hegarat-Masclé, S., Zribi, M., Alem, F., Weisse, A., & Loumagne, C. (2002). Soil Moisture Estimation from ERS/SAR Data: Toward an Operational Methodology. *IEEE Transaction on Geoscience and Remote Sensing*, 40(12), 2647-2658.
- Leavesley, G., Lichty, R., Troutman, B., & Saindon, L. (1983). *Precipitation-Runoff Modeling System: User 'S Manual* Denver: USGS.
- Lee, K.-H., Burke, E. J., Shuttleworth, W. J., & Harlow, C. R. (2002). Influence of Vegetation on SMOS Mission Retrievals. *Hydrology and Earth System Sciences*, 6(2), 153–166.
- Lewis, A. J. (1998). Geomorphic and Hydrologic Applications of Active Remote Sensing. In F. M. Henderson & A. J. Lewis (Eds.), *Principles and Applications of Imaging Radar (Manual of Remote Sensing, Volume 2)* (3rd ed., Vol. 2nd, pp. 567-630). New York [a.o.]: John Wiley & Sons.
- Lin, G.-F., & Chen, L.-H. (2004). A Spatial Interpolation Method Based on Radial Basis Function Networks Incorporating a Semivariogram Model. *Journal of Hydrology*, 288(3-4), 288-298.
- Ludwig, R., Hellwich, O., Strunz, G., Roth, A., & Eder, K. (2000). Applications of Digital Elevation Models from SAR Interferometry for Hydrologic Modelling. *Photogrammetrie - Fernerkundung - Geoinformation (PFG)*, 2, 81-94.
- Lynch, S. (2004). *Development of a Raster Database of Annual, Monthly and Daily Rainfall for Southern Africa*. Pretoria: Water Research Commission.
- Mackay, N. G., Chandler, R. E., Onof, C., & Wheeler, H. S. (2001). Disaggregation of Spatial Rainfall Fields for Hydrological Modelling. *Hydrology and Earth System Sciences*, 5(2), 165-173.
- Maidment, D. R. (2003). *Archydro: GIS for Water Resources*. Redland, CA. USA: ESRI.
- Manabe, S. (1969). Climate and the Ocean Circulation 1. The Atmospheric Circulation and the Hydrology of the Earth's Surface *Monthly Weather Review*, 97(11), 739-774.
- Marceau, D. J. (1999). The Scale Issue in Social and Natural Sciences. *Canadian Journal of Remote Sensing*, 25(4), 347-356.
-

- Märker, M. (2001). *Regionale Erosionsmodellierung unter Verwendung des Konzepts der Erosion Response Units (ERU) am Beispiel zweier Flusseinzugsgebiete im Südlichen Afrika*. Friedrich-Schiller-Universität Jena, Jena.
- Martinez, C., Hancock, G. R., Kalma, J. D., & Wells, T. (2007). Spatio-Temporal Distribution of near-Surface and Root Zone Soil Moisture at the Catchment Scale. *Hydrological Processes*, in press.
- Matthews, E. (1984). Vegetation, Land-Use and Seasonal Albedo Data Sets. *Global Change Data Base Africa Documentation, Appendix D*.
- McCuen, R. (1973). The Role of Sensitivity Analysis and Hydrologic Modeling. *Journal of Hydrology*, 18, 37-53.
- McKenzie, R. S., & Craig, A. R. (1999). *Evaporation Losses from South African Rivers* (No. WRC No. 638/1/99). Pretoria: Water Research Commission.
- Merz, B., & Plate, E. J. (1997). An Analysis of the Effects of Spatial Variability of Soil and Soil Moisture on Runoff. *Water Resources Research*, 33(12), 2909-2922.
- Midgeley, D., Pitman, W., & Middleton, B. (1994a). *Surface Water Resources of South Africa 1990- Volume I: Limpopo-Olifants (Appendices)*. Pretoria: Water Research Commission.
- Midgeley, D., Pitman, W., & Middleton, B. (1994b). *Surface Water Resources of South Africa 1990- Volume I: Limpopo-Olifants (Appendices) - Book of Maps*. Pretoria: Water Research Commission.
- Mohanty, B. P., Skaggs, T. H., & Famiglietti, J. S. (2000). Analysis and Mapping of Field-Scale Soil Moisture Variability Using High-Resolution, Ground-Based Data During the Southern Great Plains 1997 (Sgp97) Hydrology Experiment. *Water Resources Research*, 36(4), 1023-1031.
- Monteith, J. L. (1975). *Vegetation and Atmosphere, Vol. 1. Principles* (Vol. 1). London: Academic Press.
- Moran, S. M., Hymer, D. C., Qi, J., & Kerr, Y. H. (2002). Comparison of ERS-2 SAR and Landsat Tm Imagery for Monitoring Agricultural Crop and Soil Conditions. *Remote Sensing of Environment*, 79, 243-252.
- Moran, S. M., McElroy, S., Watts, J. M., & Peters-Lidard, C. D. (2006). Radar Remote Sensing for Estimation of Surface Soil Moisture at the Watershed Scale. In C. W. Richardson, A. S. Baez-Gonzalez & M. Tiscareno (Eds.), *Modeling and Remote Sensing Applied in Agriculture (Us and Mexico)* (pp. 91-106). Aguascalientes, Mexico: INIFAP Publications.

-
- Nash, J. E., & Sutcliffe, J. V. (1970). River Flow Forecasting through Conceptual Models, Part I – a Discussion of Principles. *Journal of Hydrology*, 10, 282-290.
- Njoku, E. G., & Chan, S. (2005). Vegetation and Surface Roughness Effects on AMSR-E Land Observations. *Remote Sensing of Environment*, 100(3), 190-199.
- Njoku, E. G., & Entekhabi, D. (1996). Passive Microwave Remote Sensing of Soil Moisture. *Journal of Hydrology*, 184(1-2), 101-129.
- Obhodjas, J., Sudac, D., Nadj, K., Valkovic, V., Nebbia, G., & Viesti, G. (2004). The Soil Moisture and Its Relevance to the Landmine Detection by Neutron Backscattering Technique. *Nuclear Instruments and Methods in Physics Research Section B: Beam Interactions with Materials and Atoms*, 213, 445-451.
- Obst, E., & Kayser, K. (1949). *Die Große Randstufe auf der Ostseite Südafrika und ihr Vorland: ein Beitrag zur Geschichte der jungen Heraushebung Des Subkontinents*. Hannover: Geographische Gesellschaft zu Hannover.
- Pegram, G. G. S., & Clothier, A. N. (2001). Downscaling Rainfields in Space and Time, Using the String of Beads Model in Time Series Mode. *Hydrology and Earth System Sciences*, 5(2), 175-186.
- Pellenq, J., Kalma, J., Boulet, G., Saulnier, G.-M., Woolridge, S., Kerr, Y., et al. (2003). A Disaggregation Scheme for Soil Moisture Based on Topography and Soil Depth. *Journal of Hydrology*, 276(1-4), 112-127.
- Peters-Lidard, C. D., Pan, F., & Wood, E. F. (2001). A Re-Examination of Modeled and Measured Soil Moisture Spatial Variability and Its Implication for Land Surface Modelling. *Advances in Water Resources*, 24, 1069-1083.
- Philip, J. R. (1957). The Theory of Infiltration: 4. Sorptivity and Algebraic Infiltration Equations. *Soil Science*, 84, 257-264.
- Philip, J. R. (1969). Theory of Infiltration. *Advances in Hydroscience*, 5(2), 215-296.
- Pitman, W., & Middleton, B. (1994). *Surface Water Resources of South Africa 1990*. Pretoria: Water Research Commission.
- Quattrochi, D. A., & Goodchild, M. F. (1997). *Scale in Remote Sensing and GIS*. Boca Raton [a.o.]: CRC Press, Inc.
-

- R Development Core Team (2008). R: A language and environment for statistical computing (Version 2.6.2) [Freeware], R Foundation for Statistical Computing, Vienna, Austria. ISBN 3-900051-07-0, <http://www.R-project.org>.
- Refsgaard, J. C. (1996). Terminology, Modelling Protocol and Classification of Hydrological Model Codes. In M. B. Abbott & J. C. Refsgaard (Eds.), *Distributed Hydrological Modelling* (pp. 17-40). Dordrecht: Kluwer Academic Publishers.
- Refsgaard, J. C., & Storm, B. (1996). Construction, Calibration and Validation of Hydrological Models. In M. B. Abbott & J. C. Refsgaard (Eds.), *Distributed Hydrological Modelling* (pp. 41-54). Dordrecht: Kluwer Academic Publishers.
- Reichle, R. H., Entekhabi, D., & McLaughlin, D. B. (2001). Downscaling of Radio Brightness Measurements for Soil Moisture Estimation: A Four Dimensional Variational Data Assimilation Approach. *Water Resources Research*, 37(9), 2353-2364.
- Richards, J. A., & Xiuping, J. (2006). *Remote Sensing Digital Image Analysis. An Introduction* (Vol. 4th Edition). Berlin: Springer.
- Richardson, D. M., & van Wilgen, B. W. (2004). Invasive Alien Plants in South Africa: How Well Do We Understand the Ecological Impacts? *South African Journal of Science*, 100(January/ February), 45-52.
- Richter, D. (1995). *Ergebnisse Methodischer Untersuchungen zur Korrektur des Systematischen Meßfehlers Des Hellmann-Niederschlagsmessers*. Offenbach: Deutscher Wetter Dienst.
- Rogerson, P. A. (2006). *Statistical Methods for Geography: A Student Guide* (2rd. ed.). London: Sage Publications.
- Salve, R., & Allen-Diaz, B. (2001). Variations in Soil Moisture Content in a Rangeland Catchment. *Journal of Range Management*, 54, 44-51.
- Satalino, G., Mattia, F., Davidson, M. W. J., Le Toan, T., Pasquariello, G., & Borgeaud, M. (2002). On Current Limits of Soil Moisture Retrieval from ERS-SAR Data. *IEEE Transaction on Geoscience and Remote Sensing*, 40(11), 2438-2447.
- Scheffer, F., & Schachtschabel, P. (Eds.). (2002). *Lehrbuch der Bodenkunde*. Heidelberg, Berlin: Spektrum Akademischer Verlag.

- Scheffler, C., Bäse, F., Helmschrot, J., Flügel, W.-A., & Krause, P. (2007). Anforderungen an Hydrologische Modelle für ein Nachhaltiges Wasserressourcenmanagement in semiariden Einzugsgebieten Südafrikas. *Zentralblatt für Geologie und Paläontologie* (Teil I-IV), 235-249.
- Scheffler, C., Krause, P., Flügel, W.-A., & Bongartz, K. (2007). *Development of a Validation Tool for Regional Distributed Models Using Macro-scale Soil Moisture Products, Case Study: Great Letaba River, South Africa*. Paper presented at the MODSIM 2007- International Congress on Modelling and Simulation.
- Schenk, J. H., & Jackson, R. B. (2002). The Global Biogeography of Roots. *Ecological Monographs*, 72(3), 311–328.
- Schmugge, T. J. (1983). Remote Sensing of Soil Moisture: Recent Advances. *IEEE Transaction on Geoscience and Remote Sensing*, 21(3), 336-344.
- Schmullius, C., & Furrer, R. (1992). Some Critical Remarks on the Use of C-Band Radar Data for Soil Moisture Detection. *International Journal of Remote Sensing*, 13(17), 3387-3390.
- Schoeman, J. L., Matlawa, S. M., & Howard, M. D. (2002). *Quantification of the Water Balance of Selected Rehabilitated Mine Soils under Rainfed Pastures in Mpumalanga*. Pretoria: Water Research Commission.
- Schulla, J., & Jasper, K. (1998). *Modellbeschreibung Wasim-EtH: Wasserhaushalts-Simulations-Modell Eth*. Retrieved 29. October 2007, from http://homepage.hispeed.ch/wasim/download/doku/wasim_1998_de.pdf
- Schulze, R. E. (1995). *Hydrology and Agrohydrology: A Text to Accompany the ACRU 3.00 Agrohydrological Modelling System*. Pretoria: Water Research Commission.
- Schulze, R. E., Maharaj, M., Lynch, S. D., Howe, B. J., & Melvill- Thomson, B. (1997). *South African Atlas of Agrohydrology and Climatology* Pretoria: Water Research Commission.
- Schulze, R. E., & Pike, A. (2004). *Development and Evaluation of an Installed Hydrological Modelling System*. Pretoria, South Africa: Water Research Commission.
- Schulze, R. E., & Maharaj, M. (2004). *Development of a Database of Gridded Daily Temperatures for Southern Africa*. Pretoria: Water Research Commission.

- Scipal, K. (2002). *Global Soil Moisture Retrieval from ERS Scatterometer Data*. Technische Universität Wien, Wien.
- Scipal, K., Wagner, W., Ceballos, A., Martínez-Fernández, J., & Scheffler, C. (2003). *The Potential of Scatterometer Derived Soil Moisture for Catchment Scale Modelling*. Paper presented at the Biennial Conference of the Australien Modeling and Simulation Society.
- Scipal, K., Wagner, W., Trommler, M., & Naumann, K. (2002). *The Global Soil Moisture Archive 1992-2000 from ERS Scatterometer Data: First Results*. Paper presented at the Geoscience and Remote Sensing Symposium, 2002. IGARSS '02. 2002 IEEE International.
- Shepard, D. (1968). *A Two-Dimensional Interpolation Function for Irregularly-Spaced Data*. Paper presented at the ACM Annual Conference/Annual Meeting.
- Singh, V. P. (1995). Watershed Modeling. In V. P. Singh (Ed.), *Computer Models of Watershed Hydrology*: Water Resources Publications.
- Sivapalan, M., Takeuchi, K., Frank, S. W., Gupta, V. K., Karambiri, H., Lakshmi, V., et al. (2003). IAHS Decade on Predictions in Ungauged Basins (Pub), 2003–2012: Shaping an Exciting Future for the Hydrological Sciences. *Hydrological Sciences*, 48(6), 857-879.
- Snelgrove, K. (2002). *Implications of Lateral Flow Generation on Land-Surface Scheme Fluxes*. Unpublished doctoral thesis, University of Waterloo, Waterloo, Canada.
- Statistisches Bundesamt Deutschland. (2007). Methoden und Verfahren - Zeitreihenanalyse. Retrieved 18. March 2008, 2008, from <http://www.destatis.de/jetspeed/portal/cms/Sites/destatis/Internet/DE/Content/Wissenschaftsforum/MethodenVerfahren/Einfuehrung,templateId=renderPrint.psml>
- Staudenrausch, H. (2001). *Untersuchungen zur hydrologischen Topologie von Landschaftsobjekten für die distributive Flussgebietsmodellierung*. Friedrich-Schiller-Universität Jena, Jena.
- Sugawara, M. (1995). Tank- Model. In V. P. Singh (Ed.), *Computer Models of Watershed Hydrology* (pp. 165-214). Littleton, Colorado: Water Resources Publications.
- Summer, M. E. (2000). *Handbook of Soil Science*. Boca Raton: CRC Publisher.

- Svetlichnyi, A. A., Plotnitskiy, S. V., & Stepovaya, O. Y. (2003). Spatial Distribution of Soil Moisture Content within Catchments and Its Modelling on the Basis of Topographic Data. *Journal of Hydrology*, 277(1-2), 50-60.
- Swartzendruber, D. (1997). Exact Mathematical Derivation of a Two-Term Infiltration Equation. *Water Resources Research*, 33(3), 491-496.
- Taconet, O., Vidal-Madjar, D., Emblanch, C., & Normand, M. (1996). Taking into Account Vegetation Effects to Estimate Soil Moisture from C-Band Radar Measurements. *Remote Sensing of Environment*, 56(1), 52-56.
- Tolk, J. A. (2003). Soils, Permanent Wilting Point. In B. A. Stewart & T. A. Howell (Eds.), *Encyclopedia of Water Science* (pp. 927- 929). New York,: Marcel Dekker.
- Typson, P. (1987). *Climatic Change and Variability in Southern Africa*. Cape Town: Oxford University Press.
- U.S. Geological Survey. (2003). Shuttle Radar Topography Mission (SRTM) C-Band, (Online Database). Retrieved 10. 12. 2004, from U.S. Geological Survey,,: <http://srtm.usgs.gov/data/obtainingdata.html>
- U.S. Geological Survey EROS Data Center, & NASA, u. a. w. (2007). Shuttle Radar Topography Mission (SRTM) "Finished" 3-Arc Second SRTM Format, (Online Database). Retrieved 1 October 2007, from U.S. Geological Survey: <http://edcsns17.usgs.gov/srtmbil/index.html>
- Uhlenbrook, S., Wenninger, J., & Lorentz, S. (2005). What Happens after the Catchment Caught the Storm? Hydrological Processes at the Small, Semi-Arid Weatherley Catchment, South Africa. *Advances in Geosciences*, 2, 237-241.
- Ulaby, F. T. (1974). Radar Measurements of Soil Moisture Content. *IEEE Transactions on Antennas and Propagation*, AP 22(2), 257-265.
- Ulaby, F. T., Batlivala, P. P., & Dobson, M. C. (1978). Microwave Backscatter Dependence on Surface Roughness, Soil Moisture, and Soil Texture: Part I - Bare Soil. *IEEE Transaction on Geoscience and Remote Sensing*, 16(4), 286-295.
- Ulaby, F. T., Dobson, M., & Bradley, G. A. (1981). Radar Reflectivity of Bare and Vegetation-Covered Soil. *Advances in Space Research*, 1(10), 91-104.
- Ulaby, F. T., Dubois, P. C., & van Zyl, J. (1996). Radar Mapping of Surface Soil Moisture. *Journal of Hydrology*, 184(1-2), 57-84.

- Vachaud, G., Passerat de Silans, P., Balabanis, P., & Vauclin, M. (1985). Temporal Stability of Spatially Measured Soil Water Probability Density Function. *Soil Science Society of American Journal*, 49(4), 822-828.
- Van Oevelen, P. (1998). Soil Moisture Variability: A Comparison between Detailed Field Measurements and Remote Sensing Measurements Techniques. *Hydrological Sciences- Journal, Special Issues: Monitoring and Modelling of Soil Moisture: Integration over Time and Space*, 43(4), 511- 520.
- Van Vuuren, J. A., Jordaan, H., Van der Walt, E., & Jaarsveld, V. (2003). *Luvuvhu/ Letaba Water Management Area: Water Resources Situation Assessment- Main Report* (No. P/02000/00/0101). Pretoria: Department of Water Affairs and Forestry, South Africa.
- Vegter, J. R. (1995). *Groundwater Resources of South Africa: An Explanation of a Set of National Groundwater Maps* (No. TT 74/95). Pretoria: Water Research Commission.
- Vegter, J. R. (2003). *Hydrogeology of Groundwater: Region 19 Lowveld* (No. TT 208/03). Pretoria: Water Research Commission.
- Veihmeyer, F. J., & Hendrickson, A. H. (1950). Soil Moisture in Relation to Plant Growth. *Annual Review of Plant Physiology*, 1, 285-304.
- Verdin, J., & Klaver, R. (2002). Grid-Cell-Based Crop Water Accounting for the Famine Early Warning System. *Hydrological Processes*, 16(8), 1617-1630.
- Vinnikov, K. Y., Robock, A., Speranskaya, N. A., & Schlosser, A. C. (1996). Scales of Temporal and Spatial Variability of Midlatitude Soil Moisture. *Journal of Geophysical Research*, 101(D3), 7163-7174.
- Viljoen, D. (2006). *Runoff Stations Great Letaba Catchment*. Tzaneen: Department of Water Affairs and Forestry, South Africa.
- Virdee, T. S., & Kottegoda, N. T. (1984). A Brief Review of Kriging and Its Application to Optimal Interpolation and Observation Well Selection. *Hydrological Sciences*, 29(4), 367-387.
- Vischel, T., Pegram, G. G. S., Sinclair, S., Wagner, W., & Bartsch, A. (2007). Comparison of Soil Moisture Fields Estimated by Catchment Modelling and Remote Sensing a Case Study in South Africa. *Hydrology and Earth System Sciences Discussions*, 4, 2273-2306.
- Vörösmatry, C. J., Moore, B., Grace, A. L., & Gildea, M. P. (1989). Continental Scale Models of Water Balance and Fluvial Transport: An Application to South America. *Global Biogeochemical Cycles*, 3(3), 241-265.

-
- Wackernagel, H. (1995). *Multivariate Geostatistics*. Berlin: Springer.
- Wagner, W. (1998). *Soil Moisture Retrieval from ERS-Scatterometer Data*. Wien: Technische Universität Wien.
- Wagner, W., Lemoine, G., Borgeaud, M., & Rott, H. (1999a). A Study of Vegetation Cover Effects on ERS Scatterometer Data. *IEEE Transaction on Geoscience and Remote Sensing*, 37(2), 938-948.
- Wagner, W., Lemoine, G., & Rott, H. (1999b). A Method for Estimating Soil Moisture from ERS Scatterometer and Soil Data - Empirical Data and Model Results. *Remote Sensing of Environment*, 70(2), 191-207.
- Wagner, W., Noll, J., Borgeaud, M., & Rott, H. (1999). Monitoring Soil Moisture over the Canadian Prairies with the ERS Scatterometer. *IEEE Transaction on Geoscience and Remote Sensing*, 37(1), 206-216.
- Wagner, W., Pathe, C., Doubkova, M., Sabel, D., Bartsch, A., Hasenauer, S., et al. (submitted). Temporal Stability of Soil Moisture and Radar Backscatter Observed by the Advanced Synthetic Aperture Radar (ASAR). *Sensors*.
- Wagner, W., Scipal, K., Pathe, C., Gerten, D., Lucht, W., & Rudolf, B. (2003). Evaluation of the Agreement between the First Global Remotely Sensed Soil Moisture Data with Model and Precipitation Data. *Journal of Geophysical Research*, 108(D19), 15p.
- Walker, J. P., & Houser, P. R. (2004). Requirements of Global near-Surface Soil Moisture Satellite Mission: Accuracy, Repeat Time, and Spatial Resolution. *Advances in Water Resources*, 27(8), 785-801.
- Wang, C., Qi, J., Moran, S., & Marsett, R. (2004). Soil Moisture Estimation in a Semiarid Rangeland Using ERS-2 and Tm Imagery. *Remote Sensing of Environment*, 90(2), 178-189.
- Webster, R., & Oliver, M. A. (2001). *Geostatistics for Environmental Scientists*. Chichester [a.o.]: John Wiley & Sons.
- Wegmüller, U., Mätzler, C., & Schanda, E. (1989). Microwave Signatures of Bare Soil. *Advances in Space Research*, 9(1), (1)307-(301)316.
- Western, A. W., & Blöschl, G. (1999). On the Spatial Scaling of Soil Moisture. *Journal of Hydrology*, 217(3), 203-224.
- Western, A. W., Grayson, R. B., Blöschl, G., Willgoose, G. R., & McMahon, T. A. (1999). Observed Spatial Organization of Soil Moisture and Its Relation to Terrain Indices. *Water Resources Research*, 35(3), 797-810.
-

- Wilson, D. J., Western, A. W., & Grayson, R. B. (2005). A Terrain and Data-Based Method for Generating the Spatial Distribution of Soil Moisture. *Advances in Water Resources*, 28, 43-54.
- Wood, E. F., Sivapalan, M., & Beven, K. (1990). Similarity and Scale in Catchment Storm Response. *Reviews of Geophysics*, 28, 1-18.
- Woodhouse, I. H., & Hoekman, D. H. (2000). A Model-Based Determination of Soil Moisture Trend in Spain with the ERS-Scatterometer. *IEEE Transaction on Geoscience and Remote Sensing*, 38(4), 1783-1792.
- Wu, J., & Li, H. (2006). Concepts of Scale and Scaling In J. Wu, B. K. Jones, H. Li & O. L. Loucks (Eds.), *Scaling and Uncertainty Analysis in Ecology* (pp. 3-15). Dordrecht: Springer.
- Wu, W., Geller, M. A., & Dickinson, R. E. (2002). The Response of Soil Moisture to Long-Term Variability of Precipitation. *Journal of Hydrometeorology*, 3, 604-613.
- Wythers, K. R., Lauenroth, W. K., & Paruelo, J. M. (1999). Bare-Soil Evaporation under Semiarid Field Conditions. *Soil Science Society of American Journal*, 63(5), 1341-1349.
- Yevjevich, V. (1987). Stochastic Models in Hydrology. *Stochastic Hydrology and Hydraulics*, 1(1), 17-36.
- Yu, Z., Carlson, T. N., Barron, E. J., & Schwartz, F. W. (2001). On Evaluating the Spatial-Temporal Variation of Soil Moisture in the Susquehanna River Basin. *Water Resources Research*, 37(5), 1313-1326.
- Zorita, E., & von Storch, H. (1999). The Analog Method as a Simple Statistical Downscaling Technique- Comparison with More Complicated Methods. *Journal of Climate*, 12(2), 2474-2489.
- Zribi, M., & Dechambre, M. (2002). A New Empirical Model to Retrieve Soil Moisture and Roughness from C-Band Radar Data. *Remote Sensing of Environment*, 84, 42-52.

APPENDIX

**APPENDIX A: J2000 MODEL PARAMETERS (SOURCE: KRAUSE 2001;
BÄSE 2005)**

MODULE	PARAMETER	PARAMETER DESCRIPTION
Interception	α Rain	Water storage capacity per m ² leave area (rain)
	α Snow	Water storage capacity per m ² leave area (snow)
Soil Water	SoilMaxDPS	Maximum capacity for depression storage
	SoilPolRed	Reduction parameter for the potential Evapotranspiration
	SoilLinRed	Maximum value for the MPS storage
	soilMaxInfSummer	Infiltration capacity between the months May and October
	soilMaxInfWinter	Infiltration capacity between the months November and April
	soilMaxInfsnowcover	Infiltration capacity for snow cover
	soilImpGT80	Relative infiltration capacity for areas over 80% sealing
	soilImpLT80	Relative infiltration capacity for areas below 80% sealing
	soilDistMPSLPS	Calibration parameter for infiltration distinction between LPS and MPS
	soilDiffMPSLPS	Calibration parameter for distribution of the LPS storage to MPS at the end of a model time step
	soilOutLPS	Calibration parameter for LPS out flow
	soilLatVertLPS	Calibration parameter for distribution of the LPS outflow to subsurface flow or percolation
	soilMaxPerc	Maximum percolation rate
	soilconcRD1	Time delay coefficient for surface runoff
	soilconcRD2	Time delay coefficient for subsurface flow
FCadaptation	Coefficient for field capacity adaptation	
ACAdaptation	Coefficient for air capacity adaptation	
Groundwater	gwRG1RG2dist	Calibration parameter for distribution of percolation water
	gwfacRG1	Time delay coefficient for the fast base flow
	gwfacRG2	Time delay coefficient for the slow base flow
	gwCapRise	Coefficient for capillary ascension
Reach Routing	TA	Coefficient for determination of the discharge wave

APPENDIX B: OVERVIEW ON THE RAINFALL STATIONS

SAWS- NUMBER	STATION NAME	START RECORD	END RECORD	LON	LAT	ELEVATION	% FILLED 1903-2000	% FILLED 1993-1999
635873	Serala	1903	2000	30.08	-24.02	1742	0	1
636518	Schelm	1903	2000	30.30	-24.13	826	32	92
678381	Syferkraal	1903	2000	29.70	-23.87	1259	4	5
678680	Masealama	1903	2000	29.88	-23.83	1497	12	8
678776	Haenertsburg	1903	2000	29.93	-23.93	1485	1	0
678836	Glenshiel	1903	2000	29.97	-23.93	1431	0	0
678858	Broederstrom	1903	2000	29.97	-23.85	1620	0	1
678863	Stampblokfo	1903	2000	29.98	-23.88	1426	35	0
679019	De Hoeck	1903	2000	30.02	-23.82	1274	19	50
679086	Letabadrift	1903	2000	30.05	-23.93	916	1	0
679135	Belvedere	1903	2000	30.08	-23.75	862	0	0
679141	Vergelegen	1903	2000	30.08	-23.85	1047	1	0
679164	Westfalia	1903	2000	30.10	-23.73	932	3	0
679194	Duiwelskloo	1903	2000	30.12	-23.73	850	24	3
679197	Zomerkomst	1903	2000	30.13	-23.78	763	0	0
679209	Mamathola	1903	2000	30.15	-23.97	752	3	3
679227	Merensky	1903	2000	30.13	-23.80	777	1	0
679267	New Agatha	1903	2000	30.13	-23.95	1105	1	2
679268	Monavein	1903	2000	30.12	-23.97	886	0	0
679274	Koedersrivi	1903	2000	30.17	-23.57	686	32	0
679284	Quantock	1903	2000	30.17	-23.73	832	3	0
679508	Thabina	1903	2000	30.28	-23.97	571	19	49
679562	Letaba	1903	2000	30.32	-23.87	550	42	100
679608	Modjadji	1903	2000	30.35	-23.63	916	0	0
679654	Berlyn	1903	2000	30.37	-23.90	521	21	58
680207	Gravelotte	1903	2000	30.62	-23.95	545	1	1
680225	Black Hills	1903	2000	30.65	-23.78	470	13	33
680280	Eiland	1903	2000	30.67	-23.65	548	0	0
680354	Consolidate	1903	2000	30.70	-23.90	508	0	0
680494	Kondowi	1903	2000	30.78	-23.75	421	40	100
681691	Tsende	1903	2000	31.40	-23.53	331	2	0
723231	Bontfontein	1903	2000	30.15	-23.35	740	22	46
723656	Bellevue	1903	2000	30.42	-23.42	561	43	100
724790	Shangoni	1903	2000	30.95	-23.17	426	5	0
725373	Woodlands	1903	2000	31.22	-23.22	341	15	0

**APPENDIX C: SUMMARY OF THE STATISTICAL PARAMETER FOR THE
LONG-TERM YEARLY ANALYSIS OF RAINFALL FOR EACH STATION**

STATION- NUMBER	MEAN [MM]	MEDIAN [MM]	MIN [MM]	MAX [MM]	STD [MM]
635873	769	764	402	1283	204
636518	844	802	392	1766	344
678381	416	396	229	704	124
678680	461	491	196	807	162
678776	817	827	518	1557	233
678836	1050	992	575	1846	316
678858	1751	1688	874	2876	517
678863	1205	1205	524	2303	410
679019	1634	1619	723	2563	483
679086	979	952	367	1740	312
679135	1250	1240	465	1948	396
679141	1332	1273	554	2099	391
679164	1081	1026	396	1742	371
679194	1071	1067	364	1759	364
679197	1049	998	533	1617	322
679209	1128	1118	603	1933	323
679227	961	942	410	1512	304
679267	1337	1330	693	2037	383
679268	1259	1252	722	1784	323
679274	608	488	219	1179	290
679284	1061	1043	521	1674	313
679508	636	652	259	1047	210
679562	769	783	238	1046	192
679608	725	720	392	1089	198
679654	572	541	282	858	174
680207	470	459	204	780	164
680225	506	473	286	921	160
680280	554	556	234	944	202
680354	478	484	238	802	153
680494	419	429	126	730	173
681691	428	381	194	838	170
723231	578	510	229	1002	240
723656	552	538	163	928	226
724790	477	436	270	771	157
725373	453	422	247	888	180

Std= Standard Deviation

APPENDIX D: SENSITIVITY INDEX IN REGARD TO CHANGES IN THE SOIL WATER VOLUME

	PARAMETER	PARAMETER CHANGE [%]			
		-10	-5	5	10
Soil Water Module	soilMaxDPS	-0.01	-0.01	-0.01	-0.01
	soilmaxInfSummer	-0.01	-0.01	-0.01	-0.01
	soilmaxInfWinter	-0.10	-0.10	-0.08	-0.08
	SoilDistMPSLPS	-0.04	-0.04	-0.03	-0.03
	soilDiffMPSLPS	0.00	0.00	0.00	0.00
	soilOutLPS	0.00	0.00	0.00	0.00
	soilLatVertLPS	0.00	0.00	0.00	0.00
	soilMaxPerc	-0.01	-0.01	-0.01	-0.01
	soilconcRd1	-0.05	-0.05	-0.04	-0.04
	soilconcRd2	-0.01	-0.01	-0.01	-0.01
	FCAdaptation	-0.82	-0.80	-0.78	-0.77
	ACAdaptation	-0.02	-0.02	-0.02	-0.02
Ground Water Module	gwRG1RG2dist	-0.02	-0.02	-0.03	-0.03
	gwfacRG1	0.00	0.00	0.00	0.00
	gwfacRG2	0.00	0.00	0.00	0.00
	gwCapRise	-0.01	-0.01	-0.08	-0.07
RR	TA	0.00	0.00	0.00	0.00

RR= Reach Routing

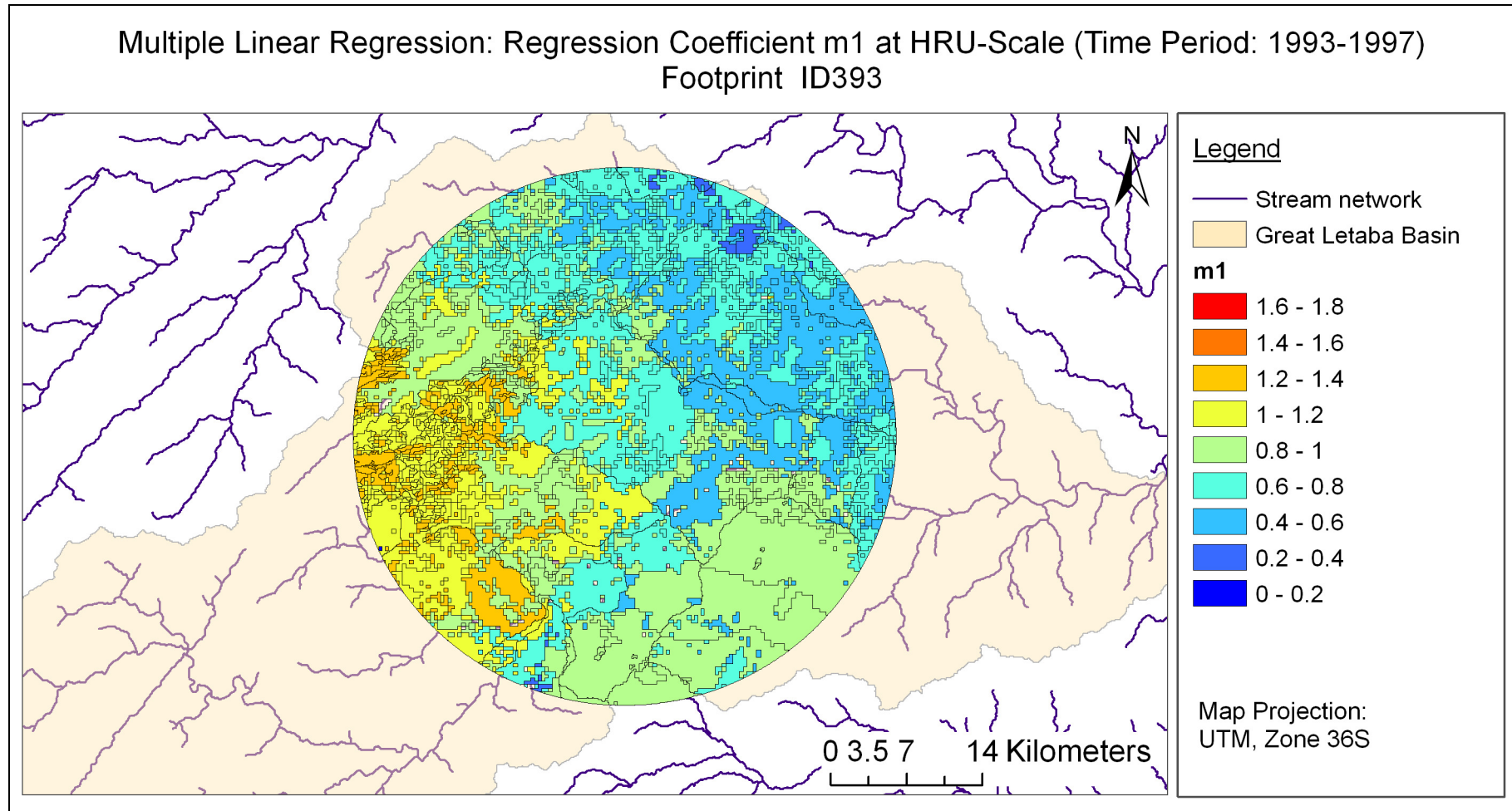
APPENDIX E: SENSITIVITY INDEX IN REGARD TO RUNOFF VOLUME CHANGES

	PARAMETER	PARAMETER CHANGE [%]			
		-10	-5	5	10
Soil Water Module	soilMaxDPS	0.03	0.03	0.03	0.03
	soilmaxInfSummer	0.09	0.08	0.07	0.07
	soilmaxInfWinter	0.37	0.35	0.31	0.29
	SoilDistMPSLPS	0.00	0.00	0.00	0.00
	soilDiffMPSLPS	0.00	0.00	0.00	0.00
	soilOutLPS	0.01	0.01	0.01	0.01
	soilLatVertLPS	0.00	0.00	0.00	0.00
	soilMaxPerc	0.07	0.07	0.07	0.06
	soilconcRd1	0.21	0.20	0.17	0.16
	soilconcRd2	0.04	0.04	0.04	0.04
	FCAdaptation	0.63	0.59	0.53	0.50
ACAdaptation	0.07	0.07	0.06	0.06	
Ground-Water Module	gwRG1RG2dist	0.19	0.19	0.19	0.19
	gwfacRG1	0.00	0.00	0.00	0.00
	gwfacRG2	0.02	0.02	0.02	0.02
	gwCapRise	-0.01	-0.01	-0.06	-0.05
RR	TA	0.00	0.00	0.00	0.00

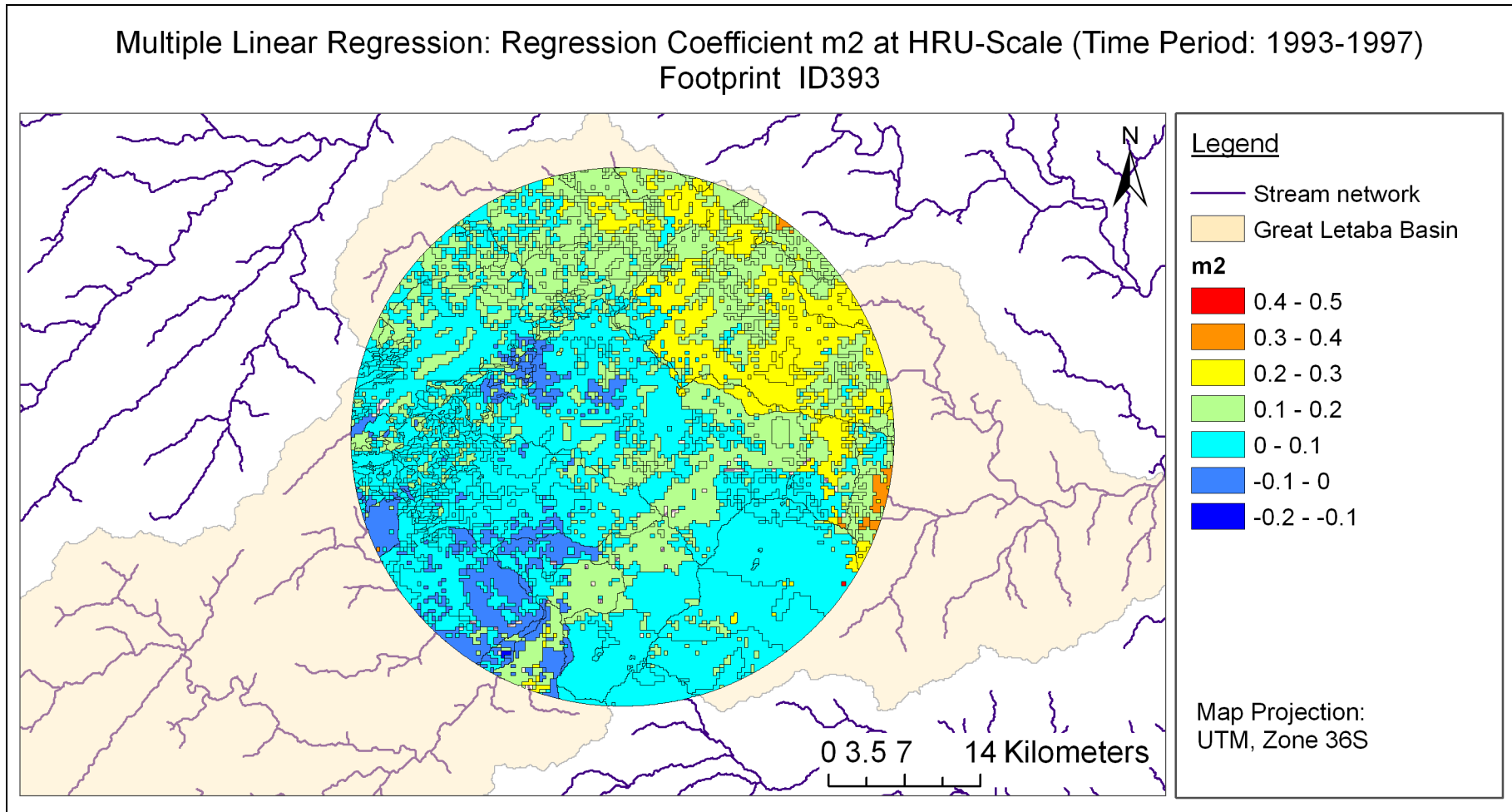
RR= Reach Routing

APPENDIX F: MULTIPLE LINEAR REGRESSION: SPATIAL VARIABILITY OF THE REGRESSION COEFFICIENT m_1 , FOOTPRINT

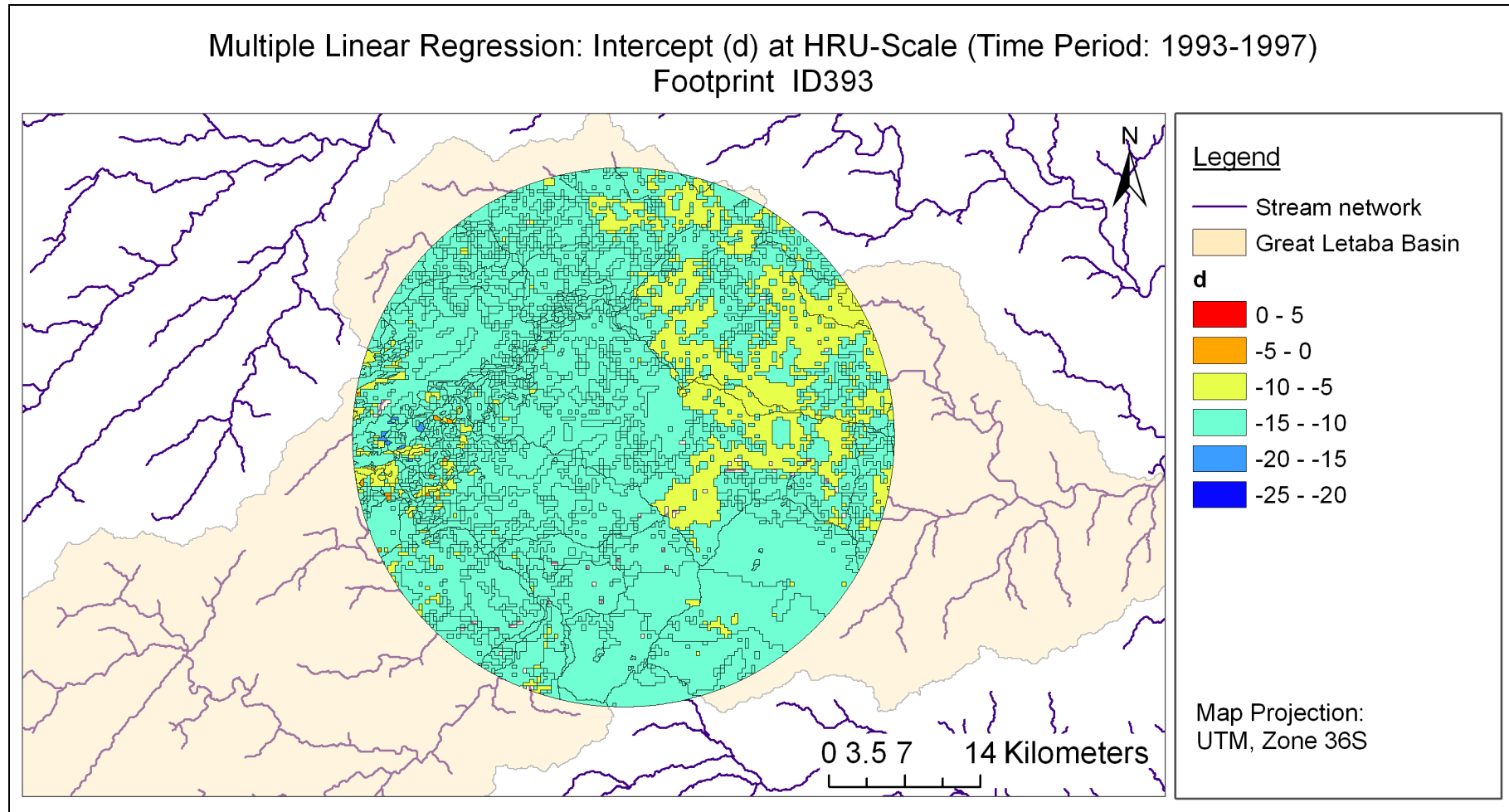
ID393



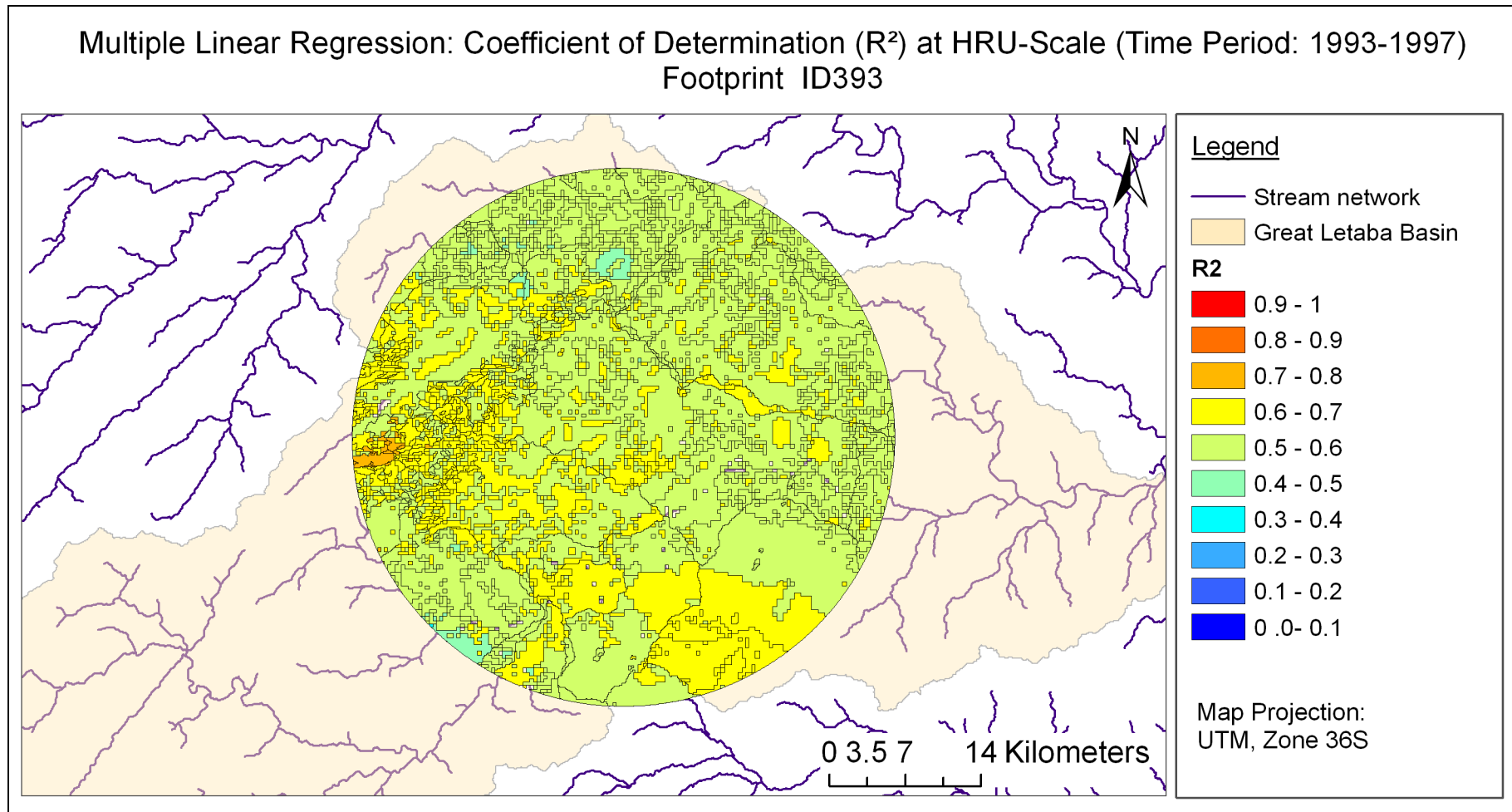
APPENDIX G: MULTIPLE LINEAR REGRESSION: SPATIAL VARIABILITY OF THE REGRESSION COEFFICIENT m_2 , FOOTPRINT ID393



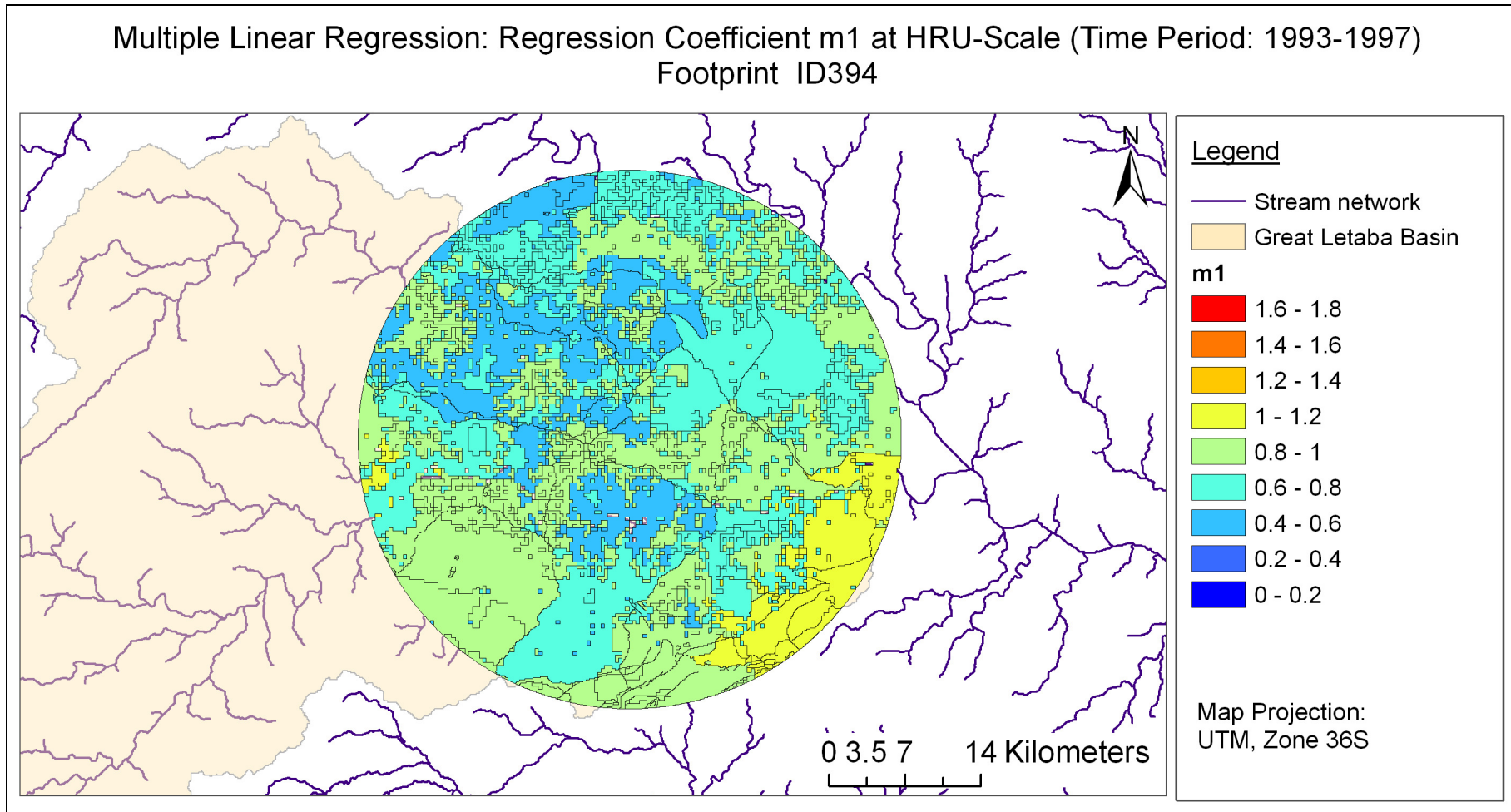
APPENDIX H: MULTIPLE LINEAR REGRESSION: SPATIAL VARIABILITY OF THE INTERCEPT d , FOOTPRINT ID393



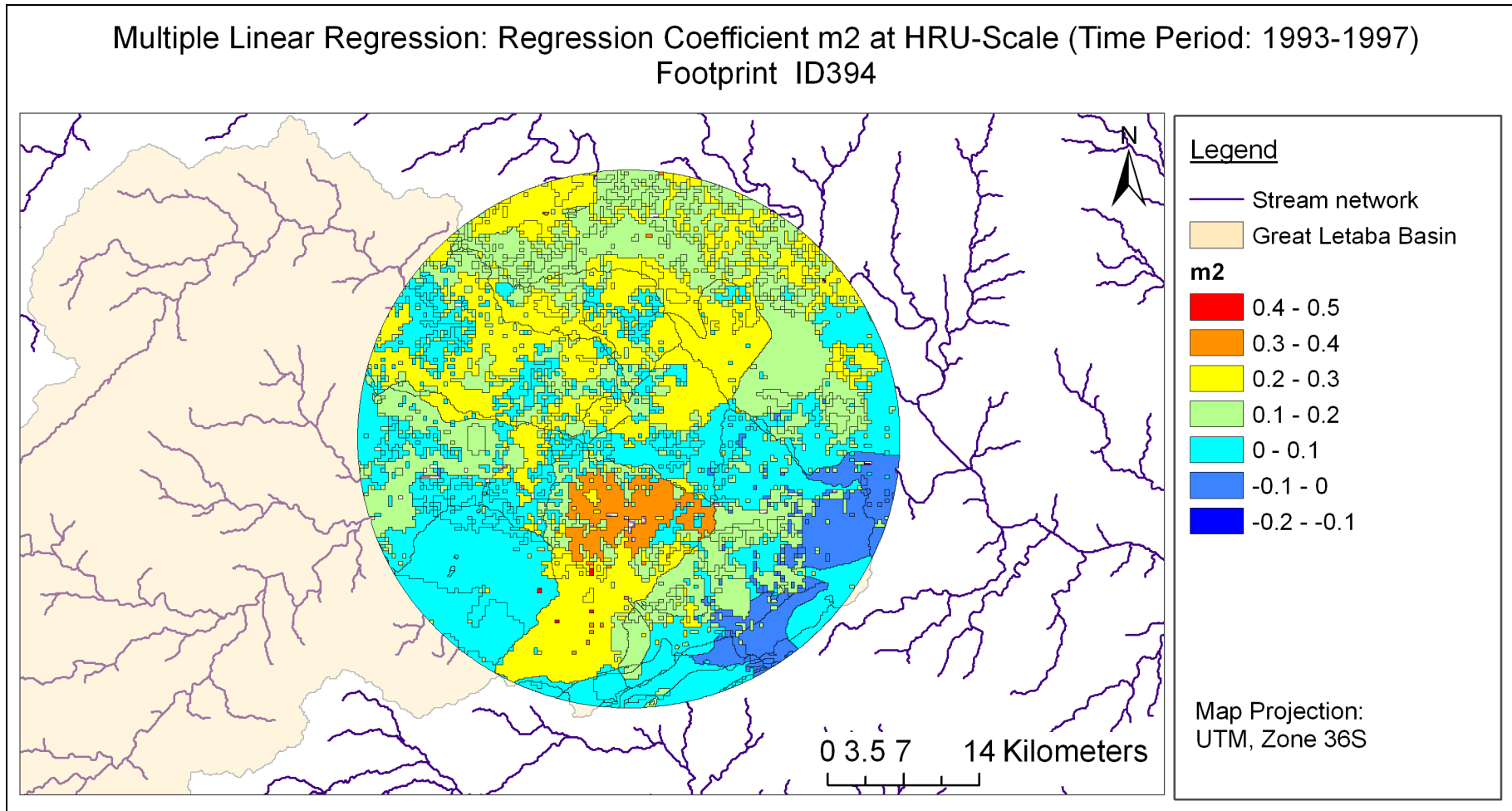
**APPENDIX I: MULTIPLE LINEAR REGRESSION: SPATIAL VARIABILITY OF THE COEFFICIENT OF DETERMINATION R^2 ,
FOOTPRINT ID393**



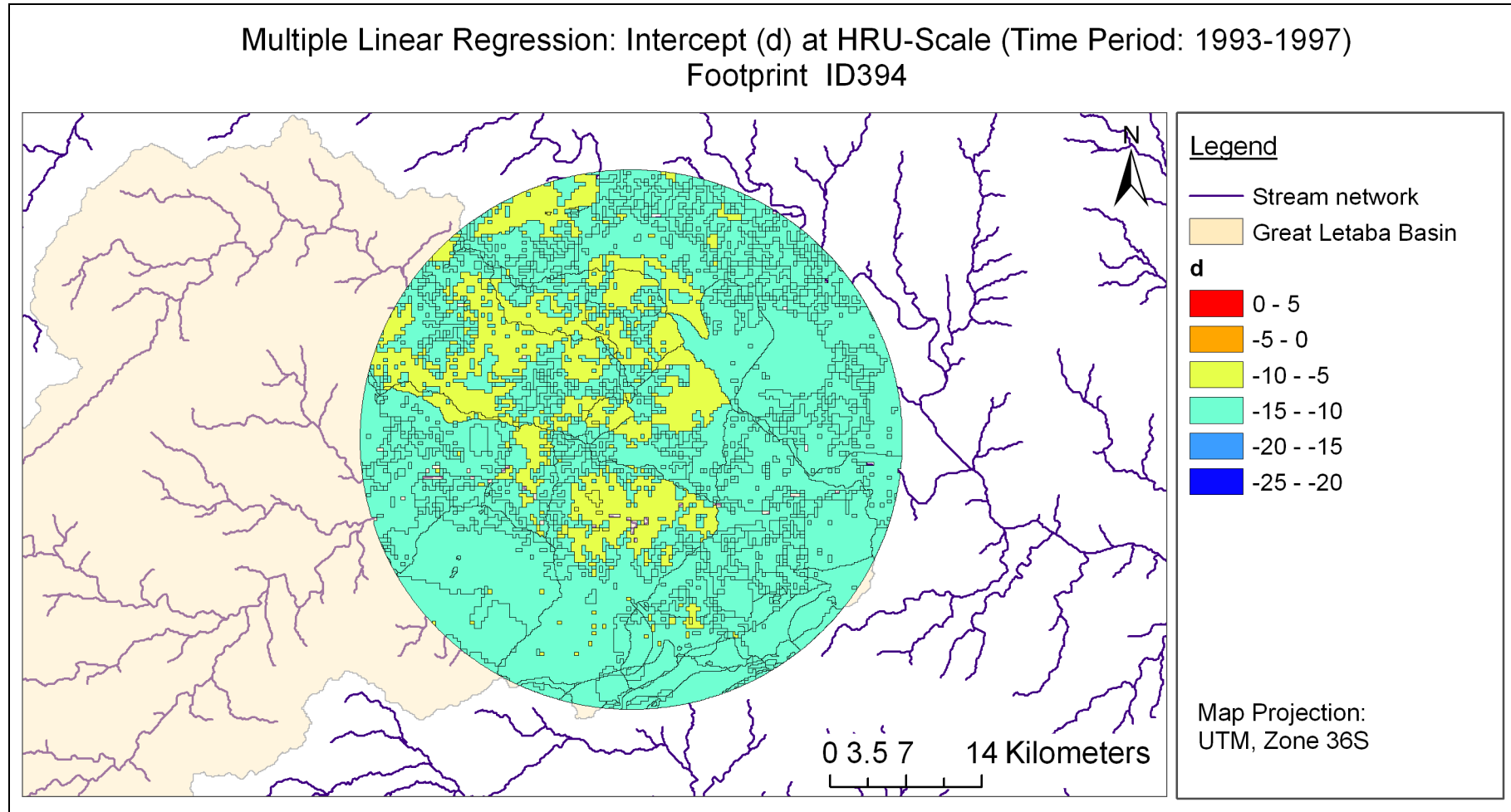
APPENDIX J: MULTIPLE LINEAR REGRESSION: SPATIAL VARIABILITY OF THE REGRESSION COEFFICIENT m_1 , FOOTPRINT ID394



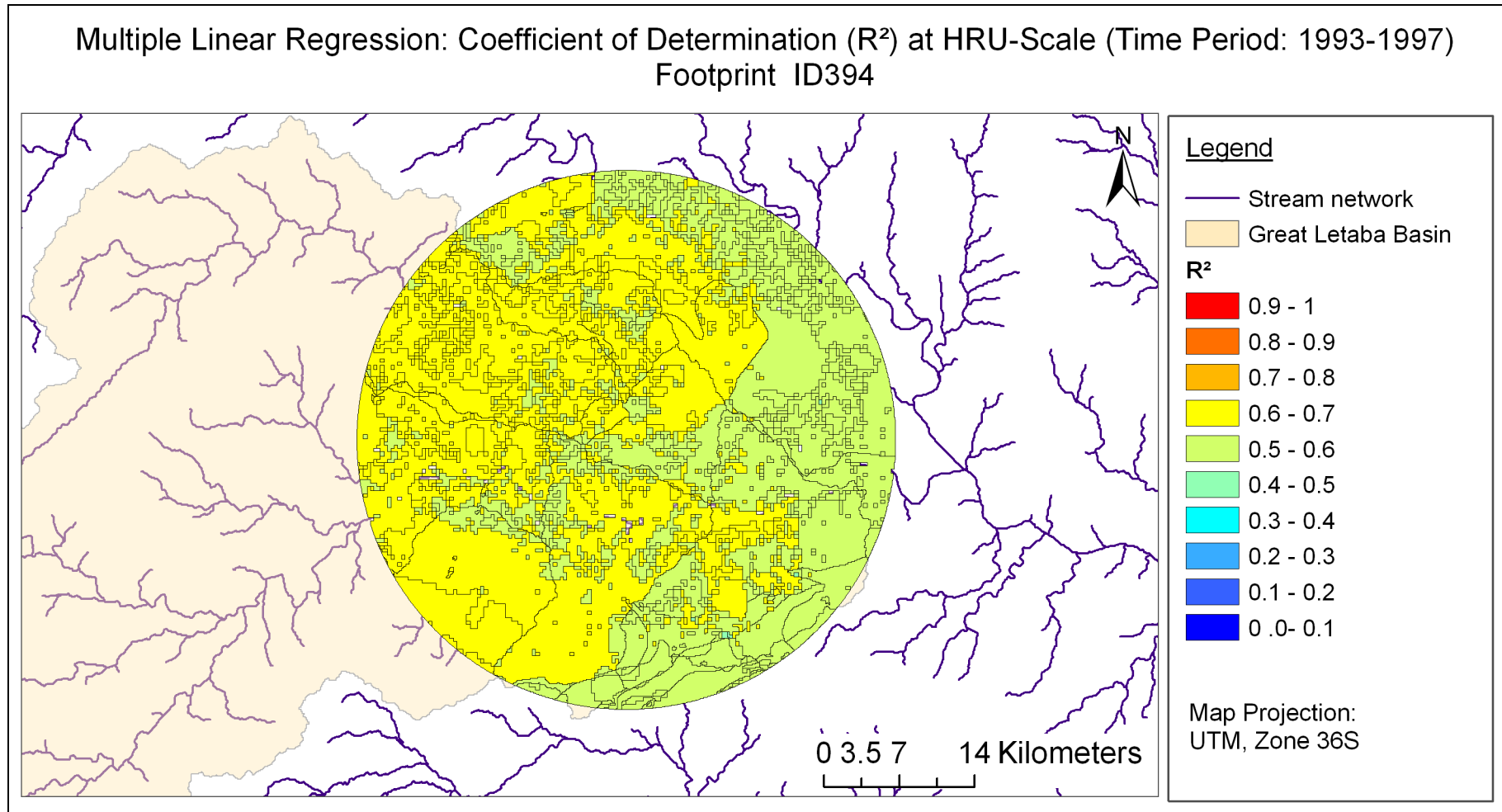
APPENDIX K: MULTIPLE LINEAR REGRESSION: SPATIAL VARIABILITY OF THE REGRESSION COEFFICIENT m_2 , FOOTPRINT ID394



APPENDIX L: MULTIPLE LINEAR REGRESSION: SPATIAL VARIABILITY OF THE INTERCEPT D, FOOTPRINT ID394



**APPENDIX M: MULTIPLE LINEAR REGRESSION: SPATIAL VARIABILITY OF THE COEFFICIENT OF DETERMINATION R^2 ,
FOOTPRINT ID394**



Selbständigkeitserklärung

Ich erkläre, dass ich die vorliegende Arbeit selbständig und unter Verwendung der angegebenen Hilfsmittel, persönlichen Mitteilungen und Quellen angefertigt habe.

Jena, 3.4. 2008

(Cornelia Scheffler)

